

**STRUCTURAL BEHAVIOUR OF REINFORCED
CONCRETE BEAMS STRENGTHENED BY
EPOXY BONDED STEEL PLATES**

By

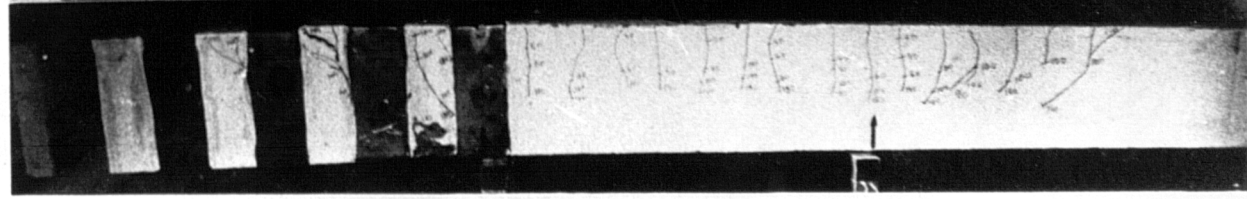
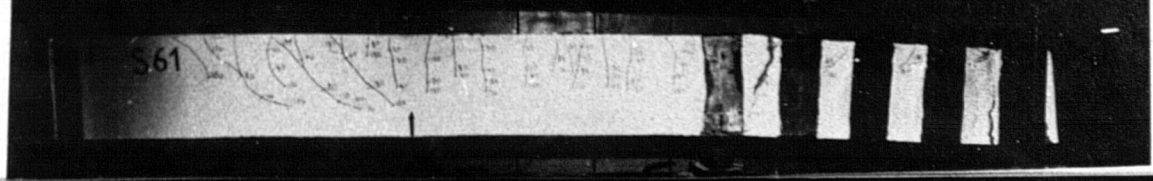
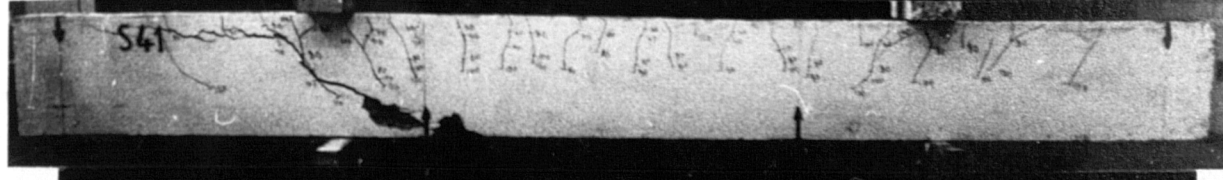
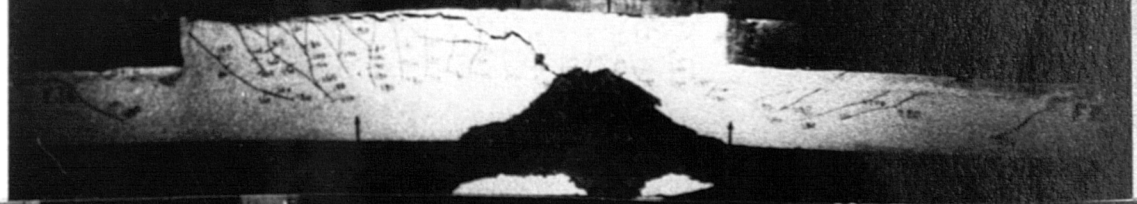
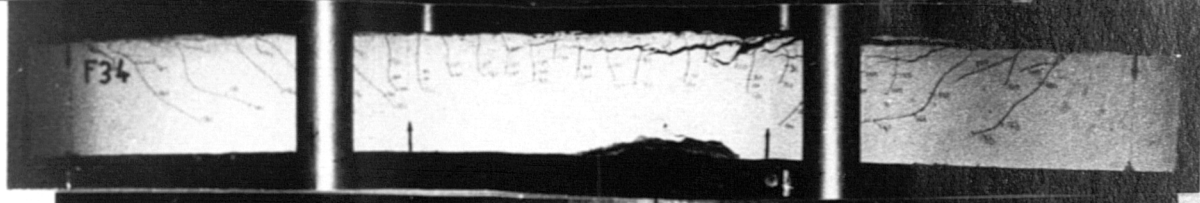
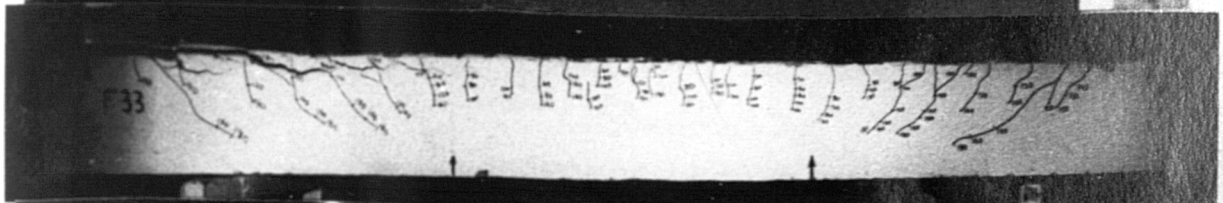
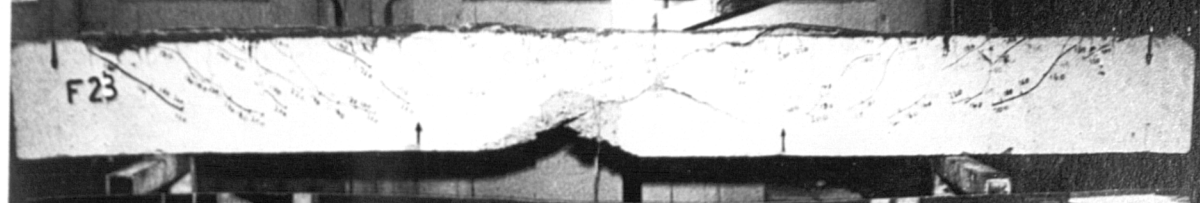
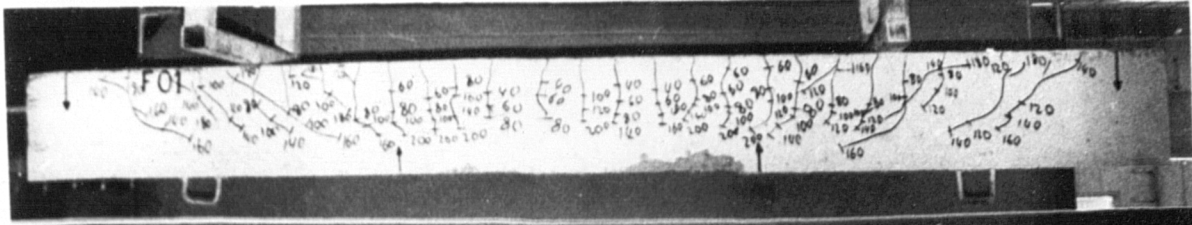
Abdelhamid CHARIF

B.Eng. (Algiers)

Thesis submitted to the university of Sheffield
for the Degree of Doctor of Philosophy
in the Faculty of Engineering

Department of Civil and Structural Engineering

July, 1983



*To the memories of my father and uncle
who paid the ultimate sacrifice,
and to my mother and sister
who fought through hard times,
to make things possible for me.*

LIST OF CONTENTS

	Page No.
LIST OF CONTENTS.....	i
LIST OF FIGURES.....	vi
LIST OF TABLES.....	viii
NOTATIONS.....	x
ACKNOWLEDGEMENTS.....	xiii
SUMMARY.....	xiv

CHAPTER ONE : GENERAL INTRODUCTION

1.1	INTRODUCTION.....	1
1.2	AIMS OF PROJECT.....	4
1.2.1	EPOXY PROPERTIES.....	5
1.2.1.1	TENSILE AND COMPRESSIVE TESTS.....	5
1.2.1.2	SHEAR ADHESION TESTS.....	6
1.2.2	PRELOADED BEAMS.....	6
1.2.3	BCND FAILURE TESTS.....	7
1.2.4	FLEXURAL BEHAVIOUR OF PLATED BEAMS.....	7
1.2.5	SHEAR BEHAVIOUR OF PLATED BEAMS.....	7
1.2.6	LONG TERM BEHAVIOUR OF PLATED BEAMS.....	7
1.3	CUTLINE OF THESIS.....	7

CHAPTER TWO : LITERATURE REVIEW

2.1	INTRDUCTION.....	10
2.2	EPOXY RESINS.....	10
2.2.1	INTRDUCTION.....	10
2.2.2	PROPERTIES OF EPOXIES.....	11
2.2.2.1	MECHANICAL PROPERTIES.....	11
2.2.2.2	DURABILITY.....	12
2.2.2.3	TEMPERATURE EFFECTS.....	13
2.2.2.4	OTHER PROPERTIES.....	13
2.2.2.5	FILLERS AND MCDIFIERS.....	14
2.2.3	BONDING PROCEDURE.....	14
2.2.3.1	SURFACE PREPARATION.....	15
2.2.3.2	MIXING.....	15
2.2.3.3	BCNDING AND CURING.....	16
2.2.3.4	SAFETY.....	17
2.3	EPOXY ADHESION TO CCONCRETE.....	17
2.3.1	INTRODUCTION.....	17
2.3.2	SHEAR ADHESION.....	18
2.3.3	WATER RESISTANCE.....	18
2.3.4	MISCELLANEOUS.....	19
2.4	EPOXY ADHESION TO METALS.....	20
2.4.1	INTRODUCTION.....	20
2.4.2	SURFACE STATE.....	22
2.4.3	TEMPERATURE EFFECTS.....	22
2.4.4	ADHESIVE THICKNESS.....	23
2.4.5	ADHERENT THICKNESS.....	24
2.4.6	DURABILITY.....	24
2.5	EXTERNALLY BCNDED REINFORCEMENT.....	25

2.5.1	INTRODUCTION.....	25
2.5.2	REINFORCEMENT GEOMETRY.....	26
2.5.3	STIFFNESS AND STRENGTH.....	26
2.5.4	BOND FAILURES.....	27
2.5.5	NEW CONCRETE WITH EXTERNAL STEEL.....	28
2.5.6	SHEAR BEHAVIOUR.....	28
2.5.7	PRACTICAL APPLICATIONS.....	29
2.6	CONCLUSIONS.....	31

CHAPTER THREE : MIX DESIGN AND MATERIAL PROPERTIES

3.1	INTRODUCTION.....	33
3.2	MATERIALS.....	34
3.2.1	CEMENT.....	34
3.2.2	FINE AGGREGATES.....	34
3.2.3	COARSE AGGREGATES.....	34
3.2.4	WATER REDUCING AGENT.....	34
3.2.5	STEEL BARS.....	36
3.2.6	STEEL PLATES.....	36
3.2.7	EPOXY RESIN.....	39
3.3	MIX DESIGN.....	39
3.3.1	MIXING PROCEDURE.....	41
3.3.2	PROPERTIES OF FRESH CONCRETE.....	41
3.3.3	PROPERTIES OF HARDENED CONCRETE.....	42
3.3.3.1	COMPRESSIVE STRENGTH.....	42
3.3.3.2	INDIRECT TENSILE STRENGTH.....	42
3.3.3.3	FLEXURAL STRENGTH-MODULUS OF RUPTURE.....	42
3.3.3.4	ELASTIC MODULUS AND POISSON'S RATIO.....	45
3.3.3.5	SHRINKAGE.....	45

CHAPTER FOUR : PROPERTIES OF EPOXY

4.1	INTRODUCTION.....	47
4.2	TENSILE TESTS ON EPOXY RESIN.....	48
4.2.1	INTRODUCTION.....	48
4.2.2	SERIES I.....	49
4.2.2.1	AMSLER TESTS.....	49
4.2.2.2	INSTRON TESTS.....	51
4.2.2.3	RESULTS OF SERIES I.....	51
4.2.3	SERIES II.....	53
4.2.3.1	VARIABLES.....	53
4.2.3.2	INSTRUMENTATION AND TESTING PROCEDURE.....	53
4.2.3.3	TEST MEASUREMENTS.....	54
4.2.3.4	DISCUSSION OF RESULTS.....	58
4.2.4	LONG TERM TENSILE TESTS ON EPOXY.....	67
4.3	COMPRESSIVE TESTS ON EPOXY.....	69
4.3.1	EXPERIMENTAL PROGRAMME.....	69
4.3.2	TEST RESULTS.....	71
4.4	SHEAR ADHESION PROPERTIES OF EPOXY.....	71
4.4.1	INTRODUCTION.....	71
4.4.2	EXPERIMENTAL PROGRAMME.....	74
4.4.2.1	PULL OUT TEST.....	74
4.4.2.2	DOUBLE AND SINGLE LAP TESTS.....	74
4.4.2.3	THEORETICAL MODELS.....	78
4.4.3	BONDING PROCEDURE.....	79
4.4.4	INSTRUMENTATION.....	79

4.4.5	CALIBRATION.....	80
4.4.6	TESTING PROCEDURE.....	80
4.4.7	MEASUREMENTS.....	81
4.4.8	DISCUSSION OF RESULTS.....	81
4.4.8.1	PULL OUT RESULTS.....	81
4.4.8.2	DOUBLE AND SINGLE LAP RESULTS.....	88
4.4.8.3	EFFECTS OF CONCRETE STRENGTH AND GLUE THICKNESS.....	94
4.4.9	LONG TERM ADHESION TESTS.....	94
4.5	CONCLUSIONS.....	97

CHAPTER FIVE : FLEXURAL BEHAVIOUR OF PLATED BEAMS

5.1	INTRODUCTION.....	100
5.2	EXPERIMENTAL PROGRAMME.....	102
5.2.1	INTRODUCTION.....	102
5.2.2	DETAILS OF BEAMS.....	103
5.2.3	MATERIALS.....	108
5.2.4	MANUFACTURING OF BEAMS.....	108
5.2.5	BONDING PROCEDURE.....	109
5.2.6	TEST MEASUREMENTS AND INSTRUMENTATION.....	111
5.2.7	TESTING APPARATUS.....	113
5.2.8	TESTING PROCEDURE.....	114
5.3	RESULTS.....	115
5.4	DEFORMATION PROPERTIES.....	119
5.4.1	DEFLECTIONS.....	119
5.4.2	ROTATIONS.....	125
5.4.3	STRAINS.....	130
5.4.3.1	CONCRETE STRAINS.....	131
5.4.3.2	BAR STRAINS.....	140
5.4.3.3	PLATE STRAINS.....	145
5.5	CRACK WIDTHS.....	150
5.6	RIGIDITIES.....	153
5.7	TENSILE STRESSES IN CONCRETE.....	157
5.8	STRENGTH PROPERTIES.....	159
5.8.1	FIRST CRACK LOADS.....	159
5.8.2	ULTIMATE STRENGTHS.....	161
5.9	INTERPRETATION OF RESULTS.....	163
5.10	CONCLUSIONS.....	172

CHAPTER SIX : PREMATURE BOND FAILURES OF PLATED BEAMS

6.1	INTRODUCTION.....	174
6.2	BOND STRESSES.....	176
6.2.1	BOND STRESSES IN THE BARS.....	176
6.2.2	BOND STRESSES IN THE PLATE.....	178
6.3	EFFECT OF PLATE CUTOFF ON BOND STRESSES.....	179
6.4	PEELING FORCES.....	183
6.5	EXPERIMENTAL INVESTIGATION.....	186
6.5.1	INTRODUCTION.....	186
6.5.2	EXPERIMENTAL PROGRAMME.....	187
6.5.3	BEAM DETAILS.....	191
6.5.4	TESTS MEASUREMENTS AND INSTRUMENTATION.....	192
6.5.5	TESTING PROCEDURE.....	192
6.6	TEST RESULTS.....	192
6.7	DEFORMATION PROPERTIES.....	193
6.7.1	DEFLECTIONS AND ROTATIONS.....	193

6.7.2	STRAINS.....	201
6.8	CRACK WIDTHS AND RIGIDITIES.....	210
6.9	TENSILE STRESSES IN CONCRETE.....	210
6.10	STRENGTH PROPERTIES.....	212
6.10.1	FIRST CRACK LOADS.....	212
6.10.2	ULTIMATE STRENGTHS.....	214
6.10.2.1	BEAM F31.....	214
6.10.2.2	BEAMS F32 AND F33.....	214
6.10.2.3	BEAMS F34 AND F35 WITH BOLTS.....	217
6.10.2.4	BEAMS F36 AND F37 WITH SIDE STRIPS.....	220
6.11	BCND STRESSES.....	224
6.11.1	EXTERNAL BOND STRESSES.....	224
6.11.2	INTERNAL BCND STRESSES.....	241
6.12	PEELING FORCES.....	245
6.12.1	COMPONENT F1.....	245
6.12.2	COMPONENT F2.....	246
6.13	CCNCLUSIONS.....	247

CHAPTER SEVEN : SHEAR BEHAVIOUR OF PLATED BEAMS

7.1	INTRODUCTION.....	249
7.2	LITERATURE REVIEW.....	251
7.3	EXPERIMENTAL PROGRAMME.....	252
7.4	DISCUSSION OF RESULTS.....	253
7.4.1	DEFORMATION PROPERTIES.....	253
7.4.2	CRACKING PROPERTIES.....	270
7.4.2.1	FLEXURAL CRACKING.....	270
7.4.2.2	DIAGONAL CRACKING.....	273
7.4.3	STRENGTH PROPERTIES.....	274
7.4.3.1	CP110 CODE.....	276
7.4.3.2	ACI CODE.....	276
7.4.3.3	CEB-FIP CODE.....	277
7.4.3.4	EFFECT OF THE LONGITUDINAL PLATE.....	278
7.4.3.5	EFFECT OF THE SHEAR SPAN.....	280
7.4.3.6	EFFECT OF THE EXTERNAL SHEAR STEEL.....	281
7.4.4	MODES OF FAILURE.....	282
7.5	CONCLUSIONS.....	287

CHAPTER EIGHT : LONG TERM BEHAVIOUR OF PLATED BEAMS

8.1	INTRODUCTION.....	289
8.2	EXPERIMENTAL INVESTIGATIONS.....	291
8.2.1	EXPERIMENTAL PROGRAMME.....	291
8.2.2	LOADING APPARATUS AND TEST MEASUREMENTS.....	293
8.3	DISCUSSION OF RESULTS.....	297
8.3.1	DURABILITY.....	298
8.3.1.1	PRISM TESTS.....	298
8.3.1.2	BEAM TESTS.....	298
8.3.2	LONG TERM DEFORMATIONS.....	299
8.3.2.1	SHRINKAGE.....	299
8.3.2.2	CREEP.....	303
8.4	CONCLUSIONS.....	311

CHAPTER NINE : LIMITATIONS, CONCLUSIONS AND
RECOMMENDATIONS FOR FUTURE WORK

9.1	LIMITATIONS OF THE PRESENT WORK.....	314
9.2	GENERAL CONCLUSIONS.....	315
9.3	RECOMMENDATIONS FOR FUTURE WORK.....	318

APPENDIX A : STRAIN GAUGE INSTRUMENTATION

A1.	STRAIN GAUGE.....	320
A2.	MEASURING CIRCUIT (WHEATSTONE BRIDGE).....	320
A2.1	QUARTER BRIDGE.....	322
A2.2	HALF BRIDGE.....	322
A2.3	FULL BRIDGE.....	322
A3.	SOURCES OF ERROR.....	322

APPENDIX B : THEORETICAL MODELS FOR PULL OUT
AND DOUBLE LAP TESTS

B1.	PULL OUT TEST.....	324
B2.	DOUBLE LAP TEST.....	327

APPENDIX C : BEAM ANALYSIS

C1.	UNCRACKED SECTION.....	331
C2.	CRACKED SECTION.....	334

APPENDIX D : ULTIMATE FLEXURAL STRENGTH

D1.	CP110 SIMPLIFIED METHOD.....	335
D2.	CP110 STRAIN COMPATIBILITY METHOD.....	336
D3.	HOGNESTAD ET AL. STRAIN COMPATIBILITY METHOD.....	339

APPENDIX E : CALCULATION OF DEFLECTIONS
ROTATIONS AND CRACK WIDTHS

E1.	DEFLECTIONS AND ROTATIONS.....	340
E1.1	UNCRACKED SECTION.....	340
E1.2	CRACKED SECTION.....	341
E1.2.1	CP110 RECOMMENDATIONS.....	341
E1.2.2	ACI RECOMMENDATIONS.....	341
E1.2.3	CEB RECOMMENDATIONS.....	342
E1.2.4	PRECASTED BEAMS.....	342
E2.	CALCULATIONS OF CRACK WIDTHS.....	342
	REFERENCES.....	347

LIST OF FIGURES

Fig. No.	Title	Page No.
2.1	Epoxy-metal joints.....	21
3.1	Grading of aggregates.....	35
3.2	Bar stress-strain curves.....	37
3.3	Plate stress-strain curves.....	38
3.4	Concrete strength development.....	43
3.5	Shrinkage in concrete.....	46
4.1	Epoxy specimen shapes used in Series I of tensile tests.....	50
4.2	Epoxy stress-strain curves in tension.....	55
4.3	Testing apparatus and instrumentation (Series II of epoxy tensile tests).....	56
4.4	Effect of loading rate in tension.....	63
4.5	Effect of specimen thickness in tension.....	64
4.6	Effect of loading rate on epoxy properties....	65
4.7	Effect of specimen thickness on epoxy properties.....	66
4.8	Epoxy stress-strain curve in compression.....	70
4.9	Failure of epoxy specimens in tension.....	73
4.10	Failure of epoxy specimens in compression.....	73
4.11 , 4.12	Pull out test rig and specimen.....	75, 76
4.13	Curing of a pull out specimen.....	76
4.14	Single and double lap test specimens.....	77
4.15	Local force distribution in pull out test.....	83
4.16	Force distribution along pull out joint.....	85
4.17	Shear stress distribution along pull out joint at different load levels.....	85
4.18	Failure of pull out specimens.....	87
4.19	Failure of double lap specimens.....	87
4.20	Local force distribution in double lap test...	91
4.21	Force distribution along double lap joint.....	92
4.22	Shear stress distribution along double lap joint at different load levels.....	92
4.23	Effect of concrete grade on bond strength.....	95
4.24	Effect of glue thickness on bond strength.....	95
5.1 , 5.2	Loading apparatus I.....	104, 105
5.3 , 5.4	Loading apparatus II and instrumentation...	105, 106
5.5	Beam details and instrumentation.....	107
5.6	Internal reinforcement cage.....	110
5.7 , 5.8	Curing of plated beams.....	110
5.9 , 5.10	Crack patterns in unplated and plated beams..	116
5.11 to 5.13	Load-deflection curves.....	121-123
5.14 to 5.16	Load-rotation curves.....	127-129
5.17 to 5.20	Load-concrete strain curves.....	133-136
5.21	Distribution of concrete strains across the beam depth.....	139
5.22 to 5.24	Load-bar strain curves.....	142-144
5.25 to 5.27	Load-plate(glue) strain curves.....	147-149
5.28	Load-average crack width curves.....	152
5.29	Transformed section of the beam.....	154
5.30	Strain model for preloaded beams.....	154
5.31	Possible stress model in beams.....	154
5.32	Crack patterns at preloading.....	168

5.33 to 5.35	Crack patterns and mode of failures.....	169-171
6.1	Bond stress in bars and plate.....	177
6.2	Transformed section of the beam.....	177
6.3	Bond stress at the plate cutoff point.....	177
6.4	System of forces acting in the joint between beam and plate.....	184
6.5	Assumed loading system in the plate.....	184
6.6 , 6.7	Details of bond failure beams.....	188,189
6.8 , 6.9	Load-deflection curves.....	196,197
6.10 , 6.11	Load-rotation curves.....	198,199
6.12 , 6.13	Load-concrete strain curves.....	204,205
6.14 , 6.15	Load-bar strain curves.....	206,207
6.16 , 6.17	Load-plate strain curves.....	208,209
6.18	Bar strain distribution in the shear span....	215
6.19	Mode of failure.....	216
6.20 , 6.21	Modes of failure.....	218,219
6.22	Mode of failure.....	221
6.23	Locations of strip strain measurements.....	222
6.24	Load-strip strain curves.....	223
6.25 to 6.28	Distribution of strains along plate at different load levels.....	225-228
6.29	Relative locations of plate, support, and load point.....	229
6.30 to 6.32	Distribution of strains along bars at different load levels.....	230-232
6.33 to 6.36	Distribution of bond stress along plate at different load levels.....	234-237
6.37	Load-plate movement curves.....	238
6.38 to 6.40	Distribution of bond stress along bars at different load levels.....	242-244
7.1	Details of shear beams without web reinforcement and instrumentation.....	254
7.2	Details of beam with external web steel.....	255
7.3	Internal reinforcement cage of beams with external shear reinforcement.....	256
7.4 , 7.5	Load-deflection curves.....	258,259
7.6 , 7.7	Load-rotation curves.....	260,261
7.8 to 7.11	Load-concrete strain curves.....	262-265
7.12 , 7.13	Load-bar strain curves.....	266,267
7.14	Load-plate strain curves.....	268
7.15	Load-external channel strain curves.....	271
7.16	Variation of ultimate shear stress with shear span.....	279
7.17	Variation of ratio of ultimate moment to flexural moment with shear span.....	279
7.18 to 7.23	Modes of failure.....	283-286
8.1	Long-term loading apparatus.....	294
8.2	Long term beams.....	295
8.3	Variation of shrinkage deformations with time.....	301
8.4 to 8.7	Variation of total concrete strain.....	306-309
8.8	Variation of neutral axis position with time.....	310
A1	Wheatstone strain gauge bridge.....	321
B1	Forces acting in pull out specimen.....	325
B2	Distribution of longitudinal force and shear stress along pull out joint.....	325
B3	Forces acting in double lap specimen.....	328

B4	Distribution of longitudinal force along double lap joint.....	328
B5	Distribution of shear stress along double lap joint.....	328
C1	Section details.....	332
D1	Stress blocks at ultimate state.....	332
D2	Strain model for preloaded beams.....	332

LIST OF TABLES

Table No.	Title	Page No.
3.1	Properties of steel bars.....	40
3.2	Properties of steel plates.....	40
3.3	Properties of fresh concrete.....	40
3.4	Properties of hardened concrete.....	44
4.1	Result of Series I of epoxy tensile tests.....	52
4.2	Results of Series II of epoxy tensile tests...	57
4.3	Ultimate strength results of Series II.....	60
4.4	Ultimate elongation results of Series II.....	61
4.5	Strains and modulus results of Series II.....	62
4.6	Long-term tensile tests on epoxy.....	68
4.7	Results of compressive tests on epoxy.....	72
4.8	Pull out test results.....	82
4.9	Single and double lap test results.....	90
4.10	Long-term epoxy adhesion test results.....	96
5.1	Control test results of flexural beams.....	118
5.2	Experimental and theoretical deflections.....	120
5.3	Measured and predicted rotations.....	126
5.4	Measured and predicted concrete compressive strains.....	132
5.5	Experimental and theoretical neutral axis depths.....	138
5.6	Measured and predicted bar strains.....	141
5.7	Measured and predicted plate(glue) strains...	146
5.8	Measured and predicted average crack widths..	151
5.9	Experimental and theoretical rigidities	156
5.10	Tensile stresses in concrete in the tension face.....	158
5.11	Experimental and theoretical strength results.....	160
5.12	Modes of failure.....	167
6.1	Bond failure beams.....	194
6.2	Modes of failure and maximum loads carried.....	194
6.3	Experimental and theoretical deflections.....	195
6.4	Measured and predicted rotations.....	195
6.5	Measured and predicted concrete compressive strains.....	202
6.6	Measured and predicted neutral axis depths...	202
6.7	Measured and predicted bar strains.....	203
6.8	Measured and predicted plate strains.....	203
6.9	Measured and predicted average crack widths.....	211
6.10	Experimental and theoretical rigidities.....	211
6.11	Tensile stresses in concrete.....	213

6.12	Experimental and theoretical strength results.....	213
7.1	Details of shear beams.....	257
7.2	Strength results of shear beams.....	272
7.3	Experimental and theoretical ultimate shear stresses.....	275
8.1	Details of long-term beams.....	292
8.2	Shrinkage deformations.....	302
8.3	Elastic strains.....	302
8.4 , 8.5	Total concrete strains.....	304,305
8.6	Weather summary.....	312

NOTATIONS

A_b, A_g, A_p	: Cross sectional area of bars, glue and plate
A_{sv}	: Cross sectional area of shear reinforcement
a	: Shear span or distance as defined
a_{cr}	: Distance from the point where the crack width is calculated to the nearest reinforcing bar
b	: Beam width
b'	: Plate width
C	: Compressive force
C_t	: Creep deformation at time t
c	: Concrete cover
c_{min}	: Minimum cover to the main reinforcing bars
d	: Beam depth
d_b, d_g, d_p	: Distance between compressive face and bars, glue and plate
E	: Excitation voltage
E_c, E_b, E_g, E_p	: Elastic modulus of concrete, bars, glue and plate
e	: Eccentricity
F	: Force as defined
f_{bb}, f_{bp}	: Bond stress in bars and plate
f_{bo}, f_{go}	: 0.2% proof stress of bars and glue
f_{gy}, f_{py}	: Yield stress of glue and plate
f_{cu}	: Concrete cube strength
f'_{cu}	: Concrete prism compressive strength
f_b	: Concrete modulus of rupture
f_{yv}	: Characteristic strength of shear reinforcement
G	: Shear modulus
I	: Second moment of area as defined

I_{cr}, I_{uncr} : Inertia of cracked and uncracked section
 K : Strain gauge factor
 K_1, K_2, K_3 : Factors related to concrete stress block
 L, l : Length as defined
 M : Bending moment
 M_c : Moment carried by concrete in tension
 M_{in} : Internal moment carried by bars, glue and plate
 M_u, M_{flex} : Ultimate and flexural moments
 P : Bar perimeter or pressure or load
 p : Load per unit width
 R : Electrical resistance
 dR : Variation of strain gauge resistance
 $1/r$: Curvature
 S_v : Spacing of stirrups
 Sh_t : Shrinkage deformation at time t
 T : Tensile force or time
 t : time
 t_c, t_g, t_p : Thickness of concrete, glue and plate
 u : Displacement
 V : Shear force or strain gauge voltage output
 v : Shear stress
 v_u : Ultimate shear stress
 W_{cr} : Crack width
 x : Neutral axis depth or distance as defined
 dx : Small increment in distance x
 y_b, y_g, y_p : Distance between the neutral axis position
and bars, glue and plate
 z : Internal lever arm

Φ :	Bar diameter
ϵ :	Strain as defined
η :	Epoxy viscosity
ω :	Pull out or double lap specimen characteristic as defined
Ω :	Ohms, unit of electrical resistance
ν :	Poisson's ratio
ρ :	Ratio of longitudinal reinforcement
γ :	Shear strain
θ :	Rotation, angle
σ :	Longitudinal stress as defined
τ :	Shear bond stress
τ_{Rd} :	Concrete shear strength
Δ :	Deflection
ΔF :	Variation of longitudinal force between two consecutive strain gauge locations
ΔL :	Distance between two consecutive strain gauges

ACKNOWLEDGEMENTS

Foremost the author would like to express his gratitude to the Algerian Ministry of Higher Education who sponsored his studies and to the Department of Civil and Structural Engineering of the University of Sheffield.

He is most grateful to his supervisors Mr R Jones and Dr R N Swamy for their help and guidance throughout the project and their assistance during the presentation of this thesis.

Special thanks are due to the technical staff of the Light and Heavy Structures Laboratories for their valuable help in the experimental work.

The author also acknowledges the assistance of the staff of the computer centre of the University of Sheffield.

SUMMARY

The development of synthetic adhesives based on epoxy resins has opened new possibilities for bonding structural materials together.

The present work was concerned with the use of epoxy resins to strengthen reinforced concrete beams by externally bonded steel plates.

It was found in the first part that the assessment of the properties of the epoxy adhesive is of paramount importance as they varied considerably with the thickness of the test specimen and the rate of loading.

The adhesive proved to offer a bond stronger than concrete in shear and resulted in a composite action between the beams and steel plates.

Preloading the beams prior to strengthening them did not have any adverse effect on their behaviour. The added strength from the plates was fully exploited even in beams which were held under a preload of 70% of their ultimate strength while being strengthened.

Stopping the plate in the shear span, short of the support, created a critical section where premature bond failure occurred beyond a certain plate thickness. Failure was caused by the combination of high peeling and bond stresses present in the region where the plate was stopped. These stresses were due to the transfer of tensile forces from the plate to the bars in that region and were higher with thicker plates.

Bonding steel plates on the tension face of the beams increased their shear capacity by 9 to 15%. This may have been due to dowelling action from the plates which had a greater contact area with concrete than an equivalent amount of internal steel bars. The use of externally bonded steel as shear reinforcement was effective but requires further investigation. The external web strips failed prematurely as compared to equivalent stirrups.

The long term deformations in plated beams were highly affected by the conditions of their environment but despite 47 month exposure no visual deterioration of the concrete-epoxy-steel joint was observed.

CHAPTER ONE
GENERAL INTRODUCTION

1.1 INTRODUCTION

The level of maintenance of structures in civil engineering is as important as their design and construction. It is unreasonable and unrealistic to expect a satisfactory response from a structure for the whole of its design lifetime without regular inspection, proper maintenance and appropriate upgradings when necessary. For numerous reasons, strengthening of existing structures may on some occasions be necessary. These upgrading requirements may be due to the need to increase the load carrying capacity of the member or to restore the structural performance because of design faults, constructional errors or following an unexpected damage. When these situations arise, considerable economic benefits can be achieved by strengthening the structure instead of replacing it.

The reasons for strengthening an existing structure are various (1) and may be broadly divided into three categories:

(a) Design or constructional shortcomings, or material deterioration, producing serviceability problems by excessive deflections, rotations or cracking of elements.

(b) A structure which has been performing in a satisfactory manner for a particular use, is required for a different purpose.

(c) Structural damage caused by effects such as settlements, earthquakes, explosions, vehicle impacts, etc.

Fire is a common cause of damage to concrete members. It causes spalling of the concrete cover to the reinforcement exposing the metal to the heat and thus resulting in a considerable reduction of its yield strength.

As far as bridges are concerned, the reasons for strengthening are more diverse (2,3). In the U.S.A. one bridge in five is considered deficient or functionally obsolete. Each year some 150 bridges sag, buckle or collapse, sometimes tragically. Basic design and execution criteria, heavier vehicle usage, environmental conditions and the level of maintenance are all involved to some extent.

The process of rehabilitating a concrete structure can vary extensively depending on its type and the corrections needed. There are four common ways in which the live load carrying capacity of a bridge (or any other structure) can be increased:

- 1- Replacing the critical members with new ones.
- 2- Strengthening the critical members by internal or external prestressing, fixing additional material by stapling or guniting or attaching external reinforcement by connections utilizing bolts extending through the member (4).
- 3- Providing supplementary supports or members to assist in carrying loads.
- 4- Reducing the dead load and thereby providing additional capacity for live loads by substituting the existing deck by a lighter yet structurally adequate one.

It is often possible to use one or a combination of these methods to strengthen a structure but the operation is very expensive and time consuming.

In recent years, polymer impregnation techniques have been used successfully to restore the structural strength of a building in North Dakota (5-7). Polymer impregnation of precast and cured concrete can increase its compressive strength from 34.5 to 138 N/mm² (5-7). However this method is only suitable in cases of compressive strength restoration (where the concrete strength has substantially deteriorated).

The development of adhesives based on synthetic epoxy resins has created new possibilities in the structural strengthening field. An attractive new alternative of structural repair is one which consists of bonding external reinforcement to the critical members by means of an epoxy adhesive. This technique requires a minimum increase in the member size, allows a larger contact area between the joined materials and solves the problem of high local stresses encountered in the traditional methods using bolting, riveting or welding. The operation is quick and easy to execute, economical and keeps the disruption on site to a minimum.

The limited research carried out so far has proved the effectiveness of the method. The technique has been put into practice in France (8), England (9), South Africa, Switzerland, Poland and Japan where over 200 bridges had been strengthened in this way by 1975.

The development of epoxy formulations capable of adhering to fresh concrete has also extended the original purpose of strength restoration to a new technology of manufacturing reinforced concrete by casting fresh concrete against steel plates or channels already coated with an adhesive layer.

The behaviour of a composite material cannot always be predicted from that of its components alone. The strengthening of reinforced concrete structures by epoxy bonded steel plates demands a confident knowledge of the three materials used and their composite behaviour. In any field of engineering, the assessment of the properties of the materials and their responses to the required applications, under every possible condition, is of primary importance. It is sometimes easy to underestimate this important aspect as many engineers are more often attracted to the challenging structural and analytical investigations than to the less exciting material research. This neglect has sometimes resulted in structural failures (2). These fatal consequences, combined with the limitations of conventional materials to perform the increasingly ambitious requirements of modern technology, have led to a general awareness of the problem. Nowadays, large amounts of money are invested in research programmes to investigate material properties and develop new, lighter, stronger and cheaper composites to suit the requirements of the engineer.

1.2 AIMS OF PROJECT

The overall objective of the present work is to study the properties of epoxy resins and produce useful information towards their confident use to bond structural materials together in general and their use to strengthen reinforced concrete beams by externally bonded steel plates in particular. The research presented in this thesis covers broadly six areas of study:

- 1- Mechanical and adhesiveness properties of the epoxy resin used in the study.

2- Effects of preloading on the subsequently strengthened beams. Performance of beams preloaded before strengthening with plates.

3- Comparison of the flexural properties of unplated and plated beams.

4- Mechanism of premature bond failures of plated beams and possibilities of avoiding them.

5- Effects of longitudinal external plates on the shear capacity of the beams and use of externally bonded steel as shear reinforcement.

6- Long term behaviour of plated beams.

1.2.1 EPOXY PROPERTIES

The successful use of an epoxy adhesive for bonding external steel to concrete requires the following basic conditions:

(a) Good adhesion of the resin to steel and concrete.

(b) Good flexibility and strength properties in order to sustain the service strains and stresses.

(c) Good durability and fatigue performances.

One of the aims of the project is to investigate these properties:

1.2.1.1 TENSILE AND COMPRESSIVE TESTS

To determine the stress-strain relationship of the epoxy resin and study the effects of the following variables: age and geometry of the specimen, rate of loading and long term exposure and immersion in water.

1.2.1.2 SHEAR ADHESION TESTS

To study the shear adhesiveness of epoxy to concrete and steel:

(a) Pull out tests:

To investigate the behaviour of the concrete-glue-steel bond in shear and study the effects of the concrete grade, glue thickness and long term exposure and immersion in water.

(b) Double lap tests:

To study the epoxy bond strength with steel adherents and the effects of the glue line thickness and long term exposure and immersion in water.

1.2.2 PRELOADED BEAMS

To assess the extent to which the method can be used in practice, two series of tests were carried out:

(a) Beams were loaded, unloaded, strengthened with a 1.5mm steel plate whilst being unloaded and then tested to failure after two weeks of bond curing.

(b) Beams were loaded then strengthened whilst still under load with a 1.5mm steel plate, and after curing of the resin, the load was increased to failure. The test variable was the preload.

The effects of the preloading on the flexural behaviour of the beams were studied in both cases.

1.2.3 BCND FAILURE TESTS

Another objective of the project is to clarify the phenomenon of premature bond failures occurring with thick plates and investigate the possibilities of avoiding them.

1.2.4 FLEXURAL BEHAVIOUR OF PLATED BEAMS

Quantitative and relative comparisons (by non-dimensional parameters) of the behaviour of plated and unplated beams have been carried out.

1.2.5 SHEAR BEHAVIOUR OF PLATED BEAMS

Another area of study is the effect of the bonded plates, in the tension face, on the shear strength of the beam (to study whether dowel action exists in the external reinforcement). The test variable was the shear span. The use of externally bonded steel strips on the beam sides as shear reinforcement is also investigated.

1.2.6 LONG TERM BEHAVIOUR OF PLATED BEAMS

Creep and shrinkage in the plated beams exposed to environmental conditions are studied by regular strain measurements on eight plated beams sustaining constant loading (creep) and one unloaded beam (shrinkage).

1.3 OUTLINE OF THESIS

Chapter two presents a critical review of past and recent research into the areas studied in this research programme. Particular emphasis is given to the general properties of epoxy resins, their use as structural adhesives and the behaviour of reinforced concrete members strengthened by externally bonded steel plates.

In chapter three, the properties of the different materials used in this project (steel bars and plates, gravel, cement, sand, water reducing agent), the design of the concrete mixes used and their properties are given.

Chapter four describes the investigations of the mechanical and adhesion properties of the epoxy glue used in the present work.

Chapter five compares the general flexural behaviour of plated and unplated beams and studies the effects of preloading on the performance of the subsequently strengthened beams.

The analytical and experimental investigations into the premature bond failures of plated beams are dealt with in chapter six.

Chapter seven is concerned with the shear behaviour of plated beams. The possible existence of a dowel action in the external plates and the use of bonded steel strips as shear reinforcement are investigated.

The time dependent deformations (creep and shrinkage) of plated beams are studied and compared to those of conventional concrete in chapter eight.

The limitations of the present work, the general conclusions and recommendations for future research are presented in chapter nine.

The electrical instrumentation and strain gauge measurements used in the project are described in Appendix A.

Appendix B describes the theoretical models for the shear adhesion tests of epoxy with concrete and steel (pull out and double lap tests).

Appendix C describes the theoretical beam analysis before and after cracking and gives the first crack loads.

Appendix D deals with the beam analysis at ultimate loads and gives the theoretical ultimate flexural strengths.

Computation of the deflections, rotations and crack widths as recommended by CP110, CEB and ACI codes is presented in Appendix E.

CHAPTER TWO
LITERATURE REVIEW

2.1 INTRODUCTION

The future potential, the economic benefits and the various other advantages of the method of strengthening existing or reinforcing new concrete members by epoxy bonded steel plates, over the traditional techniques of structural repair, are numerous.

The effective use of the technique requires, however, sound understanding of the short and long term properties of the adhesive and reliable information about its adhesion to concrete and steel. The execution of the bonding operation is of paramount importance in order to achieve and ensure an intimate contact between the joined materials.

2.2 EPOXY RESINS

2.2.1 INTRODUCTION

An epoxy resin is defined as a material whose molecules contain two or more ethylene oxide terminal groups that are capable of polymerization and combining with other molecules to form more complex ones (10) Polymerization is achieved by mixing the epoxy resin base with a curing agent which hardens the epoxy by donating a hydrogen ion. The chemical symbol of the families of epoxies is:



The first practical application of epoxy resins took place in Germany and Switzerland in the 1930's. The first known patent on epoxy was issued to Dr. Castan in Switzerland in 1936. Three years later Dr. Greenlee of the USA explored and developed several more basic epoxy formulations. Mass production and commercialization of epoxies started in the 1950's.

Epoxy was first used in the construction industry as an adhesive in 1948 to bond two pieces of hardened concrete. It proved to be a reliable structural adhesive with the capability of being stronger than the concrete it bonded together. Since then epoxies have become widely used in civil engineering applications and have performed satisfactorily as coatings (waterproof or abrasion resistant), crack sealants, adhesives, etc. (11-14).

2.2.2 PROPERTIES OF EPOXIES

There is a wide range of epoxy systems and their properties vary substantially from one formulation to another. In this section only a general review of the main properties relevant to structural repair is given.

2.2.2.1 MECHANICAL PROPERTIES

Properly used, epoxy resins can offer excellent compressive and tensile strengths and provide an adequate bond strength with most structural materials. The strength properties vary considerably from one epoxy resin to another (15-17). After the full cure is achieved, the adhesive develops a compressive strength three to five times its tensile strength. The compressive and tensile strengths vary from 10 to 200 N/mm² and 2 to 96 N/mm² respectively. The modulus of

elasticity varies between 200 and 100,000 N/mm². These high variations may be accounted for by the difference in the chemical compositions of the resins and the testing conditions used as the mechanical properties of visco-elastic materials such as epoxies are highly affected by the rate of loading and other parameters.

The published literature about the mechanical properties of epoxies is limited and the effects of important parameters such as the geometry of the specimen and the rate of loading remain unexplored. No standardized specimen size and testing method have been proposed as yet.

2.2.2.2 DURABILITY

There is very limited information about the effects of dynamic, cyclic and sustained loading on the mechanical properties of epoxy resins. Epoxy energy fracture can, however, be improved by rubber modifiers (18).

Epoxy resins react favourably to adverse environmental conditions. They are highly resistant to the attack of acids, oils, alkalis and solvents (19). A thin coating of an appropriate epoxy system can render a surface impermeable to water even when continuously inundated.

The long term mechanical properties of visco-elastic materials such as epoxy resins are important and require further investigation.

2.2.2.3 TEMPERATURE EFFECTS

The effect of the temperature on epoxies depend mainly on the type of adhesive used (20). The coefficient of thermal expansion of epoxies varies between 25 and 100 microstrains per degree Celsius. That of concrete is of the order of 10 microstrains. The considerable difference between the two coefficients requires careful attention when using the two materials together in a composite joint. The thermal expansion of the resins can however be reduced by the addition of fillers with a consequent increase in the elastic modulus (10).

The properties of epoxies are generally unaffected up to a temperature of 67°C. At higher temperatures, the properties change adversely and above 300°C., the resin chars and usually volatilizes releasing fumes which may be toxic.

2.2.2.4 OTHER PROPERTIES

(a) Mixing ratio: Mixing of the resin base and the hardener is carried out in weight ratios varying from 100:1 to 1:1.

(b) Pot life: The pot life is the time after completion of mixing and during which the adhesive remains workable with no loss of its properties. The pot life is influenced by the amount of material mixed and the ambient temperature. It can vary from a few minutes to several weeks.

(c) Exotherm: The exotherm is the heat produced by the chemical reaction when mixing is carried out and depends on the amount of material used. The resulting rise in the adhesive temperature can be as high as 200°C. in which case the cured system is literally charred.

(d) Viscosity: Varies from 100 cps (like water) to very heavy paste in which case the workability of the adhesive is

considerably reduced and the amount of air, entrained during mixing, is important and may affect the performance of the adhesive.

(e) Curing time: Depends on the ambient temperature and varies from a few minutes to several days.

(f) Shrinkage: The adhesive contraction during curing depends on the amount of glue used and the ambient conditions. It varies from 10 to 5000 microstrains. The shrinkage deformations are nevertheless considerably reduced after the adhesive is fully cured.

2.2.2.5 FILLERS AND MODIFIERS

The properties of some epoxy systems can be appropriately altered, to suit the required job conditions, by the addition of fillers or modifiers to the resin. Rubber modifiers can increase epoxy fracture energy and stress intensity by factors of 5 and 2 respectively (18). Fillers can increase the elastic modulus and reduce thermal expansion (10) whereas mixing glass fibers with the resin can reduce the stress concentration factor (ratio of maximum to mean stress) and therefore improve the overall bond strength of epoxy to concrete (21).

2.2.3 BONDING PROCEDURE

The operation of bonding two structural materials with an epoxy adhesive is tedious and requires the utmost care. Improper surface preparation, mixing, curing and poor workmanship may all cause failure (15). Standard specifications for bonding structural materials together with an epoxy resin are recommended by ACI committee 503 (22):

2.2.3.1 SURFACE PREPARATION

Surfaces to which epoxies are to be applied must be clean and free of loose and unsound materials.

(a) Concrete surface: Concrete surfaces should have their coarse aggregates newly exposed by mechanical abrasion. To remove laitance, dust and other loose particles resulting from the mechanical operation, the surface may be wire brushed and jetted with compressed air.

(b) Steel surface: Steel surfaces may be shotblasted to remove the contaminated external layer. Blast cleaning residues can be removed by compressed air. To prevent corrosion, the surface preparation should be carried out just before the application of the adhesive.

2.2.3.2 MIXING

Proportioning of the quantities of the resin and hardener must be carried out according to the manufacturer's instructions (22). This is usually facilitated by the supply of measured quantities, in the correct proportions, of base and hardener so that the contents of one component can be emptied into the other, usually hardener into resin, and then mixed together.

Mixing can be achieved by a mechanical mixer such as a low speed electric drill with a mixing paddle and continued thoroughly until a uniform and homogeneous mixture is reached. The manufacturers often facilitate this by giving the resin and hardener two distinct colours which merge to form one even colour when mixing is complete.

2.2.3.3 BONDING AND CURING

To minimize the amount of air entrained in the joint, the adhesive must be applied to both surfaces to be bonded with a roller or spray equipment at a thickness sufficient to fill with excess the gap between the substrates (23). The operation must be completed within the pot life of the epoxy.

To ensure a full and intimate contact between the substrates and to squeeze out the excess of glue and achieve a uniform joint, a uniformly distributed pressure must be applied on the joint until full cure is attained. Bresson (23) carried out a theoretical analysis to determine the value of the uniformly distributed pressure to be applied and maintained until the polymerization and hardening of the epoxy is complete. He assumed that:

- i- Epoxy is a Newtonian liquid with a viscosity independent of the velocity of the flow (Laminar flow).
- ii- There is no acceleration of the flow.

The necessary pressure P to be applied in order to squeeze out the excess of glue and vary the thickness of the adhesive layer from t_{g1} to t_{g2} during the time T is given by:

$$P.T = 2\eta L \left[\frac{1}{t_{g2}} - \frac{1}{t_{g1}} \right]$$

Where L is the length of the joint and η is the viscosity of the resin.

The time T must be less than the pot life of epoxy and should be chosen so that the viscosity of the resin can be considered constant.

To avoid internal cracking and loss of bond, the elements being bonded together must not be moved or disturbed during curing.

2.2.3.4 SAFETY

Some epoxy resins are skin irritants and sensitizers to many people. Users must avoid contact with eyes and skin, inhalation of vapors and ingestion. Safe handling can be accomplished by working in a well ventilated area and using protective and safety equipment. Disposable suits, gloves and goggles are recommended. All manufacturer's label warnings must be heeded.

2.3 EPOXY ADHESION TO CONCRETE

2.3.1 INTRODUCTION

Epoxy was first used in 1948 as an adhesive to bond together two pieces of hardened concrete (10). The bond proved to be satisfactory and had a tensile strength greater than that of the concrete. The real value of concrete is however in its compressive resistance (about ten times its tensile strength) and achieving an epoxy bond strength greater than the tensile resistance of concrete is not much of a requirement from the adhesive. If new or old concrete is to be effectively bonded to existing concrete with an epoxy resin, the adhesive must be formulated to satisfactorily transfer all the forces that the original and new concrete are expected to carry. The composite cylinder test best known as 'Arizona Slant Shear Test' (24) is an adequate method of studying the epoxy adhesion to concrete in compression.

2.3.2 SHEAR ADHESION

In many epoxy joints such as the plated beams, the mechanical action of the bond is by shearing. Many researchers (25-28) have investigated the shear adhesiveness of epoxy to concrete by tests on composite specimens steel-epoxy-concrete. Of these three materials, concrete has the lowest ultimate shear strength. Failure of the joint should therefore always occur through concrete.

The behaviour of the joint has been simulated with a mathematical model from which the shear distribution in the joint can be predicted up to failure (25). The more highly stressed end fails first and then a progressive failure of the joint follows. The predicted (25) and measured (25-28) results showed that the distribution of the longitudinal forces and shear stresses along the joint in pure shear is exponential. The ultimate shear capacity of the joint could be related to either the ultimate shear strength of concrete (25,28) or its ultimate tensile strength (26,27).

The stress concentration factor (ratio of maximum to mean stress) depends on the geometry of the specimen and elastic moduli of the adherents and adhesive. Mixing glass fibers with epoxy can reduce the stress concentration and thus increase the ultimate load (21).

2.3.3 WATER RESISTANCE

Cusens and Smith (29) reported tests on concrete prisms with 45° scarfed joints to compare the water resistance of four adhesives. In three resins there was a loss of up to 75% in strength after 8 weeks of immersion in water. There was however a slight increase in strength with the fourth resin. These

different performances of different epoxies in damp conditions were also observed by Mays and Vardy (30) whereas Utam (31) reported no loss of strength after 6 weeks of intermittent wetting and drying.

Microscopical and chemical techniques can be used to investigate the corrosion of the steel plates adjacent to the resin in epoxy bonded steel-concrete joints (32,33). After two years of exposure at industrial and marine sites with high rainfall, Lloyd and Calder (33) observed a uniformly distributed corrosion over the steel plate, which implied that corrosion was caused by migration of moisture from concrete and penetrating through the resin. The corrosion led to a reduced strength of the exposed specimens but despite that and the microcracking of the resin (observed in broken samples), the bond strength was still greater than the shear strength of concrete.

Bloxham's results (34) contradict however Lloyd and Calder's findings. He found that various sealing agents could be successfully used for coating the steel plates and joints and thereby stop the progress of moisture (in the mist room) and loss of bond strength (34). These different observations may be due to a shorter period of time (18 months) in Bloxham's case and the use of a more accurate and more sophisticated techniques by the others.

2.3.4 MISCELLANEOUS

Apart from the water resistance there is little information about the durability of steel-epoxy-concrete joints. Utam (31) reported a good fatigue performance, most specimens surviving 1.5 million cycles of loading up to 90% of

the static ultimate strength. Subsequent static tests showed that cyclic loading in fact increased the failure loads. This small increase in strength may have been the result of reduced deformations in the joint following steel hardening during cyclic loading.

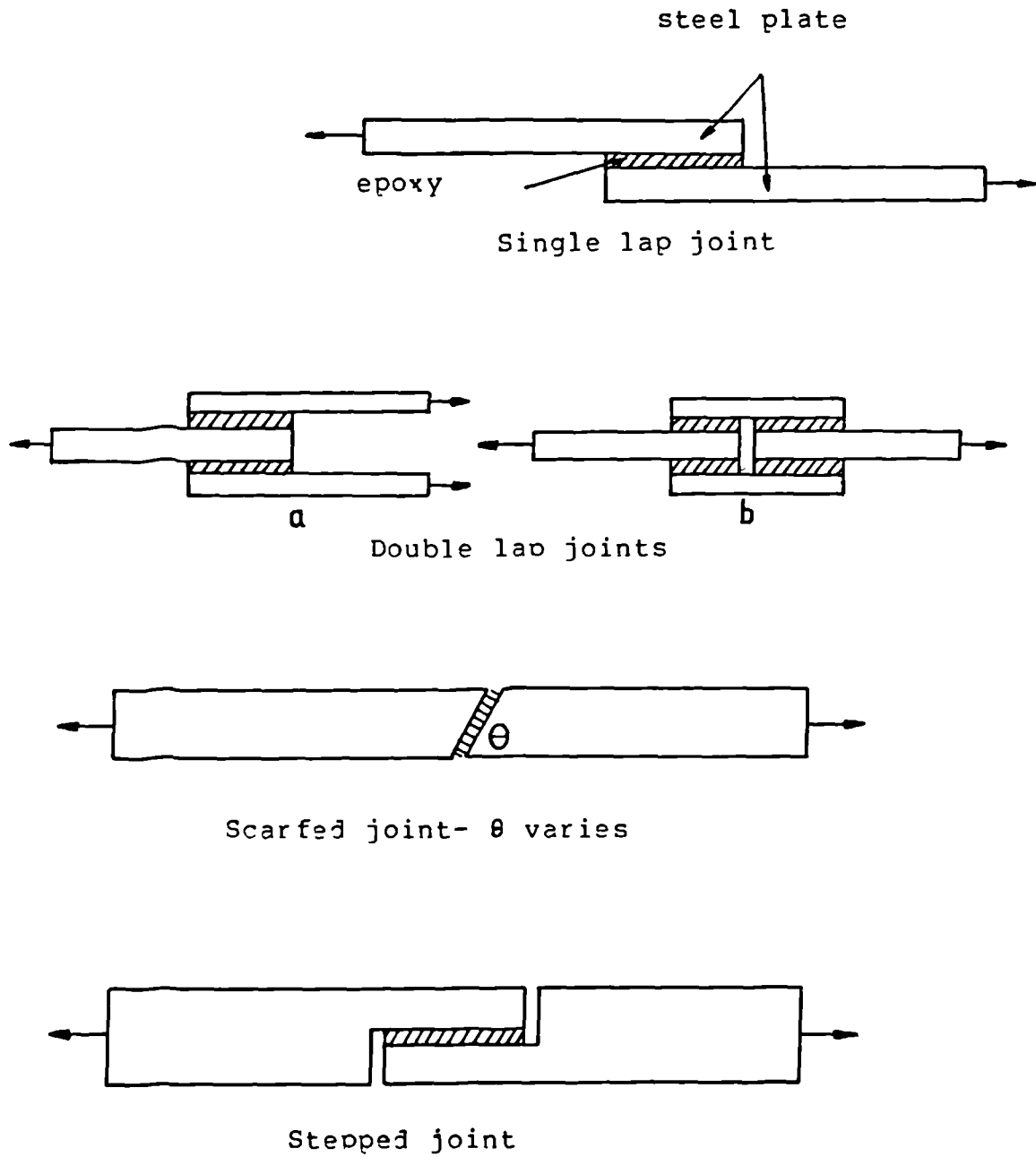
There is also a lack of information about the temperature effects on the joints. Carputi, Noto and Ermolli (21) reported no adverse effect of thermal cycling on the bond strength.

This lack of interest in the durability of the joints can probably be partly explained by the nature of the mode of failure of the joint, which is controlled by the ultimate shear strength of concrete.

2.4 EPOXY ADHESION TO METALS

2.4.1 INTRODUCTION

Testing of steel-epoxy-concrete connections, as seen in section 2.3, only studies the epoxy adhesion to concrete and does not yield sufficient information about its adhesiveness to metals (as failure always occurs through concrete-glass interface). Epoxy adhesion to metals has been investigated by tests on single lap (35-37), double lap (29,31,38-41), scarfed joints (35,37,42) and stepped joints (35-37,42) (Fig.2.1). The peeling forces present in the single lap joint (due to the unsymmetry of the specimen) result in lower average shear stresses than in symmetrical joints (35,36). Theoretical investigations (36,37,42-45) showed that as well as shear stresses, normal stresses are present in fact in all joints and that the two components are maximum at the joint ends. These tensile stresses can result either from the unsymmetry of the



There is no standardized geometry of the joints.
The adhesive and adherents dimensions vary.

Fig.2.1 : Epoxy-metal joints.

joint (35,36), or bending (42,44) or variation of the stress through the adhesive layer (36). The peeling forces may sometimes be critical and control the failure of the joint.

2.4.2 SURFACE STATE

Epoxy adhesion to metals depends on the chemical and micro geometrical properties of the adherent surfaces (31,35,38-41). It is generally agreed that the best results are achieved with a dry, clean and rough surface free of loose particles and chemical contaminants. The most common method of surface preparation used is shotblasting followed by jetting of compressed air.

The bond strength can be considerably reduced by contaminants such as oil (41) and the use of acetone as a degreaser can have an adverse effect and reduce the joint strength by up to 20%. Rust on the other hand may have a positive effect (41) by rendering the surface more rough.

2.4.3 TEMPERATURE EFFECTS

The extent of the temperature effects on epoxy joints depends mainly on the type of adhesive used (31). The performance of the joint is generally improved when the curing temperature is increased as long as it is not higher than the upper limit beyond which the properties of the resin are adversely affected (46).

Temperature cycling from -7 to +35°C can have a favourable effect as compared to a constant curing temperature of 23°C (31). This probably results from the additional curing during the warm part of the cycle.

2.4.4 ADHESIVE THICKNESS

There are some apparent disagreements in the published literature about the effect of the glue line thickness on the joint strength. Hill (35) reported no significant effect when the adhesive thickness was varied from 0.5 to 2.0mm whereas Cusens and Smith (29) found that the ductility of the specimens increased with the adhesive thickness and recommend a value equal or greater than 1.0mm. Gilibert (40) observed a variation of the joint performance with the glue thickness and found an optimum value of 0.5mm beyond which there was a considerable loss of bond strength. This reduced joint resistance with thick adhesive layers may be caused by the contraction of the glue during cure (43).

All the previous studies are based on analyses assuming that the stresses do not vary through the thickness of the adhesive and adherents. A finite element analysis with three elements representing the adhesive layer (36) showed that these assumptions are not justifiable, that the stresses varied through the glue line and that the peeling forces increased with thicker adhesive layers thus resulting in a reduced joint strength. This correlation between loss of bond strength and increase in peel stresses with thick epoxy lines seems more appropriate than explanations based on adhesive shrinkage during setting. The apparent disagreements between the various reports may also be accounted for by the different chemical compositions of the resins used.

2.4.5 ADHERENT THICKNESS

For the same epoxy glue, the ultimate shear stress in a joint is generally about 20 N/mm^2 and does not vary with the thicknesses of the adherents and adhesive. The stress concentration factor (ratio of maximum to mean stress) is however substantially reduced with thicker substrates (adherents), thus resulting in a considerable increase in the ultimate load (36). The reduction in the stress concentration factor can be as high as 16% but becomes less pronounced beyond a certain adherent thickness. This suggests the existence of an optimum value of adherent thickness beyond which the gain in overall strength is not worth the additional amount of metal used.

2.4.6 DURABILITY

The published literature shows that epoxy-metal joints respond favourably to fatigue loading (29,46-48). The loss of strength was observed on a few specimens only and was less than 16% after one million cycles.

The joints can also offer a satisfactory response to impact loading as long as the dynamic blow does not exceed a certain critical value (49).

The available literature shows that epoxy-metal joints behave satisfactorily under dynamic and fatigue loading but the information is very limited and the assessment of the joints durability requires further investigation.

2.5 EXTERNALLY BONDED REINFORCEMENT

2.5.1 INTRODUCTION

The development of synthetic adhesives based on epoxy resins has opened a new era for bonding structural materials. Epoxy adhesives offer a tenacious bond between steel and old or new concrete. Epoxy bonded steel can be used as a strengthening element for existing structures or as a reinforcement when manufacturing new concrete. This new type of concrete reinforced with glued steel sheets is also known as 'Plated Concrete'. No concrete cover is needed and the steel plates may be used as reinforcement as well as formwork. The external steel can be used as longitudinal (compression or tension) or shear reinforcement for beams, slabs or any other concrete member.

For the same amount of steel, the plated beams offer a better stiffness and strength than conventionally reinforced concrete beams because of a greater internal lever arm (50). Steel sheets used as longitudinal reinforcement of concrete members subject to bending are capable of withstanding stresses in any direction of their plane as opposed to round bars which can be utilized only in the direction of their axis. In structures where the stresses are in more than one direction such as shells or slabs the biaxial strength of the plates can be exploited and the amount of reinforcement required in one span can serve as reinforcement for the other span, thus resulting in a saving of up to 50% of metal (51,52).

2.5.2 REINFORCEMENT GEOMETRY

The use of epoxy adhesives for bonding external steel offers another advantage in the choice of the form of the reinforcement. Steel bars, strips, plates or channels can all be successfully bonded. Tests on beams with externally bonded bars or plates showed that the increase of the bond area in relation to the cross sectional area of steel resulted in a more uniform concrete strain distribution and consequently a more uniform cracking (53).

Mac Donald (54) observed that for the same amount of metal, the beam stiffness was slightly reduced with wider and thinner plates. This may have been due to the greater internal lever arm of the beams with narrow and thicker plates.

2.5.3 STIFFNESS AND STRENGTH

All the published research proves that epoxy adhesives achieve a full composite action between the external reinforcement and the existing concrete member. Laboratory (50,55-60) and field (61) tests showed that the external steel resulted in delayed cracking, reduction in deformations and increase in stiffness and strength.

The technique can be used successfully equally for under or over reinforced beams (62). Precracking did not have any adverse effect on the subsequently strengthened beams (34,59,63) and lapping techniques can be achieved satisfactorily (34,63-65).

In general the flexural behaviour of the plated beams is similar to that of conventionally reinforced beams (34,50,62) but most reports only make quantitative comparisons of the plated and unplated beams. There is little information about

the relative performance of external plates as compared with the equivalent of internal reinforcement designed to achieve the same performance.

2.5.4 BOND FAILURES

Flexural failures of under reinforced plated beams generally occur as expected by compressive crushing of concrete after yielding of the steel. There is however a limiting value of plate thickness beyond which a premature bond failure is prone to occur by sudden separation of the plate at its end (34,50,54,56,57,63,64,66). This critical value of plate thickness depends on the beam characteristics and in the published reports generally varied between 4 and 6mm. This premature failure is the result of high bond stresses due to the high transfer of tensile forces from the plate to the internal bars in the region where the plate is stopped. These bond stresses are higher with thicker plates. Jones, Swamy and Ang (66) found that there was a critical shear stress of about 2.15 N/mm^2 beyond which separation of the plate was bound to happen. This value is only a small proportion of the ultimate shear bond stress of 6 to 8 N/mm^2 determined by the pull out tests described in section 2.3. This is probably due to the fact that the value of 2.15 N/mm^2 (66) was computed in a section where the plate was fully active and the bond stress is certainly higher at the plate cutoff point.

The system of bond stresses in the joint and the tensile stresses in the plate is balanced by a normal peeling force at the end of the plate (66). The premature separation of the plate must be a combination of these bond and peeling forces. With the same cross sectional area, the increase of the bond

area with the use of wider plates can reduce the bond and peel stresses and change the concrete failure to a more ductile one (54). The plate width cannot however exceed that of the beam and the problem is bound to rise again beyond a certain plate thickness.

The mechanism of these failures is still not fully understood and the problem remains unsolved at this moment.

2.5.5 NEW CONCRETE WITH EXTERNAL STEEL

The availability of epoxy formulations capable of bonding fresh concrete to steel made it possible to extend the technique of structural repair and open a new technology of manufacturing reinforced concrete (50,56,57,67). The plated concrete is obtained by casting fresh concrete against steel plates or channels already coated with an adhesive layer. The reinforcement can serve as formwork and a sufficient bond with concrete may be achieved by the hardening of concrete in contact with the plates even without the use of epoxy (58).

Unlike the strengthening operation where the plates must be stopped short of the supports, in plated concrete sufficient and adequate anchorage lengths can be provided and the problem of bond failures thus avoided.

2.5.6 SHEAR BEHAVIOUR

The available information about the effect of the external longitudinal reinforcement on the shear capacity of concrete members is inadequate. Bouderbalah (65) reported that steel plates glued on the tensile face of the beams had no effect on their shear capacity but his observations were made on two tests only. Shear failures of sandwich beams (beams with

steel plates on both compressive and tensile faces) are brittle and the ultimate interface shear stress between steel and concrete may be related to the tensile strength of concrete (26,41,68).

The shear capacity of concrete members can however be increased by externally bonded shear reinforcement in the form of steel strips (50,55-57,69). Epoxy bonded strips on the sides of the beam improve its shear resistance showing that the strengthening technique or the manufacturing of new 'Plated Concrete' can be used in shear as well as in flexure.

Apart from the reported increase in strength, there is however a total lack of information about the relative behaviour of the external shear reinforcement as compared with internal steel stirrups. The geometry and spacings of the strips have not been investigated and no design formulae have been proposed.

The shear behaviour of plated beams remains an unexplored area. The possible presence of a dowel action in the longitudinal plates and the optimum geometry and spacings of external shear strips are all worthy of further investigations.

2.5.7 PRACTICAL APPLICATIONS

The strength properties of an existing concrete structure are determined during its construction and any subsequent intervention to strengthen it is generally a complicated operation. To determine the lack in strength or stiffness, it is necessary to make an investigation of the critical areas and carry out a check design using the original calculations. If the latter are not available, a new set of calculations should be established. A combination of the use of

a cover meter and cutting away of concrete cover may be used to find the actual size, position and placing of the reinforcement.

Despite the very limited amount of systematic research carried out, there was enough confidence in the new technique of structural repair to put it into practice. The belief may have been that if the positive effects aimed at were not achieved, there was no apparent risk for an adverse effect and further damage to the structure.

The practical applications reported are mainly concerned with bridges, in France (8,70), England (9,71), Poland (72) and Japan where 240 bridges had been strengthened this way by 1975 (63), and were carried out to solve serviceability problems in the form of excessive deflections (70) or cracking (9,71). The strengthening operations consisted of gluing steel plates on the soffits and decks of the bridges and required minimum traffic disruption. Subsequent measurements showed an increase in the bridge stiffness and a reduction in the deflections and crack openings.

The plate thicknesses used were sometimes greater than 6mm (9,71). Laboratory tests, as described in section 2.5.4, showed that despite their effectiveness at service loads, the thick plates often caused premature bond failures. In addition to the bond provided by the adhesive, the plate ends can be bolted to the concrete to avoid possible bond failures (71). The use of bolts has not however yet been proven by systematic research to be effective against the debonding of the plates and the confident use of thick plates in practical applications seems to be still premature.

2.6 CONCLUSIONS

It is evident from published literature that epoxy resins can be successfully used for bonding structural materials provided the operation is carefully executed. The large variety of epoxy formulations may however be confusing as many dramatically different performances are reported. Properly used, epoxy adhesives can offer excellent mechanical properties and bond strengths with concrete and steel opening new possibilities for structural repair.

Despite the advantages and the future potential of the new strengthening technique, only a limited amount of systematic research has been done. Many of the reports praise the effectiveness of the method by quantitative comparisons of the behaviours of plated and unplated beams. There is an absence of relative and comparative studies by non-dimensional parameters of plated and conventionally reinforced concrete beams (a plated beam may sustain a higher load than an unplated one and yet fail prematurely). There is also a lack of information about many other important parameters:

(a) Creep and other long term properties of epoxies (epoxies are visco elastic materials and creep is a very important factor).

(b) Durability (creep, shrinkage, dynamic and cyclic loading effects, temperature, water and other environmental conditions effects) of the plated beams.

(c) Bond failures: The mechanism of the premature bond failures is still not very clear and remains unsolved.

(d) The shear behaviour of plated beams is unexplored. The possible presence of a dowel action in the external

longitudinal plates and the use of external shear strips are areas worthy of further research.

CHAPTER THREE
MIX DESIGN AND MATERIAL PROPERTIES

3.1 INTRODUCTION

Sound design or analysis of a composite structure depends on reliable information about the properties of the materials to be used. The strength of a reinforced concrete member and its resistance to cracking and prevention of corrosion of reinforcement depend on many parameters, particularly on the strength properties of concrete and steel. The deformations are related to the stiffnesses of the members which in turn depend on the characteristics of their components.

Whilst there are many widely accepted methods of sampling and testing of concrete and steel, no standard method of testing epoxies is available except from those recommended by the Federation of Epoxy Resin Formulators and Applicators Limited -FERFA- (14). The properties of the concrete and steel used were determined by standard tests according to the British Standards Institution (BSI). The properties of the epoxy adhesive used were investigated by various tests and are the subject of chapter four. The design of the different concrete mixes used in the project and the properties of the various materials (except epoxy) used are presented in this chapter.

3.2 MATERIALS

The materials used in this investigation are given below. The same type of materials was used throughout the project but unavoidably they were from different deliveries.

3.2.1 CEMENT

Ordinary portland cement and rapid hardening cement with the trade name Ferrocrete complying with B.S.12 (73) were used. Rapid hardening cement was used in the shrinkage beam which was added to the long term beams designed by Bloxham (34).

3.2.2 FINE AGGREGATES

Washed natural river sand was used. The grading curve shown in Fig.3.1 lies within zone two of the grading limits of B.S.882 (74). Sampling and testing were carried out in accordance with B.S.812 (75). All sand was thoroughly dried in a mechanical dryer before use.

3.2.3 COARSE AGGREGATES

Two types of coarse aggregates were used: 10mm nominal size crushed gravel and 19mm maximum size uncrushed gravel. The grading curves shown in Fig.3.1 lie within the zones defined by B.S.882 (74).

3.2.4 WATER REDUCING AGENT

Febflow was used in the shrinkage beam mix (which was designed by Bloxham (34)) to increase the workability of the concrete. It was added to the water before adding to the dry materials in the mixing pan.

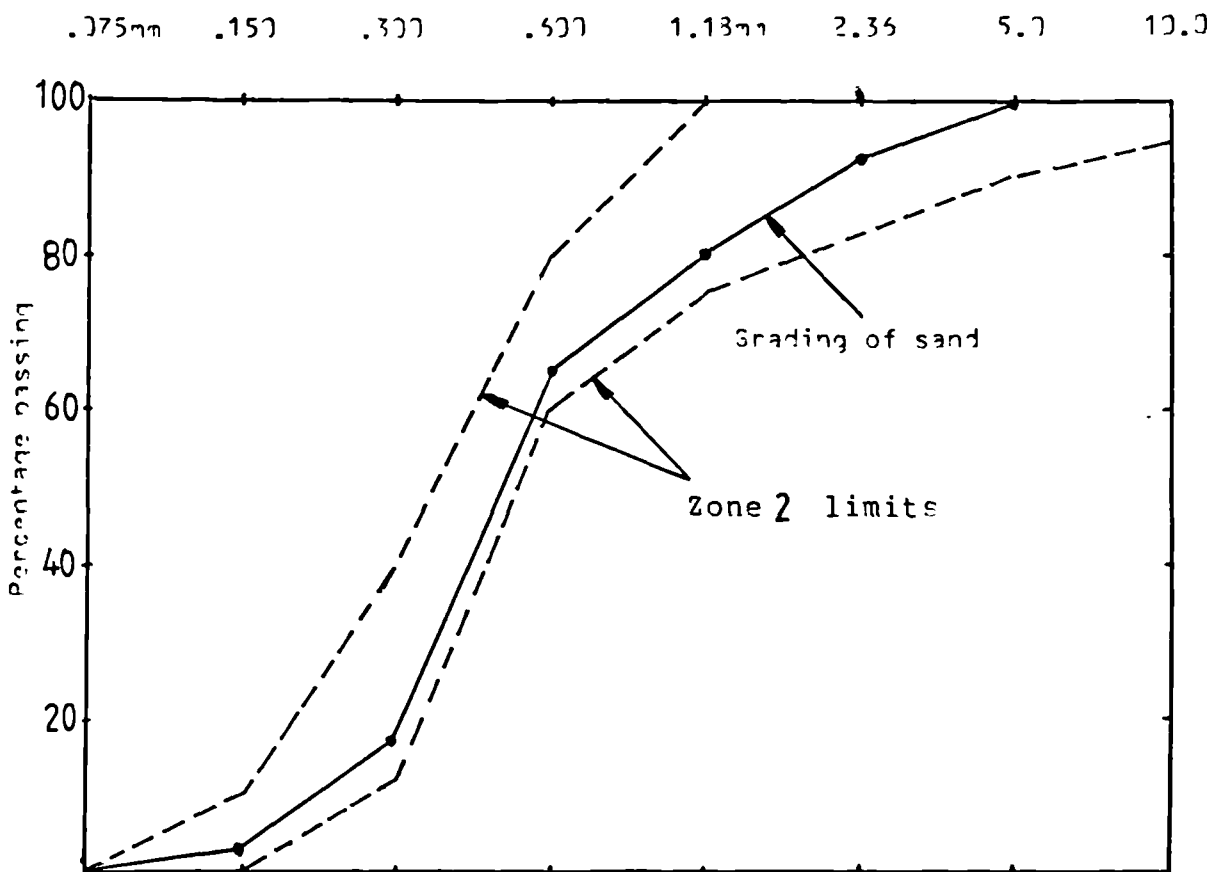
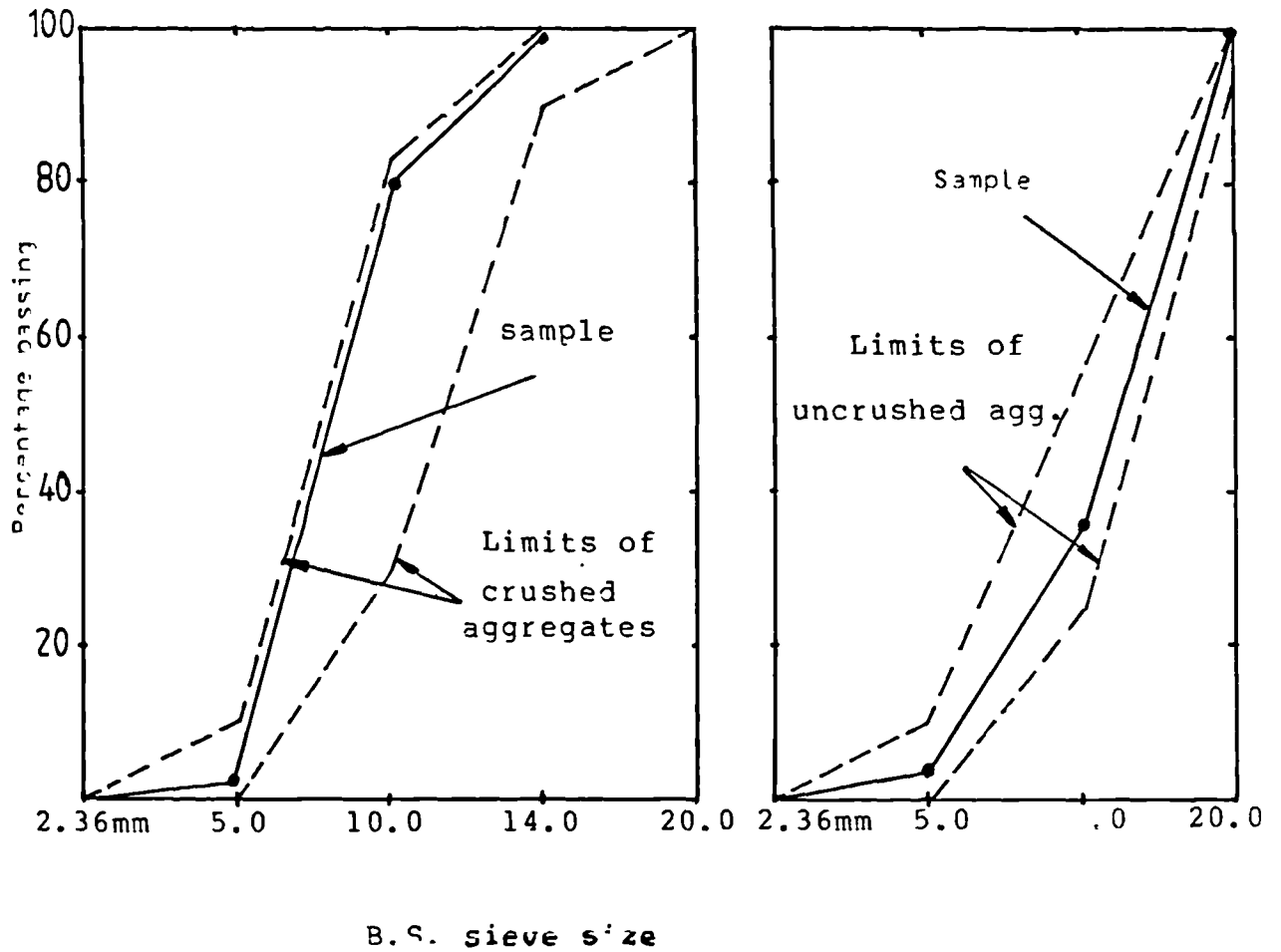


Fig.3.1 : Grading of aggregates.

3.2.5 STEEL BARS

Two types of steel bars were used: cold worked ribbed bars (Tor Bar) of 20mm diameter for longitudinal beam reinforcement and plain mild steel bars of 6mm diameter for shear reinforcement. Three specimens from each bar diameter were tested to determine the stress-strain relationships, Young's modulus, yield, proof and ultimate strength, as recommended in B.S.18: Part 2 (76). The strains were measured using an extensometer of 50mm gauge length and 2mm Kyowa electrical strain gauges. The mechanical and electrical strain measurements were carried out simultaneously in order to determine the calibration factor for future use to convert the voltage outputs (from the strain gauges) to bar strains in the beam tests. The fixing of the strain gauges needed slight grinding of the bar ribs, but the operation did not affect the behaviour as the bars performed like those without strain gauges. The electrical strain measurement is described in Appendix A. The results are shown in Fig.3.2 and Table 3.1.

3.2.6 STEEL PLATES

Mild steel plates of three different thicknesses (1.5, 3.0 and 6.0mm) were used. Three specimens from each thickness of plate were tested as recommended in B.S.18: Part 3 (76), to determine the stress-strain relationships. An extensometer of 50mm gauge length and 2mm Kyowa electrical strain gauges were used to measure the strains. The results are shown in Fig.3.3 and Table 3.2.

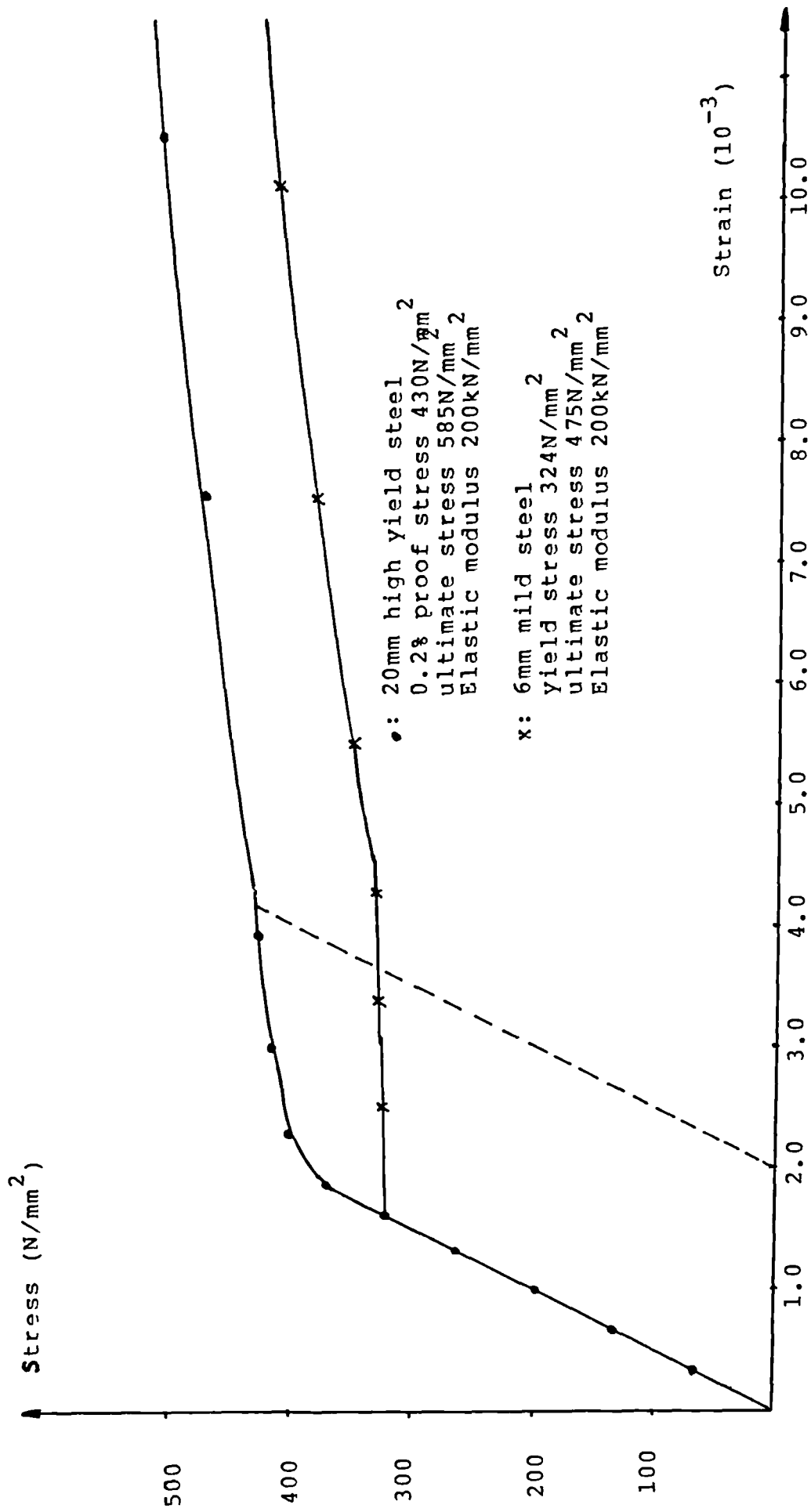


Fig.3.2 : Bar stress-strain curves.

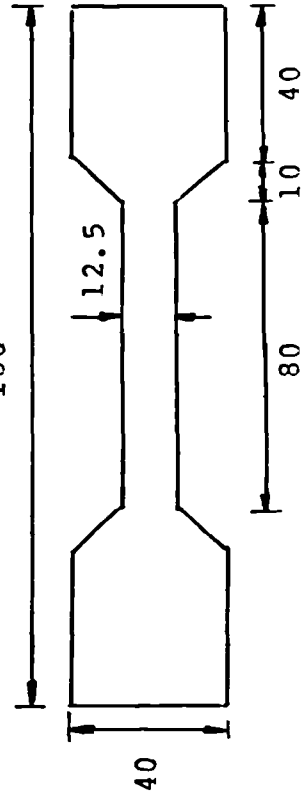
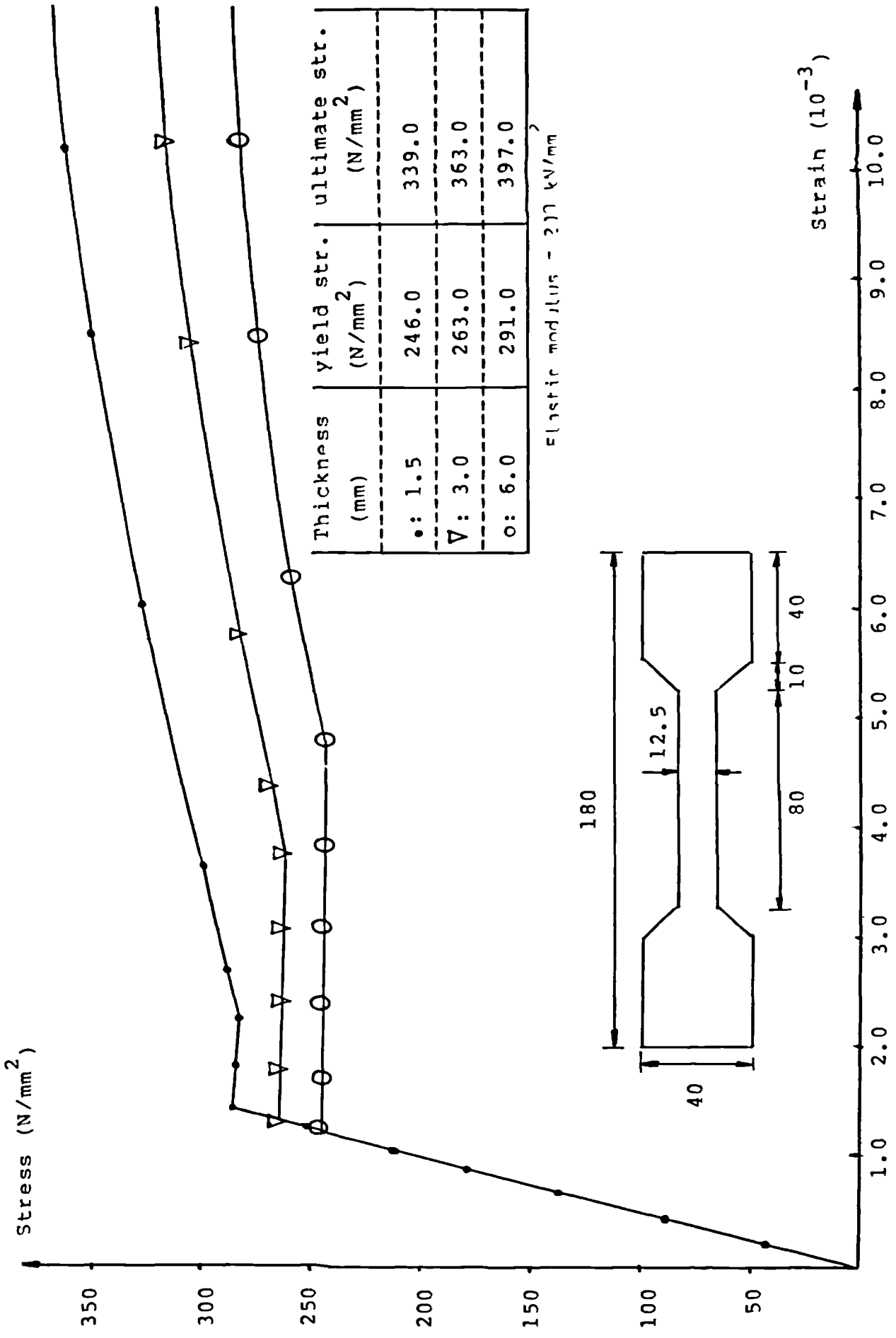


Fig.3.3 · Plate stress-strain curves.

3.2.7 EPOXY RESIN

The epoxy adhesive used in this project was manufactured and supplied by Colebrand under the code name of CXL 194. The mechanical properties of epoxy resins, their adhesion to other materials, their applications in engineering and all their properties relevant to structural repair are reviewed in detail in chapter two. The mechanical and adhesion properties of CXL 194 were studied and are described in chapter four.

3.3 MIX DESIGN

The aim was to design the most economical concrete mix sufficiently workable and attaining a specified strength at a certain age. In all five different concrete grades were used. Mix 5 was used by Bloxham (34) in the long term beams and was therefore used for the shrinkage beam added to them. Mix 4 was used for all the short term beams of the present project. The other mixes were used in the pull out tests carried out to study the effect of the concrete strength on the shear adhesion of epoxy to concrete. Apart from mix 5, the other mixes were originally designed using the method proposed by Teycheneⁿ et al. (77) but it was found that the resulting mixes were oversanded. It was subsequently decided to perform a trial mix for each concrete grade.

The final five mixes are:

Ordinary cement : Sand : Crushed gravel : Water-cement ratio

1- 1 : 2.353 : 5.235 : 0.80 (grade 25)

2- 1 : 2.000 : 2.600 : 0.56 (grade 45)

3- 1 : 1.850 : 2.100 : 0.48 (grade 60)

4- 1 : 1.750 : 2.610 : 0.54 (grade 50)

Table 3.1: Properties of steel bars.

Diam (mm)	Type	El.mod. (kN/mm ²)	0.2% pr.str (N/mm ²)	Yield str (N/mm ²)	Ult.str (N/mm ²)
6	Plain	200.0		324.0	475.0
20	Tor	200.0	430.0		585.0

Table 3.2: Properties of steel plates (mild steel).

Plate thick. (mm)	Elas.mod. (kN/mm ²)	Yield str (N/mm ²)	Ult.ten.str (N/mm ²)
1.5	200.0	246.0	339.0
3.0	200.0	263.0	363.0
6.0	200.0	291.0	397.0

Table 3.3: Properties of fresh concrete.

Mix	Cement	Gravel	Febflow	Slump (mm)	28 day cube str. (N/mm ²)
1	C.P.C	crushed	none	110.0	25.20
2	" "	" "	" "	98.0	44.90
3	" "	" "	" "	92.0	60.50
4	" "	" "	" "	101.0	52.40
5	Ferrocrr	uncrush.	yes	70.0	71.30

Mix 5 was:

5- 1 : 1.04 : 2.44 : 0.39 : 0.28 (grade 70)

Ferrocement:cement:Sand:Uncrushed gravel:Water:Febflow

Mix 5 was designed by Bloxham (34) for the creep beams (described in chapter eight) and was used for the shrinkage beam added to the creep beams to study the long term behaviour of plated beams.

3.3.1 MIXING PROCEDURE

The mixing of concrete was carried out in a non-tilting pan type mixer of 0.127 cubic meter capacity. The materials were dry mixed for two minutes and after the addition of water for a further two minutes. After mixing, concrete was poured into lightly oiled moulds in two layers and well compacted with a 25mm diameter internal poker vibrator. The specimens were then covered with polythene sheets. They were stripped after 24 hours and stored in the laboratory under uncontrolled conditions until required for testing.

With each beam, control specimens were cast as follows:

-Six 100mm cubes for compressive strength.

-Six 100mm diameter and 200mm long cylinders for indirect tensile strength.

-Six 100x100x500mm prisms for flexural strength (modulus of rupture)

3.3.2 PROPERTIES OF FRESH CONCRETE

The workability of the fresh concrete was determined by the standard slump test. The target slump was a value of about 100mm, except for mix 5 which was designed by Bloxham (34). The results are given in Table 3.3.

3.3.3 PROPERTIES OF HARDENED CONCRETE

A series of tests was conducted on 27 cubes, 18 prisms and 18 cylinders to study the compressive strength, modulus of rupture, indirect tensile strength, shrinkage and modulus of elasticity of the main concrete mix (mix 4) over a period of twelve months. Each result is the average of three values.

3.3.3.1 COMPRESSIVE STRENGTH

The compressive strength was determined from tests carried out on 100mm cubes at a stress rate of 15 N/mm^2 per minute complying with B.S.1881: Part 4 (78). The compressive strength development with age is shown in Table 3.4 and Fig.3.4. The percentage increase of the strength over that at 28 days was 6.4% after six months and 8.9% after twelve months.

3.3.3.2 INDIRECT TENSILE STRENGTH

The tensile strength was determined from tests carried out on 100mm diameter and 200mm long cylinders at a stress rate of 1.5 N/mm^2 per minute complying with B.S.1881: Part 4 (78). The results are shown in Table 3.4 and Fig.3.4. The increase of strength over that at 28 days was 7.5% at six months and 9.2% at twelve months.

3.3.3.3 FLEXURAL STRENGTH-MODULUS OF RUPTURE

The modulus of rupture was determined from tests on 100x100x500mm prisms with a loaded span of 400mm under third point loading and at a stress rate of 1.6 N/mm^2 per minute, in compliance with B.S.1881: Part 4 (78). The results, given in Table 3.4 and Fig.3.4, show that the increase of strength over that at 28 days was 8.0% at six months and 8.9% at twelve months.

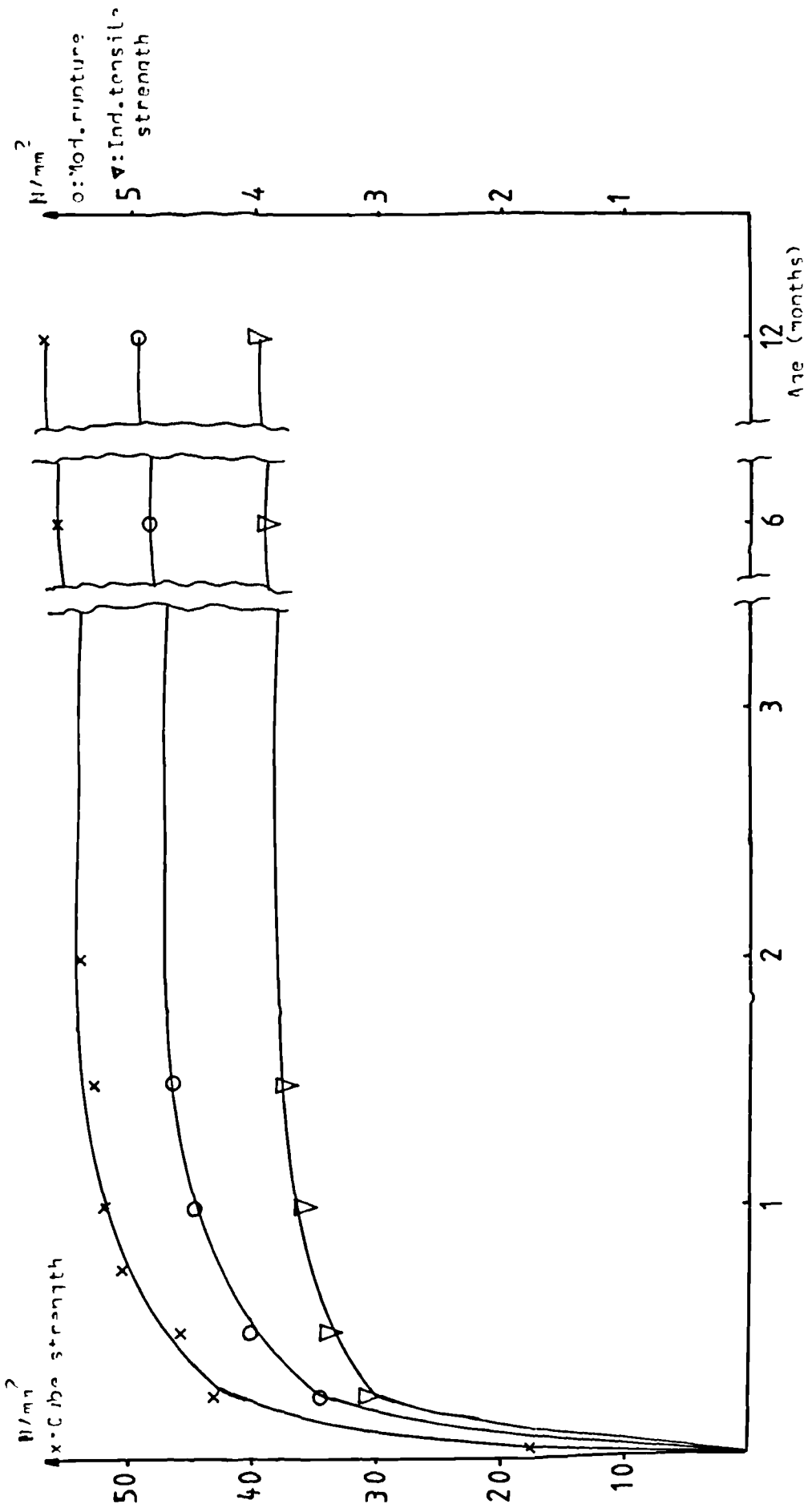


Fig. 3.4: concrete strength development

Table 3.4: Properties of hardened concrete (mix 4).

Age	Cube strength (N/mm^2)	Ind. tensile strength (N/mm^2)	Mod. of rupture (N/mm^2)	Elastic modulus (kN/mm^2)	Poisson's ratio	Shrinkage (10^{-6})
1 day	18.00					165.0
7 days	43.07	3.06	3.48			296.0
14 days	48.00	3.38	4.04			330.0
21 days	51.50					373.0
28 days	52.43	3.60	4.48	30.74	0.16	403.0
42 days	52.90	3.73	4.64	32.05	0.16	449.0
2 months	54.00			32.28	0.16	487.0
6 months	55.80	3.87	4.84			650.0
12 months	57.07	3.93	4.88			705.0

3.3.3.4 ELASTIC MODULUS AND POISSON'S RATIO

The tests were carried out on 100x100x300mm prisms in accordance with the recommendations of B.S.1881: Part 4 (78). The longitudinal strains were measured with a demec gauge over a length of 100mm in the middle third on two opposite sides of each specimen. The transverse strains were measured with a 50mm Demec gauge at the centre on two opposite sides. The results are shown in Table 3.4.

3.3.3.5 SHRINKAGE

The shrinkage of the main concrete mix was determined from longitudinal strains measured on 100x100x500mm prisms stored in the laboratory. The strains were measured with a 300mm Demec gauge on two opposite sides of the specimens. The results are shown in Table 3.4 and Fig.3.5. The increase of shrinkage over that at 28 days was 61.3% at six months and 75.0% after twelve months.

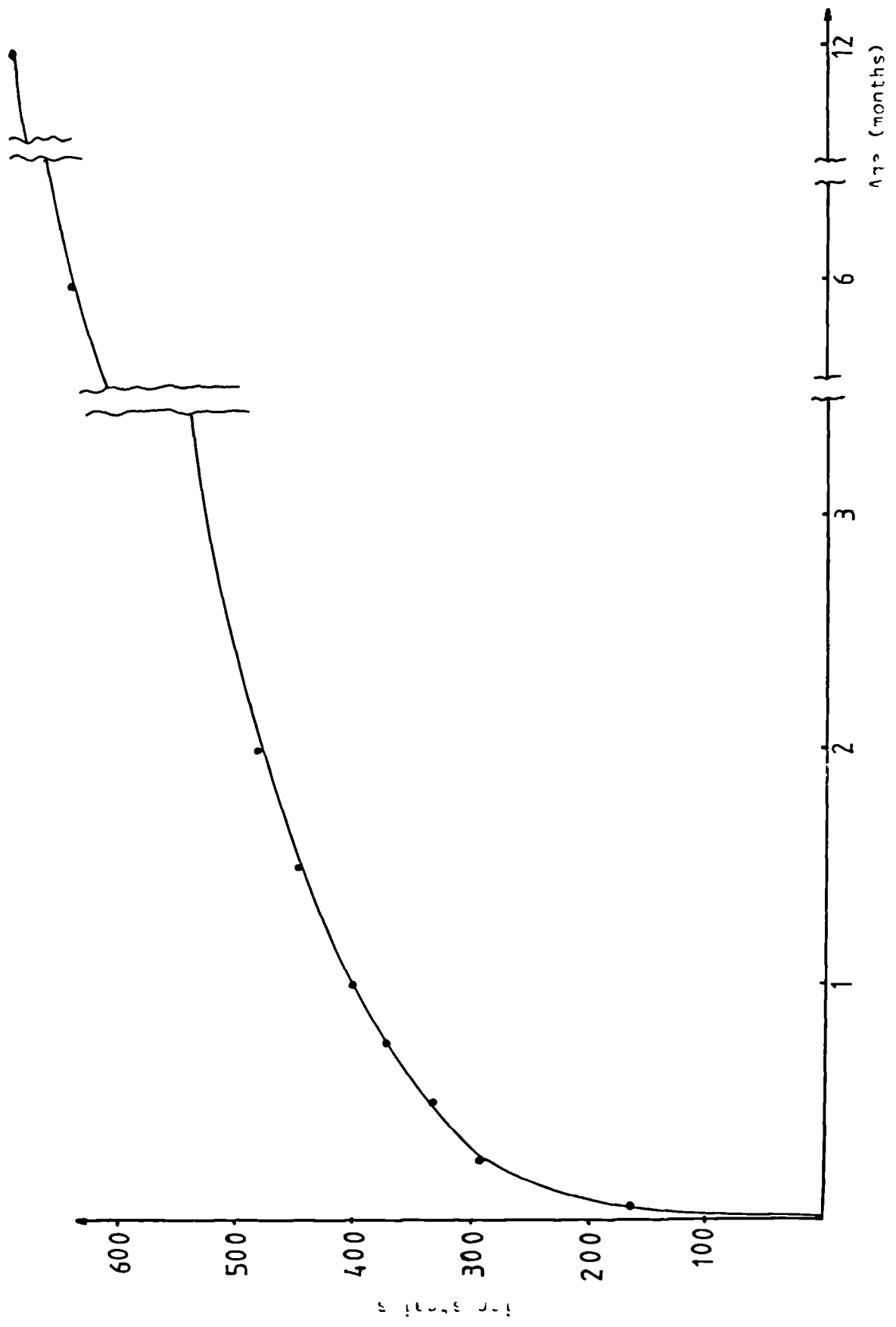


Fig. 3.5.5. Minimum in corner +

CHAPTER FOUR

PROPERTIES OF EPOXY RESIN

4.1 INTRODUCTION

The chemical composition of epoxy resins, their mechanical properties, their adhesion to other materials and all their other properties relevant to structural repair, are reviewed and discussed in detail in chapter two.

This chapter describes the mechanical and adhesion properties of the epoxy adhesive used in this project. The resin used was manufactured and supplied by Colebrand Ltd, under the code name CXL 194. Each pack contained two tins of 500g. each of the base and hardener. The manufacturer also provided instructions for the use of the adhesive and some limited test results on its tensile and shear adhesion strengths (16). The manufacturer's results and information will be referred to in the appropriate sections.

The mechanical action of the steel-glue-concrete connection, in epoxy joints such as plated beams, is mainly by shearing. The bond between the resin and the materials is partly chemical (adhesion) and partly mechanical (friction) and depends therefore on the substrates and their surface preparation. The strength of the joint will always be subject to an upper limit dictated by the lowest ultimate shear strength of the three materials or their ultimate tensile (or compressive) strength.

As well as transferring shear stresses, the epoxy joint must also be able to sustain the deformations. Assessment of the resin stress-strain relationships is therefore of vital importance. The mechanical properties of visco-elastic materials such as epoxy resins depend closely on the loading rate. These materials obey the rheological law:

$$F(d\sigma, d\varepsilon, dt) = 0$$

This means that the stress σ is a function of both the strain ε and the strain rate $\dot{\varepsilon} = d\varepsilon/dt$.

Tensile and compressive tests, on the epoxy resin used in this project, are reported in the first part of this chapter. The variables studied are the age and geometry of the specimen, rate of loading, six month exposure and water immersion.

The second part of the chapter deals with shear adhesiveness tests, with concrete and steel adherents, the main test variables being the concrete compressive strength and the glue line thickness.

4.2 TENSILE TESTS ON EPOXY RESIN

4.2.1 INTRODUCTION

The use of epoxy resins in civil engineering is relatively recent and there is still no accepted standardized test specimen size and testing procedure available. The tensile stress-strain relationship of the adhesive was studied by tests on specimens of different shapes and under different testing conditions. Mixing of the resin base and hardener was carried out according to the manufacturer's instructions (16) using a low speed drill, at 280 revolutions per minute, fitted with a paddle. The adhesive was then poured into lightly oiled moulds

in three layers. The specimens were then covered with polythene sheets for 24 hours before being stripped. They were subsequently cured in uncontrolled laboratory conditions until required for testing.

Two series of tests were carried out:

In the first, 38 specimens of four different shapes A, B, C, or D were tested (Fig.4.1). Apart from the specimens of type A, all the other specimens were cut from 50x50x150mm prisms. The specimens were cut to the required width and thickness using an electrical Bandsaw machine. The actual dimensions of each specimen were measured on many locations by a micrometer of 0.002 mm sensitivity and corrected when necessary.

In the second series, 70 specimens of the shape shown in Fig.4.2 were tested.

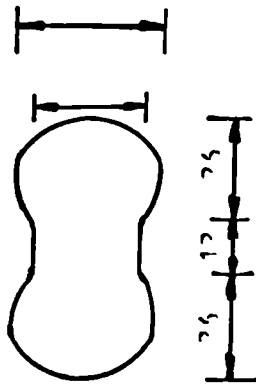
4.2.2 SERIES 1

The 38 specimens, of the shapes shown in Fig.4.1, (6 of shape A, 11 of shape B, 9 of shape C and 12 of shape D), constituting this preliminary series were tested in an Amsler machine or an Instron machine (Table 4.1).

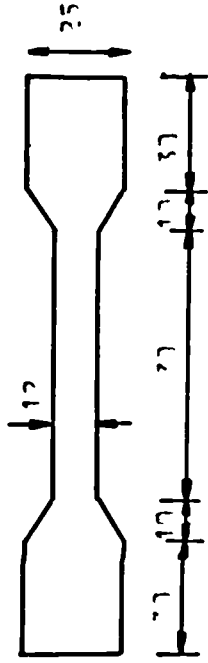
4.2.2.1 AMSLER TESTS

No accurate stress or strain rate control was possible on the Amsler machine but the tests were carried out at an approximate stress rate of 15N/mm^2 per minute. The strains were recorded by means of extensometers or demec gauges and it was found that it was practically impossible to take accurate strain measurements as the strain continued to increase when the load was kept constant. This strain variation (creep) occurred at all load levels and was probably the result of the

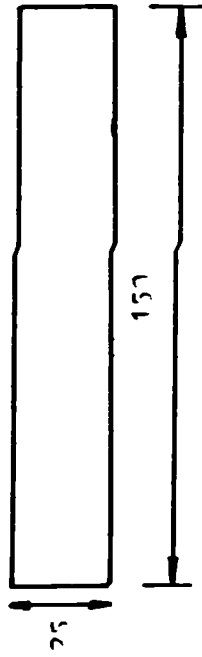
Type A, thickness: 2.5mm



Type B, thickness: 3.5mm



Type C, thickness: 3mm



Type D, thickness: 1.5mm

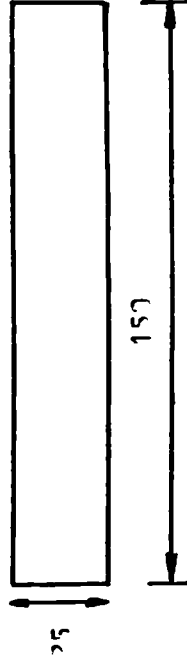


Fig. 4.1: Specimen shapes used in Series I of epoxy tensile tests

viscous properties of the epoxy resin.

4.2.2.2 INSTRON TESTS

The remaining specimens of the first series were tested in an Instron machine which provides a strain rate control over a wide range. No strains were measured (the ordered strain gauges had not arrived) but the stress-elongation curve was provided by the machine. The loading rate was equivalent to a cross-head speed of 12.7mm (0.5 inch) per minute.

4.2.2.3 RESULTS OF SERIES 1

The detailed results of the preliminary series are shown in Table 4.1. The ultimate tensile strength was deduced from the measured loads without allowing for the few air bubbles contained in the sections through which the specimens broke. The maximum elongation was deduced from the elongation curves provided by the machines. The mechanical strain measurement permitted the calculation of the elastic modulus E_g (average value of the measured slopes at different load levels) for five specimens only and, for the reasons mentioned earlier (viscous creep), the values are not very reliable.

The first major observation is that the ultimate tensile strength, the elastic modulus and the ultimate elongation varied considerably with the geometry of the specimen and the rate of loading. The strength varied from 5.13 N/mm^2 (specimen B9) to 18.54 N/mm^2 (specimen A4) and the maximum elongation from 3.21% (specimen C8) to 13.20% (specimen B10) The results also showed that full cure of the specimens was achieved after 21 days and not 7 days as specified by the manufacturer (16).

Table 4.1: Results of series 1 (epoxy tensile tests).

AMSLER TESTS										INSTRON TESTS				
Spec.	Age (days)	Ult.strength (N/mm ²)	Max. el (%)	E _g (N/mm ²)	Spec.	Age (days)	Ult.strength (N/mm ²)	Max. el (%)	Spec.	Age (days)	Ult.strength (N/mm ²)	Max. el (%)		
A1	13	13.04			D1	22	15.14	6.70	B9	32	5.13	11.30		
A2	13	15.23			D2	22	14.23	5.47	B10	32	6.08	13.20		
A3	20	15.26			D3	22	13.84	6.01	B11	32	5.52	slip		
A4	20	18.54			D4	22	14.96	6.40	C1	7	12.63	slip		
A5	20	16.14			D5	22	16.22	7.30	C2	7	11.31	4.45		
A6	20	15.72			D6	22	15.60	slip	C3	7	9.75	4.28		
B1	7	6.70	7.7	154.0	D7	30	14.09	6.95	C4	14	15.27	3.45		
B2	7	6.65	8.0	134.8	D8	30	16.40	7.60	C5	14	16.45	3.27		
B3	7	7.45	8.5	177.8	D9	30	13.96	6.77	C6	21	16.23	3.38		
B4	14	8.11	5.0		D10	30	14.65	slip	C7	21	18.18	3.50		
B5	14	7.89	4.5		D11	30	18.22	6.51	C8	28	16.59	3.21		
B6	14	8.13	4.8		D12	30	15.10	5.85	C9	28	17.08	3.61		
B7	25	8.58	3.9	280.2										
B8	25	8.95	5.3	221.0										

Some specimens of the first series were table vibrated in order to reduce the amount of air entrained but it was found that vibration did not have any effect on the properties of the adhesive.

4.2.3 SERIES 2

It was evident that the first series of tests were not conclusive enough and that a better controlled test series was needed in order to assess the influence of the different parameters. It was decided to test specimens of the shape shown in Fig.4.2 in the Instron machine using sophisticated instrumentation to record the stress-strain relationships.

4.2.3.1 VARIABLES

The test variables were the thickness of the specimen and the rate of loading.

For a specimen thickness of 1.5mm, the rate of loading was varied six times: 0.254, 1.27, 2.54, 5.08, 12.7 and 25.4mm per minute.

For a loading rate of 2.54mm (0.1 inch) per minute, the specimen thickness was varied three times: 1.5, 3.5 and 5.5mm. There were in all eight different sub-series of tests and, in each of them, a minimum of eight specimens were tested. A total of 70 specimens were tested in this series at an age of 28 days (Table 4.2).

4.2.3.2 INSTRUMENTATION AND TESTING PROCEDURE

Four 2mm Kyowa electrical strain gauges, designed for plastic materials, were fixed on two specimens of each of six sub-series, in order to record the longitudinal and transverse strains. The strain gauges were fixed on the centre sections

and on opposite faces of the specimen. To avoid the problem of strain variation during the mechanical (extensometer or demec gauge) strain measurement encountered in the preliminary series, two X-Y plotters were used to record automatically (without stopping the test) the longitudinal strain versus load and transverse strain versus load curves. For each curve, the instrumentation was as follows: The variable X of the plotter was connected to the electrical output from the load cell of the Instron machine. The variable Y was connected to the electrical output from the Wheatstone bridge of four strain gauges formed by the two active strain gauges on the test specimen and two similar 'dummy' strain gauges on a similar specimen at rest (Appendix A).

The stress-strain curves are derived from those recorded by the X-Y plotters. In addition, the elongation-load curve was provided by the machine. The elongation was measured between the grips of the machine and was converted to percentage values by dividing by the free gauge length of the specimen (90 mm, which was the initial distance between the grips of the machine).

The testing apparatus and the electrical instrumentation are shown in Fig.4.3.

4.2.3.3 TEST MEASUREMENTS

From the stress-strain (longitudinal and transverse) curves up to failure, the ultimate tensile strength, the maximum longitudinal and transverse strains, the elastic modulus and Poisson's ratio were all determined and the average results are given in Table 4.2. The stress-strain relationship is not perfectly elastic. The modulus of 'elasticity' and

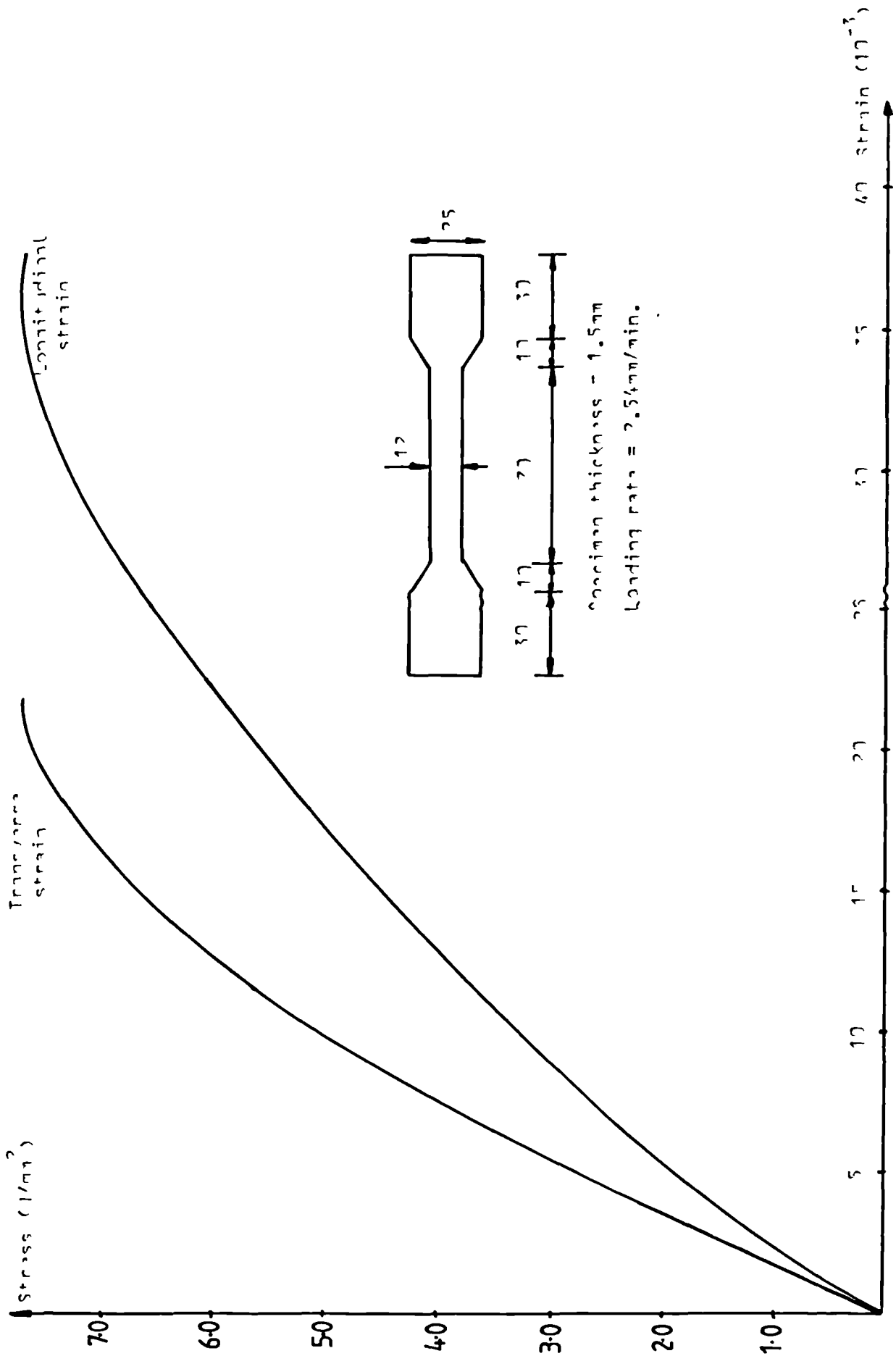
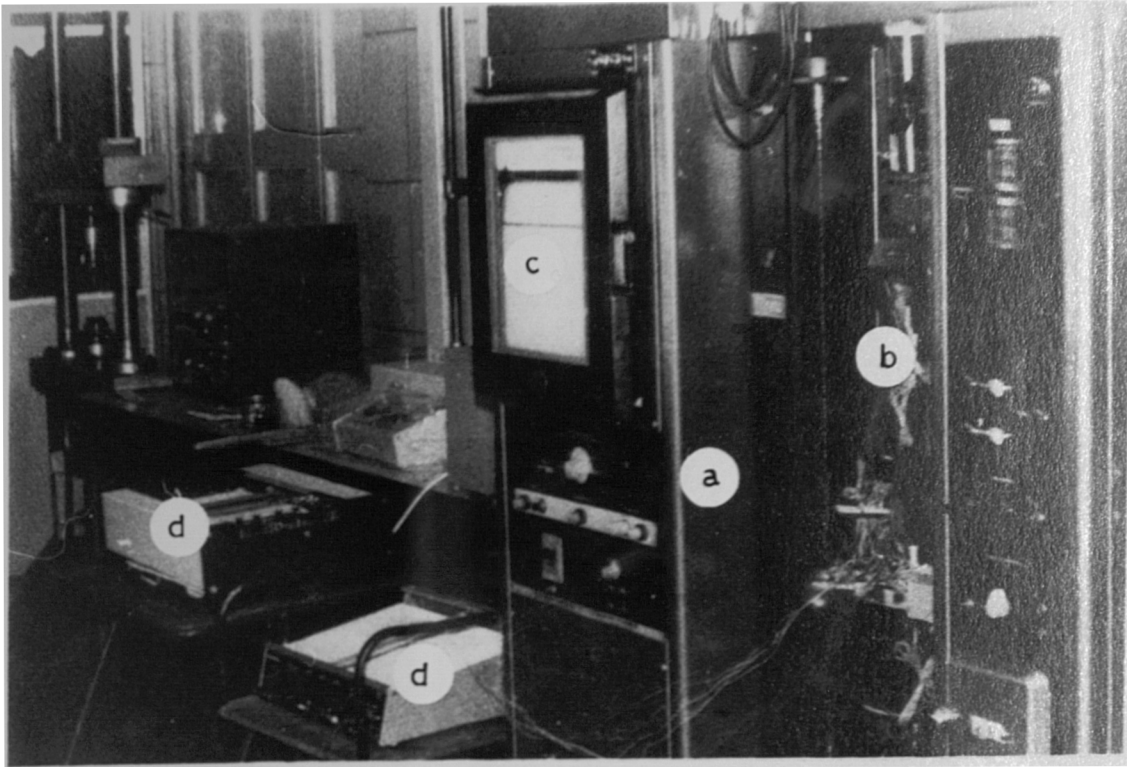


Fig. 6.2. Typical stress-strain curves for a specimen in tension.



- (a): Instron testing machine
- (b): Test specimen
- (c): Elongation curve
- (d): X-Y plotters

**Fig.4.3: Testing apparatus and instrumentation
(Series II of epoxy tensile tests)**

Table 4.2: Results of series 2 (epoxy tensile tests).
(average values)

Loading rate (mm/min)	Spec. thick (mm)	No. of spec.	Ult. strength (N/mm ²)	Max. elong. (%)	Ult. long. strain (10 ⁻³)	Ult. transv. strain (10 ⁻³)	E ₁ (N/mm ²)	E ₂ (N/mm ²)	ν_1	ν_2
0.254	1.5	8	6.39	3.76	43.34		435.3	221.7		
1.27	1.5	8	6.90	2.62						
2.54	1.5	10	7.82	2.41	37.76	21.07	801.0	278.9	.70	.58
5.08	1.5	8	9.79	1.83						
12.7	1.5	8	9.90	1.50	26.51		2030.7	468.3		
25.4	1.5	8	9.98	1.15	19.52		1140.1	510.0		
2.54	3.5	10	9.45	1.97	29.81	17.19	881.0	394.6	.70	.63
2.54	5.5	10	13.32	1.70	25.04	12.31	1322.4	641.0	.58	.51

Poisson's ratio were computed twice: E_1 is the initial modulus of elasticity determined by the tangent at the origin of the stress-strain curve. E_2 is the secant modulus determined as an average value over a longitudinal strain of 0.02.

ν_1 and ν_2 are the corresponding values of Poisson's ratio. E_1 and ν_1 are determined visually by the initial tangents to the curves and are not therefore very accurate. This particular value of 0.02 strain was chosen to compare the results to those of the manufacturer (16) determined at the same strain. E_1 and E_2 are both different from the modulus E_g determined in Series 1 as an average value over the recorded strains. The ultimate elongation was determined from the curve provided by the testing machine.

4.2.3.4 DISCUSSION OF RESULTS

It was observed that failure of the specimens always occurred through sections containing some air bubbles. The subtraction of the cross-sectional area of the bubbles, which was estimated by means of a microscope, resulted in more consistent values of stresses falling within a variation of 5.7%. The average results of the eight sub-series of series 2 are given in Table 4.2.

Tables 4.3, 4.4 and 4.5 show the individual results for each specimen of series 2 of ultimate tensile strengths, ultimate elongations, and ultimate strains and elastic moduli respectively. The coefficient of variation for the strength and elongation results for the eight sub-series is equal to or less than 6% and 10% respectively. The results shown in Table 4.5 are those of the specimens where strain gauges were fixed.

The stress-strain curves and stress-elongation curves were different but had similar shapes. They both varied considerably with the rate of loading and thickness of the specimen. Typical curves are shown in Figs.4.2, 4.4 and 4.5. This makes the comparison of these results with those of the manufacturer (16) rather difficult as their test specimen and loading rate were different and their elastic moduli were determined from the stress-elongation curves. The manufacturer's ultimate tensile strength, maximum elongation and 2% secant modulus results varied between 5.15 and 11.50 N/mm², 1.1% and 4.5%, and 284.2 and 460.6 N/mm² respectively. Their test specimen had a gauge length of 70mm, a width of 12.5mm and was 1.0 mm thick. The loading rate used was 1.27mm per minute. Their elastic modulus results are of little significance as the present tests showed that the stress-strain and stress-elongation curves were different. The present test ultimate strength results, for specimens of 1.5mm thickness and a loading rate of 1.27mm per minute, varied from 6.49 to 7.50 N/mm² (Table 4.3) and the maximum elongation results from 2.62% to 2.83% (Table 4.4). The high variation in the manufacturer's results may be due to the non-allowance for the air contained in the cured specimens.

The variation of the ultimate tensile strength, elastic moduli, maximum strains and elongations, and Poisson's ratios with the rate of loading and specimen thickness are shown in Figs.4.6 and 4.7.

For specimens of 1.5mm thickness, the average ultimate strength varied from 6.4 to 10.0 N/mm², the average maximum elongation from 3.8 to 1.2% and the average secant modulus at 2% strain

Table 4.3: Ultimate tensile strength results of series 2 (N/mm²)

Specimen	SPECIMEN THICKNESS = 1.5MM					LOADING RATE = 2.54MM/MIN				
	Loading rate (mm/min)					Specimen thickness (mm)				
	0.254	1.27	5.04	12.7	25.4	1.5	3.5	5.5		
1	6.30	7.08	9.90	9.83	9.59	7.65	9.33	12.95		
2	6.26	7.50	9.67	10.31	10.01	7.54	9.44	13.67		
3	6.87	6.79	10.13	10.47	10.33	7.56	9.83	14.10		
4	6.37	6.57	9.70	9.97	10.11	8.31	10.30	13.16		
5	5.98	7.17	9.82	9.55	10.18	7.85	9.57	13.71		
6	6.37	6.49	9.60	9.80	10.14	8.53	8.96	12.75		
7	6.67	6.70	9.77	9.72	9.54	7.87	9.45	14.38		
8	6.33	6.90	9.75	9.53	9.95	7.63	9.68	13.91		
9						7.50	9.12	11.98		
10						7.80	8.84	12.61		
Average	6.39	6.90	9.79	9.90	9.98	7.82	9.45	13.32		
Stand. dev. (N/mm ²)	0.269	0.337	0.164	0.339	0.281	0.343	0.430	0.756		
Coef. of var. (%)	4.21	4.88	1.68	3.42	2.82	4.39	4.55	5.68		

Each line gives different test results and each column gives the ultimate strength results of one sub-series in N/mm².

Table 4.4: Ultimate elongation results of series 2 (%).

Specimen	SPECIMEN THICKNESS = 1.5MM					LOADING RATE = 2.54MM/MIN				
	Loading rate(mm/min)									
	0.254	1.27	5.04	12.7	25.4	1.5	3.5	5.5		
1	3.69	2.58	1.73	1.52	Slip	2.61	2.04	Slip		
2	3.83	2.62	1.85	1.62	1.07	2.29	2.00	1.78		
3	4.31	2.49	1.94	1.71	1.10	2.33	1.78	1.82		
4	3.71	2.83	1.80	1.43	1.05	2.35	1.86	1.88		
5	3.55	2.70	2.01	1.34	1.12	2.41	1.90	1.59		
6	3.70	2.49	1.78	1.41	1.21	Slip	1.98	1.66		
7	3.76	2.58	1.79	1.57	1.11	2.43	2.21	1.65		
8	3.52	2.64	1.76	1.41	1.38	2.54	1.95	1.72		
9						2.37	1.92	1.61		
10						2.38	2.03	1.60		
Average	3.76	2.62	1.83	1.50	1.15	2.41	1.97	1.70		
Standard deviation	0.245 %	0.112 %	0.096 %	0.126 %	0.114 %	0.103 %	0.117 %	0.105 %		
Coef.of variation	6.52 %	4.27 %	5.25 %	8.37 %	9.91 %	4.26 %	5.93 %	6.16 %		

Each column gives the ultimate elongation results in % for one sub-series.

Table 4.5: Strains and elastic modulus results of series 2
(specimens with strain gauges).

	SPECIMEN THICKNESS = 1.5mm				LOADING RATE = 2.54mm/MIN.									
	Loading rate(mm/min)								Specimen thickness(mm)					
	0.254mm/min	12.7mm/min	25.4mm/min	25.4mm/min	1.5mm	3.5mm	5.5mm							
Max. long. Strain	44.17	42.50	27.33	25.68	18.87	20.16	37.91	36.67	38.70	28.79	30.82	24.33	26.52	24.27
(10 ⁻³)														
Max. transv. Strain							21.12	19.44	22.64	16.21	18.17	12.34	13.44	11.16
(10 ⁻³)														
E ₁ ² (N/mm ²)	442.5	428.1	1979.7	2081.7	1124.0	1156.2	798.2	790.7	814.1	860.2	901.7	1400.0	1281.1	1286.1
E ₂ ² (N/mm ²)	230.4	212.9	481.2	455.3	517.5	502.4	271.3	266.7	298.8	399.3	389.9	648.7	611.3	663.0
v ₁							0.69	0.68	0.72	0.68	0.72	0.61	0.57	0.55
v ₂							0.58	0.55	0.61	0.61	0.64	0.53	0.51	0.48

Each column gives the results of one individual test.

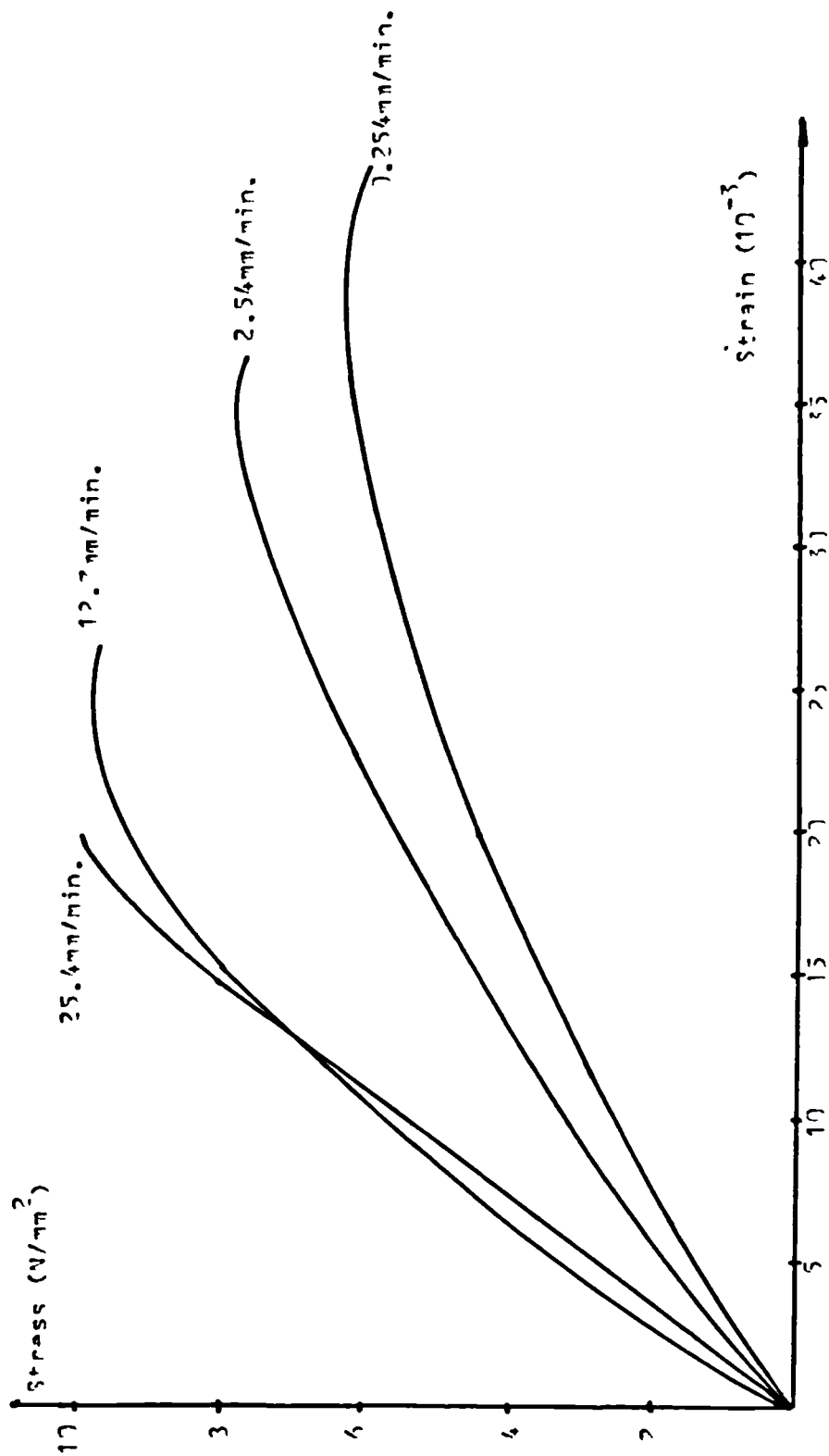


Fig.4.4: Epoxy stress-strain curves in tension
Effect of loading rate
(specimen thickness = 1.5mm)

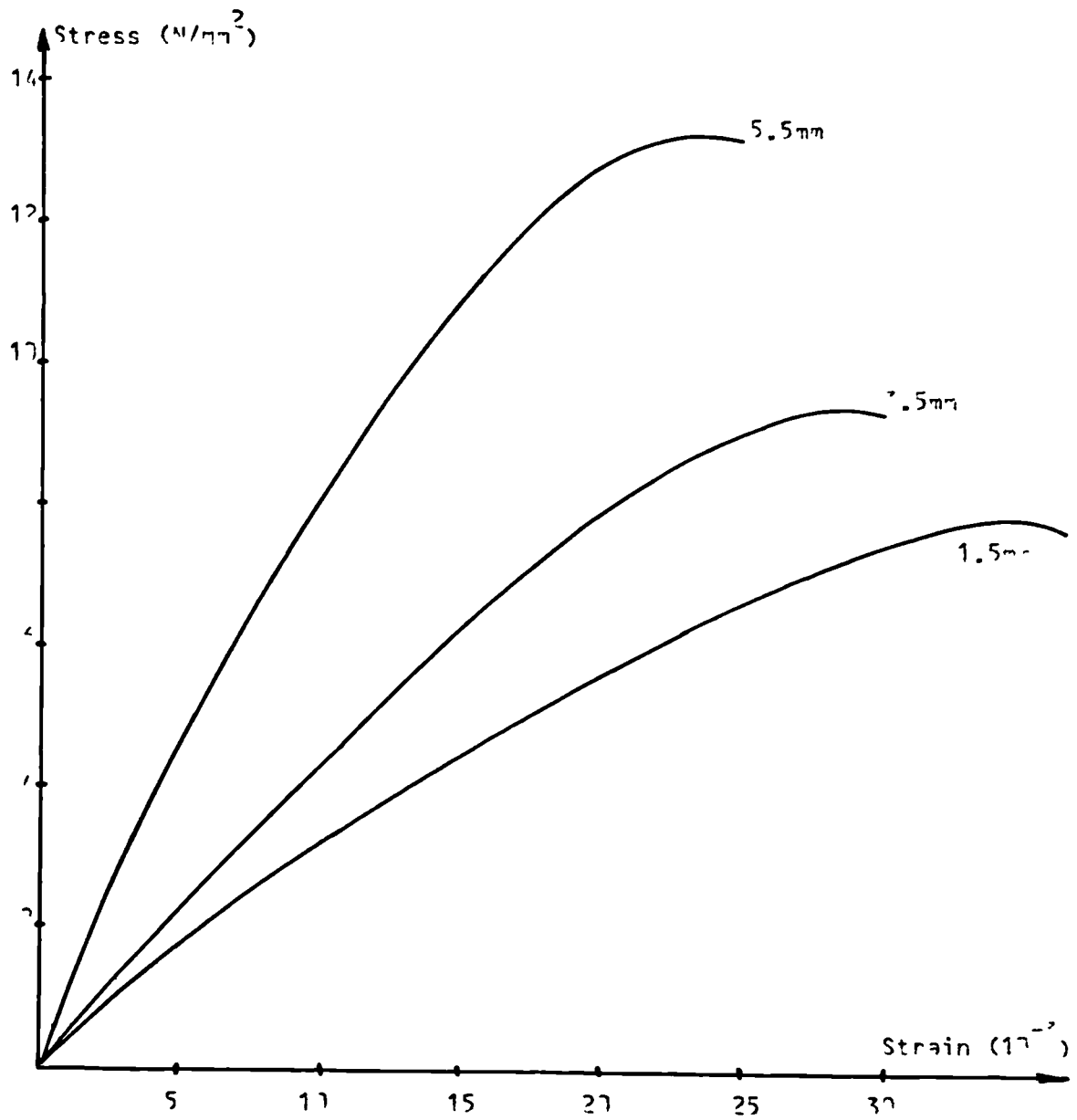


Fig.4.7: Epoxy stress-strain curves in tension
 Effect of specimen thickness
 (loading rate = 2.54mm/min.)

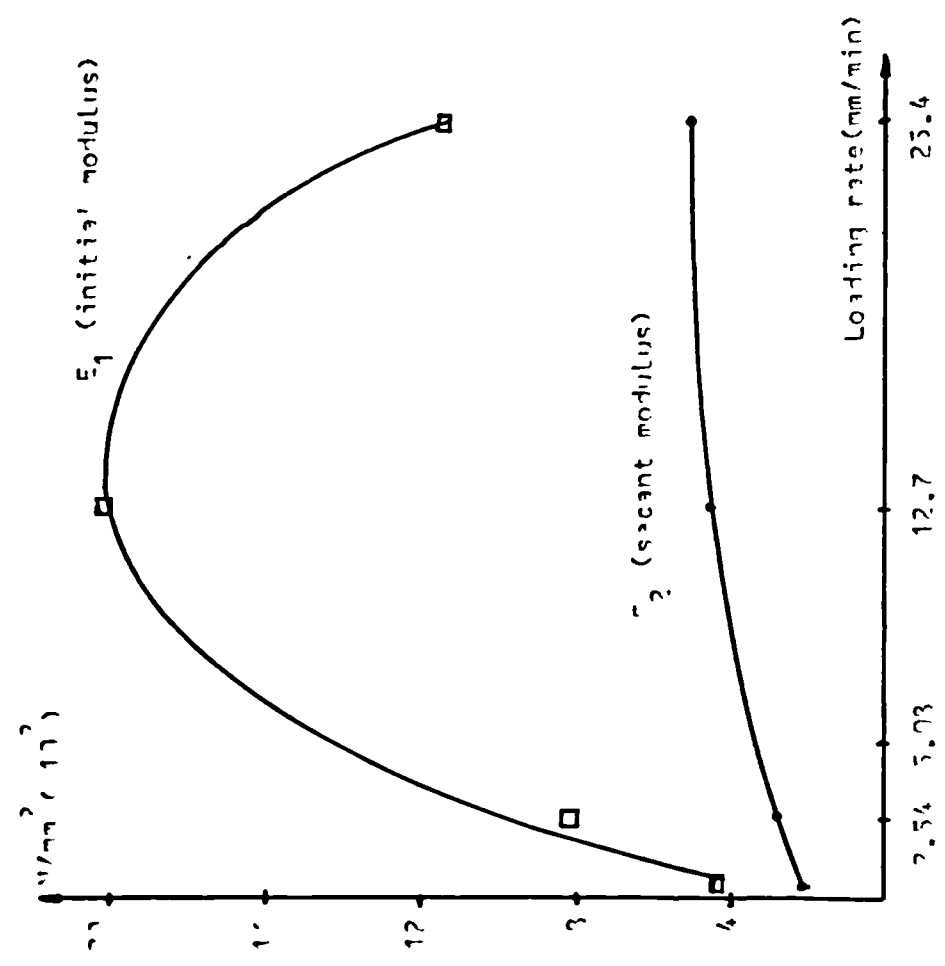
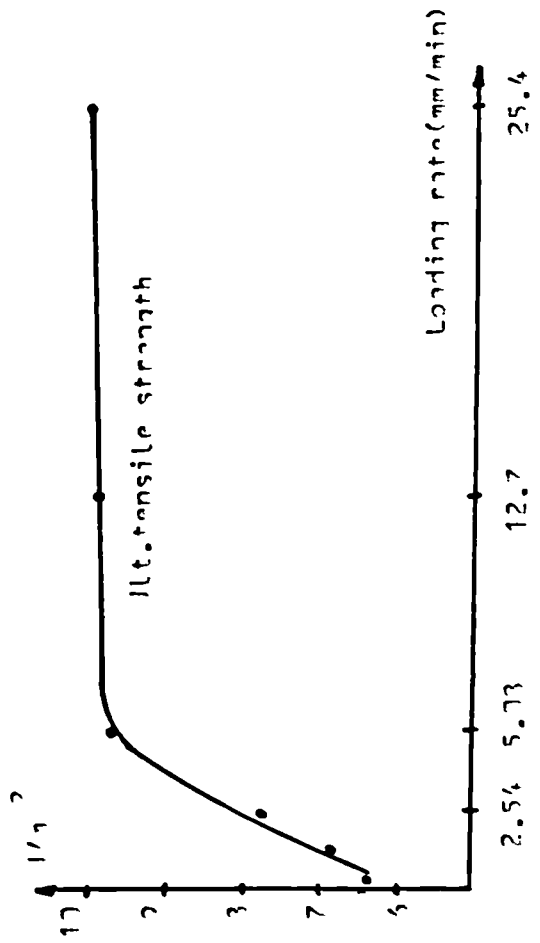
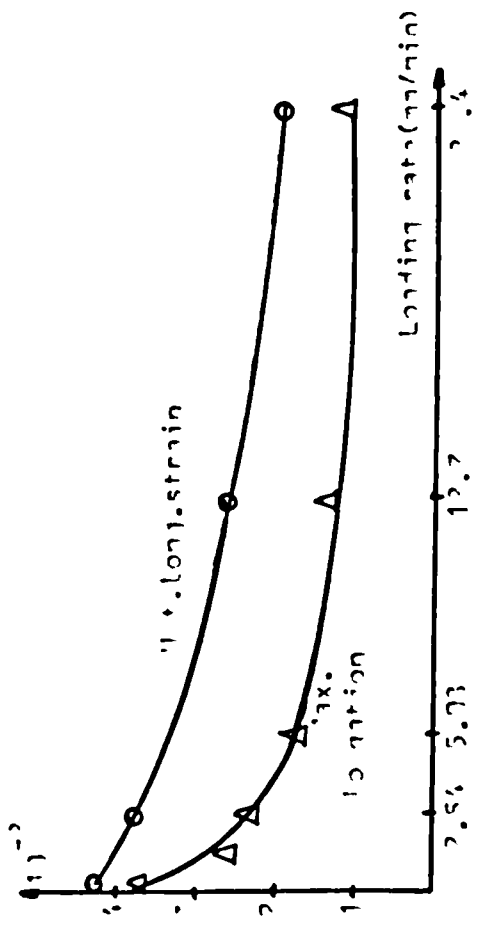
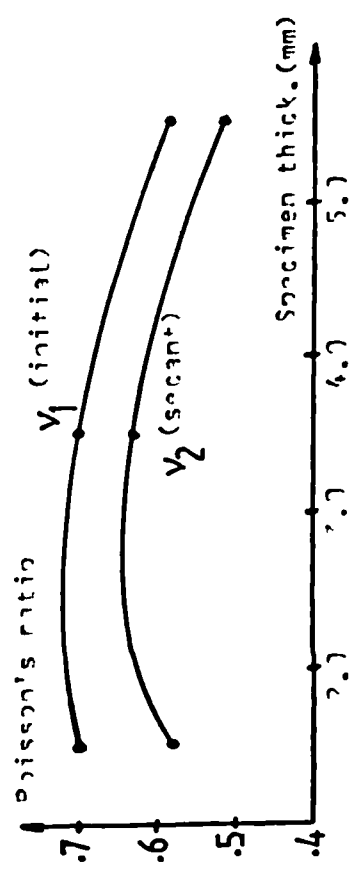
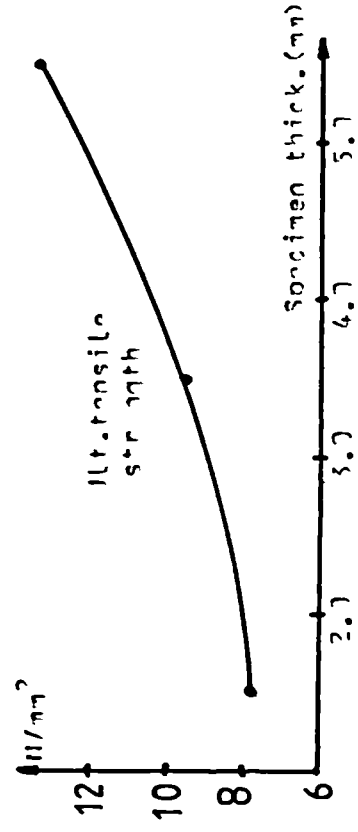
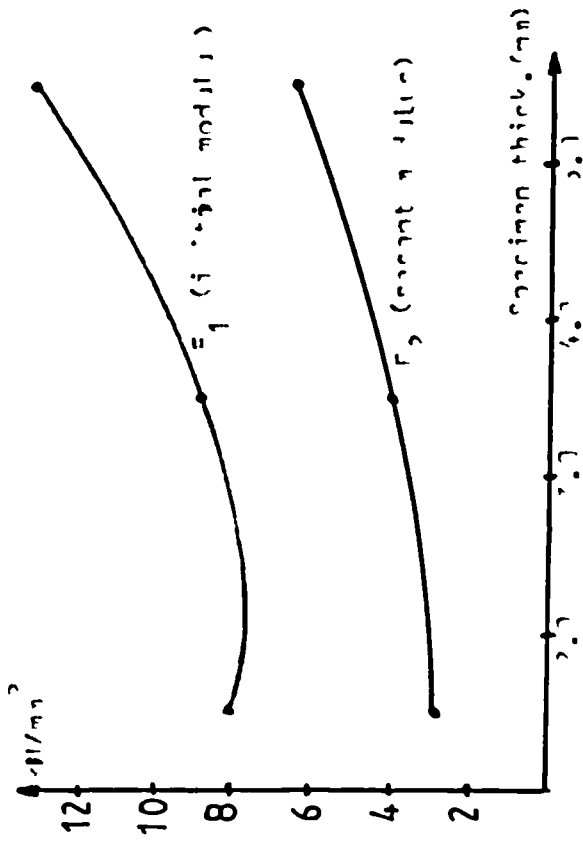


Fig. 4.6: Effect of loading rate on epoxy properties (plate thickness = 1.5mm)



ν

Fig. 4.7: Effect of specimen thickness on alloy properties (loading rate = 2.54mm/min.)

from 222.0 to 510.0 N/mm², when the loading rate was varied from 0.254 to 25.4 mm/min. (Fig.4.6).

For a loading rate of 2.54 mm/min, the average ultimate strength varied from 7.8 to 13.3 N/mm², the average maximum elongation from 2.4 to 1.7% and the average secant modulus from 279.0 to 641.0 N/mm², when the specimen thickness was varied from 1.5 to 5.5mm (Fig.4.7).

In general the stiffness of the specimen increases with its thickness or the loading rate (Figs.4.3 and 4.4) except for a rate of loading of 25.4 mm/min. where the initial stiffness (E_1) was less than that at a rate of 12.7 mm/min. (Figs.4.4 and 4.6). The reason for this behaviour is not quite clear and may be due to some kind of dynamic effect of the high loading rate of 24.5 mm/min. The tests for that rate lasted six to eight seconds only whereas those carried out at a loading rate of loading of 0.254 mm/min. lasted up to thirty minutes.

These results illustrate the close interrelation between the stress-strain relationship and the loading rate and specimen geometry of epoxies.

4.2.4 LONG TERM TENSILE TESTS ON EPOXY

Twenty specimens identical to those of series 2 and of 1.5mm thickness were tested in the same manner at a loading rate of 2.54mm per minute after 6 months. Ten specimens were kept outside the laboratory exposed to weather conditions and the other ten were immersed in water and kept in the laboratory. The results are shown in Table 4.6. Unfortunately, no specimens were kept in dry conditions in the laboratory for direct comparison. The average ultimate strength was 8.62 N/mm² for the specimens immersed in water and 8.78 N/mm² for the

Table 4.6: Long term tensile tests on epoxy.

6 MONTH IMMERSION			6 MONTH EXPOSURE		
IN WATER			TO WEATHER CONDITIONS		
Specimen	Ult. strength (N/mm ²)	Max. el (%)	specimen	Ult. strength (N/mm ²)	Max. el (%)
W1	8.53	2.46	EX1	9.82	2.57
W2	8.50	2.40	EX2	8.56	2.20
W3	9.40	2.92	EX3	7.96	2.10
W4	7.94	2.25	EX4	9.08	2.39
W5	8.61	2.73	EX5	9.11	2.54
W6	9.01	2.85	EX6	8.63	2.16
W7	8.51	2.30	EX7	9.41	2.61
W8	9.04	2.68	EX8	8.50	2.03
W9	7.91	2.25	EX9	9.03	2.53
W10	8.78	2.55	EX10	8.71	2.36
Average	8.62	2.54	Average	8.78	2.35
Standard deviation	0.467 N/mm ²	0.245 %	Standard deviation	0.523 N/mm ²	0.213 %
Coef. of variation	5.42 %	9.72 %	Coef. of variation	5.89 %	9.08 %

exposed specimens.

These represent increases over that at 28 days of 10.2 and 13.6% respectively. The maximum elongations were 2.54 and 2.35% respectively, which are equivalent to variations of +5.4 and -2.5% respectively over the value at 28 days. These results show that immersion in water or exposure to weather conditions of the specimens for 6 months had no adverse effect on their tensile strength. The slight increase in strength registered may have been due to the ageing of the specimens. This contradicts however the limited results of series 1 which suggested that the specimens were fully cured after 21 days. Further investigation over a longer period of time is therefore needed to assess the long term tensile strength of epoxy.

4.3 COMPRESSION TESTS ON EPOXY

4.3.1 EXPERIMENTAL PROGRAMME

These tests were conducted on either 50mm cubes or 50x50x150mm prisms. The specimens were cast and cured in the same manner as described before. The tests were carried out at an approximate stress rate of 15N/mm^2 per minute. The strains were measured on the prisms only and as in the tensile tests, the mechanical measurement of strains was impossible because of their variations when the load was stopped for recording purposes. The same instrumentation, as in the series 2 of tensile tests, was therefore used with the same X-Y plotters and similar strain gauges to record automatically the stress-strain curves. The electrical output of the stress was taken from a 200kN calibrated load cell positioned between the test prism and the loading plate.

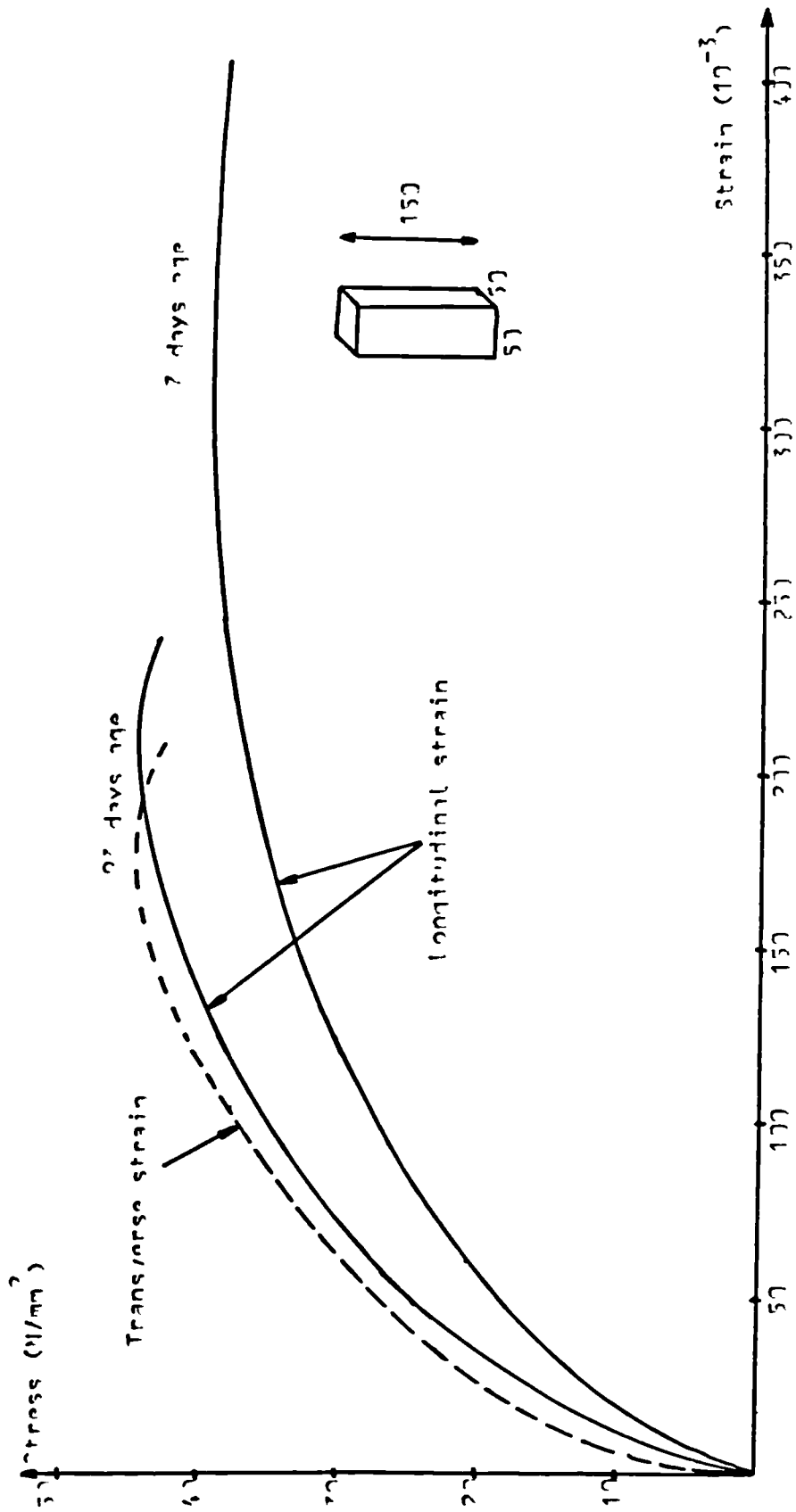


Fig. 4.3: Epoxy stress-strain curves in compression
(Loading rate = 15N/mm^2 per min.)

The manufacturers of the glue (16) stated that the full cure of the resin was achieved after 7 days, but it was soon observed that the specimen strength increased at a later age. It was therefore decided to study this variability by a series of tests on 27 cubes and 6 prisms tested at different ages.

4.3.2 TEST RESULTS

The detailed results of the compressive tests are shown in Table 4.7. It was found that the full cure of the specimens was completed after 21 days in uncontrolled laboratory conditions. Fig.4.8 shows the stress-strain curves before and after the full cure was achieved.

The average ultimate cube compressive strength (of fully cured specimens) was 46.6 N/mm^2 (about 5 times the tensile strength), the average secant modulus and Poisson's ratio at 2% strain were 711.9 N/mm^2 and 0.67 respectively, and the average maximum longitudinal and transverse strains were 253.0 and 217.8 millistrains respectively (about 6 times the ultimate strains in tension).

4.4 SHEAR ADHESION PROPERTIES OF EPOXY

4.4.1 INTRODUCTION

The main action of epoxy bond in plated beams is by shearing. The shear adhesiveness of epoxy to concrete and steel was studied by two series of tests:

(a) The first series was conducted on concrete and steel adherents (pull out tests).

(b) As failure in the pull out specimens always occurred through the concrete-glue bond, it was decided to study the epoxy shear adhesion to steel by tests with steel adherents

Table 4.7: Results of compressive tests on epoxy.

50MM CUBE TESTS				50x50x150MM PRISM TESTS							
Age	No. of spec.	Ult. strength (N/mm ²)	spec.	Age (days)	Ult. strength (N/mm ²)	Max. long. strain (10 ⁻³)	Max. transv. strain (10 ⁻³)	E ₁ (N/mm ²)	E ₂ (N/mm ²)	ν ₁	ν ₂
1	3	11.4	1	7	38.6	406.08		845.0	251.0		
3	3	28.0	2	7	37.4						
7	6	41.6	3	7	42.0						
14	3	45.2	4	93	43.2	230.16	203.64	1141.9	735.4	.59	.67
21	3	47.0	5	93	46.4	274.58	237.95	1254.3	690.3	.58	.67
28	3	46.6	6	93	41.8	254.33	211.72	1434.5	710.0	.62	.66
93	3	46.2									
320	3	46.6									

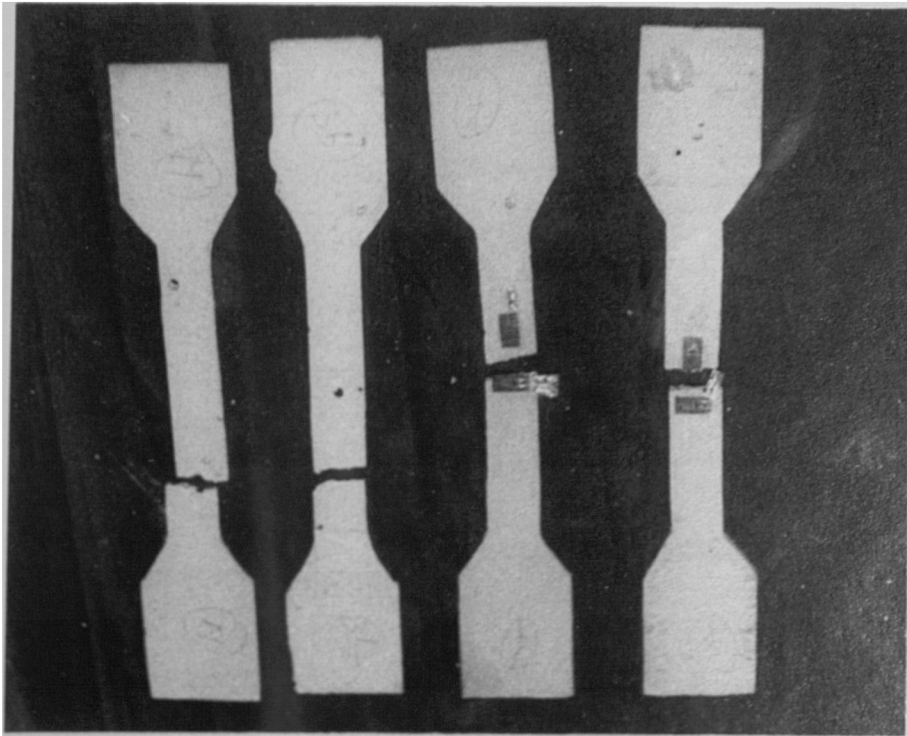


Fig.4.9: failure of epoxy specimens in tension

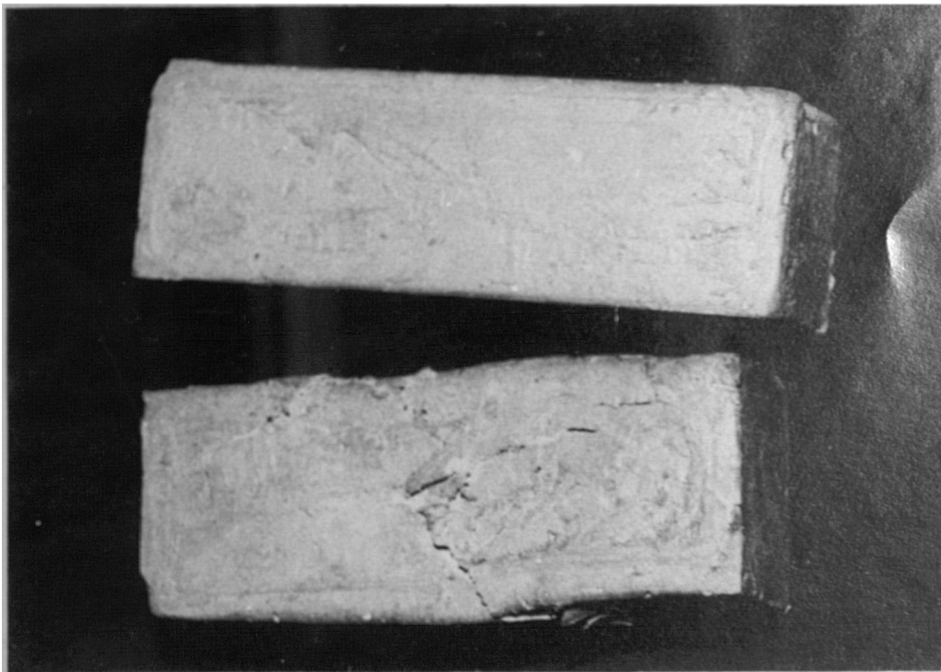


Fig.4.10: Untested and tested epoxy prisms in compression

only (single and double lap tests).

4.4.2 EXPERIMENTAL PROCEDURE

4.4.2.1 PULL CUT TEST

The pull out test specimen, shown in Figs.4.11 and 4.12, is similar to the one used by Solomon (26). Two plates P 3mm thick and 60 mm wide are glued to the opposite sides of a 60x60x150 mm prism. The two plates are put into tension through the rod A1 which is fixed to the piece P1 to which the plates are bolted. The reaction is taken by the two rods A2 (which are fixed to the pieces P2 and P3). A rotule R is positioned between the pieces P3 and P4 in order to distribute the load as uniformly as possible at the end of the concrete prism. The steel plates thus in tension transfer their load to the concrete prism through the glue layer.

The test variables were the glue thickness which was varied from 0.5 to 3.0mm and the concrete cube strength which was varied from 25 to 70N/mm². The concrete mixes used are described in chapter three. For each glue thickness and cube strength, 6 specimens were tested. In all 42 specimens were tested in the short term pull out series at 28 days.

4.4.2.2 DOUBLE AND SINGLE LAP TESTS

The double lap test specimen is shown in Fig.4.14. When the inner plate (6mm thick and 60 mm wide) is put in tension, the load is transferred to the outer plates through the glue layer. The reaction is then taken by the plate P to which the outer plates (3mm thick and 60 mm wide) are bolted. In order to distribute the loads as uniformly as possible at the ends of the plates as is assumed in the theoretical model (25), the

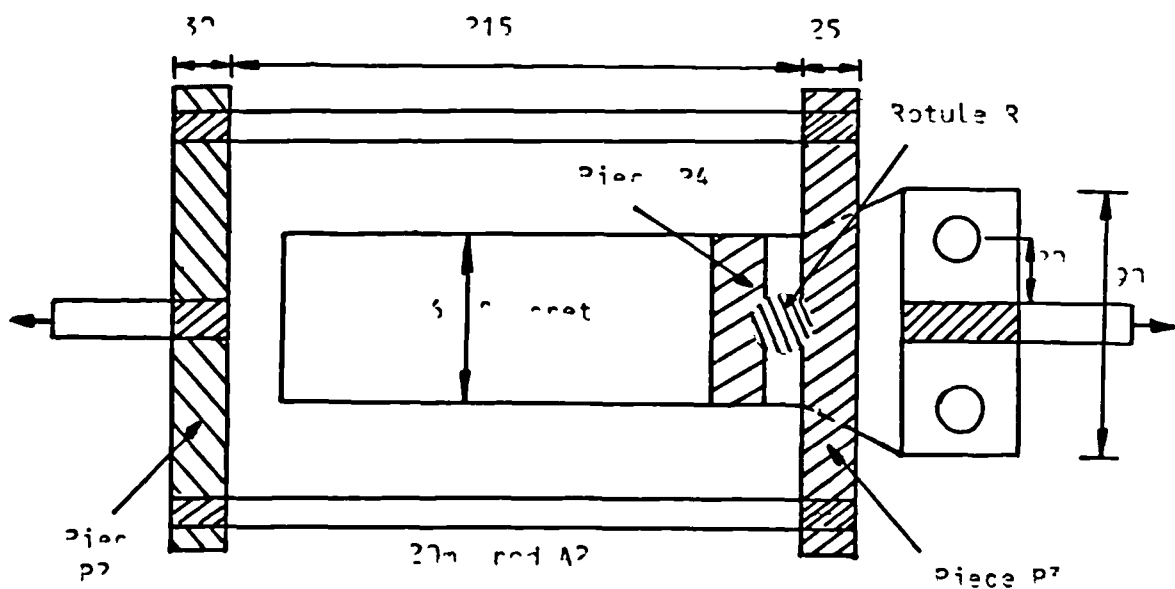
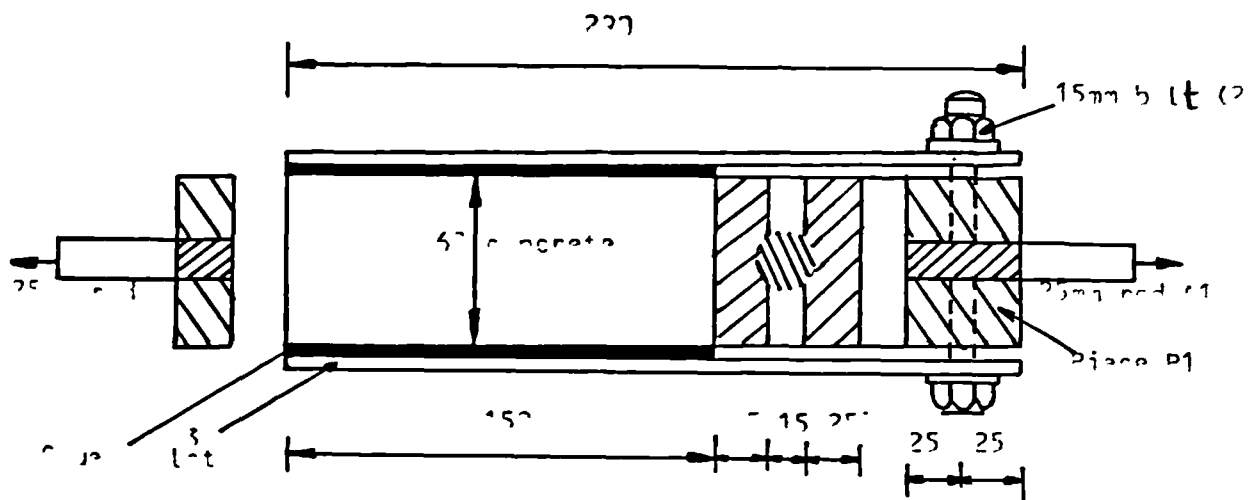
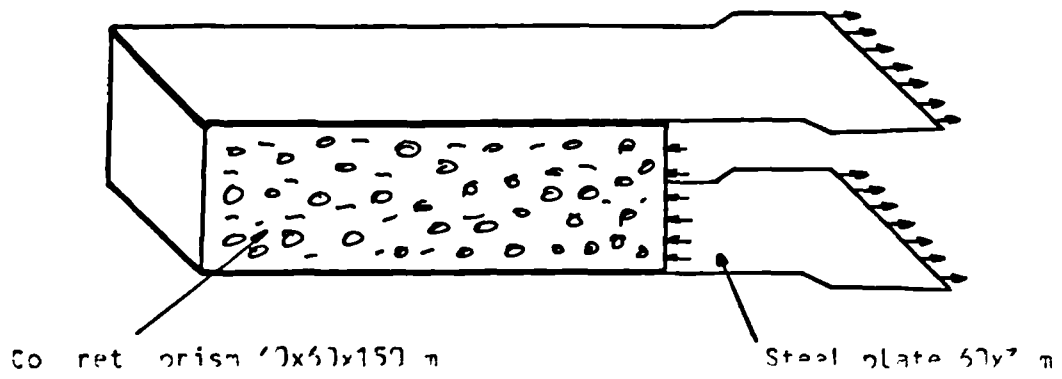


Fig. 4.11 Pull out test on pipe
(All distances in mm)

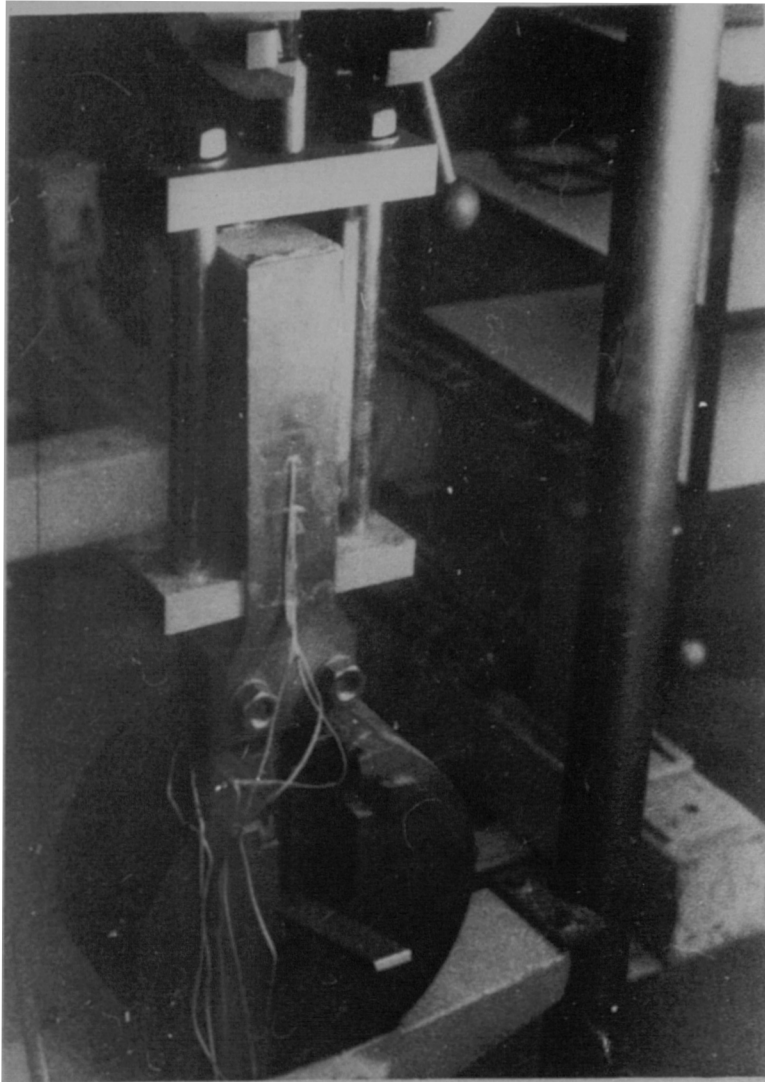


Fig.4.12: Pull out test rig and specimen

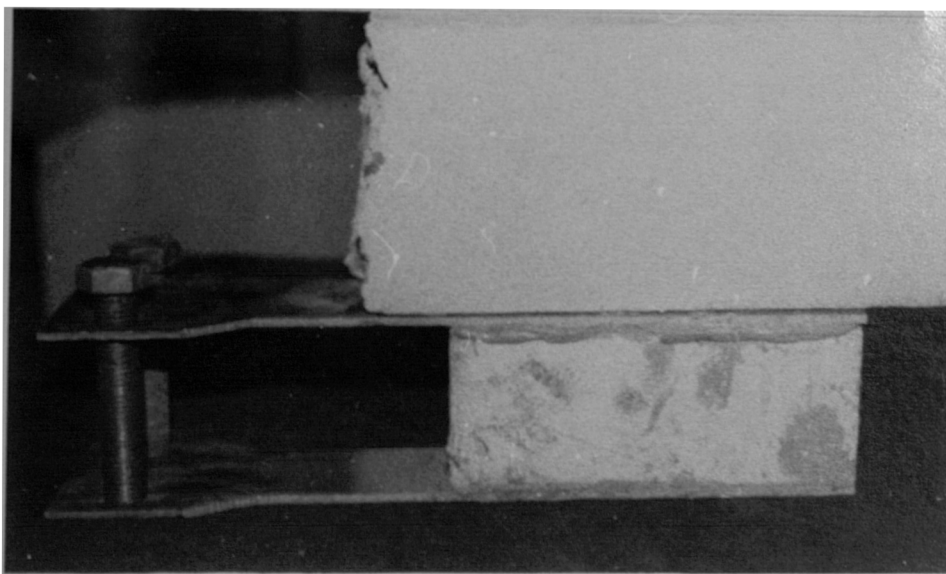


Fig.4.13: Curing of a pull out specimen

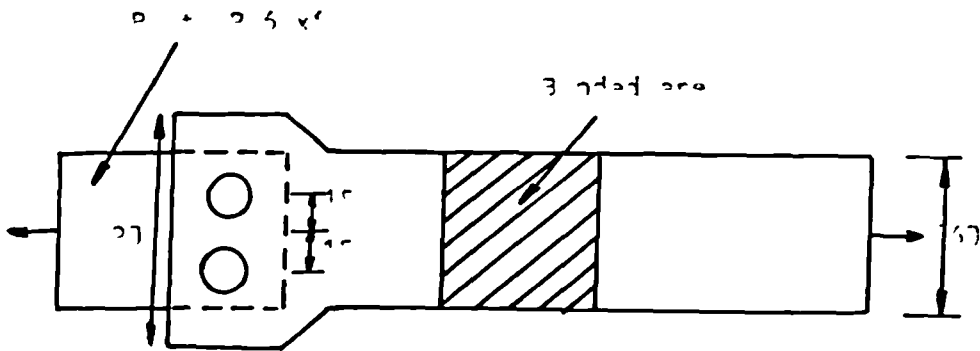
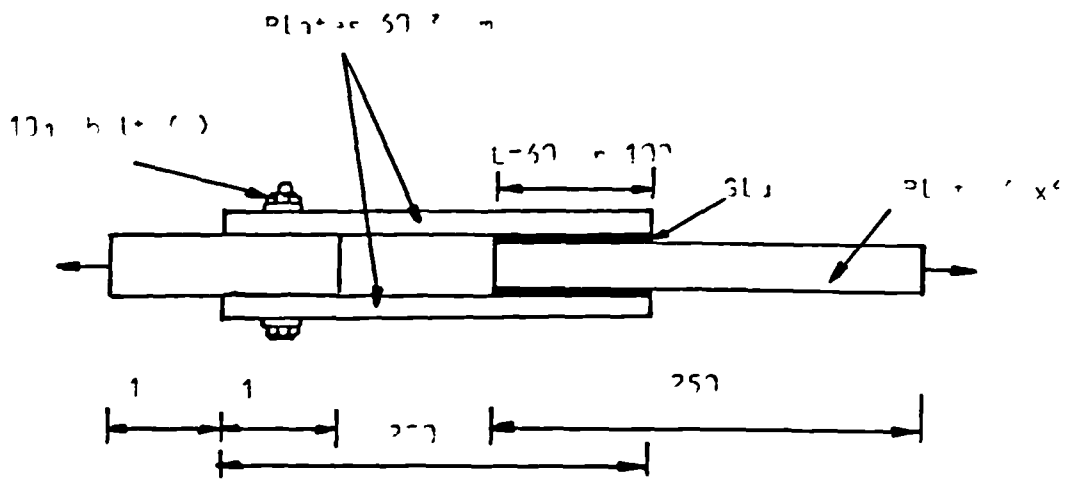
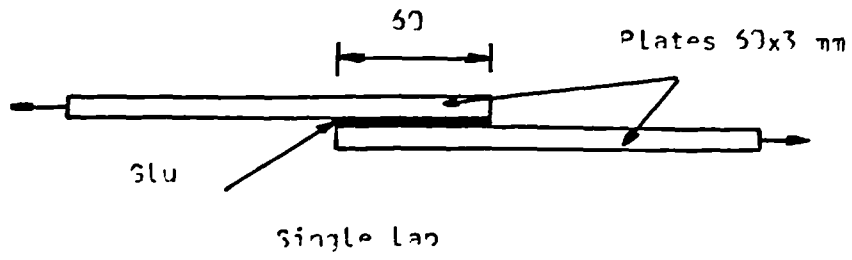


Fig. 4.14. Single lap joint specimen
(All distances in mm)

Amsler testing machine was fitted with friction grip jaws capable of accepting the whole width of the plates.

The main test variable was the glue thickness. All the joints were 60mm long and 60mm wide except three specimens which had a 100mm long joint. These last three tests were carried out to study the behaviour of the bond when the steel yields.

Three single lap tests were also carried out for comparison. The single lap specimens had identical plates as the double lap specimens and 60mm long joints.

In all sixteen 60mm long and three 100mm long double lap specimens and three 60mm long single lap specimens were tested in this short term series at 28 days.

4.4.2.3 THEORETICAL MODELS

The theoretical model for the pull out test, first proposed by Bresson (25) and described in Appendix B, makes the following assumptions:

- 1- The materials (steel, epoxy, concrete) obey Hook's law.
- 2- The epoxy layer carries nothing but shear stresses.
- 3- The normal stresses are uniformly distributed in the adherents.

The theoretical model for the double lap test was developed with the same approach and assumptions. The two models are both described in detail in Appendix B.

4.4.3 BONDING PROCEDURE

After two weeks of curing in uncontrolled laboratory conditions, the concrete prisms were prepared for bonding. Prior to glueing the materials, the concrete surfaces were abraded with an electrical disc grinder to remove laitance and expose the aggregates. They were then wire brushed and vacuum cleaned to remove all loose particles. The face of the steel plates to receive the adhesive was shotblasted using steel grit of 340 microns mean particle size and at a pressure of 0.75 N/mm². The epoxy adhesive was mixed according to the manufacturer's instructions as described in section 4.2. The glue was then applied to both the concrete surface and steel plate. The joint thickness was controlled by four small hardened epoxy spacers. The plates were then applied and held in position by weights. The alignment was ensured by putting bolts through the plate holes during setting (Fig.4.13).

4.4.4 INSTRUMENTATION

After four weeks of bond curing, 2mm Kyowa strain gauges were fixed along the centre line of both plates of three specimens for each sub-series. The strain gauge positions are shown in Fig.4.15 for the pull out tests and Fig.4.20 for the double lap tests. The strain gauges were used to record the deformations along the joints from which the longitudinal force and shear stress distribution could be deduced. The accuracy of the computed shear stresses depends on the distances between consecutive strain gauges. The strain gauge spacings were therefore smaller near the most stressed end of the joint where (according to the theoretical model) the longitudinal force and shear stress are maximum.

A portable Solartron data logger was used to record automatically the electrical outputs from the strain gauges.

4.4.5 CALIBRATION

Although the factor of conversion of voltage output from the strain gauges to strains was given by the suppliers (Kyowa) and although the longitudinal force could be obtained directly by multiplying the recorded strain by the cross-sectional area of the plate and its elastic modulus, it was decided to carry out calibration tests (direct tensile tests) on 2 similar plates with similar strain gauges. These calibration tests permitted the direct conversion of voltage outputs to strains or longitudinal forces. The recorded calibration factor was only 2% greater than the conversion factor given by the product of the strain gauge factor, the cross-sectional area of the plate and its elastic modulus. In addition, 2 strain gauges were fixed outside the joint (where the longitudinal force is known) and were used as references. The electrical strain measurement is described in Appendix A.

4.4.6 TESTING PROCEDURE

After 28 days of epoxy curing (when the concrete prisms were 42 days old), the specimens were tested in an Amsler machine at approximate stress rates of 2 N/mm^2 per minute for the pull out tests and 6 N/mm^2 per minute for the double lap (and single lap) tests. The data logger was monitored to take continuous readings (without stopping the test) up to the breaking point.

4.4.7 MEASUREMENTS

From the recorded voltages and using the calibration factors, three different series of curves were plotted:

1- Local longitudinal force versus applied load for each strain gauge location (Figs.4.15 and 4.20). The local longitudinal force is obtained by multiplying the recorded strain by the calibration factor.

2- Force distribution along the joint at different load levels (Figs.4.16 and 4.21). The distribution of the longitudinal force along the joint at each load level is obtained by joining the points given by the local longitudinal force for each strain gauge position at each load level.

3- Shear stress distribution along the joint at different load levels (Figs.4.17 and 4.22). The shear stresses were calculated assuming a linear variation of the longitudinal force along the plate between consecutive strain gauge positions. For this reason the strain gauge spacings were smaller at the ends of the joints where the shear stresses were expected to be higher.

$$\text{Shear stress } \tau = \frac{\Delta F}{b \cdot \Delta L} \quad (4.1)$$

where ΔF is the Variation of longitudinal force between 2 consecutive strain gauges, ΔL the distance between the 2 strain gauge positions and b the width of the joint.

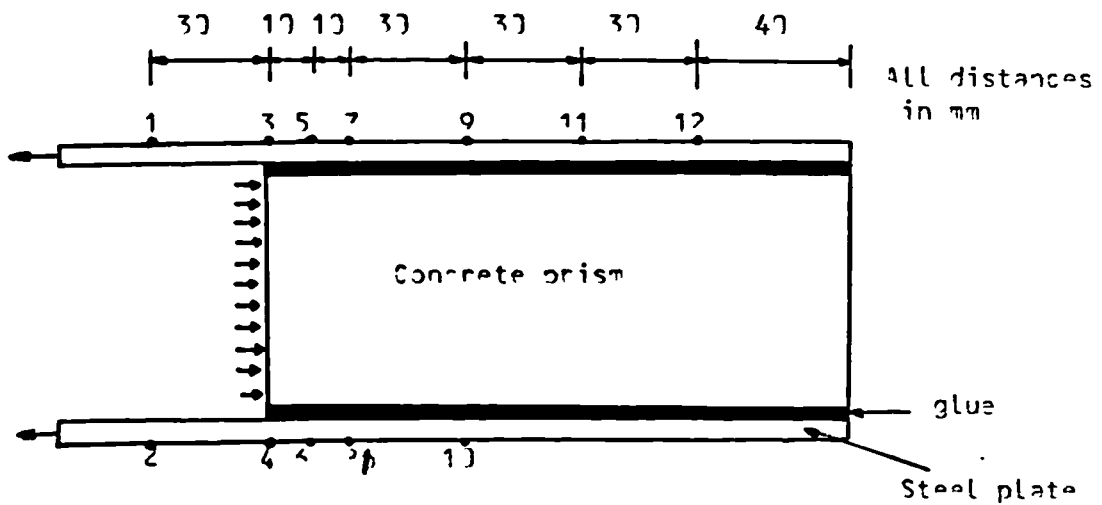
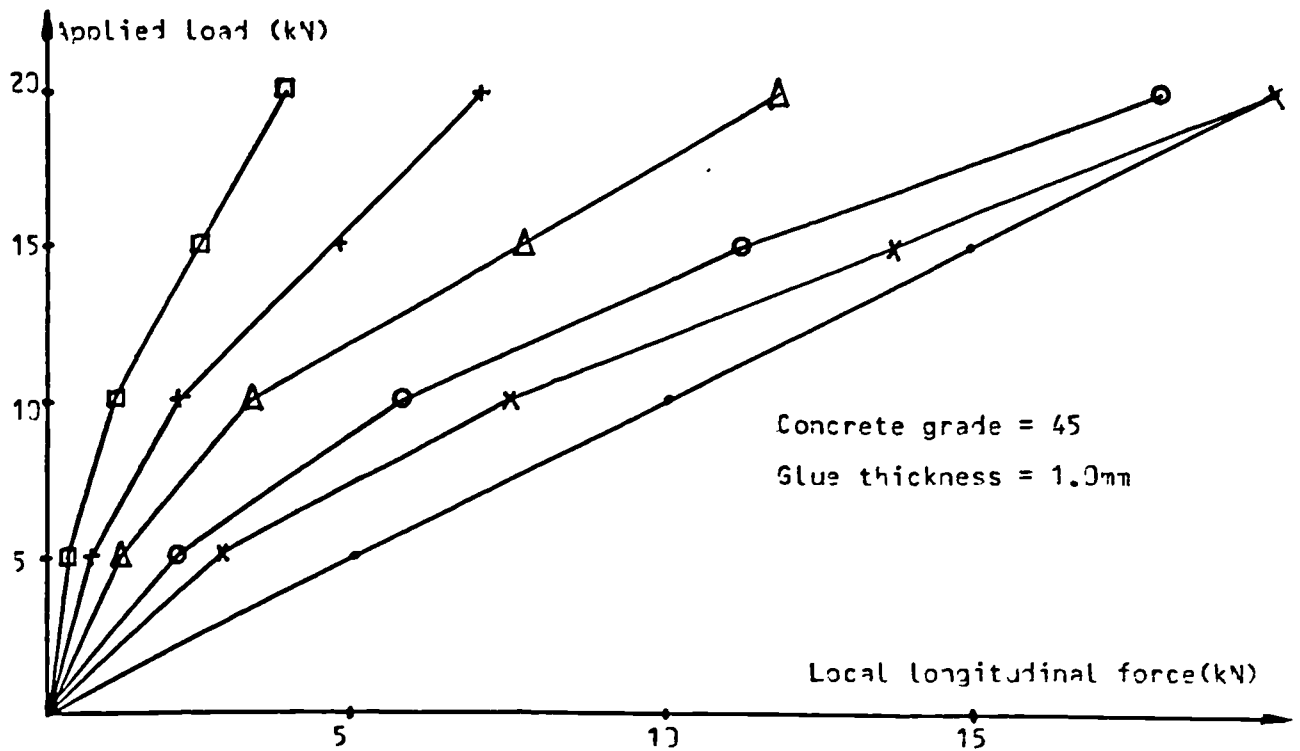
4.4.8 DISCUSSION OF RESULTS

4.4.8.1 PULL OUT RESULTS

The detailed results of the pull out tests are shown in Table 4.8. Fig.4.15 shows that the local longitudinal forces (for each strain gauge location) are proportional to the applied load and that the slopes change at regular intervals.

Table 4.8: Pull out test results.

EFFECT OF CONCRETE STRENGTH				EFFECT OF GLUE THICKNESS			
(glue thickness = 1.0mm)				(concrete grade = 45N/mm ²)			
Concrete cube strength (N/mm ²)	No.of spec.	Mean shear stress (N/mm ²)	Max. shear stress (N/mm ²)	Glue line thick. (mm)	No.of spec.	Mean shear stress (N/mm ²)	Max. shear stress (N/mm ²)
25.1	6	2.17	6.0	0.5	6	2.42	6.9
44.9	6	2.52	6.8	1.0	6	2.52	6.8
60.2	6	2.77	7.4	1.6	6	2.38	6.7
71.3	6	3.33	8.3	3.0	6	2.83	6.9
Maximum deviation (N/mm ²)	standard			Maximum deviation	standard		
		0.21	0.38			0.17	0.42
Maximum variation (%)	coef.of (%)	8.43	5.59	Maximum variation	coef.of (%)	7.14	6.27
Joint (epoxy) age = 28 days				Mean stress = Ult.load/bond area			
Concrete age = 42 days				Max.stress: From recorded distribution			



Strain gauge locations

- ∴: Aver. of strain gauges 1,2,3,4
- x: Aver. of strain gauges 5,6
- o: Aver. of strain gauges 7,8
- Δ: Aver. of strain gauges 9,10
- +: Strain gauge 11
- : Strain gauge 12

Fig.4.15: Local force distribution in the pull out specimen

This probably results from the parabolic nature of the stress-strain relationships of concrete and epoxy and therefore contradicts the simplified elastic relationships assumed in the theoretical model (25). At high loads, the local longitudinal force near the stressed end of the joint increases rapidly until it reaches the value of the applied load (Fig.4.15). This means that no force is transferred from the plate to concrete in that area. This could be the result of cracking in concrete or the joint or both. Fig.4.16 showing the force distribution along the joint at different load levels confirms the previous observation. At low loads the distribution is exponential but at higher loads it tends to become more and more horizontal near the stressed end following the reduction in the transfer of forces from the plate to concrete in that region.

The deduced shear stress distribution along the joint at different load levels, represented by histograms (Fig.4.17), is exponential at low loads. At higher loads however the shear stresses are reduced in the stressed end region and near the ultimate load, the bond stress becomes equal to zero in the first 10mm of the joint (Fig.4.17).

At low loads, the longitudinal force and shear stress distributions along the joint are exponential (as suggested by the theoretical model described in Appendix B) (Figs.4.16 and 4.17). At higher loads (60% of the ultimate load) however the joint starts failing at the most stressed end but the variation still remains exponential in the remaining region of the joint. Near the ultimate load, the most stressed end fails completely reducing the effective length of the joint by approximately 10 to 20 mm or 6.67 to 13.33% of its initial length. Fig.4.17

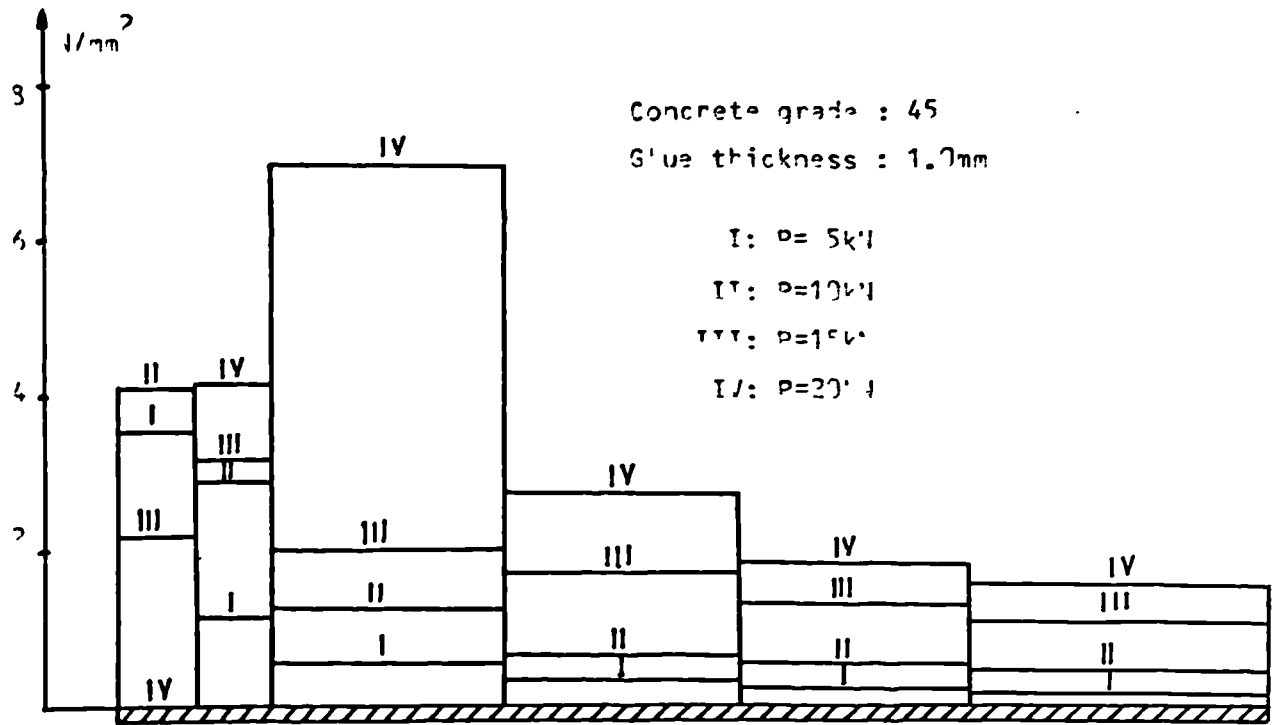


Fig. 4.17 Stress distribution at ball out joint at different load levels

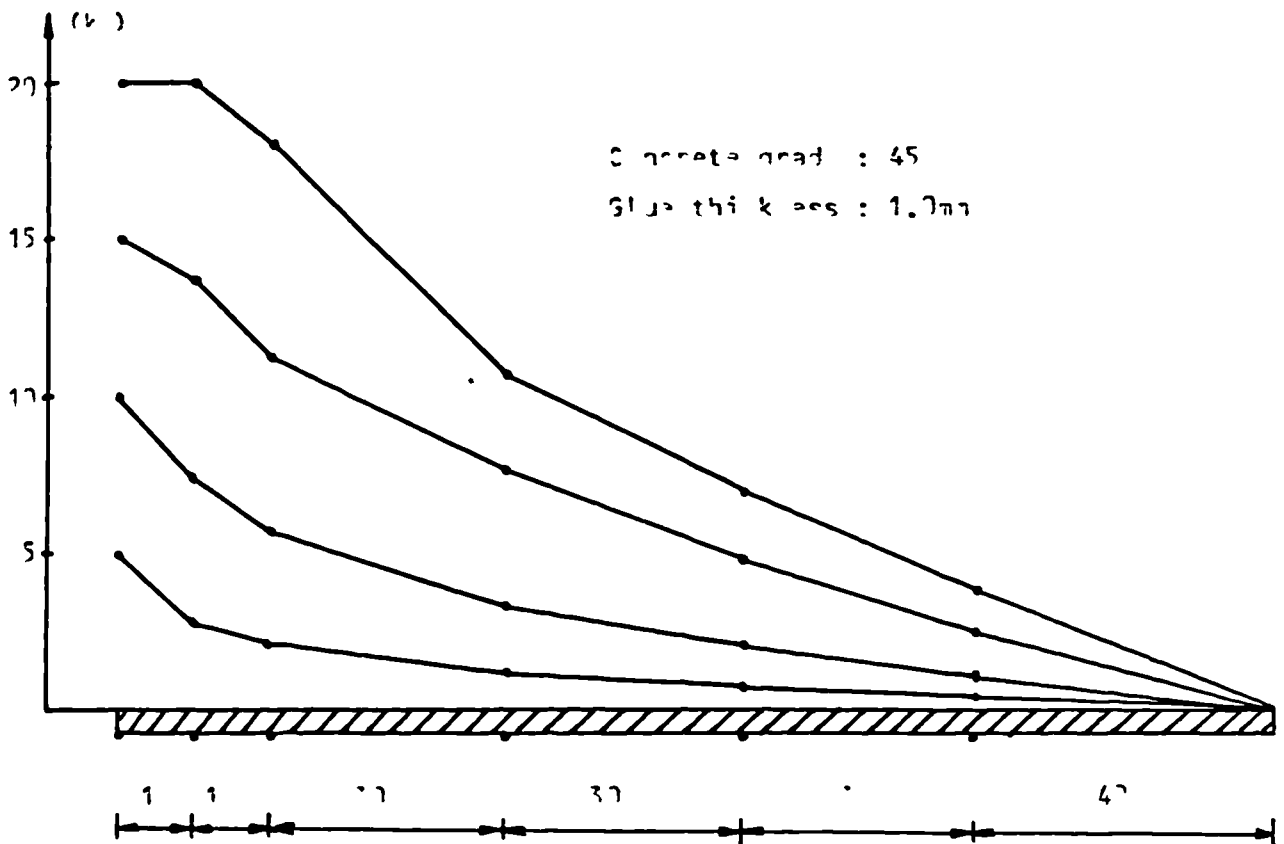


Fig. 4.18 Stress distribution at ball out joint at different load levels

shows that at a load of 20kN, the shear stress in the first 10mm of the stressed end was equal to zero. The maximum shear stress recorded near the edge of the joint was about 4.1 N/mm^2 , 60% only of the recorded value at a location distant 20mm from the edge (Fig.4.17). The joint seems therefore to offer a weaker bond strength at its edge. This phenomenon of lower bond strength at the edge of the joint was not reported by Bresson (25) or Solomon (26) but was observed by Van Gemert (27). He found that the stressed end starts failing at a shear stress of 2.6 N/mm^2 whereas the maximum value registered at a distance of 50mm was 6.0 N/mm^2 . Van Gemert observed that the bond strength reduction occurred over a distance of 125mm or 42% of the initial joint length. This greater reduction in the effective length of the joint may have been due to the difference in the elastic properties of the materials he used and to the greater joint length (300mm) of his specimens. Van Gemert proposed a simplified linear design model relating the ultimate joint strength to the ultimate tensile strength of concrete. The concrete he used had a compressive strength of 56 N/mm^2 and a tensile strength of 4.5 N/mm^2 . This interrelation between the tensile strength of concrete and the bond strength was also reported by Solomon (26) and was probably suggested by the relatively lower values of ultimate bond stresses recorded. These lower values (2.64 to 3.95 N/mm^2) were probably the result of higher spacings between consecutive strain gauges (25mm in Van Gemert's tests and 30mm in Solomon's tests). The ultimate shear stresses recorded in the present tests varied between 6.0 and 8.3 N/mm^2 (Figs.4.23 and 4.24), much higher than the tensile strength of concrete (4.5 N/mm^2), and

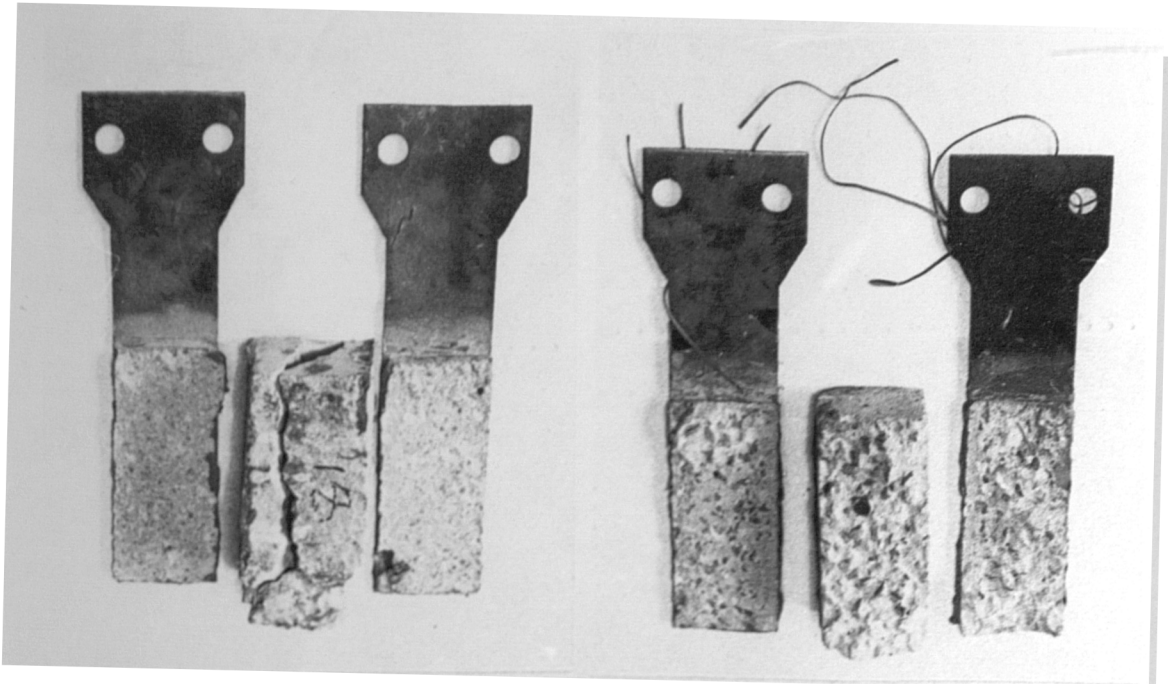


Fig.4.18: Failure of pull out specimens



Fig.4.19: Failure of double lap specimens

agree satisfactorily with Bresson's results of 6.0 to 8.0 N/mm² (25).

The results of these tests suggest that the distribution of the shear stresses is exponential as predicted by Bresson's model (25) but that there is a reduction of 6.67 to 13.33% in the joint length at high loads due to an unclear edge effect. A possible explanation to this reduced bond strength at the edge may be the presence of tensile stresses at the end of the joint.

The average values of the mean and maximum shear stresses varied from 2.17 to 6.0 N/mm² respectively for a concrete grade of 25 and from 3.33 to 8.3 N/mm² respectively for a concrete grade of 70 (Fig.4.23). The mean shear stress is obtained by dividing the maximum load by the area of the joint. The maximum shear stresses recorded are greater than the splitting tensile of concrete (3.1 to 4.0 N/mm²).

Failure of the specimens always occurred through concrete (Fig.4.18) proving that the epoxy resin can offer a bond stronger than concrete in shear. The ultimate shear strength of concrete seems therefore to be the upper limit of the joint strength and the interrelation between the two may be more appropriate than that relating the joint capacity to the tensile resistance of concrete.

4.4.8.2 DOUBLE AND SINGLE LAP RESULTS

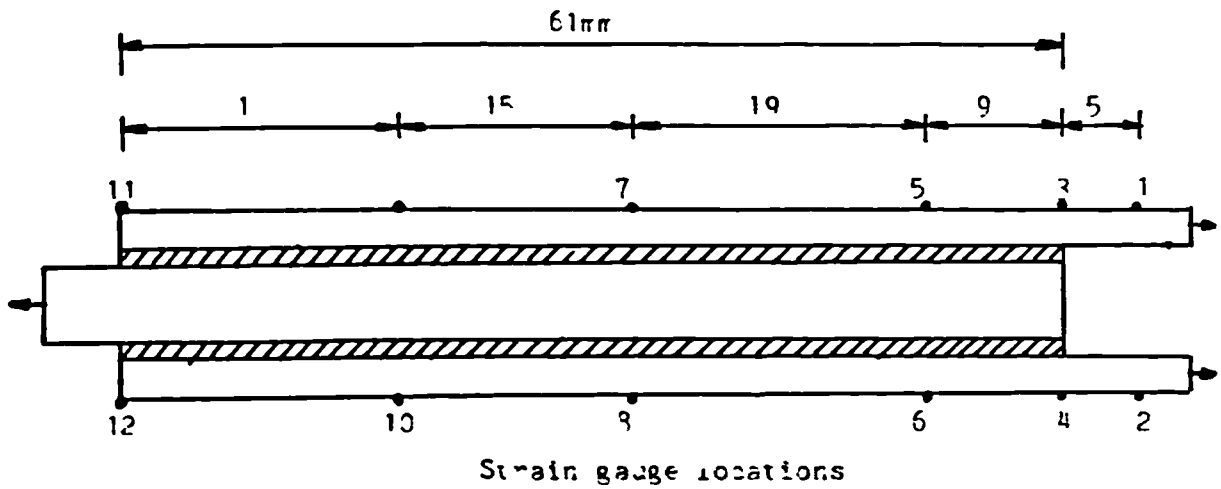
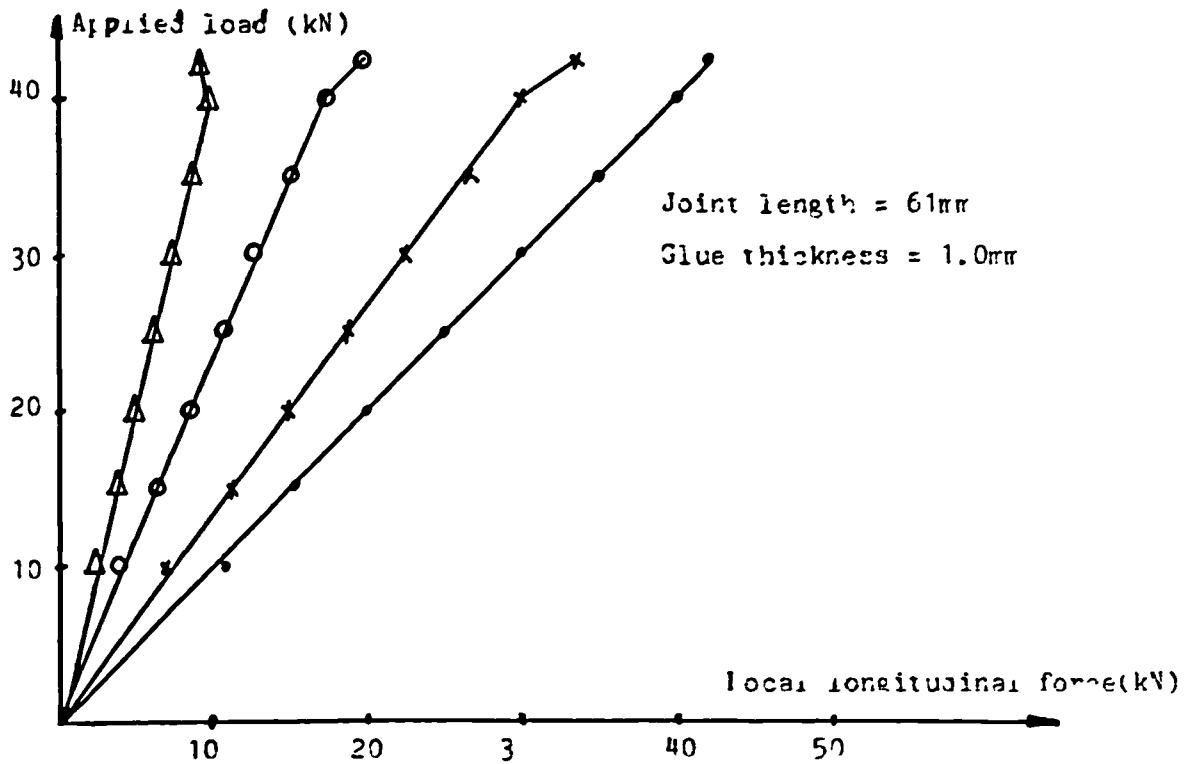
The detailed results of the double and single lap tests are given in Table 4.9. At all strain gauge positions, the local longitudinal forces are proportional to the applied load and keep the same slope up to failure (Fig.4.20). This means that the changes in the slopes, observed in the pull out tests,

were probably not due to the inelastic behaviour of epoxy but to the parabolic relationship between stresses and strains in concrete or microcracking of concrete near the interface. The distribution of the longitudinal forces and shear stresses along the joint is exponential as suggested by the model described in Appendix B (Figs.4.21 and 4.22). The theoretical model predicts a stress distribution symmetrical about the axis passing through the middle of the joint with a maximum value at both ends of the joint and minimum value in the middle (Appendix B). The unsymmetry of the recorded shear stress distribution is probably due to the different strain gauge spacings used. The average values of the mean and maximum shear stresses in the double lap specimens of 60mm length were 12.7 and 18.2 N/mm² respectively. This maximum value is greater than 15.8 N/mm² reported by Gilibert et al.(39). The difference may be accounted for by the differences in the epoxies and test specimens used or the greater spacings between the strain gauges (18.5mm). Cusens and Smith (29) found that the mean shear stress varied with the type of adhesive used between 13.5 and 22.0 N/mm². They did not measure the deformations along the joints and could not therefore deduce the experimental maximum values. Their values of mean shear stresses (up to 22.0 N/mm²) are much higher than those of the present tests (12.7 N/mm²) or those reported by others (39). This may be due to the different version of the double lap test specimen (specimen b shown in Fig.2.1) used by Cusens and Smith (29) or the difference in the properties of the materials. The reported results show that the steel adherents used must have been of high yield strength. The difference in the performances of the adhesives (29) and

Table 4.9: Single and double lap results.

DOUBLE LAP TESTS						SINGLE LAP TESTS					
Joint length (mm)	Glue line thic (mm)	No.of spec.	Mean shear stress (N/mm ²)	Max. shear stress (N/mm ²)	Joint length (mm)	Glue line thic (mm)	No.of spec.	Mean shear stress (N/mm ²)	Max. shear stress (N/mm ²)		
60	0.5	4	12.86	18.2	60	1.0	3	10.2	18.1		
60	1.0	4	12.50	18.0							
60	1.6	4	12.71	18.2							
60	3.0	4	12.89	18.3							
100	1.0	3	9.68	13.8							
Max. standard		0.85		1.07		Max. standard		0.98		1.31	
dev. (N/mm ²)						dev. (N/mm ²)					
Max. var.		6.69		5.88		Max. var.		9.61		7.24	

Joint age = 28 days (epoxy cured for 28 days)
 Mean stress = Ult.load/bond area
 Max.stress: from recorded distribution



- ∴: Aver. of strain gauges 1, 2, 3, 4
- x: Aver. of strain gauges 5, 6
- o: Aver. of strain gauges 7, 8
- ▲: Aver. of strain gauges 9, 10

Fig.4.20: local force distribution in the double lap specimen

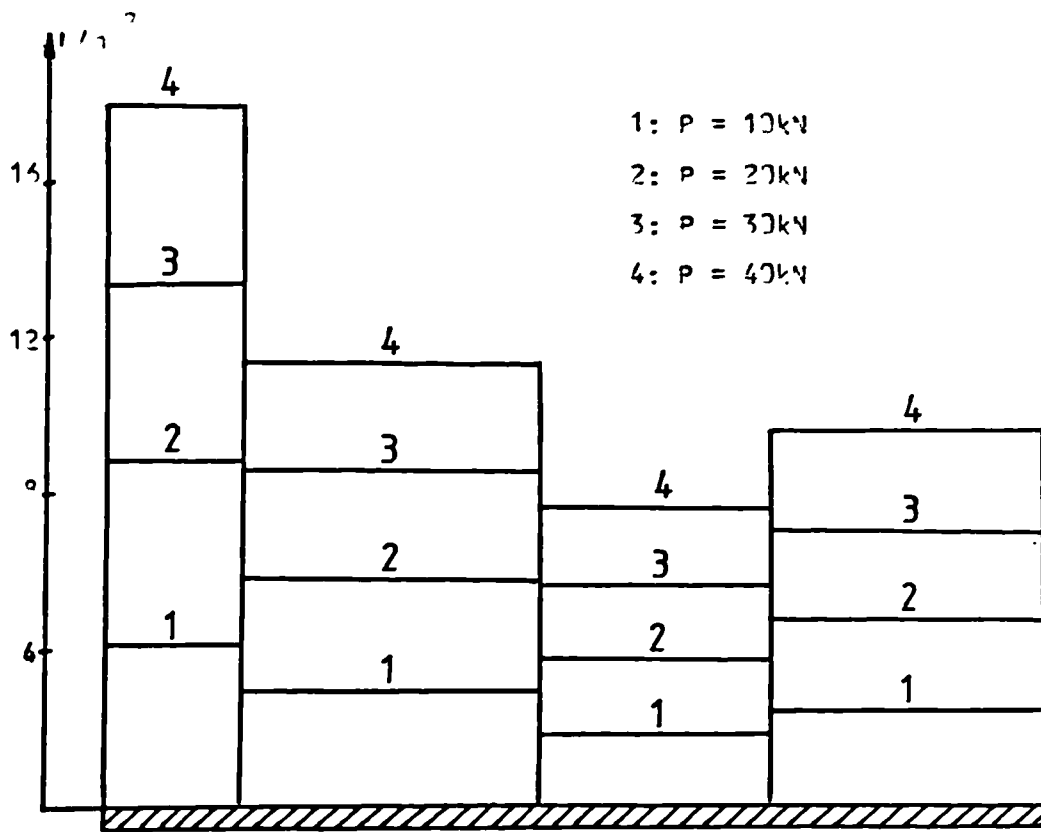


Fig. 4.20. Force distribution along double lap joint at different load levels

(Joint length = 51mm)
(Plate thickness = 1.7mm)

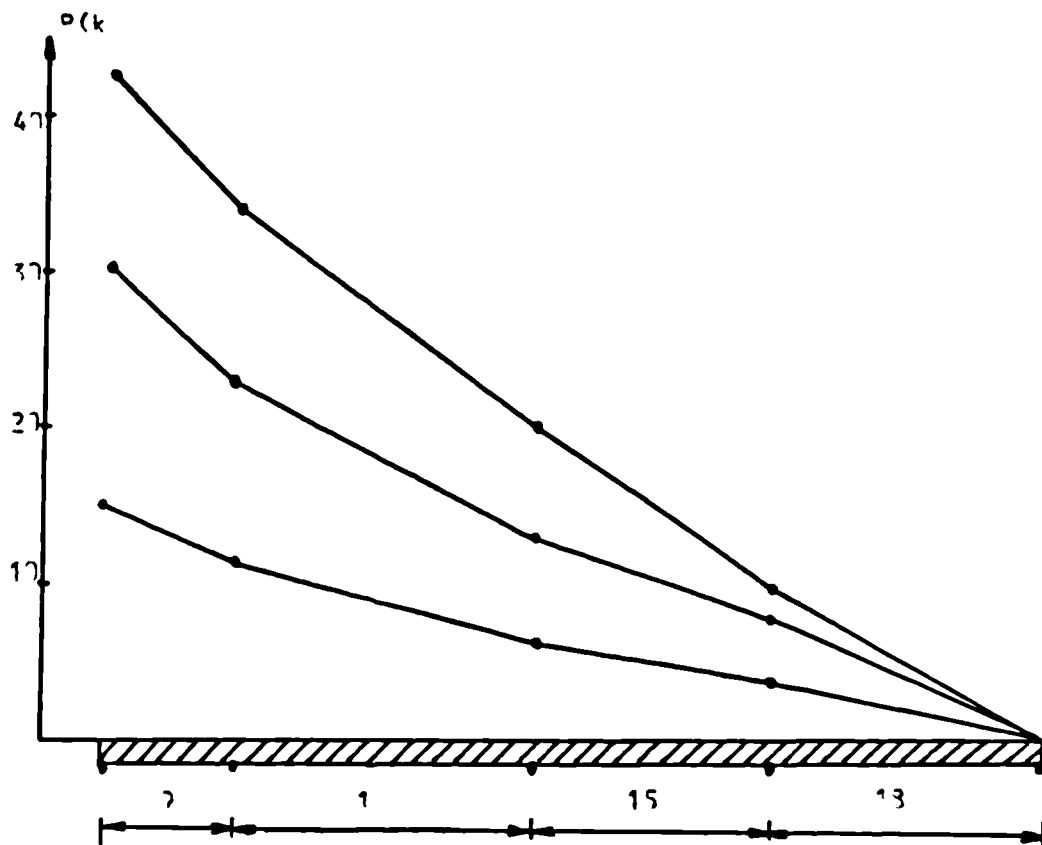


Fig. 4.21. Force distribution along double lap joint at different load levels (joint length = 51mm) (plate thickness = 1.7mm)

the difference in the testing conditions (specimen geometry, rate of loading...) used, make a direct and full comparison of the various results rather difficult.

The double lap joints of 100mm length behaved in the same manner and sustained higher loads than the 60mm long joints. They failed however at mean and maximum shear stresses of 9.68 and 13.8 N/mm² respectively, lower than those recorded in the 60mm long joints. This early separation (compared to shorter double lap joints) was caused by the yielding of the steel plates which resulted from the higher loads sustained by the longer joints. This may be due to the limitations of epoxy joints in sustaining high deformations or a higher stress concentration factor possibly resulting from a stress redistribution following the yielding of the plates.

The single lap specimens, tested for comparison, failed at an average shear stress of 10.2 N/mm², which is 19.7% lower than the double lap value. The manufacturer's single lap tests on the same adhesive gave an average result of 12.25 N/mm² but again no complete comparison can be done as many important test parameters (specimen size, loading rate...) are not reported. This low resistance of the single lap specimens (compared to the double lap tests) is probably the result of the combination of the shear stresses and peeling forces present in the unsymmetrical specimen. This suggests that the single lap test is an unreliable method of studying the shear bond strength of epoxies.

Failure of the specimens occurred by separation of the plates. Subsequent observation of the failed specimens suggested that failure was a combination of adhesion (at the

interface steel-glyue) and cohesion (through the glyue) failures (Fig.4.19) confirming other findings (16,29).

4.4.8.3 EFFECTS OF CONCRETE STRENGTH AND GLUE THICKNESS

Fig.4.23 shows that the shear bond strength of epoxy to concrete varies almost linearly with the concrete cube strength. This is probably due to the nature of failure which is controlled by the shear strength of concrete.

Although the theoretical models suggest that the joint strength should increase with the glue line thickness, the experimental results showed no apparent effect of the adhesive layer thickness over a range 0.5-3.0mm on the strength of the pull out and double lap specimens (Fig.4.24). This apparent contradiction may be accounted for by the high shrinkage deformations during setting occurring in the thick resin layers or the presence of normal stresses in joints with thick adhesive layers (36).

4.4.9 LONG TERM ADHESION TESTS

Twelve pull out specimens and ten double lap specimens were tested after 6 months immersion in water or exposure to weather conditions. Six of the pull out and five of the double lap specimens were immersed in water and kept in uncontrolled laboratory conditions. The other specimens were exposed to weather conditions on the roof of the university building. The glue layer was 1.0mm thick for all specimens. The concrete used was of grade 45 with a cube strength of 44.9 N/mm² after 42 days dry curing in the laboratory, and 46.3 and 47.1 N/mm² after 6 months immersion in water or exposure to environmental conditions respectively. The joints and all the exposed steel

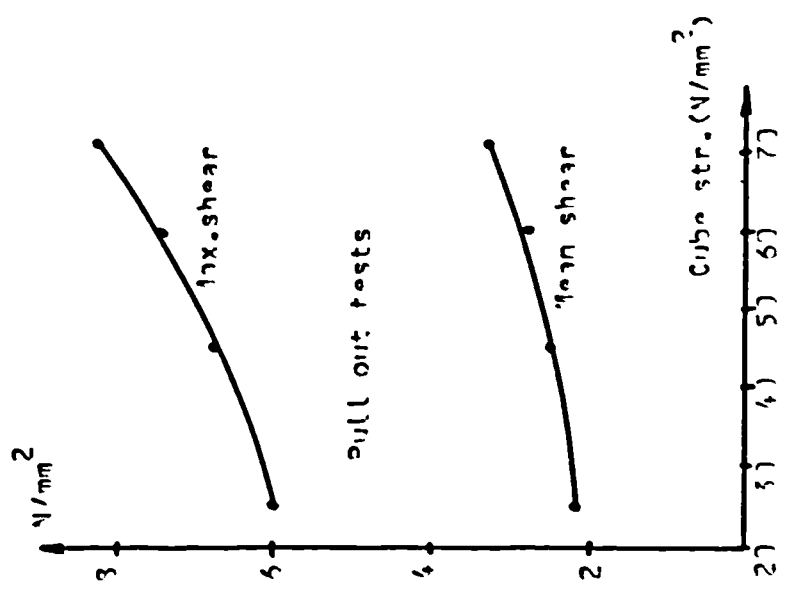
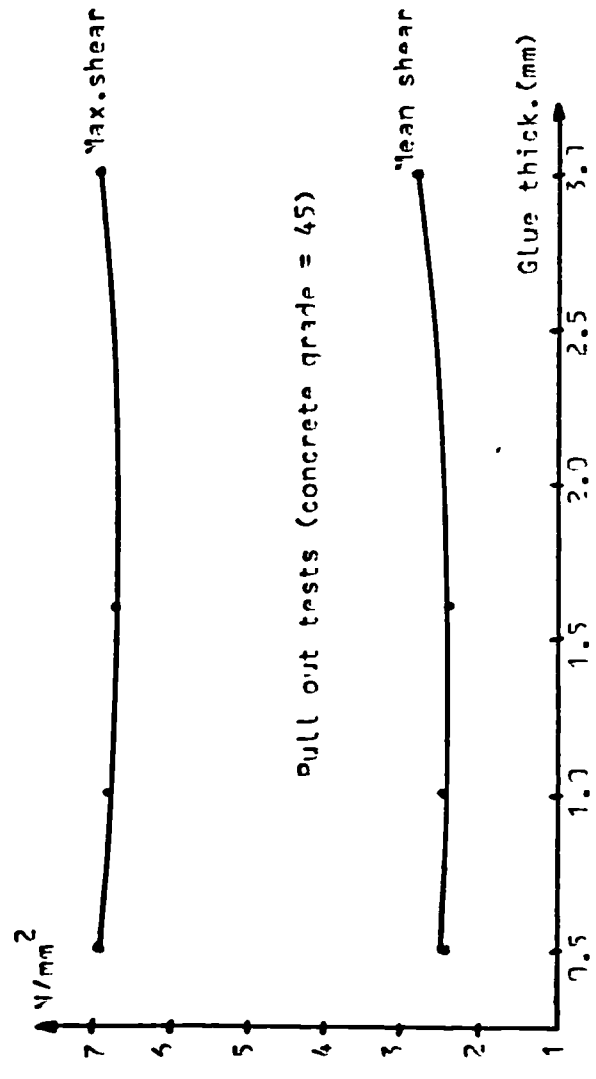
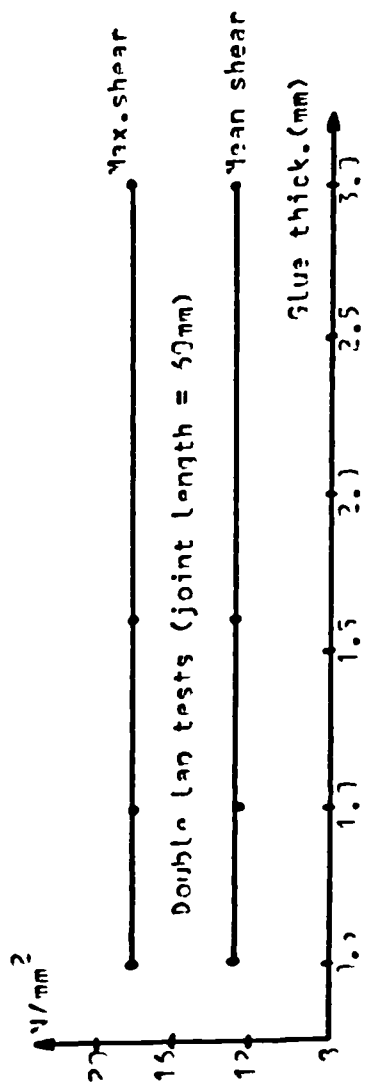


Fig. 4.23: Effect of concrete strength on epoxy bond to concrete (Glue thickness = 1.0mm)

Fig. 4.24: Effect of glue thickness on epoxy bond to concrete and steel

Table 4.10: Long term epoxy adhesion test results.

LONG TERM PULL OUT TESTS			LONG TERM DOUBLE LAP TESTS		
6 month immersion in water (conc. cube strength 46.3 N/mm ²)	6 month weather exposure (conc. cube strength 47.1 N/mm ²)	6 month immersion in water	6 month weather exposure	6 month immersion in water	6 month weather exposure
Specimen	Mean shear stress (N/mm ²)	Specimen	Mean shear stress (N/mm ²)	Specimen	Mean shear stress (N/mm ²)
POW1	2.63	POEX1	2.68	DLW1	12.65
POW2	2.81	POEX2	2.86	DLW2	11.88
POW3	2.54	POEX3	2.29	DLW3	11.94
POW4	2.49	POEX4	2.56	DLW4	12.07
POW5	2.77	POEX5	2.70	DLW5	12.76
POW6	2.23	POEX6	2.78		
Average	2.58	Average	2.65	Average	12.26
Stand. dev. (N/mm ²)	0.22	Stand. dev. (N/mm ²)	0.20	Stand. dev. (N/mm ²)	0.41
Coef. of var. (%)	8.20	Coef. of var. (%)	7.58	Coef. of var. (%)	3.38
		Concrete cube strength at 42 days = 44.9 N/mm ²			
				Average	12.39
				Stand. dev. (N/mm ²)	0.33
				Coef. of var. (%)	2.65

plate surfaces were Aluminium painted for protection. After six months the specimens were tested in the same manner as the short term ones. The detailed results are shown in Table 4.10.

For the pull out tests the average shear stress was 2.58 N/mm^2 for the specimens immersed in water and 2.65 N/mm^2 for those exposed to weather conditions. These represent increases over the short term strength of 2.4% and 5.2% respectively. These small increases are probably due to the ageing and increase in concrete cube strength (3.1 and 4.9% respectively).

The average shear stress of the double lap tests was 12.26 N/mm^2 for the specimens immersed in water and 12.39 N/mm^2 for the exposed ones. These are equivalent to decreases over the short term strength of 1.9% and 0.9% respectively.

These negligible variations mean that 6 month exposure or immersion in water did not have any adverse effect on the epoxy shear adhesion to concrete and steel. They also mean that the edge effect observed and reported in the short term pull out tests was not enhanced by exposure to weather conditions and immersion in water for 6 months.

4.5 CONCLUSIONS

The following conclusions drawn from the tensile, compressive and shear adhesion tests on epoxy can only apply to the adhesive formulation CXL 194 used in this project:

1- The stress-strain relationships of epoxy depend closely on the rate of loading and geometry of the specimen. The ultimate tensile strength increased by 56% when the loading rate varied from 0.254 to 25.4 mm/min. (specimen thickness = 1.5mm) and by 70% when the thickness of the specimen varied from 1.5 to 5.5 mm (loading rate = 2.54 mm/min.).

2- The rheological law $F(d\sigma, d\epsilon, dt)=0$ of the visco-elastic materials is not appropriate enough to describe the mechanical behaviour of epoxy resins as it does not take into account the influence of the specimen shape.

3- Full cure of the specimens is only achieved after 21 days and not 7 days as stated by the manufacturer.

4- Table vibration of the specimens did not have any effect on the properties of the resin.

5- Immersion in water and exposure to environmental conditions of the specimens for 6 months did not have an adverse effect on the tensile strength of the adhesive. There was on the contrary an increase of 10.2 and 13.6% respectively over the 28 days strength.

6- Epoxy glue ensures full composite action of concrete and steel and achieves a bond stronger than concrete in shear.

7- The epoxy bond with concrete is weaker at the edge but the experimental results agree satisfactorily with the theoretical predictions.

8- The bond with concrete increases with the cube strength.

9- Variation of the glue thickness did not have any effect on the bond strength with concrete or steel.

10- The theoretical model predicts satisfactorily the behaviour of the double lap tests (steel adherents).

11- The results of tests on double lap specimens of 100mm length show that the epoxy bond does not sustain high deformations and breaks as soon as the steel adherents start yielding.

12- Due to the presence of peeling forces, the single lap test is not a reliable method of studying the shear strength of

epoxy joints.

13- Immersion in water and exposure to weather conditions for 6 months did not have any ill effect on on the shear adhesion of epoxy to concrete and steel. There were increases of 2 and 5% in the pull out tests and 3 and 5% in the double lap tests (over the 28 days strength).

CHAPTER FIVE
FLEXURAL BEHAVIOUR OF PLATED BEAMS

5.1 INTRCDUCTION

The flexural behaviour of a composite member depends on the properties of its component materials. Concrete has a low tensile strength of about one tenth of its compressive strength and little resistance to crack propagation. This poor tensile resistance and the brittle nature of the failures connected with it render the use of concrete in tension undesirable, uneconomical and unsafe. The main objective of reinforced concrete is to exploit the compressive strength of concrete in flexure and impart the tensile forces to the reinforcing steel bars. The reinforcement provides tensile resistance in the member but does not, however, improve the tensile strength of the surrounding concrete or its resistance to cracking. Concrete cracks at a tensile strain of about 100 to 150 microstrains, only a fraction of the ultimate strain of the reinforcing bars it covers. Cracking is therefore unavoidable in reinforced concrete members. Tensile stresses can be transferred through narrow cracks but the overall strength of concrete in tension is considerably reduced after the appearance of cracks. For this reason it is common in reinforced concrete design codes to ignore the tensile strength of concrete when estimating the flexural strength of a member.

Most limit design theories are based on plastic properties of reinforced concrete. The advantage of this is to allow moment redistribution in statically indeterminate

structures. The moment transfer depends on the hinging and deformational capacity of the member. The prediction and control of the deformations has therefore become very important.

Control of cracking is also vital. Wide cracks are aesthetically unpleasant and may lead to corrosion of the steel bars and consequently a reduction of the member strength. Excessive deformations (deflections, rotations, strains) and cracking are undesirable and may give rise to public concern. The modern codes of practice recommend limiting values for deflections and crack widths which are not to be exceeded.

The present trend towards using refined design methods, with higher allowable stresses for both steel and concrete, produces structures in which the serviceability conditions can be more critical than the strength considerations.

Previous field and laboratory tests have shown the effectiveness of epoxy resins in successfully bonding steel to concrete. Glueing external reinforcement to existing members results in delayed and reduced cracking and increases in stiffness and ultimate strength.

This part of the project investigates the flexural behaviour of plated beams and compares the deformational, cracking and strength properties of unplated and plated beams. The role of the epoxy adhesive and the effect of preloading are also studied.

5.2 EXPERIMENTAL PROGRAMME

5.2.1 INTRODUCTION

When strengthening an existing structure by bonding external reinforcement, the internal steel bars are already under load, due to the self weight and dead load. To make the strengthening element effective, the structure must undergo further deformation or loading. Unless the structure is completely relieved of its existing dead load, the added strength may not therefore be fully exploited (even assuming a composite action between the beam and the plate).

This part of the experimental programme included nine beams in all divided in three Series:

(a) SERIES I

Beams tested at 42 days in rig 1 shown in Figs.5.1 and 5.2 (which is described later):

F01: No glue and no plate.

F02: 3mm thick glue layer and no plate (to investigate whether the adhesive cracks with concrete).

F11: Strengthened with a 1.5mm thick plate (the epoxy bond being 1.5mm thick) at 28 days age and tested at 42 days.

(b) SERIES II

Beams loaded to 30, 50 or 70% of their ultimate flexural capacity (from the experimental maximum load of beam F01) unloaded, strengthened with a 1.5mm thick plate on the same day at 28 days (the epoxy bond being 1.5mm thick), and then tested two weeks later in rig 1. Although the epoxy tensile tests described in chapter four showed that the full cure of the specimens was achieved after three weeks, the epoxy joint was

cured enough after two weeks to be stronger than concrete in shear.

F12: Preloaded to 65kN or 31% of ultimate strength.

F13: Preloaded to 110kN or 52% of ultimate strength.

F14: Preloaded to 150kN or 71% of ultimate strength.

(c) SERIES III

Beams Loaded to 30, 50 or 70% of their ultimate strength and strengthened (under a constant load) with a 1.5mm plate on the same day at 28 days age (the epoxy bond being 1.5mm thick) in rig 2 (shown in Figs.5.3 and 5.4, and described later). The beams were then kept under their preloads for two weeks (to allow the epoxy bond to cure) before increasing the load up to failure at 42 days:

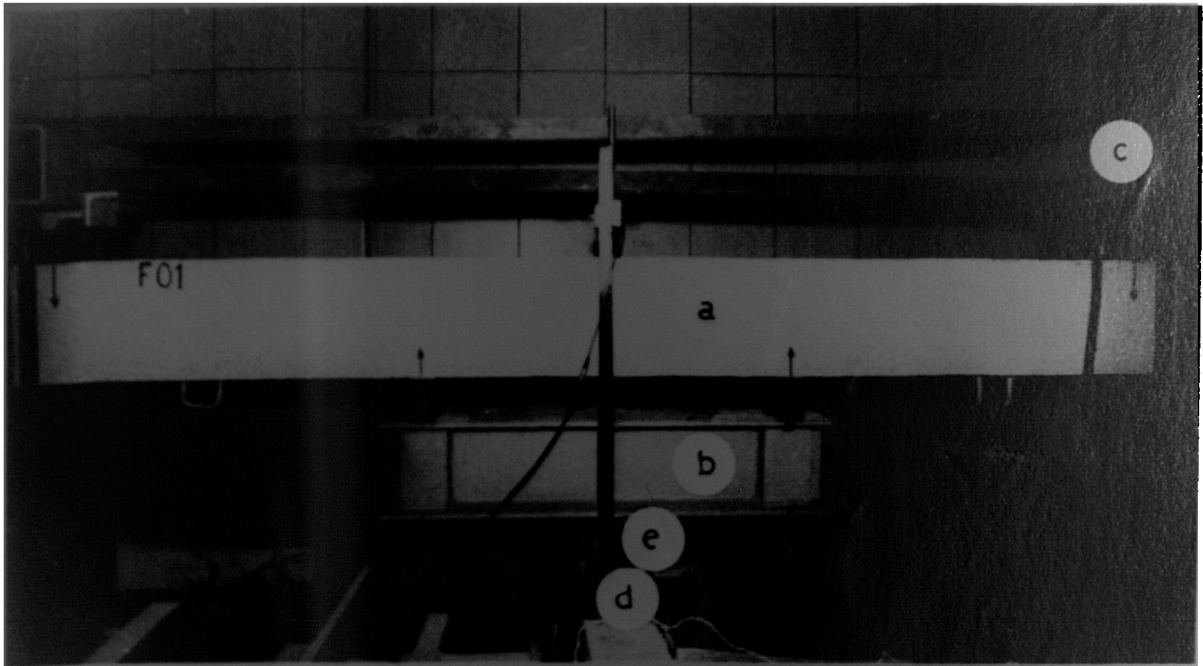
F22: Preloaded to 65kN or 31% of ultimate strength.

F23: Preloaded to 110kN or 52% of ultimate strength.

F24: Preloaded to 150kN or 71% of ultimate strength.

5.2.2 DETAILS OF BEAMS

All the beams had the same section, length and internal reinforcement (which was equal to 55% the value for balanced conditions). To avoid shear failures, 6mm diameter mild steel stirrups at 75mm centres were provided in the shear spans. The beams were 2.5m long, 155mm wide and 255mm deep. The plates were 2.2m long and 125mm wide. The epoxy adhesive layer was 1.5mm thick for all the beams. The beam details are shown in Fig.5.5.



- (a): Test beam
- (b): Spreader beam
- (c): Reaction frames
- (d): Hydraulic jack
- (e): Load cell

Fig.5.1: Loading rig 1

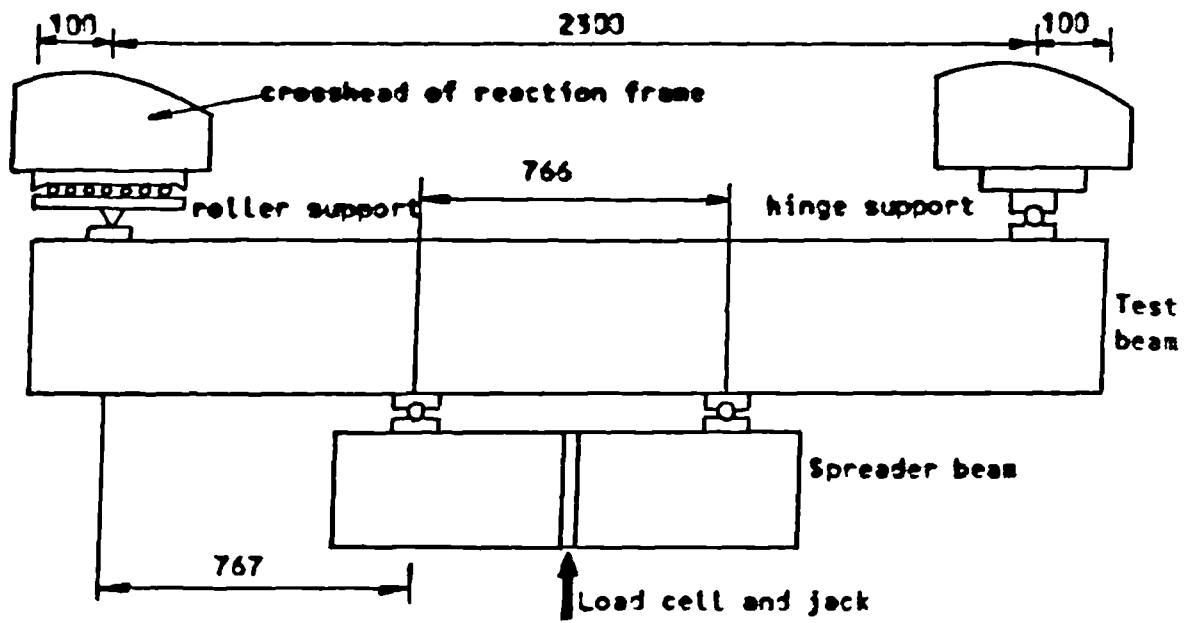


Fig.5.2: Loading rig 1 (hydraulic jack)

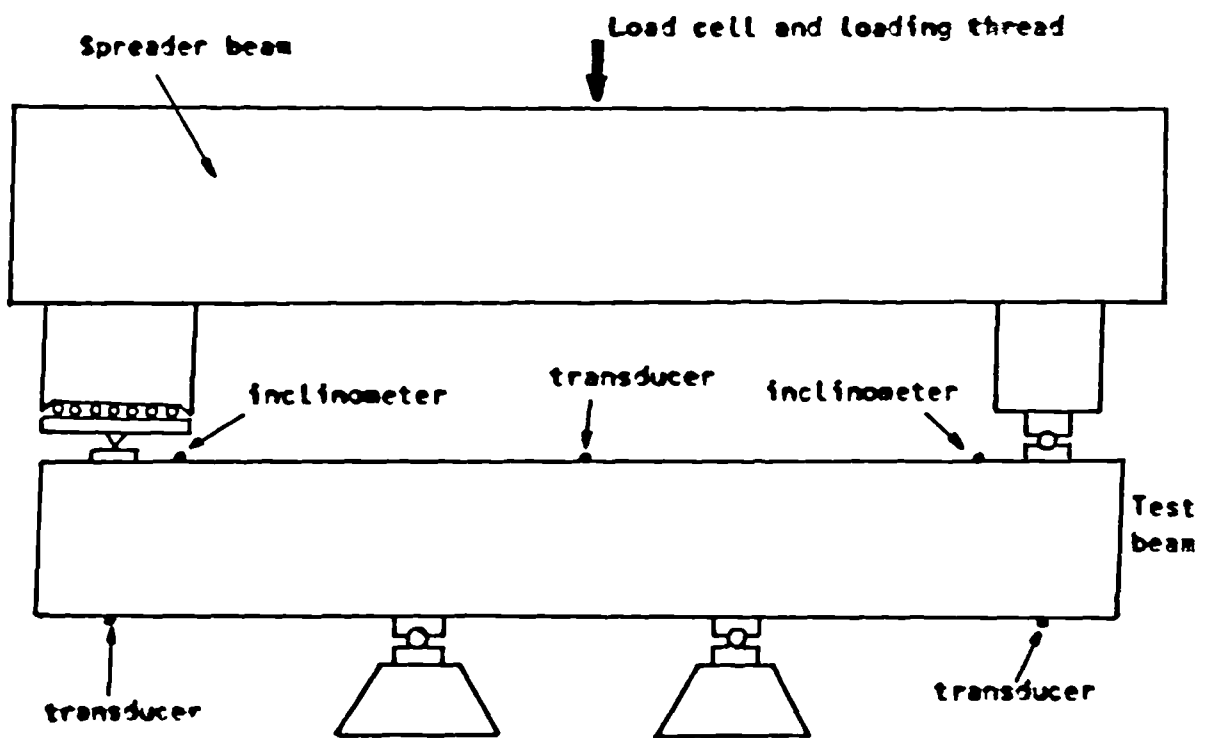
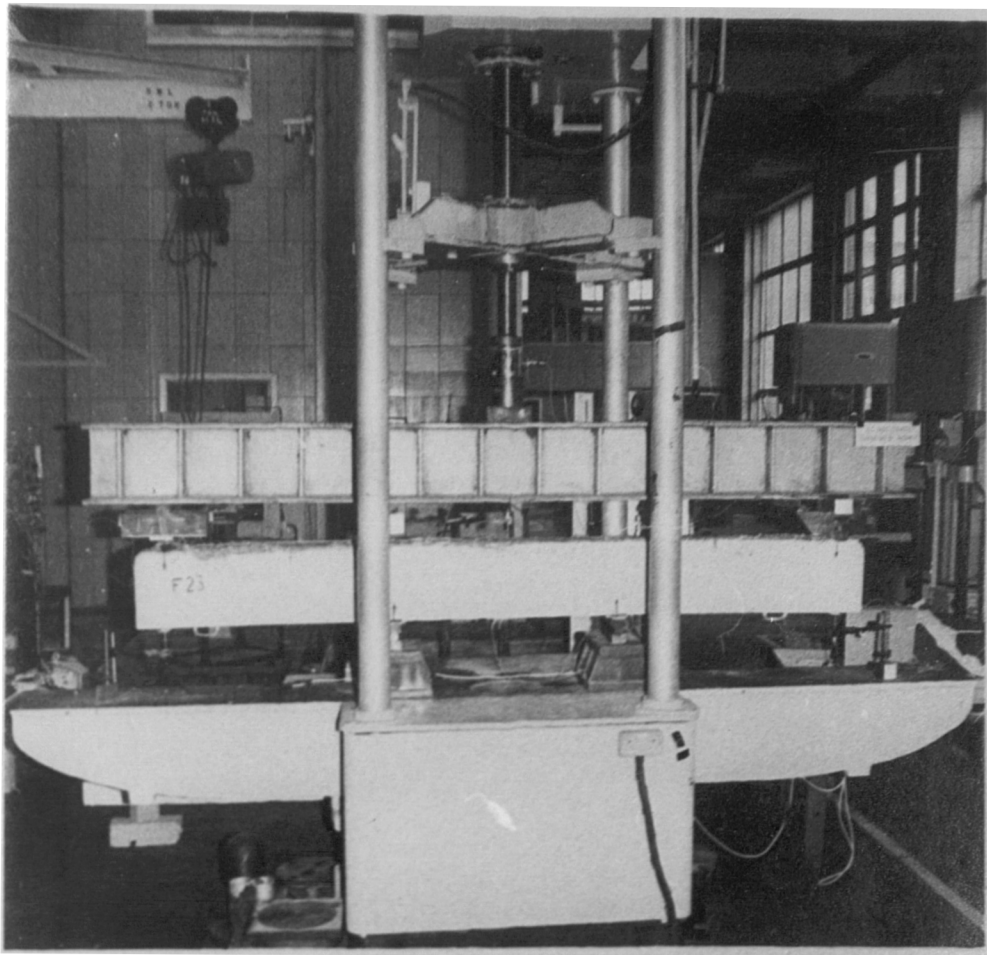
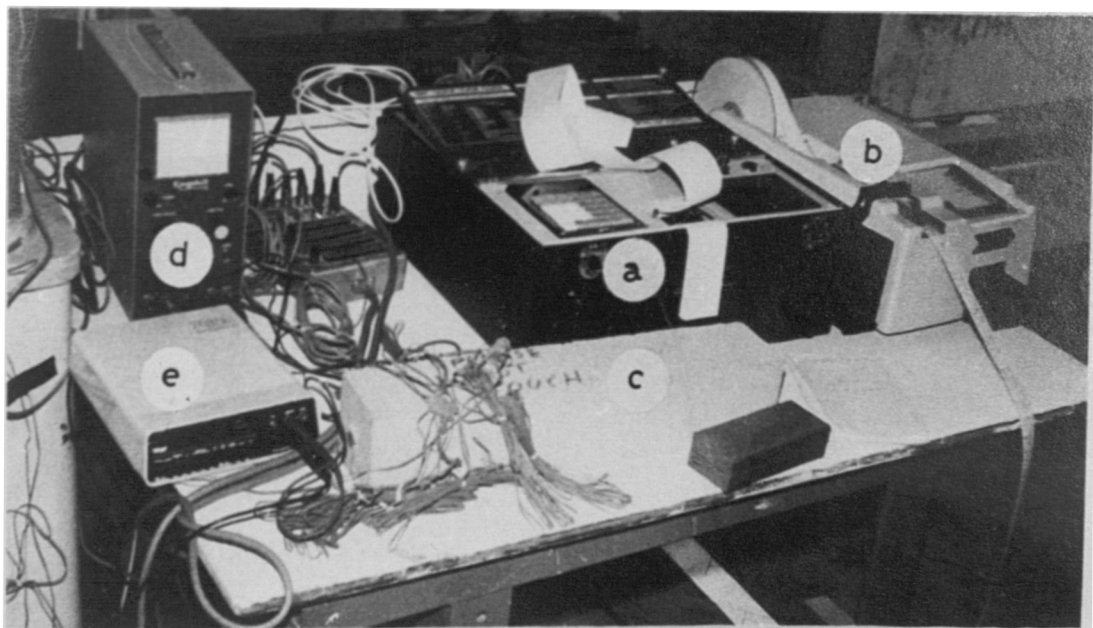


Fig.5.3: Loading rig 2 (Denison machine) and instrumentation



Denison machine



- (a): data logger
- (b): paper punch
- (c): Dummy strain gauges
- (d): Power supply
- (e): Voltmeter

Fig.5.4: Loading rig 2 and instrumentation

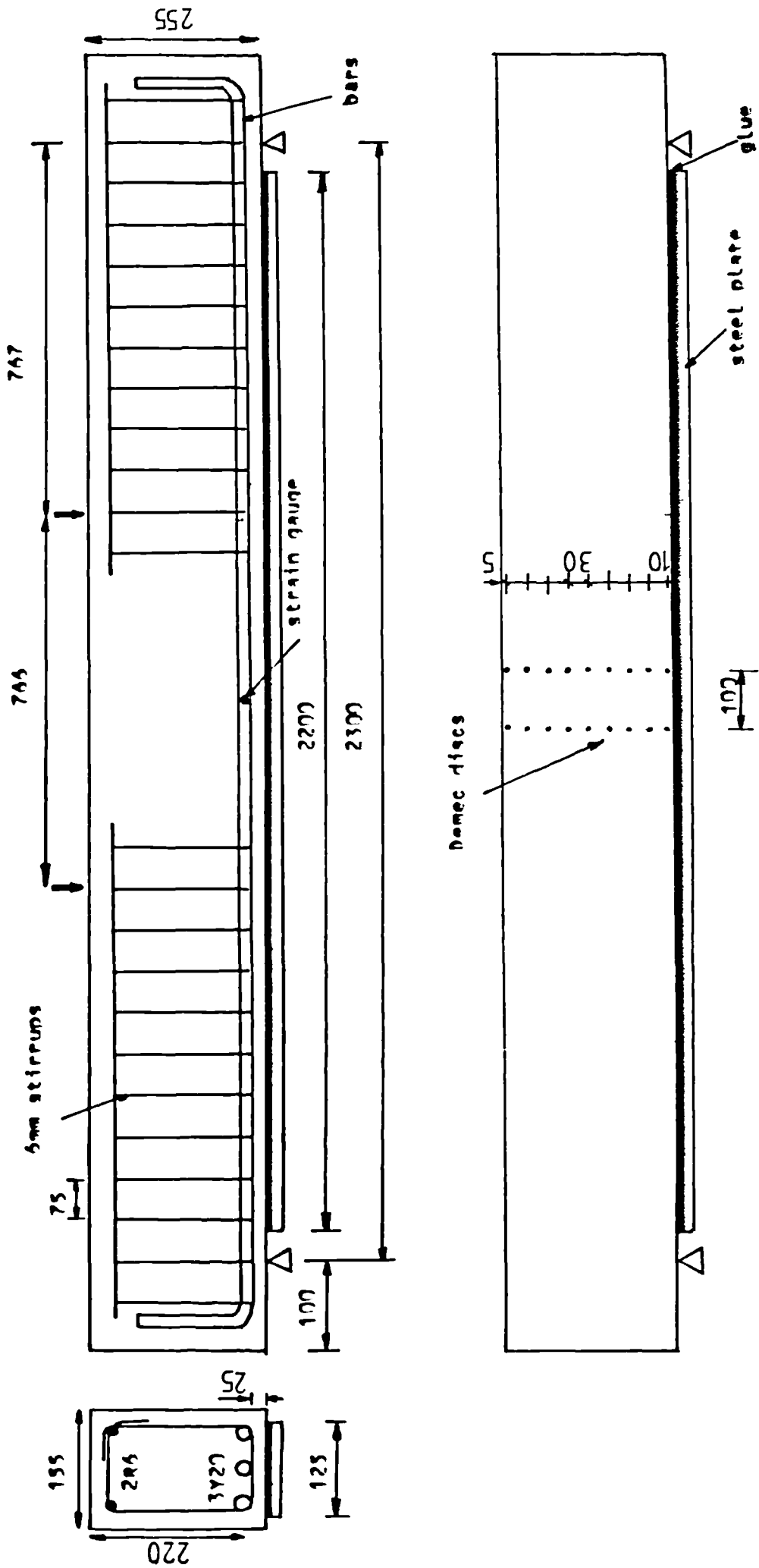


Fig. 3.5: beam details and instrumentation

5.2.3 MATERIALS

The properties of the materials and the concrete mix used in the manufacturing of the beams are described in detail in chapter three.

20mm diameter high yield steel bars were used. The 6mm diameter plain bars for shear stirrups and the external plates used were of mild steel.

The concrete mix used is the mix 4 described in chapter three. Crushed aggregates of a nominal size of 10mm, ordinary portland cement and dried river sand were used. The mix had a 28 days cube strength of 52.4 N/mm^2 . The concrete mix was used with the following weight ratios:

Cement : Sand : Cravel : Water

1 : 1.75 : 2.61 : 0.54

The properties of the components (cement, gravel and sand) and the manufacturing of concrete are described in chapter three. Also reported in chapter three are the properties of fresh and hardened concrete as recommended by the British Standards Institution -BSI- (78).

The epoxy resin used was manufactured by Colebrand under the code name of CXL 194. The properties of the adhesive are described in chapter four.

5.2.4 MANUFACTURING OF BEAMS

Prior to preparing the steel cage consisting of the longitudinal bars and stirrups (Fig.5.6), the bars were wire brushed to remove the millscale of the external surface.

Concrete was mixed in the same manner as described in chapter three. Six 100mm cubes for compressive strength, six 100mm diameter and 200mm long cylinders for indirect tensile strength and six 100x100x500mm prisms for modulus of rupture, were cast with each beam. The beams and control specimens were cast in two layers and thoroughly vibrated after each layer using a poker vibrator. They were then covered with polythene sheets for 24 hours before being stripped. After demoulding, the beams and control specimens were cured in uncontrolled laboratory conditions until required for testing.

5.2.5 BONDING PROCEDURE

After 28 days, the beams and steel plates were prepared for bonding. The bonding procedure was identical to that described in chapters two and four. Because of their large size, the plates were taken to a shotblasting company where they were abraded with steel grit of 340 micron mean size. To prevent warping of the plates, both faces of the plate were shotblasted.

Mixing of the epoxy adhesive was carried out in the same manner as described in chapters two and four. The adhesive was applied to both the concrete and plate surfaces. The joint thickness was 1.5mm and was controlled by small metal spacers. The plate was then applied and held in position by a uniformly distributed pressure obtained by a heavy metal beam clamped to the test beam (Figs.5.7 and 5.8). The pressure was maintained for four days and the beams were left for a further ten days before being tested at 42 days age.

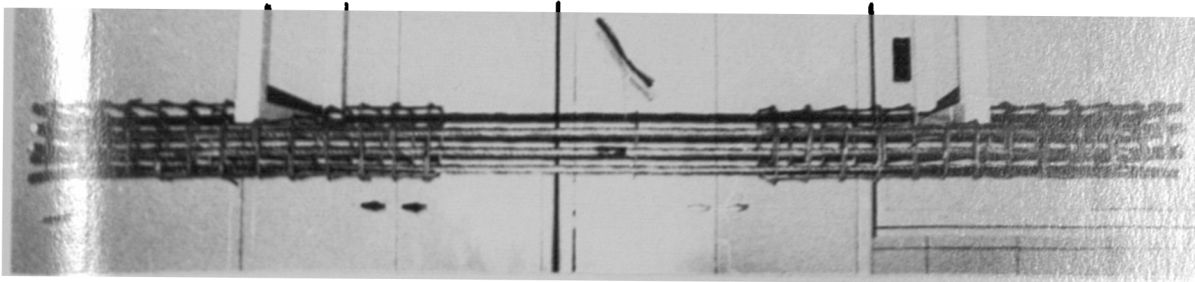
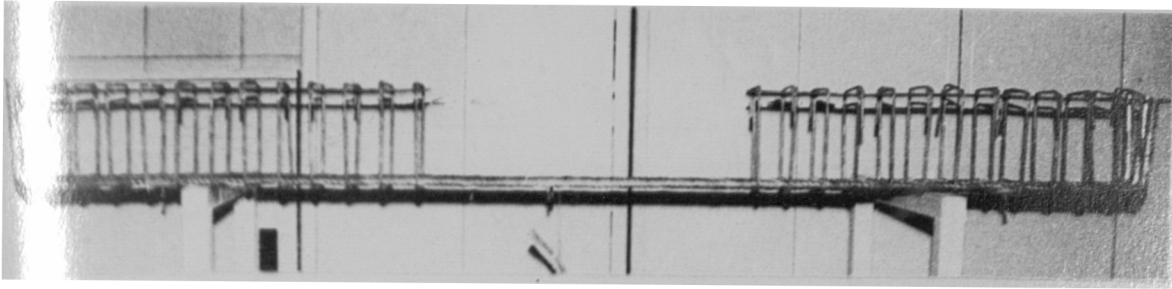


Fig.5.6: Internal reinforcement cage

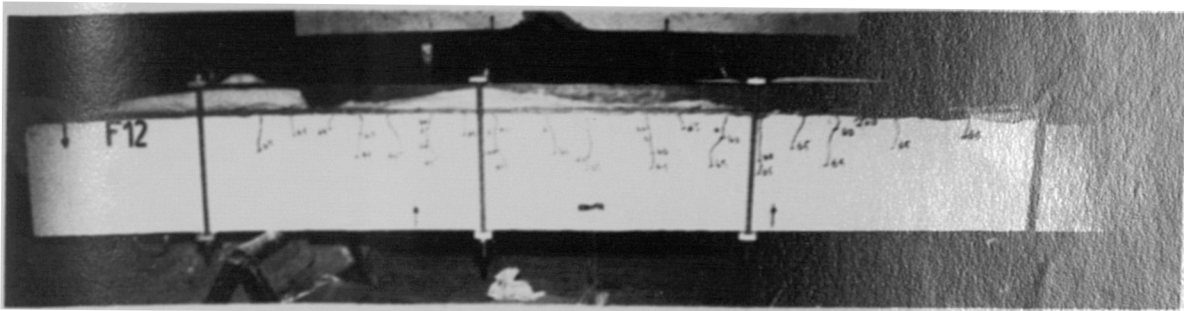


Fig.5.7: Curing of a beam of Series I and II

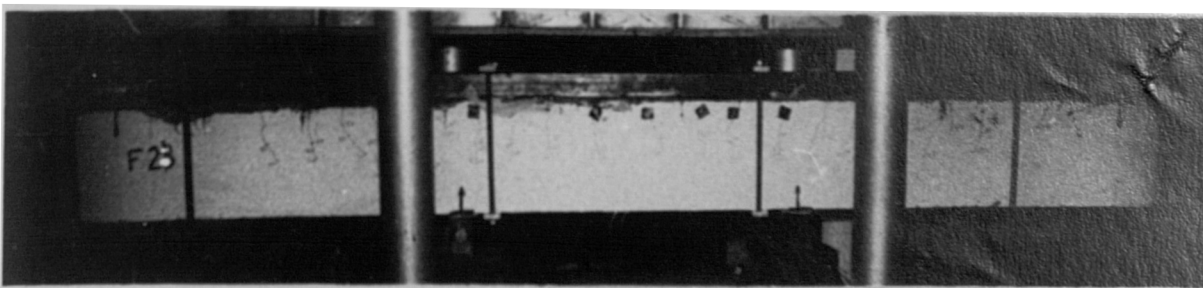


Fig.5.8: Curing under load of a beam of Series III

For the preloaded beams (Series II and III), preloading and subsequent plating were carried out at 28 days and testing to failure at 42 days age.

For the beams of Series III, the surface preparation was conducted before preloading and the bonding procedure after, under a constant load (Fig.5.8).

To facilitate crack viewing, all the beams were whitewashed the day prior to preloading or testing.

5.2.6 TEST MEASUREMENTS AND INSTRUMENTATION

For all the beams, the first crack load, central deflection, support rotations, concrete and steel strains, crack widths and ultimate load were measured.

(a) DEFLECTIONS: The deflections were measured at the middle section of the beam using calibrated electrical Linear Variable Displacement Transducers (LVDT).

(b) ROTATIONS: The rotations were recorded near the supports with an inclinometer with a sensitivity of one minute over a gauge length of 150mm and resting on small steel balls glued to the beam.

(c) CONCRETE STRAINS: The concrete strains were measured in the middle face of the beam at different positions across the beam depth (Fig.5.5). They were recorded using a mechanical demec extensometer of 100mm gauge length with a sensitivity of 16 microstrains. The demec discs were glued on the beam with 'Plastic Padding'.

(d) STEEL STRAINS: The internal steel bar strains were recorded using 2mm Kyowa electrical strain gauges using the calibration factors determined by the direct tensile tests on the bars described in chapter three. The measuring Wheatstone bridge was formed by one active strain gauge and three similar 'dummy' strain gauges fixed on a bar covered by concrete. The dummy gauges were used to balance any undesirable variation of resistance that may be caused by the environmental conditions. This is more explained in Appendix A. The plate strains were measured along the middle line with a 100mm demec gauge. The bar and plate strains were recorded at the middle section of the beam. The epoxy resin strain was measured only on beam F02 with a glue layer and without plate.

(e) CRACK WIDTHS: The appearance of first cracks and their propagation was detected visually using a magnifying glass. The development of cracks was marked with a pencil after each load increment. The widths of the first eight flexural cracks were measured in the constant moment region with a microscope with a sensitivity of 0.02 mm at the level of the internal steel bars.

(f) LCADS: Loading was controlled and measured with a linear differential voltmeter connected to a calibrated 50 ton load cell.

A portable Imp data logger and a paper punch were used to record the electrical outputs from the load cell, strain gauges and transducers.

5.2.7 TESTING APPARATUS

The beams were loaded at third point over a span of 2300mm with their tension face uppermost to facilitate plate strain measurements and the bonding procedure for the preloaded beams of Series III. Two rigs were used in the testing:

In the first rig, the load was applied upwards at positions 383mm on either side of the midspan by means of a stiffened 200mm deep, wide flange, steel spreader beam resting on a 50 ton capacity hand operated hydraulic jack at its mid-point. The electrical load cell was positioned between the jack and the spreader beam. The reactions were provided by two pairs of 50mm diameter Macalloy bars up to crossheads that were secured at the top. One end was a fixed support and the other moving on rollers longitudinally. Both supports allowed rotation. Rig 1, shown in Figs.5.1 and 5.2, was used for all the beams except for the preloaded beams of Series III which needed to be kept under a constant load (to allow the glue to cure) for two weeks before increasing the load up to failure. It was decided to use another device where the load losses would be minimum.

Rig 2 is a 50 ton Denison machine with an excellent controllable strain loading system. The static loading was identical to that of rig 1 except that the load was applied downwards through the load cell and a stiffened 280mm deep steel beam spreading over a span of 2300mm. The load was monitored by the speed of the vertical movement of the 70mm diameter steel thread of the Denison machine. Rig 2 is shown in Figs.5.3 and 5.4.

5.2.8 TESTING PROCEDURE

The total load on the test beam was taken to be equal to the applied load from the hydraulic jack or the Denison machine, plus the weight of crossheads (rig 1) or the spreader beam (rig 2). The self weight of the test beam was ignored. The load was applied in increments of 5kN until the first crack appeared and subsequently in increments of 20kN until the preloading or failure load was reached. After each increment, the different test measurements were recorded and the development of cracks marked with a pencil. After failure, the cracks were outlined by thick black marking and the beams photographed.

The preloaded beams of Series II were unloaded in similar increments, removed from the testing rig, then strengthened and tested to failure two weeks later.

The beams of Series III were strengthened under a constant load and kept under the same load for two weeks to allow the cure of the epoxy bond. The load was adjusted twice daily. After 14 days, the load was increased up to failure of the beams.

The manual test measurement (rotations, concrete and plate strains, crack propagation and crack widths) and the electrical measurements (deflections, bar strains, loads) were all recorded at each load level during the preloading, unloading (curing under constant load) and testing. At ultimate loads, the data logger and paper punch were monitored to take continuous readings in order to record the ultimate loads, deflections and strains. The paper tapes were subsequently fed into a computer with the other test results for data analysis and graph plotting. The analysis of the sections of the beams,

the computation of the deformations, crack widths and strengths, and the computer flowcharts used are described in Appendices C, D and E.

5.3 RESULTS

All beams failed as under reinforced beams by compressive crushing of concrete after yielding of the reinforcement. There was an increase in the stiffness and strength of the plated beams and a reduction in their deflections, rotations, strains and crack widths as compared to the unplated beam. There was a delay in the appearance of first cracks. The crack pattern of the plated beams was similar to that of the unplated beam at service loads but at higher loads there was a significant difference in the crack pattern:

The plates prevented the principal cracks from widening freely and this resulted in a Δ shaped cracking developing from the principal cracks in the concrete cover towards the plate (Figs.5.9 and 5.10). Testing of the beam F02 of Series I, with a glue layer only, showed that for the amount of internal reinforcement used (55% of the balanced conditions ratio), the epoxy layer did not crack with concrete and remained uncracked until failure. It was therefore justified to consider the epoxy glue not only as an agent transmitting stresses from concrete to steel but also as a full participant in the resistance of the beam. Epoxy glue was therefore taken into account in the structural calculations of the composite sections of the plated beams (which had a higher ratio of reinforcement than beam F02). It must be pointed out that taking epoxy resin into account cannot be justified in beams with a lower ratio of total reinforcement than that of beam F02. Epoxy may well crack

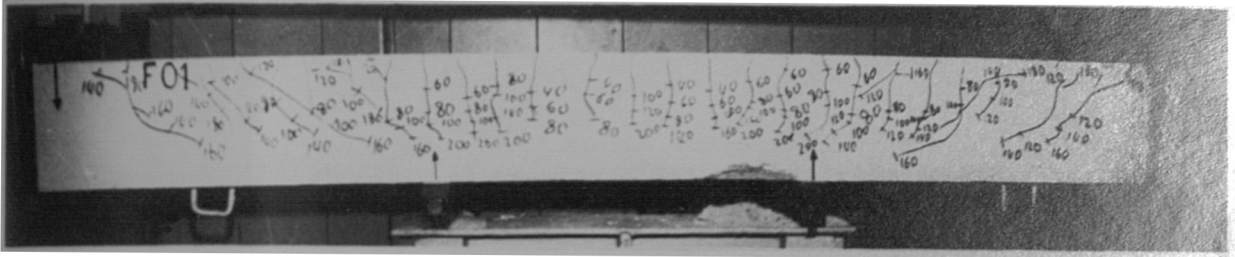


Fig. .9: rack pattern in an unplated beam

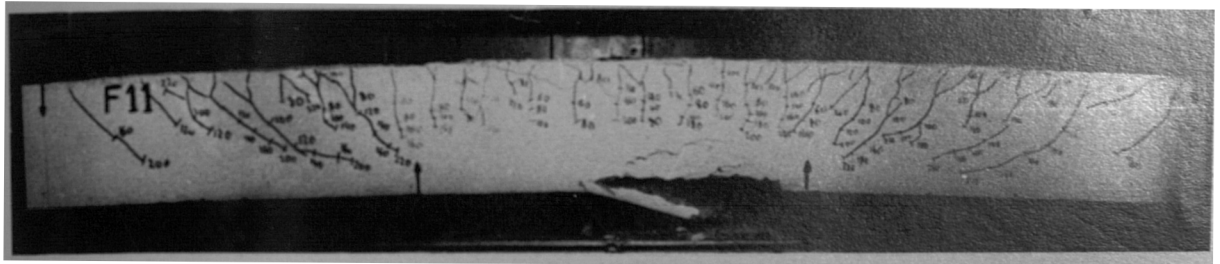


Fig.5.10: Crack pattern in a plated beam

before breaking point in very under reinforced beams (with less than 15% of steel) and where failure is likely to occur by breaking of the steel bars after excessive plastic deformations. Tensile tests on epoxy, described in chapter four, showed that the ultimate strain of the adhesive was about 20,000 microstrains, which is less than the ultimate tensile strain of steel. Furthermore, direct tension tests on steel strips coated with an epoxy layer showed that the adhesive cracked before breaking of the specimens.

Absolute and quantitative comparison of the results of the unplated and plated beams is of little importance as the effectiveness of the additional reinforcement has already been proven. A plated beam may sustain a higher load than an unplated one and yet fail prematurely before developing its full flexural strength. The following sections concentrate more on relative studies of the results by comparing non-dimensional parameters such as the ratios of experimental to theoretical strength or deformation or crack width. The theoretical models used were derived from elastic theory or methods proposed by various codes of practice or other researchers. Although the proposed formulae were only valid in serviceability conditions, they were also used at low and high loads. The predicted results were therefore not always very satisfactory but they were very useful in a relative study and comparison of the behaviour of plated and unplated beams.

The strength and elastic modulus of the materials (concrete, steel and epoxy), used in the analysis of the beams, were those determined by the tests described in chapters three and four. Table 5.1 shows the control test results of the flexural beams.

Table 5.1: Flexural beams.

Beam No.	F01	F02	F11	F12	F13	F14	F22	F23	F24
Age				28	28	28	28	28	28
(1)									
(2)		28	28	28	28	28	28	28	28
(3)	42	42	42	42	42	42	42	42	42
Cube strength				50.3	50.5	49.7	49.9	50.3	51.0
(1)									
(3)	52.4	52.0	53.3	55.1	53.1	52.2	52.1	52.4	52.1
Mod. rupture									
(3)	4.93	4.56	4.93	4.48	4.71	4.49	4.58	4.64	4.93
Ind. tensile strength									
(3)	3.93	3.37	3.52	3.73	3.93	3.31	3.48	3.50	3.42
Glue thick.									
(mm)	-	3.0	1.5	1.5	1.5	1.5	1.5	1.5	1.5
Plate thick.									
(mm)	-	-	1.5	1.5	1.5	1.5	1.5	1.5	1.5

(1): At preloading
(2): At strengthening
(3): At testing

The cube strength at testing varied from 52.0 to 55.1 N/mm² and the modulus of rupture from 4.48 to 4.93 N/mm². The use of the cube strength of 53.0 N/mm² (determined by the material tests described in chapter three) results in a variation of 1.0% only in the ultimate flexural strength of the beams. As the value of the modulus of elasticity of concrete used was the same for all the beams (32.05 kN/mm² determined by the material tests described in chapter three), it was decided to use the same cube strength in the analysis of the beams.

The deformation, cracking, stiffness and strength results of the flexural beams are presented and analysed in detail in the following sections.

5.4 DEFORMATION PROPERTIES

5.4.1 DEFLECTIONS

Figures 5.11 to 5.13 show the load-deflection curves of the flexural beams. Table 5.2 gives the theoretical and experimental deflections at different load levels before and after cracking.

The theoretical deflections were computed using three methods derived from those of CP110 (79), CEB (80) and ACI (81) codes. Computation of the deflections is described in Appendix E.

For the preloaded beams of Series III, the deflections were determined as a superposition of two components:

$$\text{Defl.} = \text{Defl.1} + \text{Defl.2}$$

Defl.1: Deflection of the unplated beam under the preloading load.

Defl.2: Deflection of the plated beam under a load equal to the considered load minus the preload.

During the two weeks of bond curing under a constant load, the

Table 5.2: Experimental and theoretical deflections at different load levels.

Beam NO.	Experimental deflections (mm)			Theoretical deflections (mm)						Exp./Theo. (CEB)			
	20kN	100kN	200kN	20kN		100kN		200kN		20kN	100kN	200kN	
				(1)	ACI	CEB	CP110	ACI	CEB	CP110			
F01	1.14	6.10	16.10	0.543	4.91	5.62	4.80	9.94	12.26	9.78	2.09	1.09	1.31
F02	1.14	5.78	14.70	0.543	4.73	5.40	4.60	9.51	11.48	9.35	2.10	1.07	1.28
F11	0.92	4.85	13.34	0.542	3.98	4.60	3.89	8.05	9.98	7.92	1.70	1.05	1.34
F12	0.97*			.543*							1.79*		
	0.87	4.62	12.30	0.542	3.98	4.60	3.89	8.05	9.98	7.92	1.61	1.00	1.23
F13	0.90*	5.20*		.543*	4.91*	5.62*	4.80*				1.66*	0.93*	
	0.86	4.90	11.90	0.542	3.98	4.60	3.89	8.05	9.98	7.92	1.59	1.07	1.19
F14	1.13*	5.94*		.543*	4.91*	5.62*	4.80*				2.08*	1.06*	
	0.80	4.60	10.70	0.542	4.91	5.62	4.80	8.05	9.98	7.92	1.48	1.00	1.07
F22	1.00*	5.37E	11.9E	.543*	4.18	5.17	4.33	8.49	10.55	8.36	1.84*	1.04E	1.12E
		7.42	13.90								1.43	1.32	
F23	0.98*	5.97*	12.2E	.543*	4.91*	5.62*	4.80*	8.99	11.12	8.79	1.80*	1.06*	1.10E
			14.25										1.28
F24	1.20*	6.20*	12.7E	.543*	4.91*	5.62*	4.80*	9.28	11.62	9.17	2.21*	1.10*	1.09E
			15.70										1.35

£: Excluding variations during the 2 weeks of bond curing

*: Values at preloading (unplated)
(1): CP110, ACI and CEB

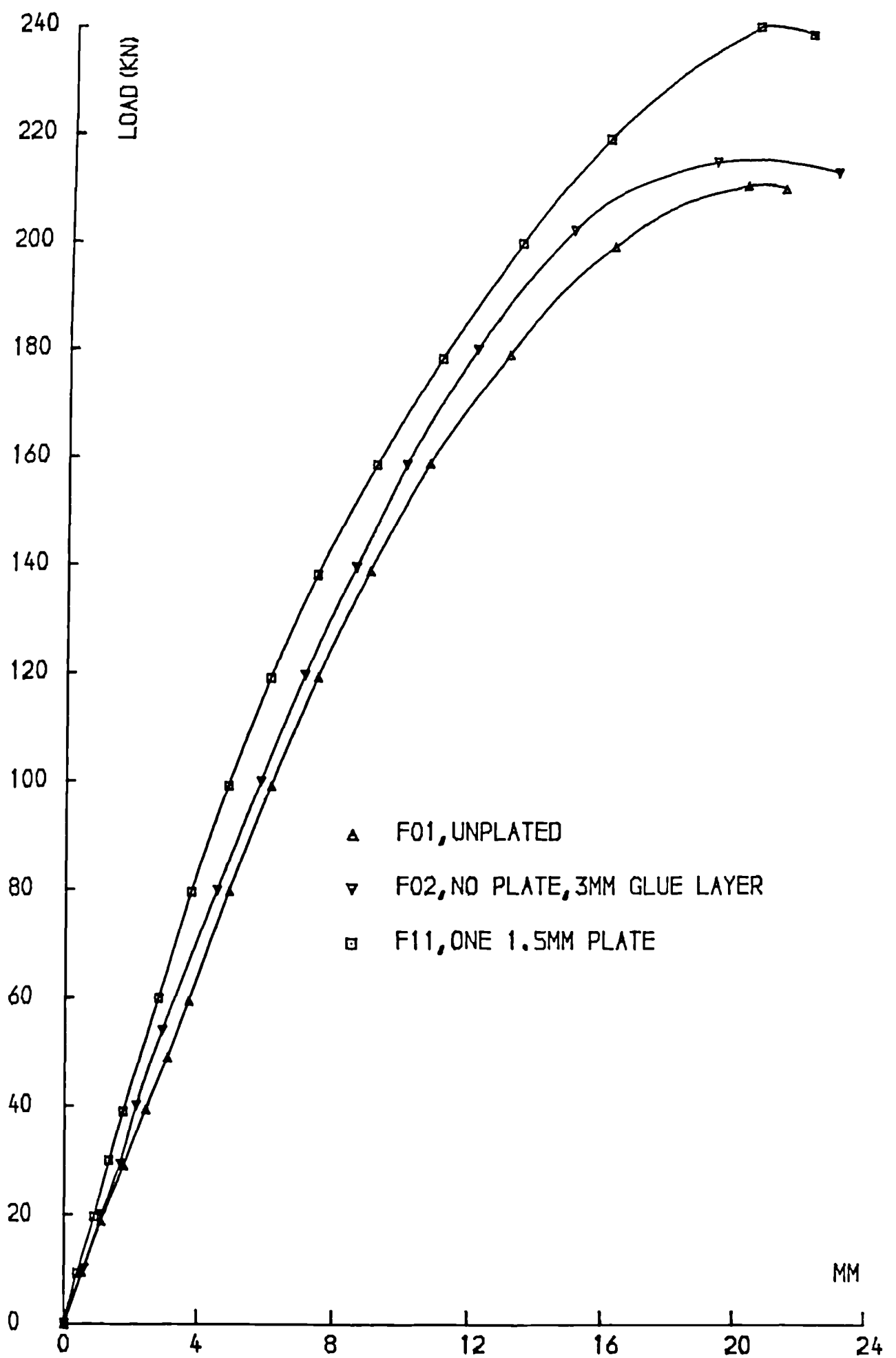


FIG.5.11 ,LOAD-DEFLECTION CURVES

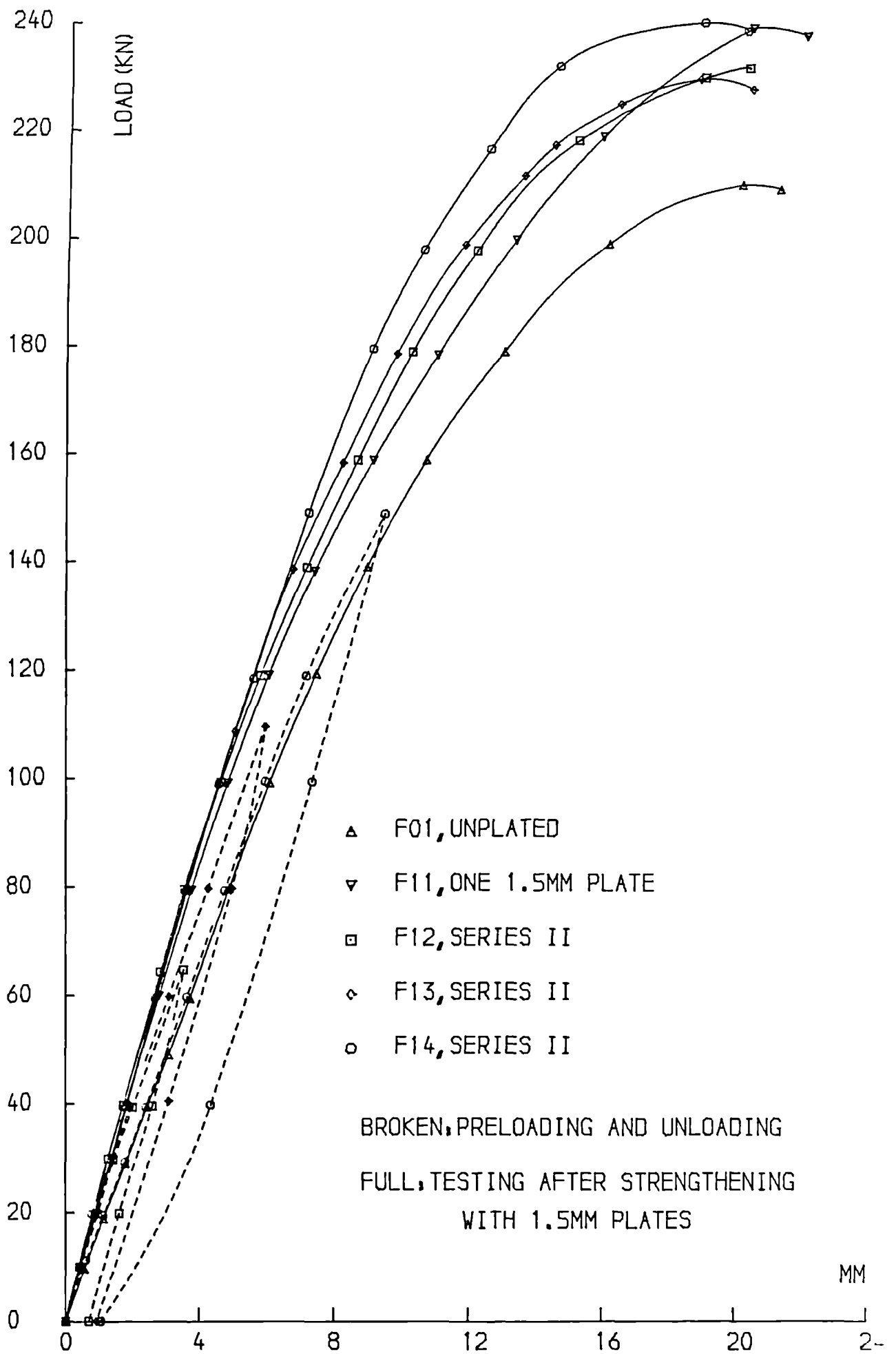


FIG.5.12 ,LOAD-DEFLECTION CURVES

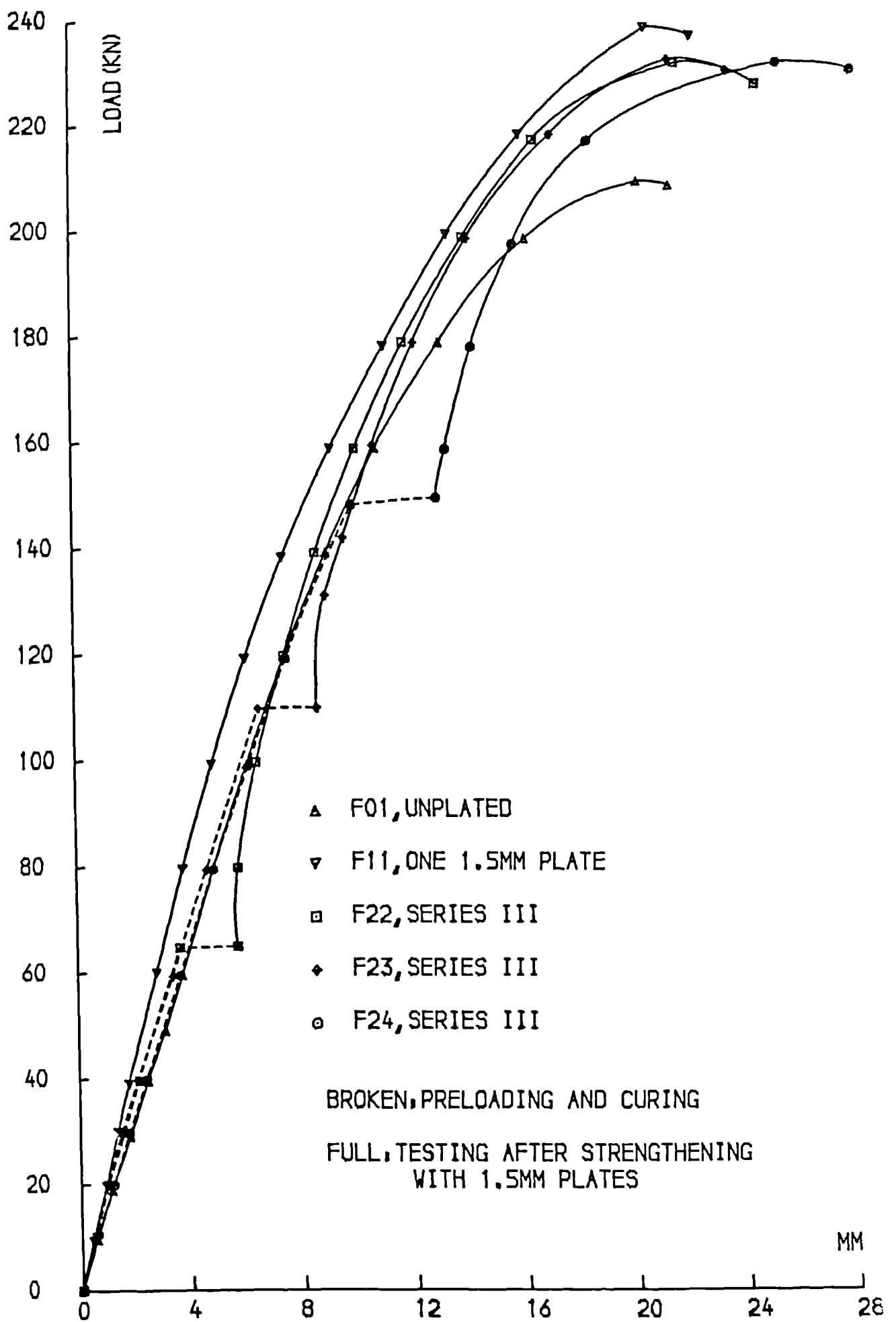


FIG.5.13 ,LOAD-DEFLECTION CURVES

preloaded beams F22, F23, F24 underwent further deflections. This time variation was higher with higher preloading loads (Table 5.2 and Fig.5.13). The theoretical predictions do not allow for these time variations.

In general the CEB formula gave better predictions. For all beams, the ratio of experimental to theoretical deflection was near unity at service loads and greater for lower or higher loads confirming that the methods of the three codes are more suitable in service conditions.

The preloaded, unloaded and subsequently strengthened beams F12, F13, F14 of Series II behaved like the unplated beam F01 during preloading and like the plated beam F11 during testing (after they were plated). Fig.5.12 shows the deflections at preloading, unloading and testing. The deflections of the preloaded beams were the same or slightly less than those of beam F11. After unloading, the beams had to be taken out of the loading rig to be strengthened. The residual deflections could not therefore be measured and were consequently not taken into account at the testing. The slight increase in the stiffness of the preloaded beams of Series II (Table 5.2) may therefore be the result of the non-allowance for the residual deflections.

The load-deflection curves of the preloaded beams F22, F23, F24 of Series III (Fig.5.13) shows the time variations of the deflections during the two weeks of bond curing under a constant load and also illustrates the stiffening effect of the plates when the load was increased to failure.

At a load of 100kN, the ratio was 1.05 for unplated beams and 1.03 for the beams with 1.5mm plates. The unplated beam result is the average from the testing of the beam F01 (unplated) and the preloading of the beams F13 and F14 (Series II), and F23 and F24 (Series III). The 1.5mm plate result is the average from the testing of beam F11 and beams F12, F13 and F14 (after they were strengthened). These ratios suggest that the stiffening effect of the external steel plates may be slightly greater than that of an equivalent amount of internal reinforcement designed to achieve the same performance.

5.4.2 ROTATIONS

The theoretical rotations were computed using three models derived from those of CP110 (79), CEB (80) and ACI (81) codes (see Appendix E). The predicted and recorded values before cracking, at service loads and near ultimate loads, are given in Table 5.3.

The rotation results (Figs.5.14 to 5.16 and Table 5.3) were similar to those of the deflections and the same conclusions can be drawn.

The CEB method gave better predictions. The ratios of measured to predicted values were near unity at service loads and greater before cracking or near ultimate loads.

At a load of 100kN, the ratio was 1.05 for the unplated beams and 1.01 for beams with a 1.5mm thick plate, again suggesting that the stiffening effect of the external plates is greater than that of conventional reinforcement designed to produce the same performance.

Table 5.3: Measured and predicted rotations at different load levels.

Beam No.	Experimental rotations(min)		Theoretical rotations(min)						Exp./Theo. (CEB)			
	20kN	100kN	20kN	100kN		200kN		20kN	100kN	200kN		
			(1)	ACI	CEB	CP110	ACI	CEB	CP110			
F01	3.90	25.50	2.44	22.02	25.20	21.53	44.61	54.99	43.88	1.60	1.01	1.44
F02	3.50	25.50	2.44	21.78	24.87	21.01	43.98	54.12	43.13	1.43	1.03	1.41
F11	2.83	22.01	2.43	17.87	20.65	17.47	36.10	44.75	35.54	1.17	1.07	1.43
F12	4.6*		2.44*							1.89*		
	2.83	20.98	2.43	17.87	20.65	17.47	36.10	44.75	35.54	1.17	1.02	1.46
F13	3.3*	25.1*	2.44*	22.0*	25.2*	21.5*				1.35*	1.00*	
	3.05	20.00	2.43	17.87	20.65	17.47	36.10	44.75	35.54	1.26	0.97	1.25
F14	4.4*	28.7*	2.44*	22.0*	25.2*	21.5*				1.80*	1.14*	
	2.66	20.42	2.43	17.87	20.65	17.47	36.10	44.75	35.54	1.10	0.99	1.45
F22	4.1*	21.4E	2.44*	18.75	23.21	19.43	38.07	47.31	37.51	1.68*	0.92E	1.30E
		24.00								1.03	1.35	
F23	4.1*	26.9*	2.44*	22.0*	25.2*	21.5*	40.32	49.87	39.43	1.68*	1.07*	1.29E
												1.38
F24	3.8*	26.3*	2.44*	22.0*	25.2*	21.5*	41.63	52.15	41.14	1.56*	1.04*	1.23E
												1.40

£: Excluding variations during the 2 weeks of bond curing. *: Values at preloading (unplated) (1): CP110, ACI and CEB

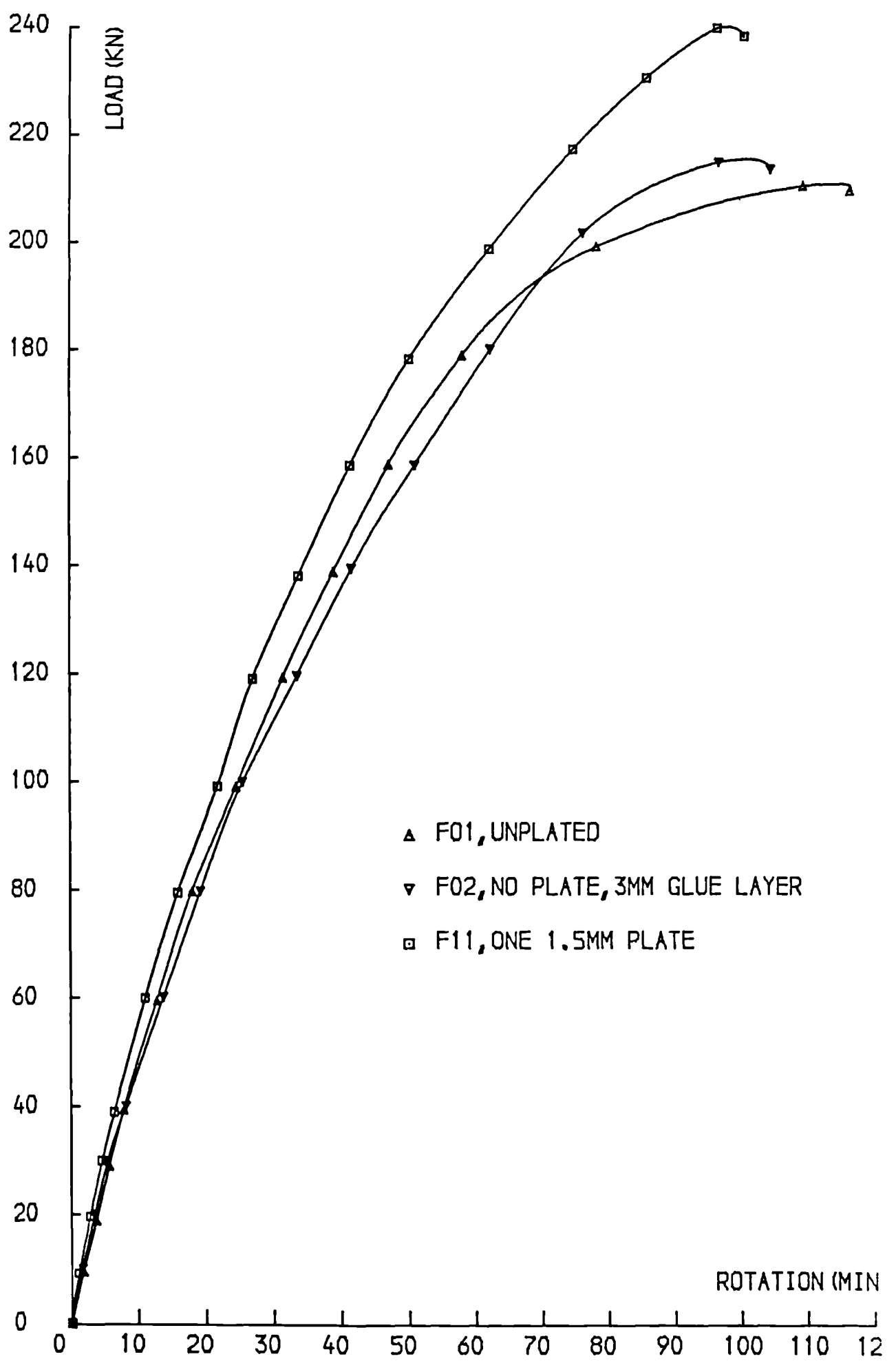


FIG.5.14 ,LOAD-ROTATION CURVES

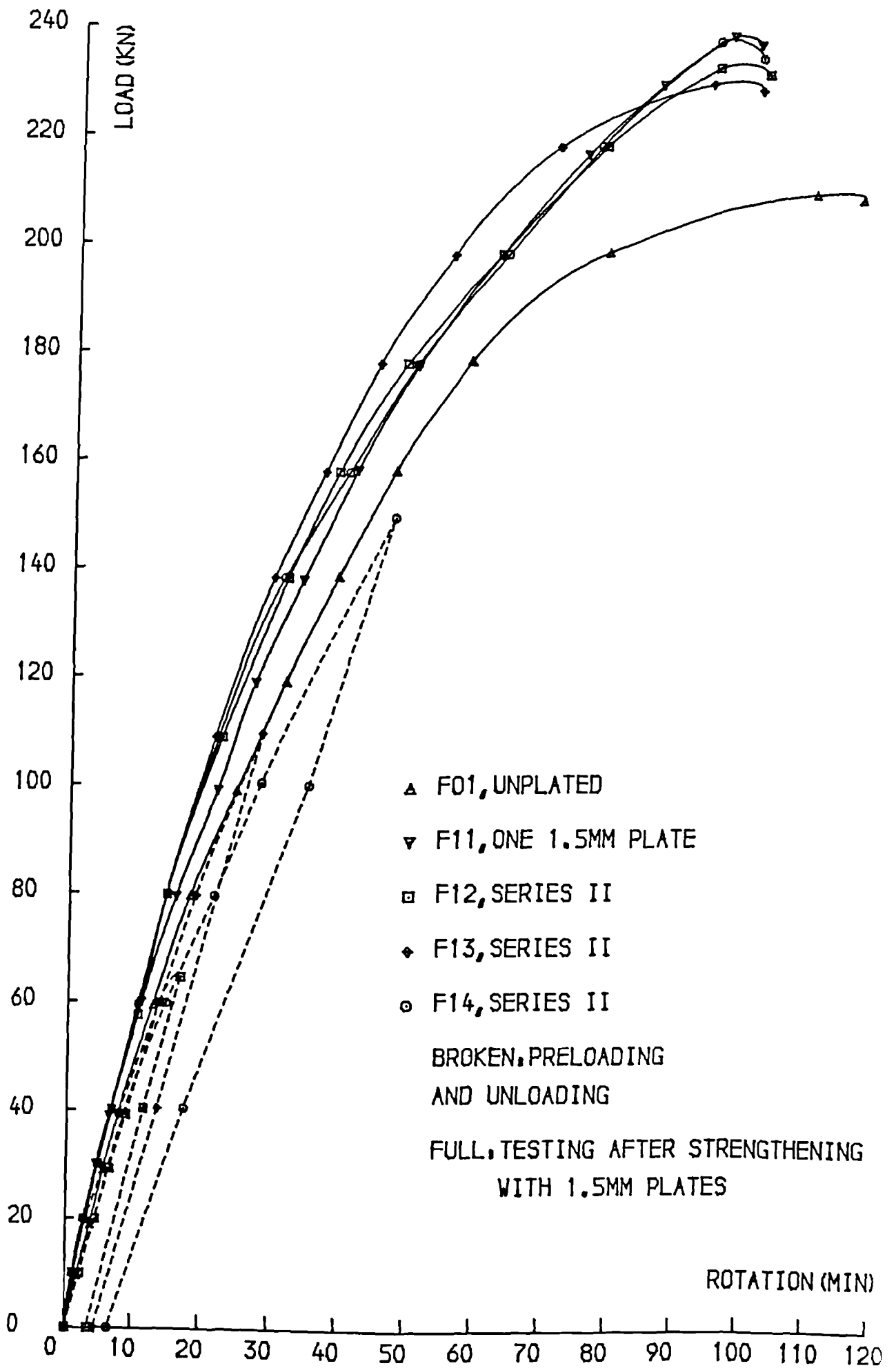


FIG. 5.15 , LOAD-ROTATION CURVES

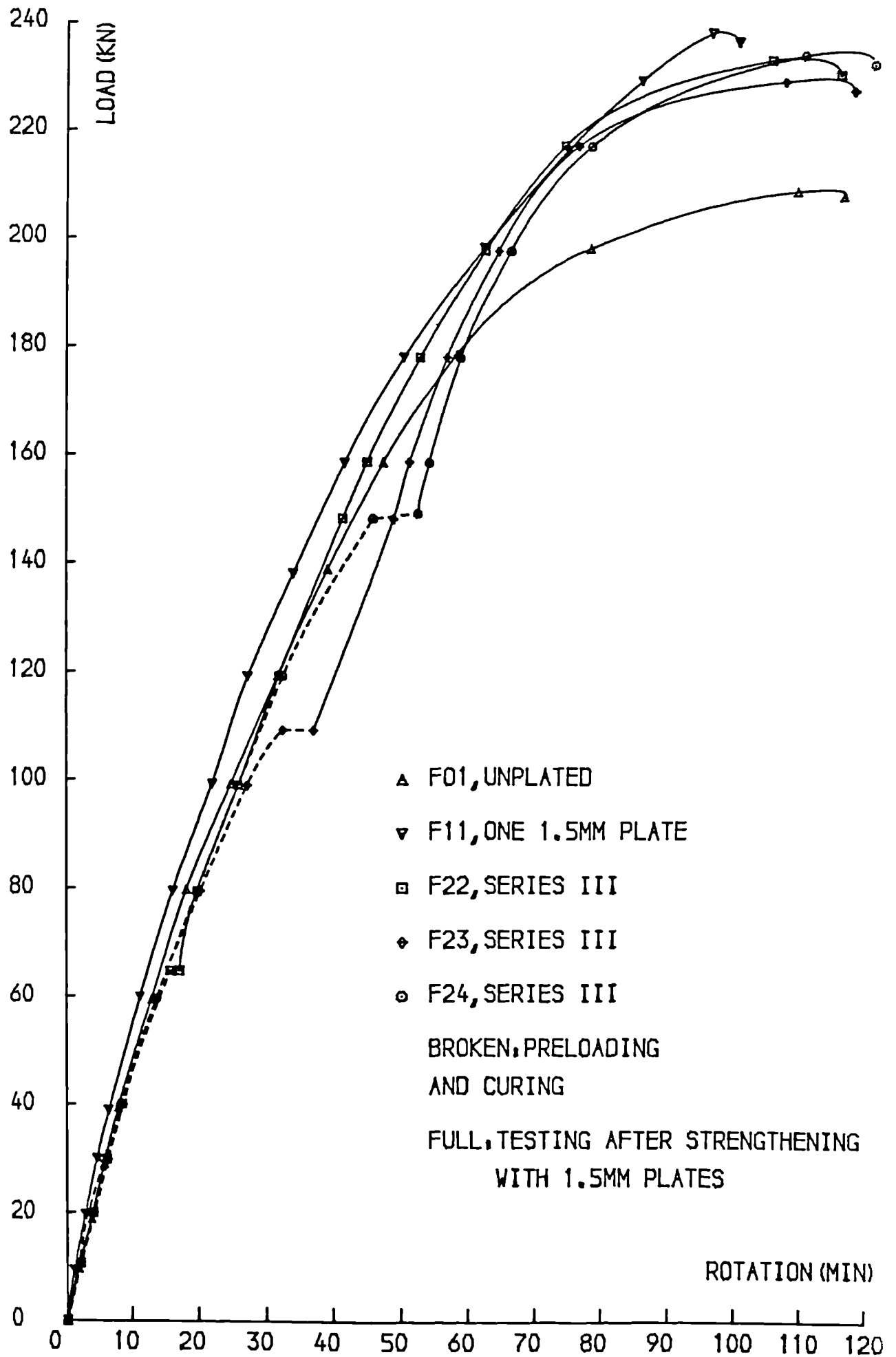


FIG.5.16 ,LOAD-ROTATION CURVES

There was no significant difference in the rotational behaviour of the preloaded, unloaded and subsequently strengthened beams F12, F13, F14 of Series II and the plated beam F11 (Fig.5.15).

As expected, the preloaded beams F22, F23, F24 of Series III behaved as unplated beams at the preloading stage and as plated beams thereafter. There was a slight increase in their rotations during the two weeks of bond curing under a constant load (Table 5.3 and Fig.5.16). This time variation was more pronounced with higher preloading loads.

5.4.3. STRAINS

The theoretical strains for concrete, bar reinforcement and steel plate were computed at different load levels using an elastic analysis and the cracked transformed sections. The value of the concrete modulus of elasticity used was that determined by prism tests according to the BSI recommendations (78) as described in chapter three. The recommended elastic modulus was the average value measured on the prism at a load equivalent to a third of the ultimate cube strength (78). The theoretical model was therefore more suitable in service conditions. The model was nevertheless used at low and high load levels as a means of comparison between the unplated and plated beams.

Tables 5.4, 5.6 and 5.7 show the experimental and theoretical concrete, bar and plate strains at different load levels. Two important observations can be made:

(a) For the same beam, the ratio of measured to predicted strain increases with the load. This can be explained by the fact that the theoretical model is based on an ideally elastic

concrete whereas the actual stress-strain of concrete is non-linear and the secant modulus decreases with the load.

(b) For the same load, the ratio of experimental to predicted strain decreases from the unplated beams to the plated ones. At a load of 100kN, the ratio of measured to predicted bar strain was 0.99 for unplated beams and 0.80 for beams with 1.5mm thick plates. Again, the unplated beam result is the average from the testing of beam F01 and the preloading of beams F13, F14, F23 and F24. The 1.5mm plate result is the average from the testing of beam F11 and beam F12, F13 and F14 (after they were strengthened). This also can be explained by the same reason: The theoretical model is designed for a certain service load. A given load does not represent the same percentage of the ultimate strength for unplated or plated beams. A load of 100kN is equivalent to 48% and 42% respectively of the ultimate flexural capacities of unplated beams and beams with 1.5mm plates. The parabolic stress-strain relationship of concrete means that the lower the percentage of load considered, the higher the stiffness of the beam.

5.4.3.1 CONCRETE STRAINS

The theoretical and experimental concrete compressive strains are given in Table 5.4. The experimental strains were measured across the beam depth (Fig.5.5). The compressive strain was given by the gauge at 5mm from the compression face. The tensile strain was given by the gauge at 10mm from the tension face.

At a load of 100kN, the ratio of measured to predicted strain was 1.21 for unplated beams and 1.14 for plated beams, supporting the conclusions drawn before.

Table 5.4: Measured and predicted concrete compressive strains at different service loads.

Beam No.	Experimental concrete compressive strain (10^{-3})				Theor. concrete compressive strain (10^{-3})			Exp./Theo.		
	50kN	100kN	150kN	Max.	50kN	100kN	150kN	50kN	100kN	150kN
F01	.48	1.08	1.86	4.70	.42	.84	1.26	1.14	1.29	1.48
F02	.51	1.13	1.85	5.50	.42	.84	1.25	1.21	1.35	1.48
F11	.44	.94	1.40	4.50	.41	.81	1.22	1.07	1.16	1.15
F12	.49*				.42*			1.17*		
	.43	.91	1.36	4.81	.41	.81	1.22	1.05	1.12	1.12
F13	.51*	1.08*			.42*	.84*		1.21*	1.29*	
	.42	.90	1.86	6.25	.41	.81	1.22	1.02	1.11	1.53
F14	.48*	.97*	2.05*		.42*	.84*	1.25*	1.14*	1.16*	1.64*
	.44	.93	1.39	5.23	.41	.81	1.22	1.07	1.15	1.14
F22	.50*	1.00E	1.70E	5.46*	.42*	.83	1.24	1.19*	1.21E	1.37E
		1.52	2.22	5.98					1.83	1.79
F23	.49*	1.00*	1.84E	5.61E	.42*	.84*	1.25	1.17*	1.19*	1.47E
			2.54	6.31						2.03
F24	.47*	.97*	1.59E	5.20E	.42*	.84*	1.26	1.12*	1.16*	1.26E
			2.64	6.25						2.10

£: Excluding creep and shrinkage during the 2 weeks of epoxy curing

*: Values at preloading (unplated beams)

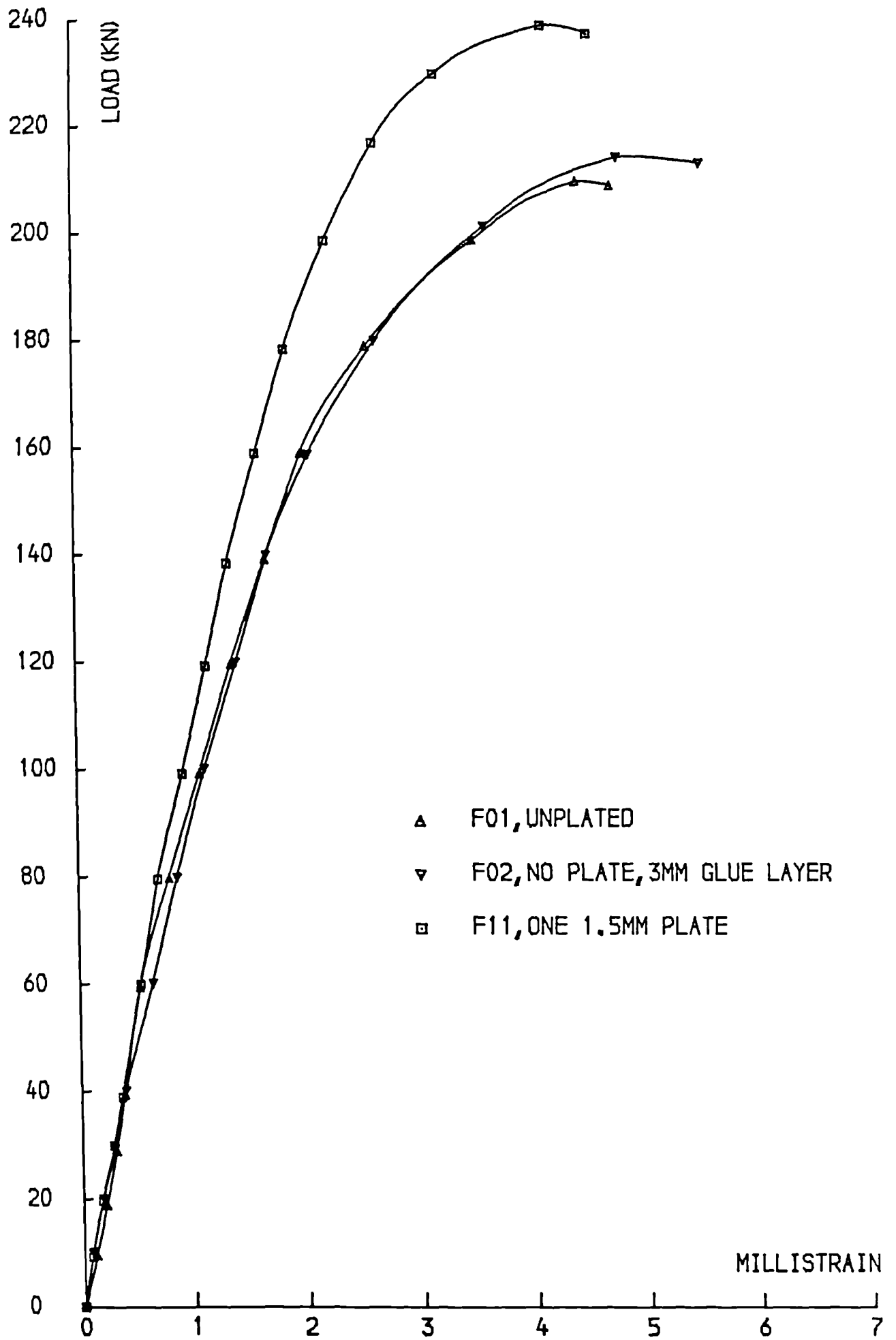


FIG.5.17 ,LOAD-CONC.COMP.STRAIN CURVES

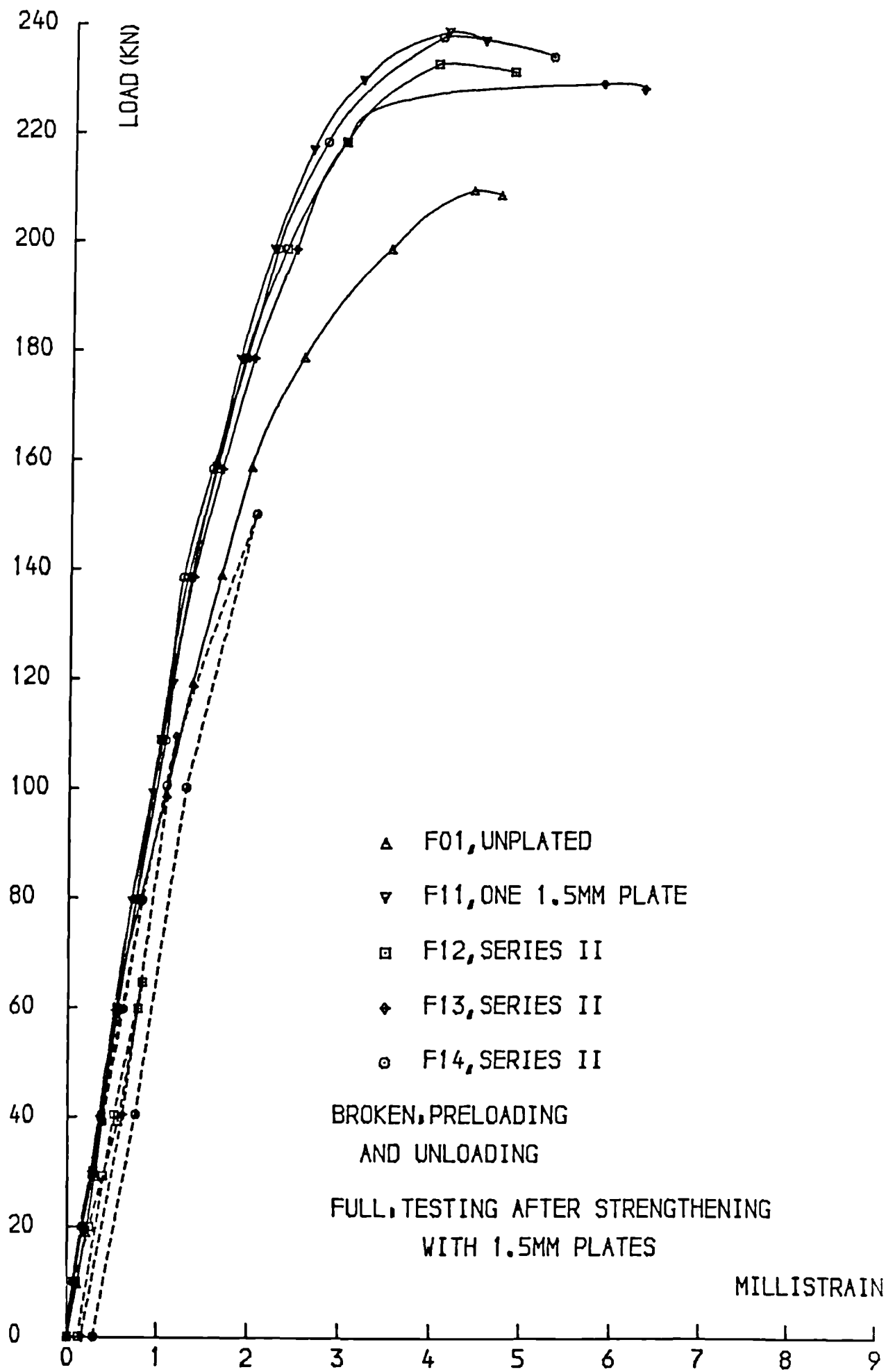


FIG.5.18 ,LOAD-CONC.COMP.STRAIN CURVES

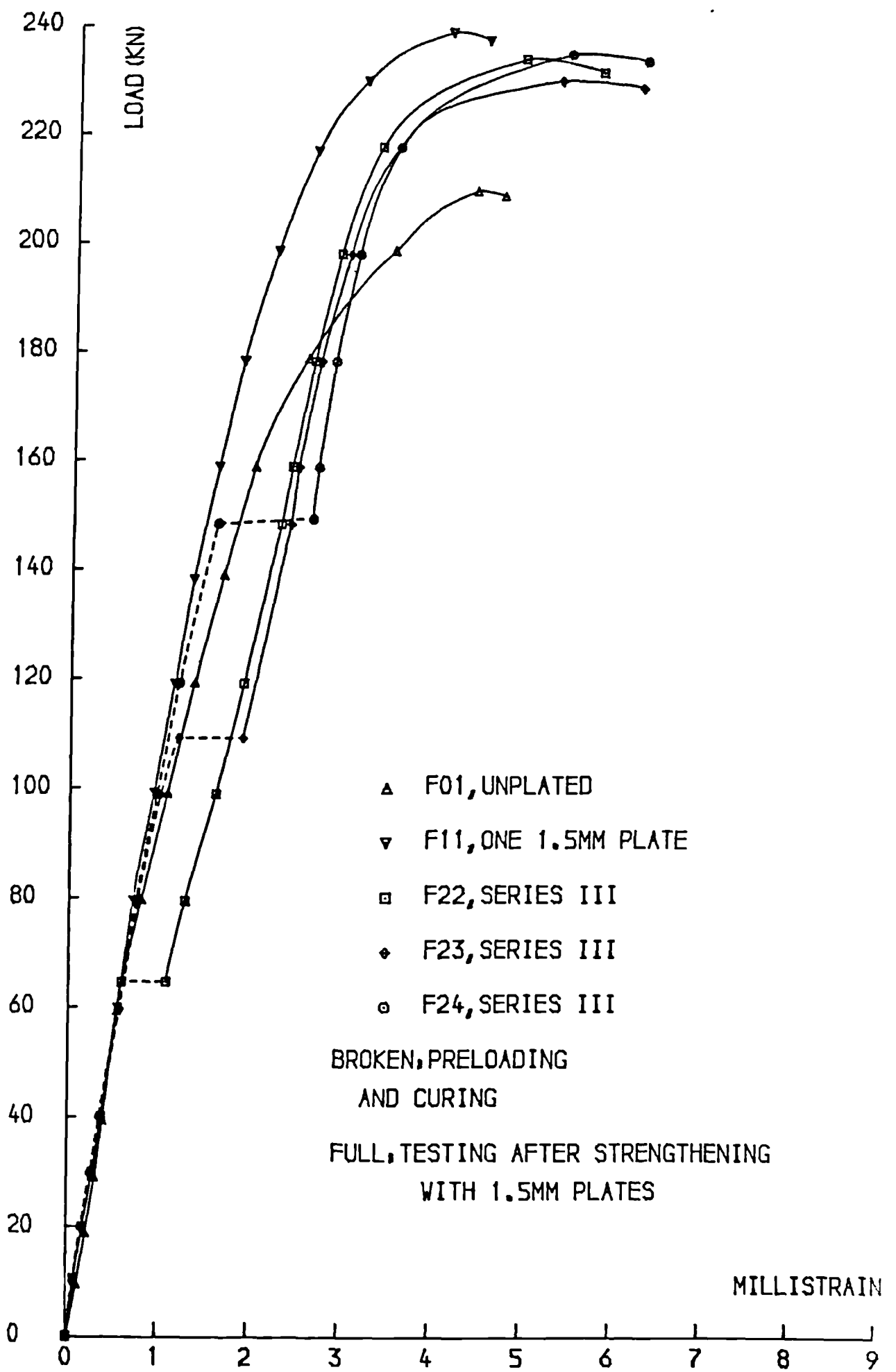


FIG. 5.19 ,LOAD-CONC.COMP.STRAIN CURVES

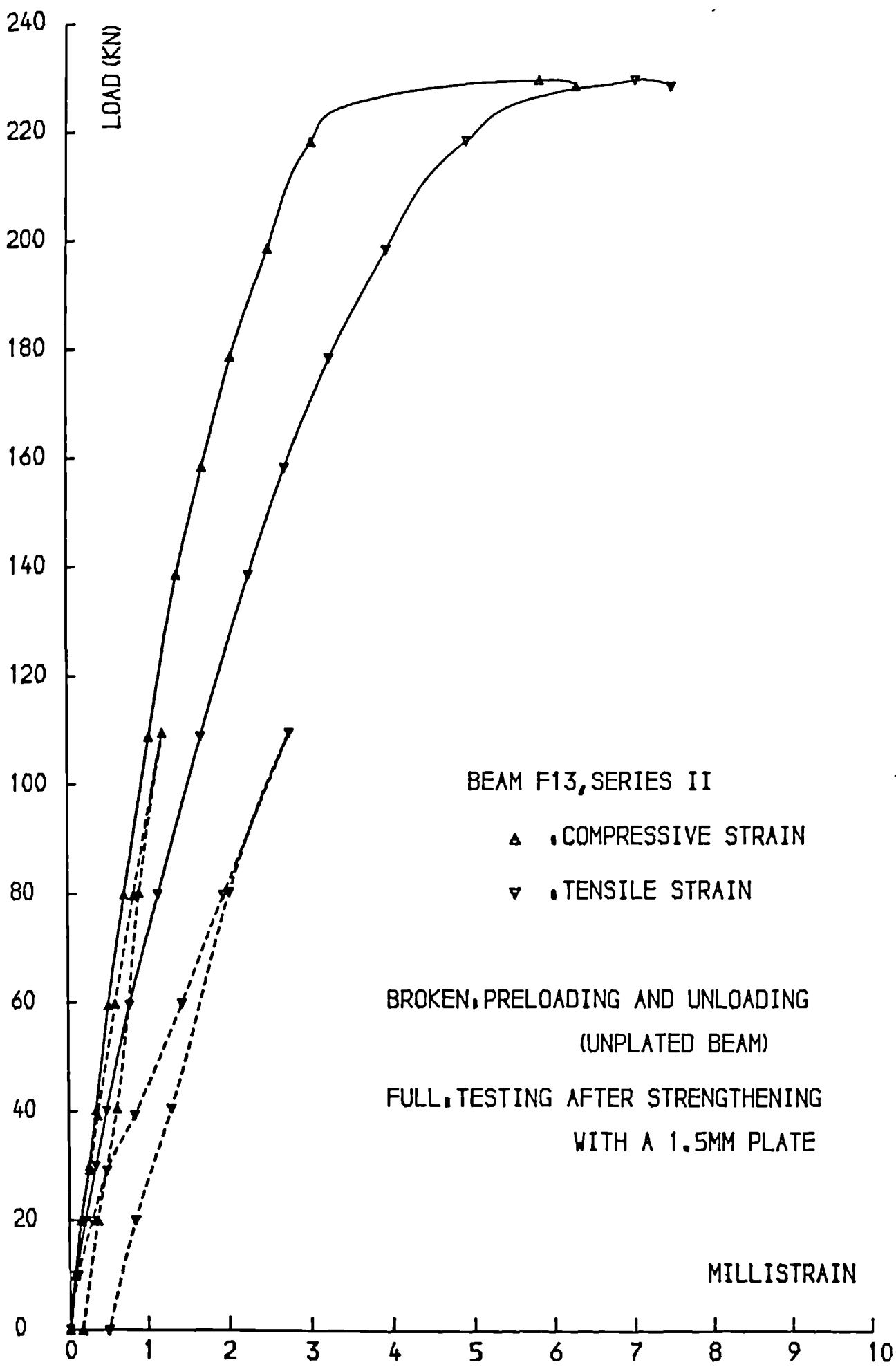


FIG.5.20 LOAD-CONCRETE STRAIN CURVES

Figs.5.17 to 5.20 show the load-concrete compressive strain and the load-concrete tensile strain curves. The measured tensile strain is a combination of the actual tensile strain and the openings of the cracks present in the 100mm gauge length over which the measurement was made. The same demec gauges and discs were used at the preloading, unloading and testing of the preloaded beams of Series II. It is particularly interesting to notice the load-concrete tensile strain of beam F13 (Fig.5.20). The curve shows the appearance and free widening of the cracks at the preloading stage. The significant restraining effect of the plate on the same cracks is illustrated by the curve at the testing. At testing, the concrete strains of the preloaded beams of F12, F13 and F14 of Series II were similar to those of beam F11 (Fig.5.18).

The variation in the concrete strains of the preloaded beams F22, F23 and F24 of Series III during the two weeks of bond curing includes creep and shrinkage. The creep was, as expected, higher with higher preloading loads (Table 5.4 and Fig.5.19).

The ultimate concrete compressive strains recorded varied between 4500 and 6250 microstrains for all the beams. The recorded ultimate strain of concrete was greater than the value of 3500 microstrains recommended by the CP110 code (79). The load corresponding to the CP110 value was however equal to or greater than 96% of the ultimate load for all beams (Figs.5.17 to 5.19).

Fig.5.21 shows the concrete strain distribution across the beam depth at different load levels and justifies the assumption of plane strains on which all the theoretical models

Table 5.5: Experimental and theoretical neutral axis depths at different load levels.

Beam No.	Experimental N.A. depth(mm)			Theoretical N.A. depth(mm)					Exp./Theor.					
	20kN	100kN	200kN	20kN		100kN		200kN		20kN	100kN	200kN		
				A	B	C	D	E	A	B	C	D	E	
F01	119.0	107.1	100.5	138.0	97.3	89.9	89.9	104.2	.86	1.10	1.12	1.12	.96	
F02	122.2	108.8	104.0	139.2	99.8	93.0	93.0	106.8	.88	1.09	1.12	1.12	.97	
F11	138.2	121.0	115.0	141.5	106.7	102.1	102.0	118.4	.98	1.13	1.13	1.13	.97	
F12	118.2*			138.0*					.86*					
	139.0	122.2	115.0	141.5	106.7	102.1	102.0	118.4	.98	1.15	1.13	1.13	.97	
F13	118.7*	106.0*		138.0*	97.3*				.86*	1.09*				
	135.7	119.0	114.0	141.5	106.7	102.1	102.0	118.4	.96	1.12	1.12	1.12	.96	
F14	116.9*	107.2*		138.0*	97.3*				.85*	1.10*				
	135.0	118.8	113.6	141.5	106.7	102.1	102.0	118.4	.95	1.11	1.11	1.11	.96	
F22	120.2*	124.3E	116.1E	138.0*	106.7	102.1	101.9	118.2	.87*	1.16	1.14	1.14	.98	
F23	121.1*	106.9*	115.0E	138.0*	97.3*	102.1	101.8	118.1	.88*	1.10*	1.13	1.13	.97	
F24	116.4*	103.3*	113.5E	138.0*	97.3*	102.1	101.6	118.0	.84*	1.06*	1.11	1.12	.96	

A: Elastic theory, uncracked section

B: " " cracked " "

C: Ult.CP110 simplified method

D: " strain comp.(rect. block)

E: " " Hognestad block

*: Values at preloading (unplated)

E: Including creep and shrinkage during bond curing

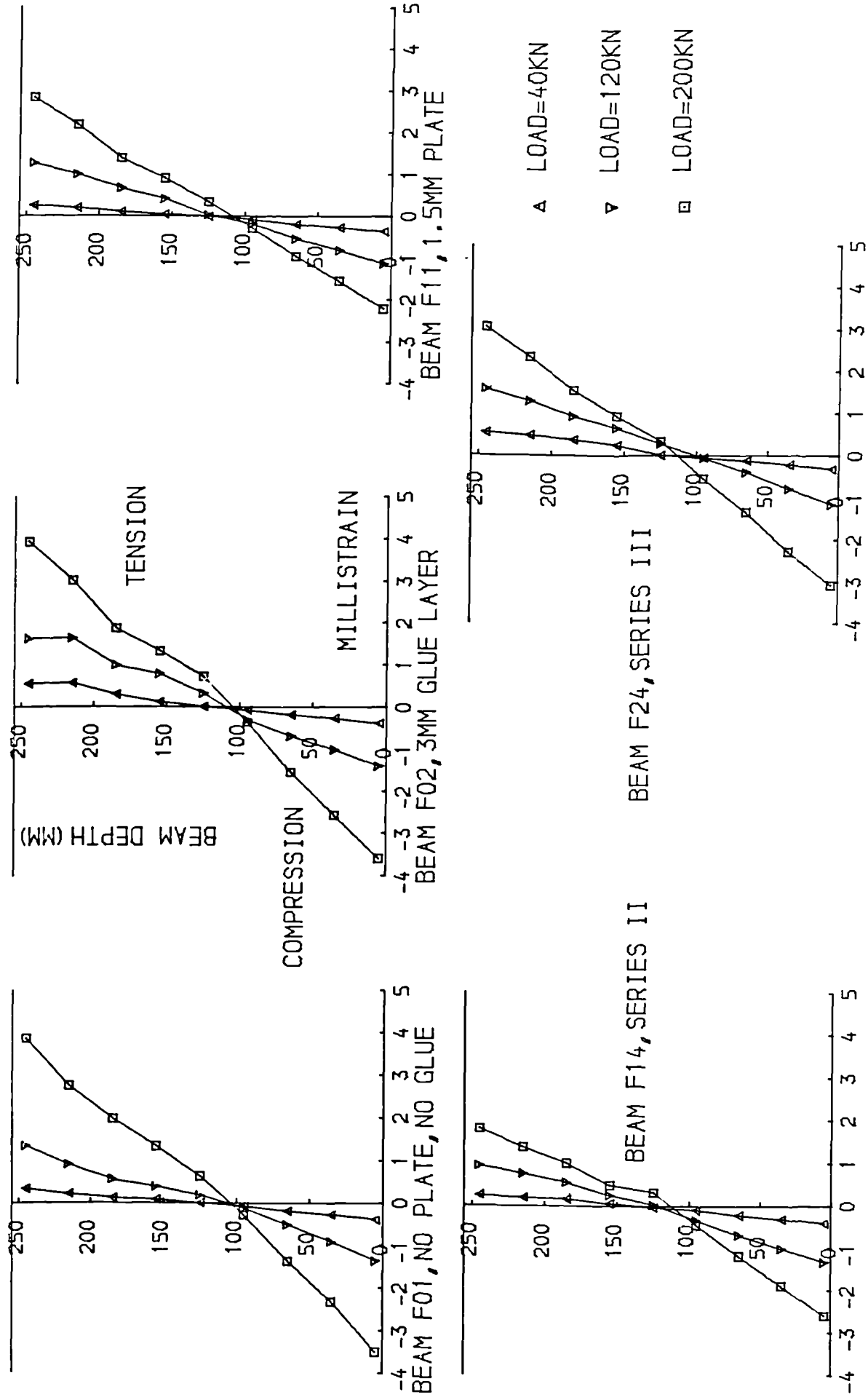


FIG.5.21 CONCRETE STRAIN DISTRIBUTION

of this project are based. After cracking, the linearity of the tensile strains is affected by the crack openings. The neutral axis position moves towards the compressive face of the beam at higher loads (Table 5.5) confirming that the beams were under reinforced.

The experimental and predicted neutral axis depths at different load levels are given in Table 5.5. Three different methods were used to compute the theoretical values:

- (a) BEFORE CRACKING: Elastic theory and transformed uncracked sections.
- (b) SERVICE LOADS: Elastic theory and transformed cracked sections.
- (c) NEAR ULTIMATE LOADS: The three methods used for ultimate strengths (see Appendix D).

The different methods gave satisfactory predictions of the neutral axis depths. The theoretical values were slightly overestimated before cracking and slightly under estimated at service and near ultimate loads.

5.4.3.2 BAR STRAINS

The load-bar strain curves are shown in Figs.5.22 to 5.24. Table 5.6 gives the theoretical and experimental bar strains at different levels of loading. The theoretical strains were computed using an elastic analysis.

At a load of 100kN, the ratio of measured to predicted value was 0.99 for unplated beams and 0.80 for plated beams. The same ratios were 1.05 and 0.95 respectively at a load of 150kN.

Table 5.6: Measured and predicted bar strains at different service loads.

Beam No.	Experimental ₃ bar strain(10^{-3})			Theoretical ₃ bar strain(10^{-3})			Exp./Theor.			
	50kN	100kN	150kN	Max.	50kN	100kN	150kN	50kN	100kN	150kN
F01	.47	1.00	1.62	4.97	.528	1.056	1.584	.89	.95	1.02
F02	.37	.86	1.52	5.11	.508	1.004	1.450	.73	.86	1.05
F11	.26	0.62	1.26	4.35	.432	0.865	1.297	.60	.72	.97
F12	.48*	.30	.72	4.46	.528*	.865	1.297	.91*	.83	0.99
F13	.47*	1.04*	1.18	4.31	.528*	1.056*	1.297	.89*	.99*	0.91
F14	.44*	1.09*	1.71*	3.97	.432	.865	1.584*	.83*	1.03*	1.08*
F22	.50*	.92E	1.38E	4.62E	.528*	.989	1.421	.95*	.93E	.97E
F23	.51*	1.05*	1.48E	5.02	.528*	1.056*	1.507	.97*	1.33	1.25
F24	.49*	1.05*	1.64E	6.55E	.528*	1.056*	1.584*	.93*	0.99*	.98E
			2.15	7.06						1.25
										1.04E
										1.35

£: Excluding strain variations during the 2 weeks of epoxy curing * : Values at preloading (unplated beams)

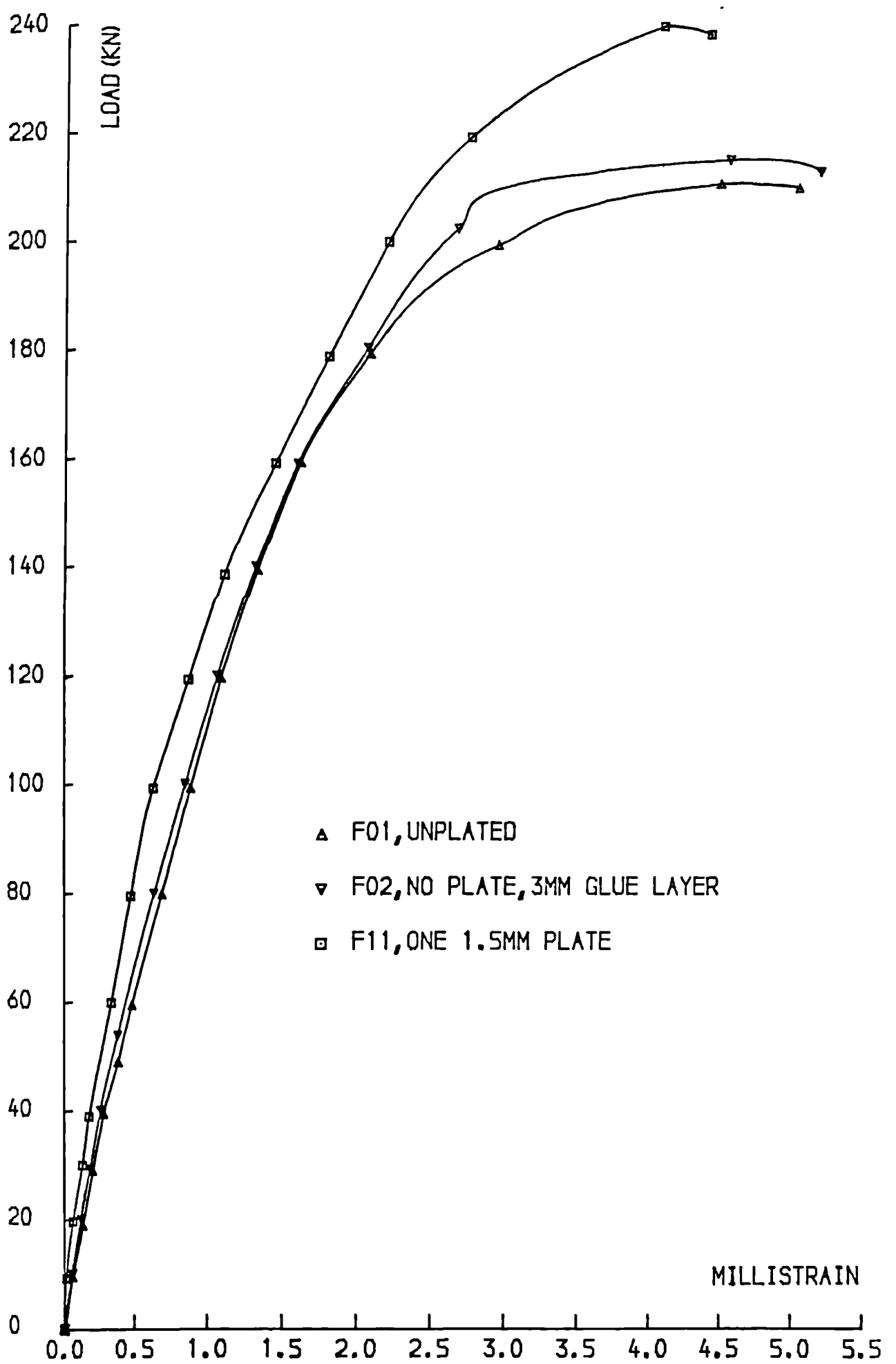


FIG.5.22 ,LOAD-BAR STRAIN CURVES

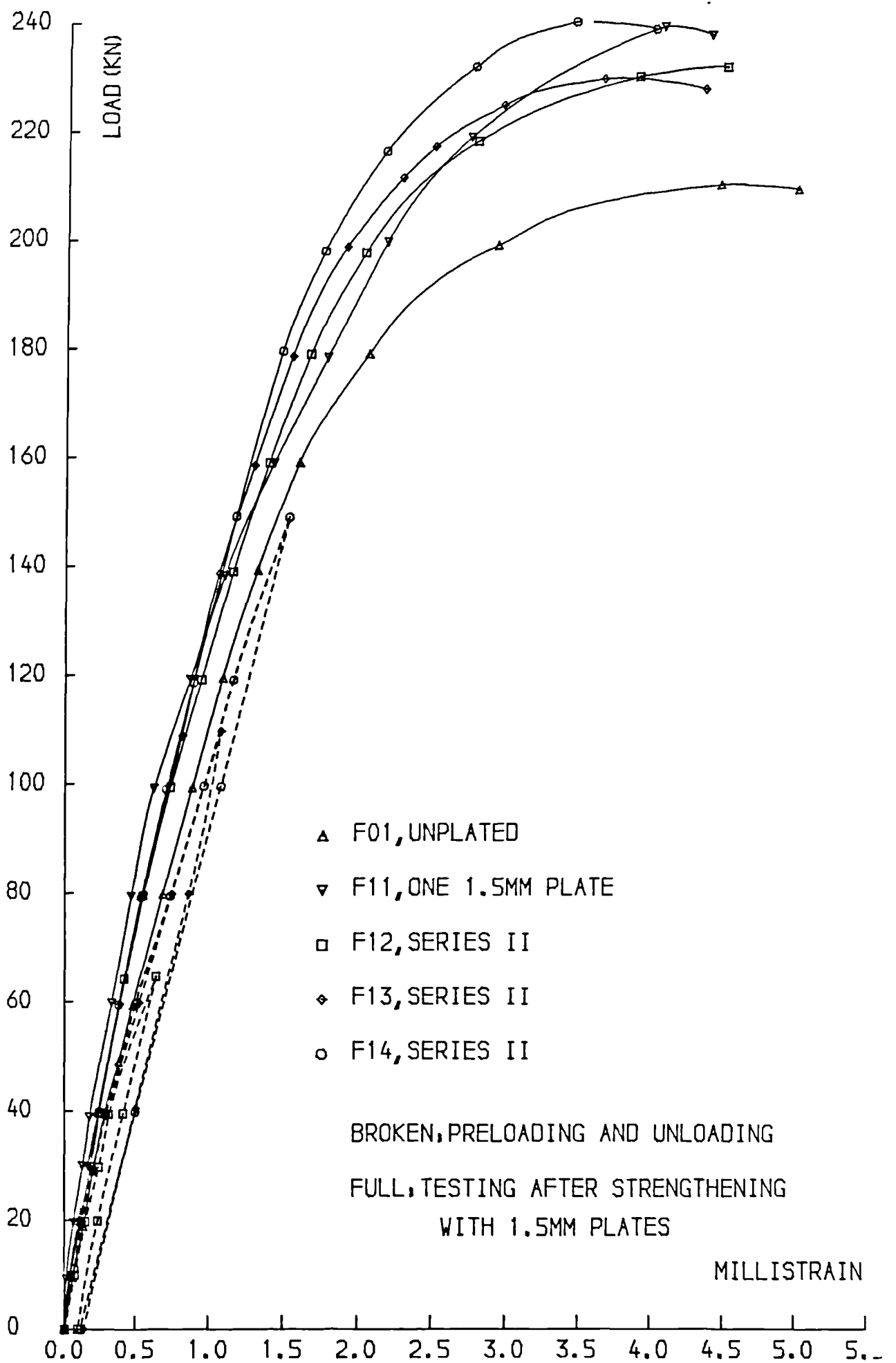


FIG. 5.23 , LOAD-BAR STRAIN CURVES

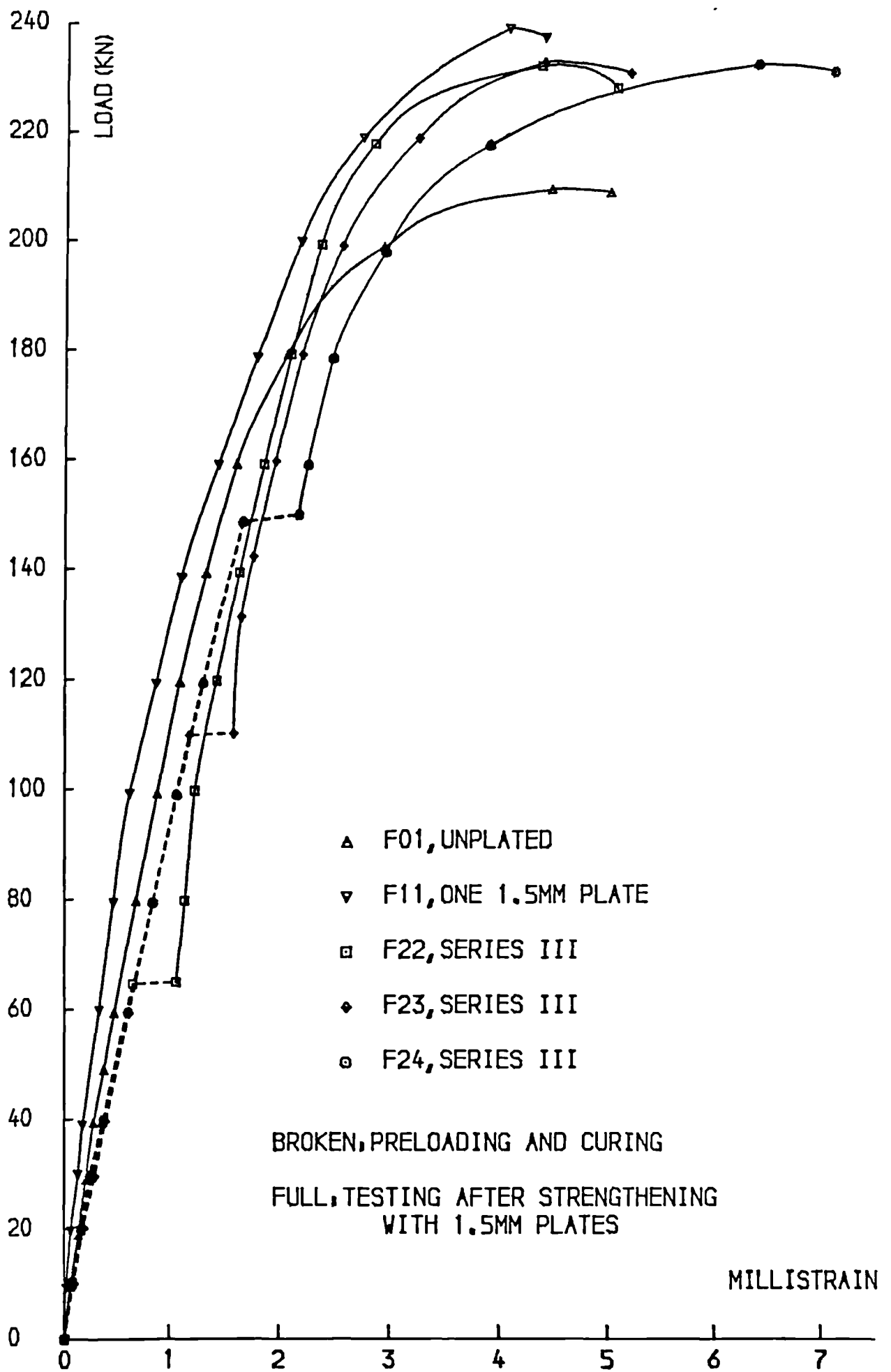


FIG. 5.24 , LOAD-BAR STRAIN CURVES

There was no significant difference in the bar strains of the preloaded beams F12, F13 and F14 of Series II and those of beam F11. The bar strains in the preloaded beams were however slightly greater than those of beam F11 at low loads and slightly less at higher loads but the differences were less than 5% (Fig.5.23 and Table 5.6).

The preloaded beams F22, F23 and F24 of Series III behaved as expected. Bonding of the plate increased the beam stiffness and reduced the subsequent increase in the bar strains. There was a variation of up to 504 microstrains in the steel bars during the two weeks of bond curing (Fig.5.24 and Table 5.6).

The maximum bar strains recorded were higher than the 0.2% proof value (2000 microstrains) and varied between 3970 and 7060 microstrains.

5.4.3.3 PLATE STRAINS

The theoretical (elastic) and experimental plate strains are given in Figs.5.25 to 5.27 and Table 5.7.

At a load of 100kN, the ratio of measured to predicted value was 0.95 for 1.5mm thick plates. The same ratio was 1.07 at 150kN.

The plate strains in the preloaded beams F12, F13 and F14 of Series II were identical to those of beam F11 (Table 5.7 and Fig.5.26).

Fig.5.27 shows that the plates in the preloaded beams F22, F23 and F24 of Series III were active before the load was increased. There was a stress transfer from the beam to plate during bond curing under a constant load. This stress transfer is illustrated by the strain variation in the plates of up to

Table 5.7: Measured and predicted plate(glue) strains at different load levels.

Beam No.	Experimental ₃ plate strain(10^{-3})			Theoretical plate strain(10^{-3})			Exp./Theor.			
	50kN	100kN	150kN	Max.	50kN	100kN	150kN	50kN	100kN	150kN
F02@	0.62	1.49	2.51	7.30	.741	1.482	2.223	.84	1.01	1.13
F11	0.44	1.10	1.85	7.10	.573	1.147	1.720	0.77	0.96	1.08
F12	0.45	1.09	1.83	6.80	"	"	"	0.79	0.95	1.06
F13	0.49	1.08	1.83	6.93	"	"	"	0.86	0.94	1.06
F14	0.44	1.10	1.84	7.20	"	"	"	0.77	0.96	1.07
F22		.341* .422	1.04* 1.118	5.93		0.401	0.975		0.85* 1.05	1.07* 1.15
F23			0.45* 0.551	5.25			0.459			0.98* 1.20
F24			0.00* 0.227	3.90			0.000			

*: Excluding strain variation during the 2 weeks of bond curing @:Glue strain

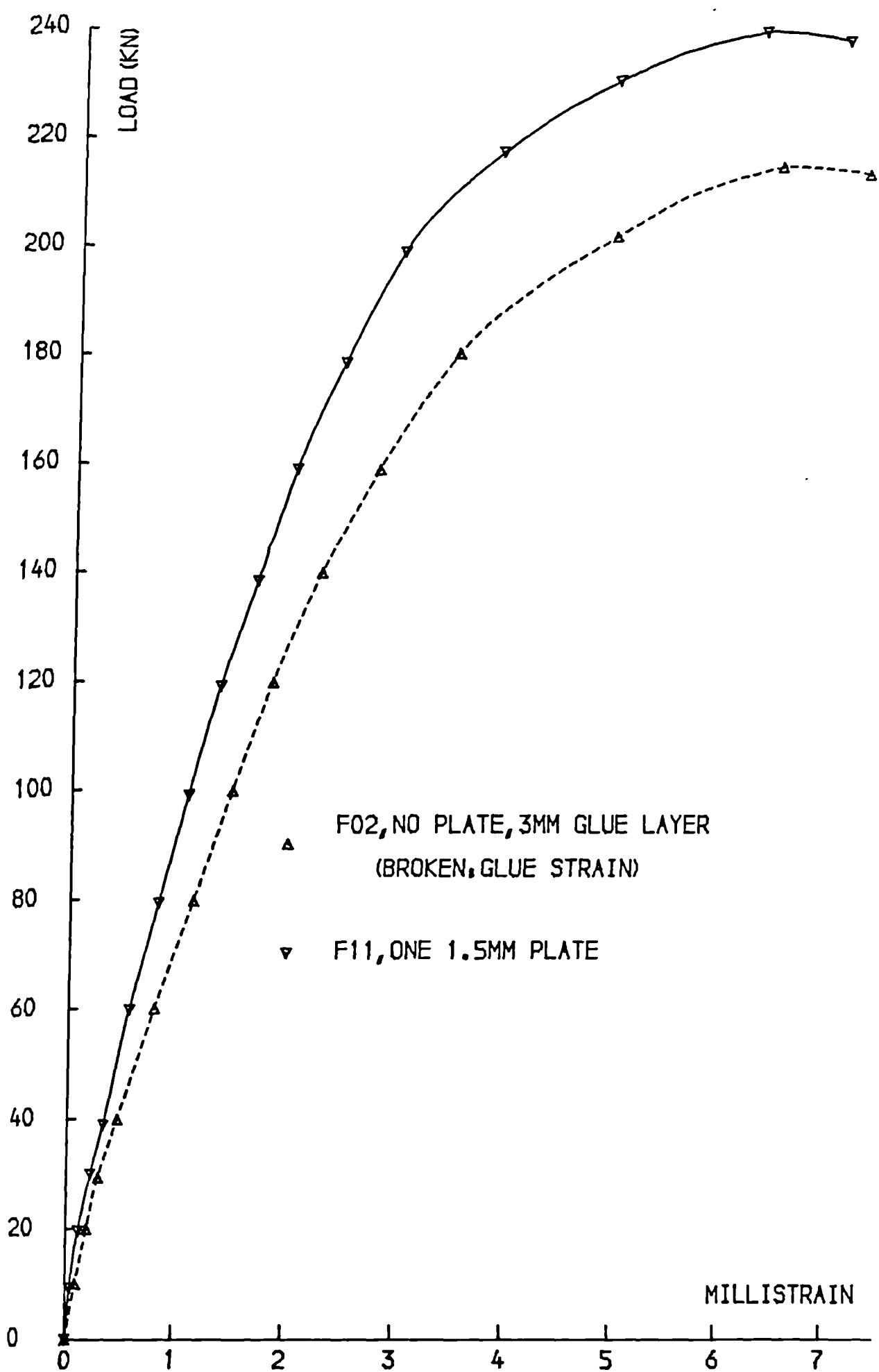


FIG.5.25 ,LOAD-PLATE STRAIN CURVES

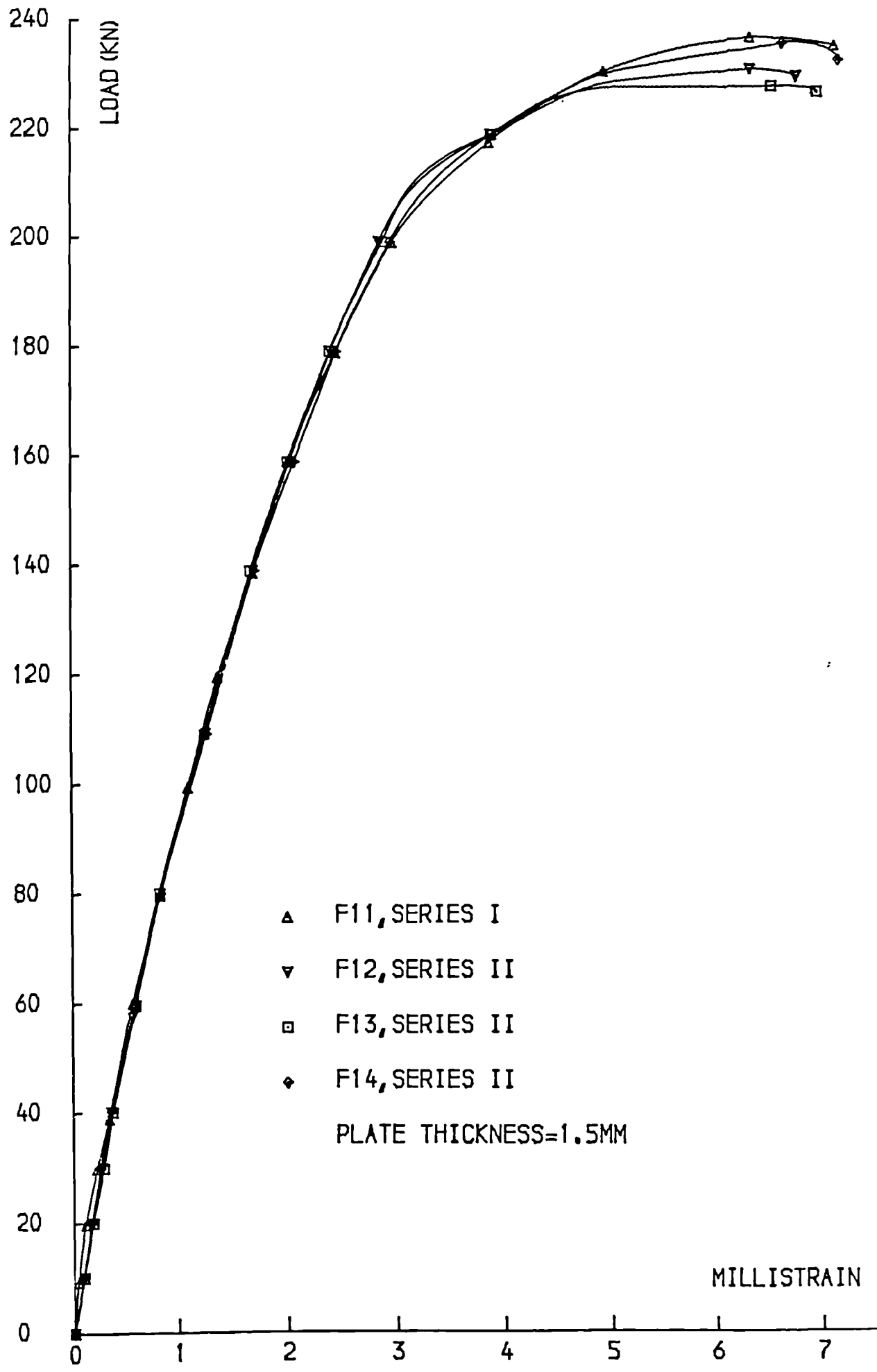


FIG.5.26 ,LOAD-PLATE STRAIN CURVES

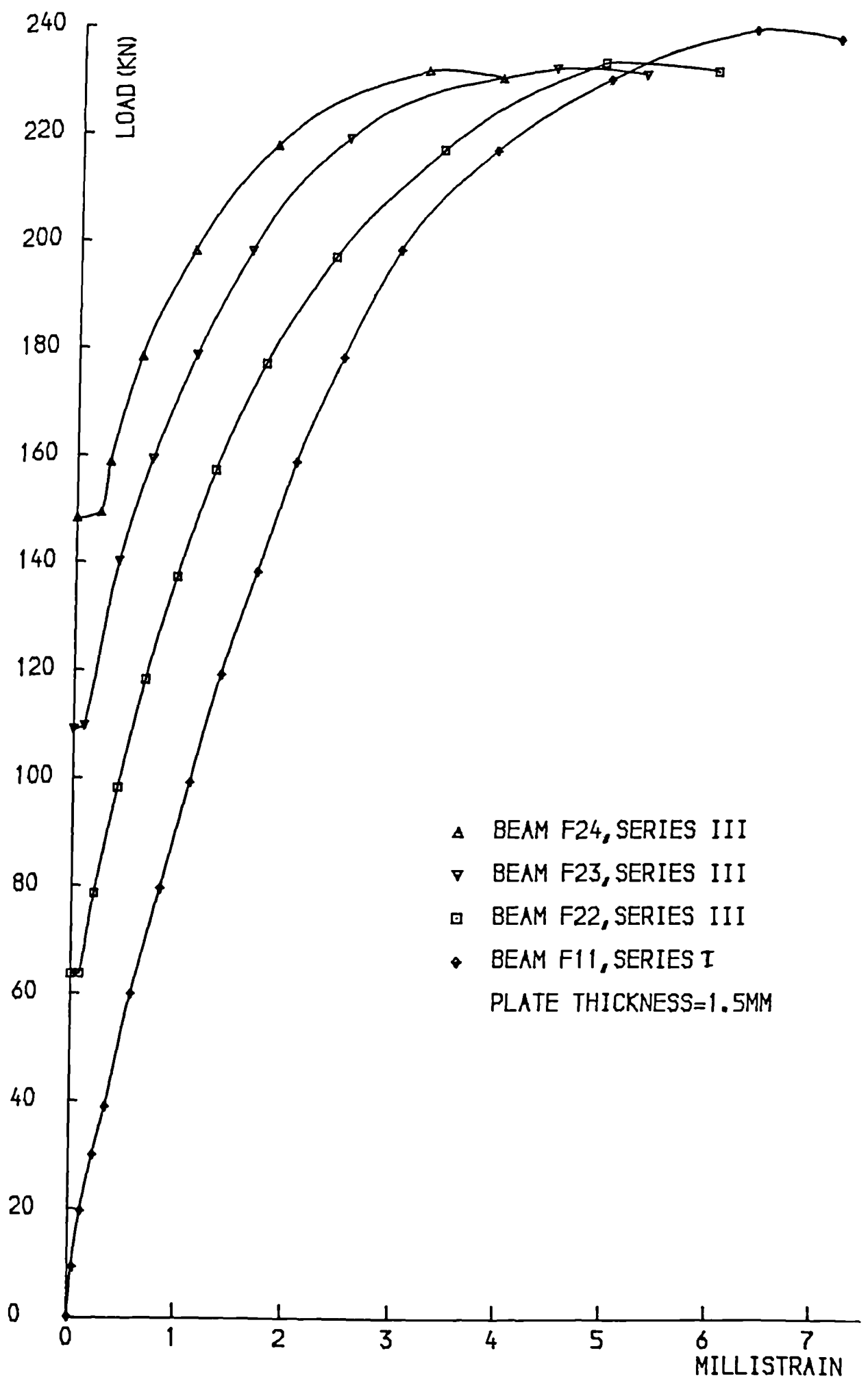


FIG.5.27 LOAD-PLATE STRAIN CURVES

227 microstrains (Fig.5.27). The actual strain variation in the plates was probably higher than the recorded one as the plate strains were measured only over the last 10 days of the two weeks of bond curing, after the removal of the steel beam which was clamped to the test beam to provide the curing pressure. The predicted elastic strain for beam F23 at 150kN was 459 microstrains. The actual measured value was 551 microstrains. This difference can be accounted for partly by the non-validity of the elastic model at high loads. It is also the result of the plastic properties of the steel bars, which made it possible to exploit the full capacity of the plates.

The maximum plate strains recorded varied between 3900 and 7300 microstrains (Table 5.7) which were higher than the yield value of 1400 microstrains.

5.5 CRACK WIDTHS

Cracking is a random phenomenon and the limited experimental results are used here in a comparative study only. The theoretical average crack widths were calculated using the method proposed by the CP110 code(79) (Appendix E). Fig.5.28 shows typical load-average crack width curves. The measured and predicted average crack widths at service loads and at higher loads are given in Table 5.8. The method could not be used near ultimate loads, as the CP110 code specifies that the formula should be restricted only to cases where the strain in the steel is less than 80% of the yield value. At a load of 100kN, the ratio of experimental to theoretical average crack width was 1.04 for unplated beams and 0.89 for plated beams.

Table 5.8: Measured and predicted average crack widths at different load levels.

Beam No.	Exper. average crack width (mm)		CP110 average crack width (mm)		Exp./Theo.	
	100kN	200kN	100kN	200kN	100kN	200kN
F01	.078	.320	.074	.154	1.05	@
F02	.070	.200	.068	.140	1.03	@
F11	.046	.115	.054	.115	0.85	1.00
F12	.050	.115	.054	.115	.93	1.00
F13	.082*		.074*		1.11*	
	.047	.120	.054	.115	0.87	1.04
F14	.713*		.074*		0.96*	
	.050	.118	.054	.115	0.93	1.03
F22	.057£	.126£	.060	.121	0.95£	1.04£
	.065	.134			1.08	1.11
F23	.080*	.138£	.074*	.130	1.07*	1.06£
		.156				1.20
F24	.073*	.142£	.074*	.139	0.99*	1.02£
		.165				1.19

*: Values at preloading (unplated beams)

£: Excluding variations during the 2 weeks of bond curing.

@: The CP110 method is not applicable if steel strain is more than 80% of yield value.

~~\$: Extrapolated~~ § Extrapolated

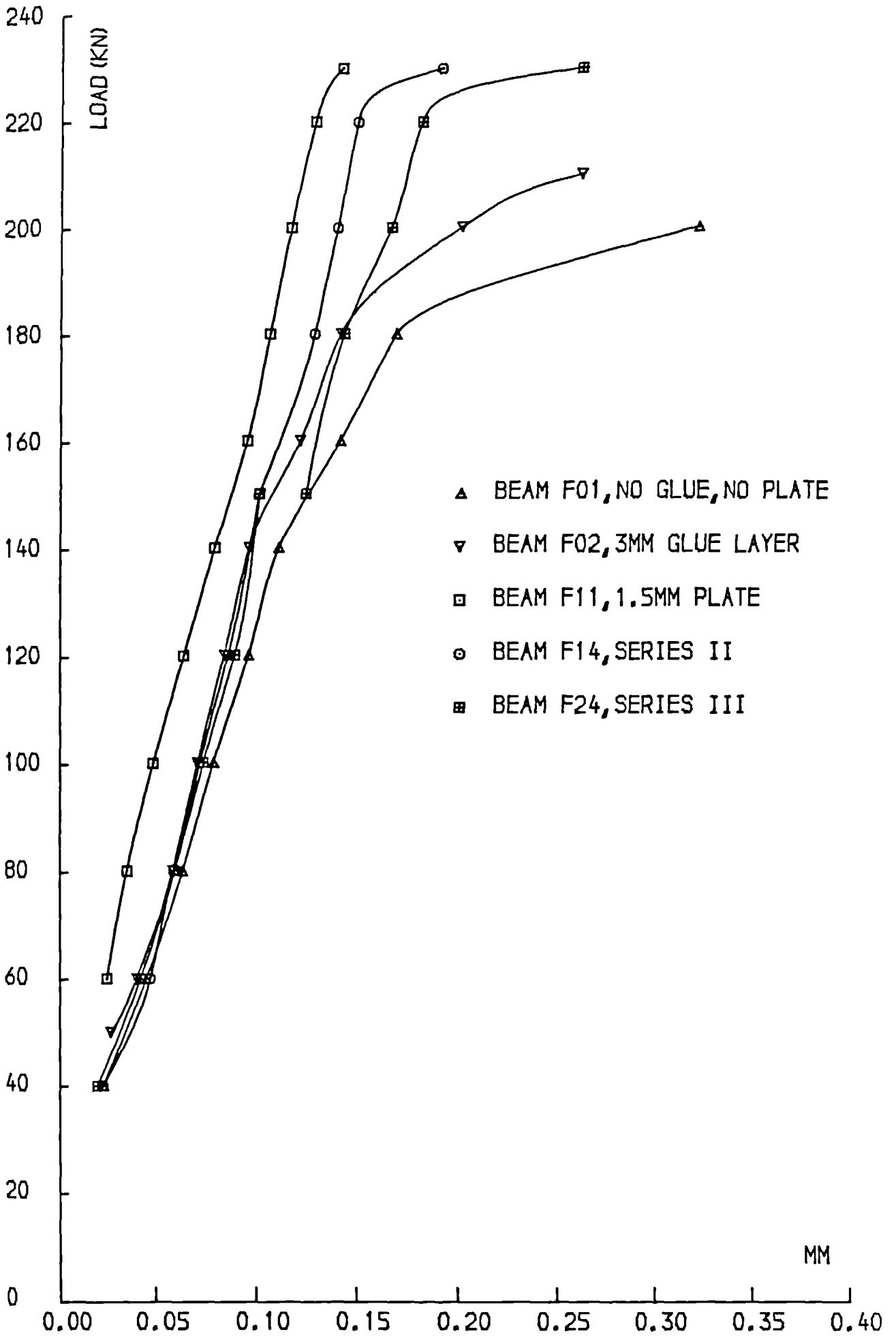


FIG.5.28 LOAD-CRACK WIDTH CURVES

The crack widths of the preloaded beams F12, F13 and F14 of Series II were slightly higher than those of beam F11. The difference was higher at low loads and less pronounced beyond the preloading load. The effect of the plates on the crack widths seems therefore to be more apparent when the beam is loaded beyond the original preload. The crack openings of the preloaded and subsequently plated beams were nevertheless less than those of the unplated beam F01.

The crack widths of the preloaded beams F22, F23, F24 of Series III were similar to those of the unplated beam F01 at the preloading stage but the addition of the plates reduced the subsequent crack openings. Despite the increase in the widths during the fourteen days of bond curing (under a constant load), the total crack openings of the preloaded beams were less than those of the unplated beam.

5.6 RIGIDITIES

The theoretical inertia of the beam was calculated using the elastic transformed section (uncracked or cracked). The rigidity was then obtained by multiplying the inertia by the elastic modulus of concrete determined by prism tests described in chapter three.

Considering the diagram shown in Fig.5.29, the stress in the compression face of concrete is given by:

$$\sigma_c = \frac{M \cdot x}{I} \quad \text{so} \quad I = \frac{M \cdot x}{\epsilon_c E_c} \quad \text{therefore} \quad E_c I = \frac{M \cdot x}{\epsilon_c} \quad (5.1)$$

The experimental rigidity of the beam was obtained by multiplying the experimental neutral axis depth by the applied moment and dividing by the measured concrete compressive

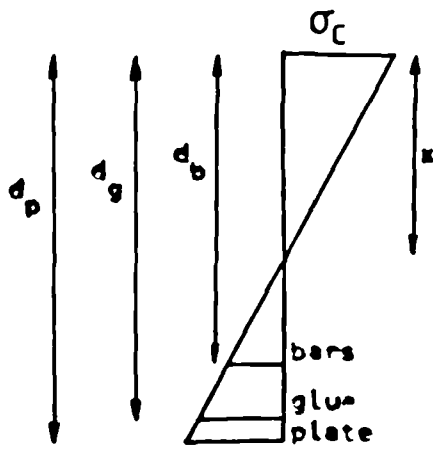


Fig.5.29: Transformed section

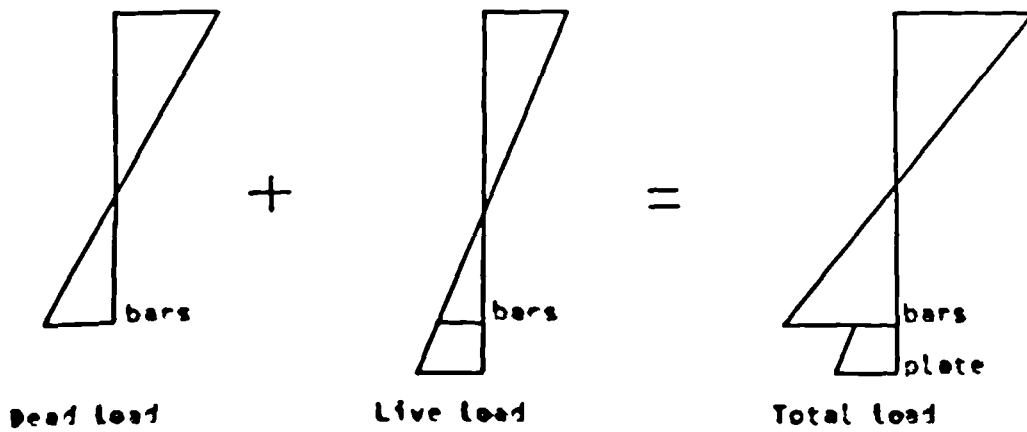


Fig.5.3 - Sim plified strain model f r beams of Series III

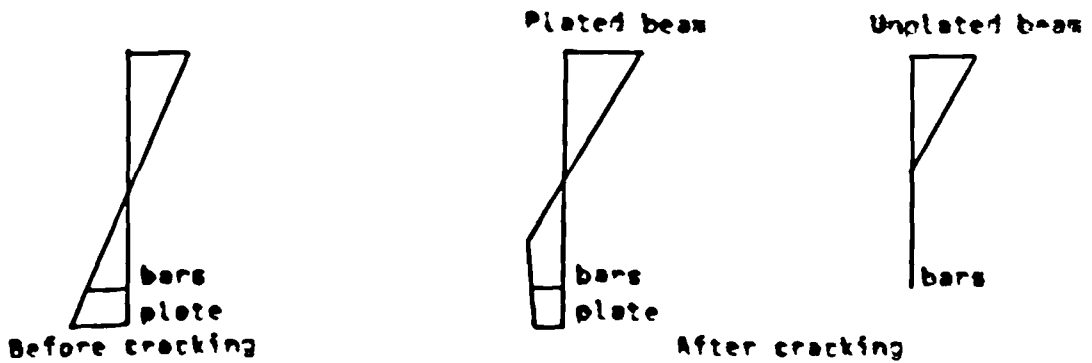


Fig.5.31: Possible simplified stress model

strain. The concrete in tension was neglected.

The experimental and predicted rigidities before and after cracking are given in Table 5.9.

At a load of 20kN (before cracking), the experimental rigidities were 533.6×10^{10} N.mm² for unplated beams and 648.8×10^{10} N.mm² for beams with a 1.5mm plate.

At 100kN (after cracking), the rigidities were 398.8×10^{10} and 502.8×10^{10} N.mm² respectively.

At 20kN, the ratio of experimental to predicted rigidity was 0.67 for unplated beams and 0.76 for plated beams. The same ratios were 0.92 and 0.94 at 100kN. Although the actual stiffness at 20kN is greater than at 100kN, the ratios of recorded to predicted rigidities are higher at 100kN than at 20kN. This may be due to the fact that the theoretical model after cracking (at 100kN) ignores the stiffening effect of concrete in tension. It could also be due to the presence of some cracking in concrete at 20kN for which the theoretical model did not allow.

It is however interesting to note that the rigidities of the plated beams are underestimated when compared to those of the unplated beams: The ratio of experimental to theoretical value was slightly greater in plated beams. This again supports the conclusion that the restraining effect of the external plates could be greater than that of an internal reinforcement designed to achieve the same performance.

Table 5.9: Experimental and theoretical rigidities before and after cracking.

Beam No.	Rigidity EI (10^{12} N.mm ²)					
	Exp. EI		Theor. EI		Exp./Theo.	
	20kN	100kN	20kN	100kN	20kN	100kN
F01	5.30	3.97	7.952	4.337	.67	.92
F02	5.38	4.14	8.035	4.562	.67	.91
F11	6.47	5.02	8.539	5.362	.76	.94
F12	5.30* 6.50	5.04	7.952* 8.539	5.362	.67* .76	.94
F13	5.32* 6.47	4.00* 5.00	7.952* 8.539	4.337* 5.362	.67* .76	.92* .93
F14	5.34* 6.51	3.96* 5.05	7.952* 8.539	4.337* 5.362	.67* .76	.91* .94
F22	5.31*	4.77£ 3.136	7.952*	5.362	.67*	.89£ .59
F23	5.40*	3.98*	7.952*	4.337*	.68*	.92*
F24	5.38*	4.08*	7.952*	4.337*	.68*	.94*

*: Values at preloading
£: Excluding variations during bond curing.

5.7 TENSILE STRESSES IN CONCRETE

The experimental glue strain ϵ_g is deduced from the measured bar and plate strains ϵ_b and ϵ_p (Fig.5.29). Assuming an elastic distribution in the concrete at low loads and using the experimental value x of the neutral axis depth, the internal moment M_{in} carried by the bars, glue and plate is:

$$M_{in} = A_b E_b \epsilon_b \left[d_b - \frac{x}{3} \right] + A_g E_g \epsilon_g \left[d_g - \frac{x}{3} \right] + A_p E_p \epsilon_p \left[d_p - \frac{x}{3} \right] \quad (5.2)$$

Where A_b, A_g, A_p and E_b, E_g, E_p are the cross-sectional areas and elastic moduli of the bars, glue and plate respectively.

The difference between the applied moment M and the internal moment M_{in} is equal to the moment M_c carried by concrete in tension: $M_c = M - M_{in}$.

Assuming an elastic distribution of stresses in concrete in tension, the tensile stress in concrete (at the tensile face) is given by:

$$M_c = \sigma_f \frac{b(d-x)}{2} \frac{2d}{3} \quad \text{therefore} \quad \sigma_f = \frac{3M_c}{bd(d-x)} \quad (5.3)$$

Where b and d are the width and depth of the beam.

The tensile stresses in concrete thus obtained are given in Table 5.10.

At a load of 2 kN, the stress was 1.45 N mm^2 for the unplated beams and 2.3 N mm^2 for the plated beams.

At 100kN, the stress was 0.92 N mm^2 for the unplated beams and 2.67 N/mm^2 for beams with a 1.5mm plate.

Similar observations were made by Bloxham(34) who found that the contribution of concrete in tension increased with the plate thickness up to a value of 6 N mm^2 (which is greater than

Table 5.10: Tensile stresses in concrete at the tension face before and after cracking.

Beam No.	Internal moment carried by bars glue and plate (kN.m)		Moment carried by concrete in tension (kN.m)		Tensile stress in concrete (N/mm ²)	
	20kN	100kN	20kN	100kN	20kN	100kN
	F01	4.93	36.42	2.74	1.93	1.53
F02	4.87	36.31	2.80	2.04	1.60	1.06
F11	4.56	33.64	3.11	4.71	2.02	2.67
F12	4.95*		2.72*		1.51*	
	4.55	33.63	3.12	4.72	2.04	2.70
F13	4.99*	36.56*	2.68*	1.79*	1.49*	0.91*
	4.45	33.58	3.22	4.77	2.05	2.66
F14	4.85*	36.38*	2.82*	1.97*	1.55*	1.01*
	4.49	33.61	3.18	4.74	2.01	2.64
F22	5.09*	34.11£	2.58*	4.24£	1.45*	2.46£
F23	5.25*	36.59*	2.42*	1.76*	1.37*	.90*
F24	5.06*	36.71*	2.61*	1.58*	1.43*	.79*

*: Values at preloading (unplated beams)
 £: Excluding variations during bond curing

the tensile strength of concrete). He did not however take into account the contribution of the glue in his calculations (which would have reduced the numerical values but without changing the trend).

These results suggest that the beams do not only benefit from the added stiffness and strength provided by the plates but also from a better contribution of concrete in tension. This higher resistance of tensile concrete in plated beams, could be the reason for the higher ratios of experimental to theoretical rigidities and lower ratios of measured to predicted deflections, rotations, crack widths and strains.

5.8 STRENGTH PROPERTIES

5.8.1 FIRST CRACK LOADS

The first crack loads were calculated using the transformed uncracked section with the value of the modulus of rupture from the test prisms and the values of the elastic moduli of the materials (concrete, steel and epoxy) obtained from the material tests as described in chapters three and four (see Appendix C). The experimental first crack loads were observed visually with a magnifying glass and determined within load increments of 5kN. The theoretical and experimental first crack loads are given in Table 5.11.

For the unplated beams, the experimental value was 1.15 time the theoretical one. The same ratio was 1.39 for beams with 1.5mm thick plates.

The ratio of first crack load to the CP110 ultimate load was 0.15 for unplated beams and 0.18 for beam F11 with a 1.5mm thick plate. The tensile strain in concrete at first cracking was 154 microstrains for unplated beams and 178 microstrains

Table 5.11: Experimental and theoretical strength results.
(first crack and ultimate loads).

Beam No.	First crack load(kN)		M ximum l d(kN)									1 st crack load over	1 st crack concrete tensile strain (10 ⁻⁶)
	Exp.	Theo.	Exp.			Theo.ult.flex.			Exp./Theo.				
F01	30.0	26.10	1.15	210.0	202.21	202.21	194.05	1.04	1.04	1.08	0.15	162	
F02	30.0	26.95	1.11	214.2	206.18	206.18	200.22	1.04	1.04	1.07	0.15	170	
F11	40.0	28.89	1.39	239.0	227.25	227.25	216.99	1.05	1.05	1.10	0.18	178	
F12	30.*	26.1*	1.15*	232.0	"	"	"	1.02	1.02	1.07	0.15*	100*	
F13	"	"	"	230.0	"	"	"	1.01	1.01	1.06	"	205*	
F14	"	"	"	240.0	"	"	"	1.06	1.06	1.11	"	162*	
F22	30.*	26.1*	1.15*	232.2	227.25	227.05	228.10	1.02	1.02	1.02	0.15*	170*	
F23	"	"	"	233.0	"	226.71	227.69	1.03	1.03	1.02	"	120*	
F24	"	"	"	232.3	"	219.31	221.14	1.02	1.06	1.05	"	162*	

A: CP110-simplified method

B: Strain compatibility(rect.stress block)

C: " (Hognestad et al.)

*: (see Appendix D for these 3 methods).

*: Values at preloading(unplated beams)

for beam F11 with a 1.5mm plate.

Although the experimental first crack loads are obtained visually and are not very accurate, the comparison of the previous ratios suggest that the restraining effect of the plate may be greater than that of conventional reinforcement designed to achieve the same performance.

5.8.2 ULTIMATE STRENGTHS

The ultimate flexural strength was computed using three methods:

(a) Simplified method of CP110 (79) with a rectangular concrete stress block and based on a failure criteria of the reinforcement reaching its yield strain and concrete reaching its ultimate compressive strain. This simplified method is based on the assumption that the plastic properties of the reinforcement allow concrete to reach its ultimate strain after the steel has yielded (in under reinforced beams), but it is more suitable in the case of balanced sections.

(b) Strain compatibility method with a rectangular concrete stress block and based on a ultimate concrete compressive strain of 0.0035.

(c) Strain compatibility method with the concrete stress block and ultimate strain proposed by Hognestad et al. (82).

The plastic properties of steel were taken into account in the strain compatibility methods and the calculations were made by successive iterations by means of a computer. The three methods and the computer flowcharts used are described in Appendix D. The theoretical and measured ultimate strengths are shown in Table 5.11.

All the beams reached their ultimate flexural strengths and failed as under reinforced beams by compressive crushing of concrete following the yielding of the reinforcement (Table 5.12).

Preloading did not have any adverse effect on the ultimate strength of the subsequently unloaded and strengthened beams F12, F13 and F14. The preloaded beams F12, F13, F14 reached ultimate strengths comparable to that of beam F11.

Despite the fact that the plates were active only when the load was increased beyond the preloading value, the preloaded beams F22, F23, F24 of Series III also developed ultimate strengths comparable to that of beam F11. This may be explained by the fact that although the total bar strain was greater than that of the plate, the lower yield strain of the plates (mild steel) and the plastic properties of steel permitted the full exploitation of the external reinforcement. Applying the principle of superposition to the strain distribution as is shown in Fig.5.30 and depending on the preloading value of dead load, the total bar and concrete strains could be so much higher than the total plate strain that the latter may not reach its yield value before concrete reaches its ultimate compressive strain. The added strength from the plates may therefore not be fully used. This is more likely in cases of high preloading values and high yield steel plates or mild steel bars.

In such cases, the use of the simplified method of CP110 is not recommended. The method is based on the criteria that both reinforcements yield before failure, which may overestimate the beam strength. The best and most appropriate analysis to use

would certainly be a strain compatibility method based on a given ultimate concrete compressive strain and taking into account the plastic properties of steel.

Table 5.11 shows that the simplified CP110 method predicts the same value of ultimate strength for beam F11 and the preloaded beams F22, F23, F24. This is due to the fact that this simplified method does not take into account the difference in the strains and assumes that the reinforcement and the concrete reach their limit strains at failure.

The strain compatibility methods however give different predictions. The differences are very small and negligible in these beams for the reason mentioned earlier: the plates (mild steel) have a lower yield strain than the bars (high yield steel).

This shows that despite the preloading of the existing reinforcement up to 70% of the ultimate strength of the beam, the added strength from the plates can still be fully exploited if they are appropriately chosen (with a lower yield strain than the existing bars).

5.9 INTERPRETATION OF RESULTS

The plated beam results showed that bonding 1.5mm thick steel plates, on the tensile face of the beams by means of an epoxy adhesive layer, improved the performance of the beams. The increases in the stiffnesses were however greater than expected as is illustrated by the comparisons of the following non-dimensional parameters:

- (1) The ratio of measured to predicted deflection at a load of 100kN, was 1.05 for unplated beams and 1.03 for plated beams.
- (2) For the rotations at 100kN, these ratios were 1.04 and 1.01

respectively.

(3) The concrete compressive strain ratios at 100kN were 1.21 and 1.14 respectively.

(4) The bar strain ratios were 0.99 and 0.80 at 100kN and 1.05 and 0.95 at 150kN respectively.

(5) The crack width ratios at 100kN were 1.04 and 0.89 respectively.

(6) The rigidity ratios at 100kN were 0.92 and 0.94 respectively.

(7) The ratios of recorded and predicted first crack loads were 1.15 and 1.39 respectively.

These higher ratios of rigidities and first crack loads and lower ratios of deformations and crack widths may be explained partly by the fact that the theoretical formulae are based on a value of concrete elastic modulus determined in service conditions and the parabolic stress-strain relationship of concrete means that the actual stiffness is greater at lower loads. A load of 100kN represents 48 and 42% respectively of the ultimate strengths of the unplated beams and beams with a 1.5mm plate. These lower percentages of a given load to the ultimate strength with plated beams explain partly the observations mentioned earlier.

The previous explanations cannot however justify the higher values of concrete tensile strains at cracking and concrete tensile stresses after cracking in plated beams. The tensile strain in concrete at first cracking and the tensile stress in concrete in a cracked state were the only non-dimensionless parameters studied.

The recorded tensile strains in concrete at first cracking were

154 and 178 microstrains respectively for unplated beams and beam F11 with a 1.5mm plate.

Before cracking (at 20kN), the calculated tensile stress in concrete was 1.48 N/mm^2 for unplated beams and 2.03 N/mm^2 for beams with a 1.5mm plate.

After cracking the tensile stress in concrete dropped to 0.92 N/mm^2 in unplated beams justifying the assumptions of various codes of practice to ignore the concrete in tension or limit its contribution to 1 N/mm^2 (79).

Despite cracking at 100kN the calculated tensile stress in concrete was 2.67 N/mm^2 in the plated beams.

The presence of the plates seem to enable concrete to carry more stresses in tension, in a cracked state, which thus results in an increase of the overall stiffness of the beam. The mechanism by which the plates improve the performance of concrete in tension is not very clear. The crack pattern in a reinforced concrete member depends on the ratio of the steel area to the contact area with concrete. In conventional RC structures, cracking is initiated in the external surface of the member where there is a great number of heterogeneities due to the wall effect or another mechanical action. If a glue layer and a steel plate are bonded to the member, they will tend to eliminate the imperfections by impregnating the external surface of concrete, thus producing a delay in the appearance of cracks. The external reinforcement and the greater bond area will also prevent the principal cracks from widening freely. This reduction in the crack openings will produce a higher transfer of tensile stresses between the cracks, thus resulting in a greater contribution of concrete in

tension and consequently a higher stiffness of the transformed section. The effect of the plate on the crack opening is well illustrated by Fig.5.20, showing the concrete tensile strain (including the widths of the cracks present in the gauge length over which the measurement was made) at the preloading stage and after strengthening for beam F13. The restraining of the free widening of the principal cracks results in the appearance of neighbouring secondary cracks developing from the principal cracks and extending towards the plates and forming a Δ shaped cracking (Fig.5.10). A possible simplified stress model to explain this behaviour is shown in Fig.5.31. The presence of the plates may result in a somewhat plastic behaviour of concrete in tension after the first crack load is reached. It has already been shown that concrete behaves this way in certain conditions. Hillerborg (83) carried out tests on plain concrete beams to investigate the fracture mechanics of concrete. He found that varying the beam depth affected the contribution of concrete in tension. The plasticity of concrete in tension was increased with slender beams.

This plastic behaviour of concrete in tension may be the result of the restraining effects of the plates on the free widening of principal cracks and would explain the increase in the beam rigidity, the reduction in the deflections, rotations, crack widths and strains, and the high tensile stresses of concrete in the plated beams.

Bloxham (34) carried out tests on small scale plated beams and found that he had to take a glue tensile strength of 60 N/mm^2 (6 times the real value) in order to predict the strength responses of the beams. He suggested that the considerable

Table 5.12: Modes of failure and maximum loads carried.

Beam	Maximum load (kN)	Mode of failure
F01	210.0	Flexural crushing of concrete after yielding of the bars
F02	214.2	" " "
F11	239.0	Flexural crushing of concrete after yielding of bars and plate
F12	232.0	" " "
F13	230.0	" " "
F14	240.0	" " "
F22	232.2	" " "
F23	233.0	" " "
F24	232.3	" " "

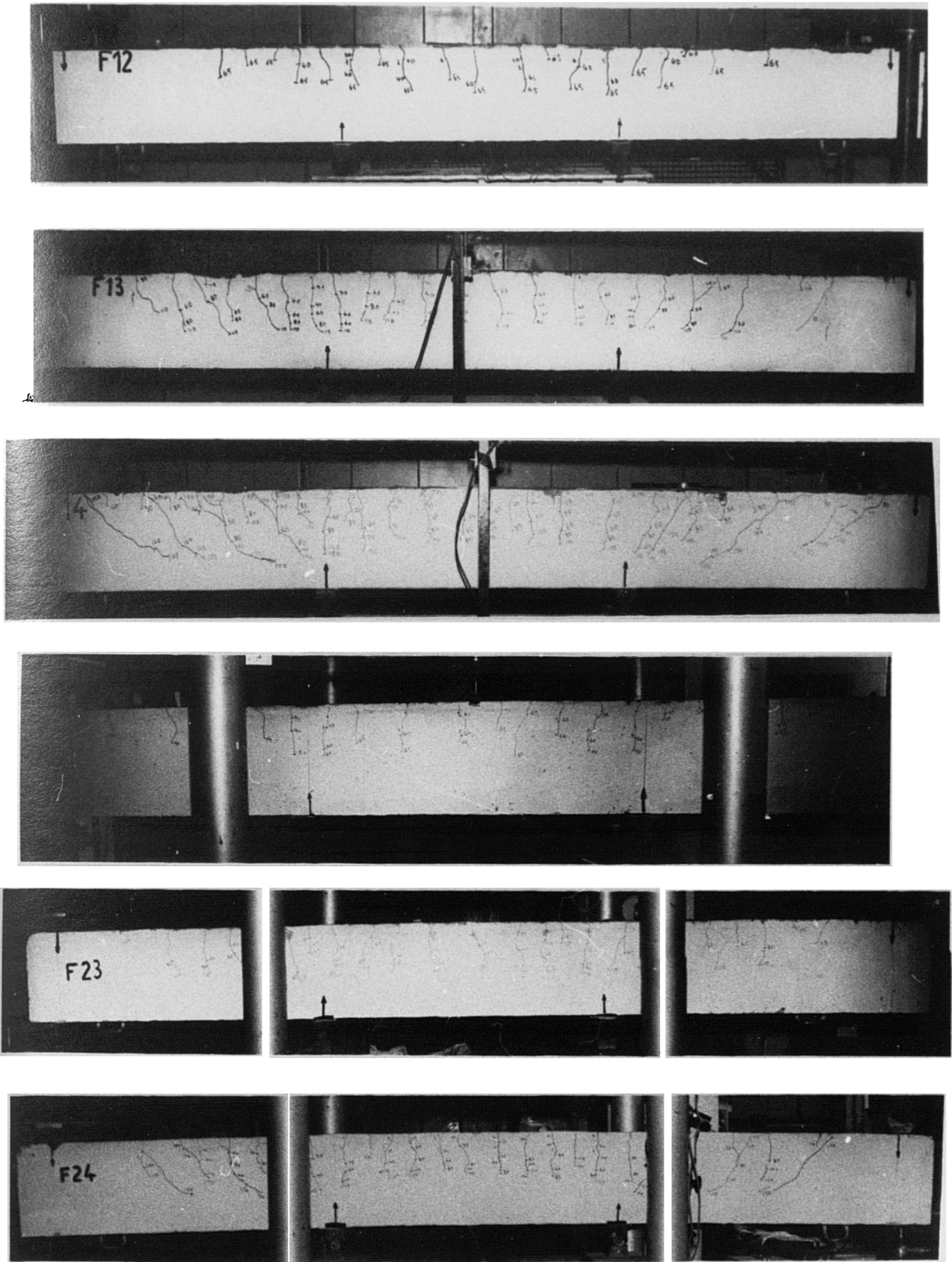
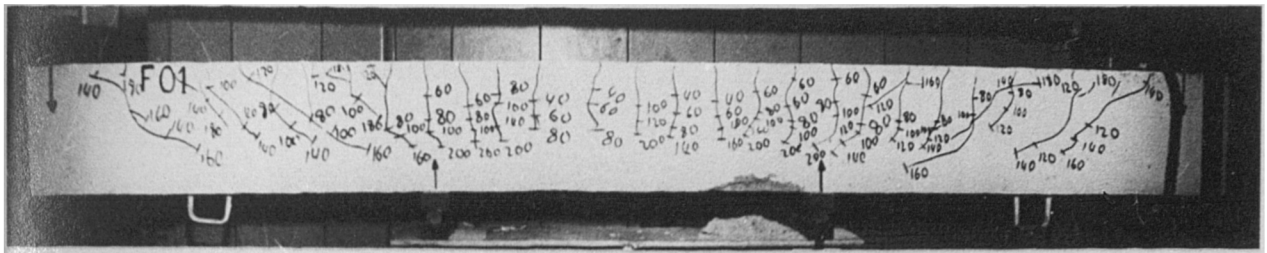
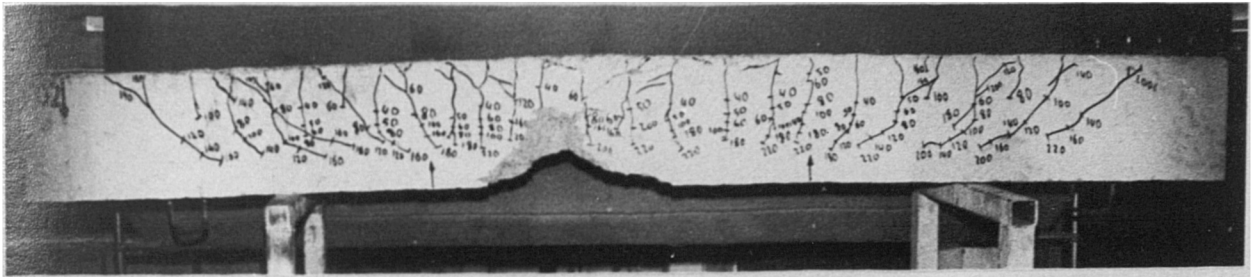


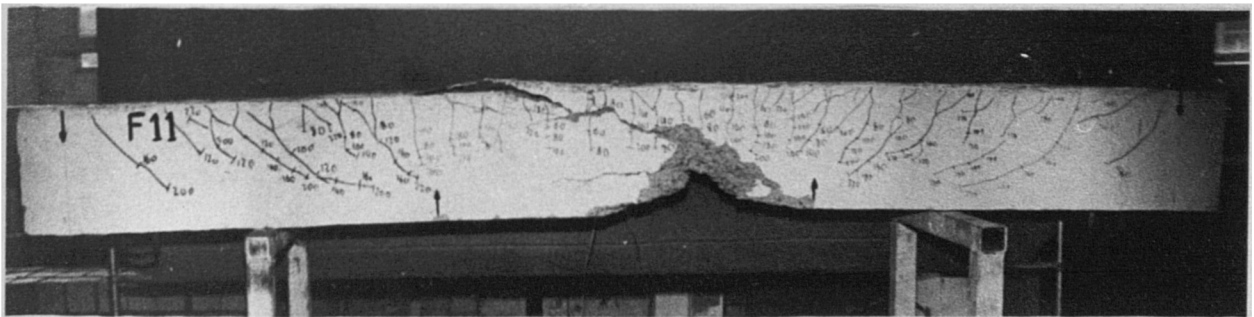
Fig.5.32: Crack patterns at the preloading stage of beams of Series II and III



F01: no glue and no plate

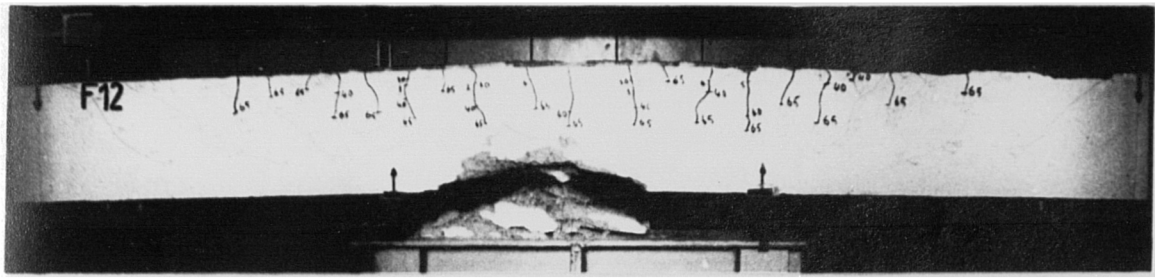


F02: 3mm glue layer

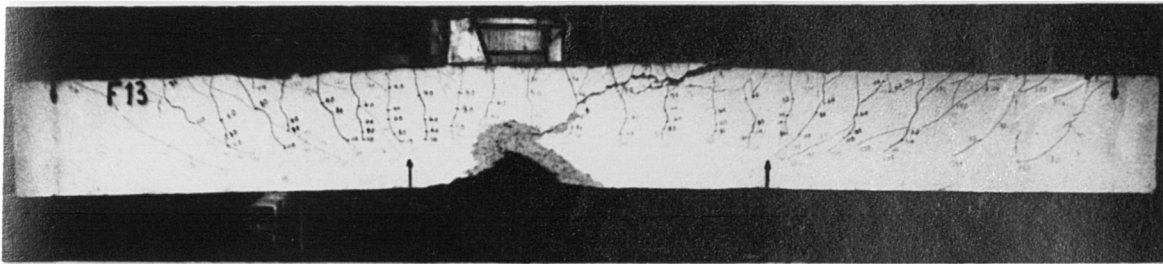


F11: one 1.5mm plate

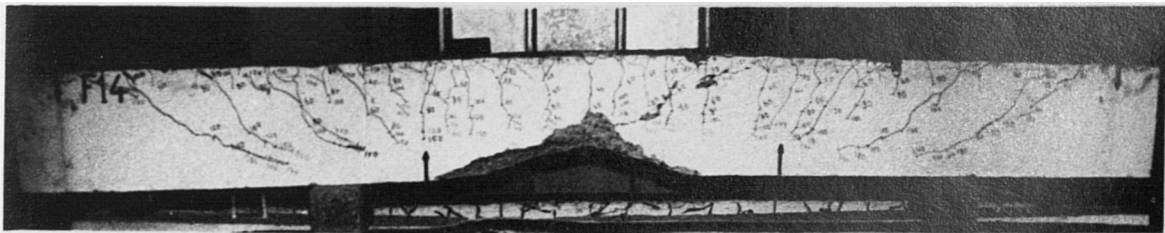
Fig.5.33: Crack patterns and modes of failure of beams of Series I



F12: preloaded to 30%



F13: preloaded to 50%

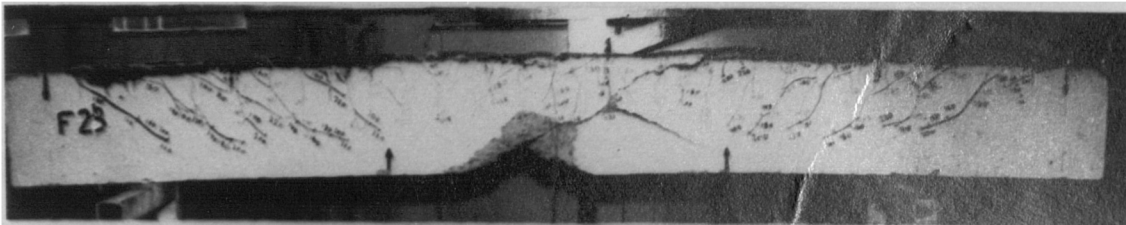


F14: preloaded to 70%

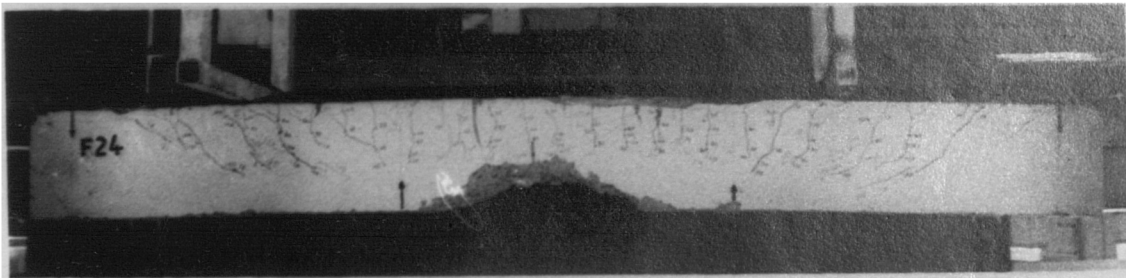
Fig.5.34: Crack patterns and modes of failure
of beams of Series II
(preloaded, unloaded and then strengthened
with a 1.5mm steel plate)



F22: preloaded to 30%



F23: preloaded to 50%



F24: preloaded to 70%

**Fig.5.35: Crack patterns and modes of failure
of beams of Series III
(preloaded and strengthened whilst under the preload
with a 1.5mm steel plate)**

increase in stiffness and strength could be explained by the assumption that the composite material plate-glass may be performing as a material two to three times stiffer and stronger than could be deduced from the separate properties of each material. Tests on composite specimens (tensile tests on steel plates with a glue layer and flexural tests on concrete prisms with a glue layer) contradicted his propositions and showed that the composite specimens behaved predictably. His observations can be better explained by the model of 'plastic' behaviour of concrete in plated beams.

This assumption of a better performance of concrete in tension would be worth studying by tests on conventional RC beams and plated beams designed to produce the same flexural performance. L'hermite and Bresson (50) reported tests on one conventionally reinforced concrete beam and another one externally reinforced with the same amount of steel. They observed a better performance of the plated beam but they explained the difference by the greater internal lever arm (distance between the neutral axis position and the reinforcement) in the plated beam. An ideal comparison would have therefore to take into account the difference in the lever arms when designing the two beams.

5.10 CONCLUSIONS

From the flexural studies of the plated beams, the following conclusions can be drawn:

- 1- Epoxy resin ensures full composite action of the reinforced concrete beams and the bonded steel plates and results in an increase of the stiffness and strength of the plated beam.
- 2- For the amount of internal reinforcement used in this

investigation (55% of balanced conditions ratio), the glue layer does not crack before failure and therefore acts not only as a stress transfer agent but as a full participant in the structural resistance of the beam.

3- Preloading of up to 70% of the ultimate strength, did not have any adverse effect on the flexural behaviour of the subsequently unloaded and strengthened beams. The restraining effect of the plates on the existing cracks was however more pronounced when the load was increased beyond the original preloading value.

4- The ultimate deformations and crack widths of the preloaded beams of Series III (which were strengthened whilst under their preloads) were greater than those of a plated beam but despite the increases during two weeks of bond curing under a constant load, they were less than those of an unplated beam.

5- The plastic properties of the steel bars and the lower yield strain of the plates permitted the full exploitation of the added plates (although they were active only beyond the existing preload) in the preloaded and subsequently strengthened (whilst under their preloads) beams.

6- Apart from the predictable increase in stiffness and strength, the external steel plates seem to be restraining the free widening of the cracks and allow a higher stress transfer between the cracks resulting in an improved performance of concrete in tension and thus a higher overall beam stiffness as compared to conventional reinforcement designed to achieve the same performance.

CHAPTER SIX
PREMATURE BOND FAILURES OF PLATED BEAMS

6.1 INTRODUCTION

In conventional reinforced concrete, the bond between the steel bars and the concrete cover is a combination of chemical adhesion and mechanical friction. Variation of the applied bending moment is the major cause of the bond and shear stresses. These stresses are interrelated and their interaction is even closer after the appearance of shear cracks (84-86). The dowel action which follows may cause the concrete cover to be broken off. This kind of failure gave rise in the past to confusion whether it was a bond or shear failure (87).

The bond stress distribution in the shear span is not uniform and is highly influenced by the cracks crossing the bars. The bond stresses are usually critical near the supports and can cause premature failures by debonding of lapped bar splices following a large crack in the cover along the line of the bars (88). Premature bond failures can also result from stopping a splice of bars at the same section in the shear span (89,90).

In the technique of strengthening existing concrete beams by glueing external reinforcement, the plate width cannot exceed that of the beam. There is therefore an upper limit to the bond area and the amount of external steel can only be increased by bonding thicker plates. Unlike in the internal reinforcement where the bond area, which is equal to the bar perimeter, increases with the cross section area of the bar,

the bond area in the external steel does not increase with the plate thickness. As the bond stresses are proportional to the steel area, this will limit the amount of external reinforcement that can be added.

Furthermore, when dealing with existing beams, the plates are always stopped in the shear span, thus creating a critical section. The transfer of tensile forces from the plate to the bars in the region where the plate is stopped results in high gradients of strains and stresses. These variations are higher with thicker plates.

In addition, the eccentricity between the tensile forces in the plate and the balancing bond forces in the epoxy joint will result in normal forces which will tend to lift the plate. These peeling forces are higher with thicker plates and critical at the plate cutoff section.

The premature bond failures occurring with thick plates and reported by various researchers (34,50,54,62-64,66) could be caused by one or a combination of these bond and peel stresses.

Analytical investigations into the bond and peel stresses present in the joint are first presented in this chapter. The effect of the plate cutoff in the shear span on these stresses is also studied.

The second part of the chapter describes the experimental investigations to clarify the mechanism of premature bond failures and the different operations attempted to solve the problem.

A study of the flexural properties and a comparison of the predicted and measured bond and peel stresses are finally presented.

6.2 BOND STRESSES

In plated beams, there are two types of bond between steel and concrete: bond between the internal bars and the surrounding concrete and bond between the plate and the beam through the epoxy layer.

The bond stresses are caused by the variation of tensile forces along the reinforcement resulting from the variation of the bending moment in the shear span.

6.2.1 BOND STRESSES IN THE BARS (ELASTIC THEORY)

The forces acting in an element length dx of the bars in the shear span are shown in Fig.6.1. The difference in the longitudinal forces (resulting from the variation of the bending moment) is balanced by the bond stresses:

$$T+dT-T=f_{bb}P \cdot dx \quad \text{therefore:}$$

$$f_{bb} = \frac{1}{P} \frac{dT}{dx} = \frac{1}{P} \frac{E_b A_b d\epsilon_b}{dx}$$

Where :

f_{bb} : Bond stress in the bars

P: Perimeter of the bars

dT: Variation of tensile force over the distance dx

E_b : Elastic modulus of bars

A_b : Cross section area of bars

$d\epsilon_b$: Variation of strain in bars over the distance dx

$d\sigma_b$: Variation of tensile stress in bars over the distance dx

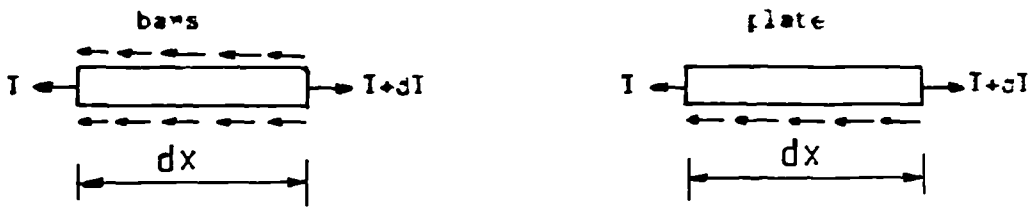
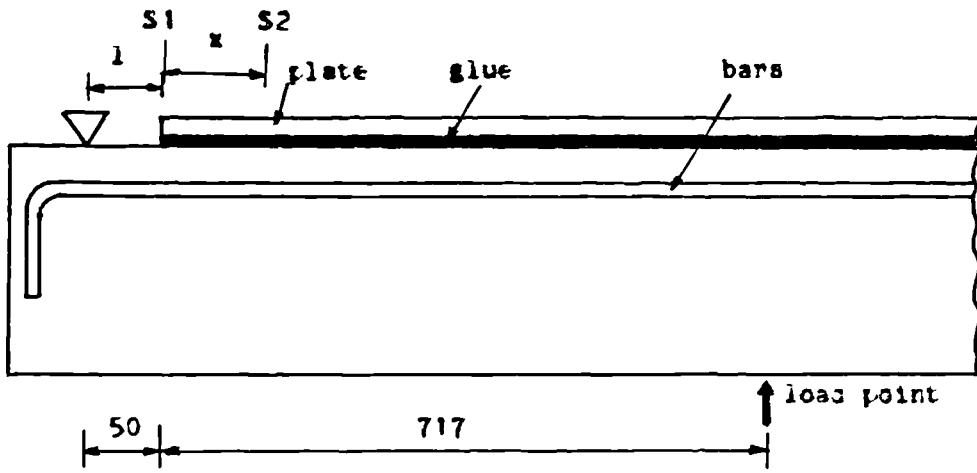


Fig.6.1: Bond stresses along bars and plate

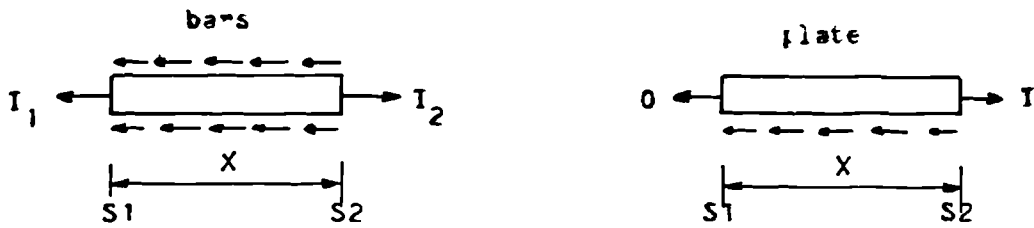


Fig.6.3: Bond stresses in the plate cutoff region

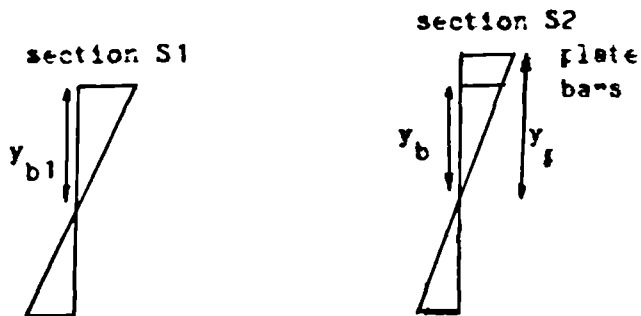


Fig.6.2: Transformed sections at sections S1(unplated) and S2(plated)

and $d\sigma_b = E_b d\epsilon_b$

If M is the applied moment, y_b and y_p the distance from the neutral axis to the bars and plate respectively, and I the second moment of area of the transformed section (cracked or uncracked), then considering the transformed section shown in Fig.6.2, the stress in the bars is:

$$\sigma_b = M \frac{y_b}{I} \quad \text{so} \quad d\sigma_b = \frac{y_b}{I} dM \quad \text{therefore} \quad d\epsilon_b = \frac{y_b}{E_b I} dM$$

and $dM = V \cdot dx$ where V is the shear force.

The internal bond stress is therefore given by:

$$f_{bb} = \frac{V A_b y_b}{P \cdot I} \tag{6.1}$$

If there was no external reinforcement the quantity $I/A_b \cdot y_b$ would be equal to the internal lever arm z_b and the well known equation $f_{bb} = V/P \cdot z_b$ would be found.

6.2.2 BOND STRESSES IN THE PLATE (ELASTIC THEORY)

The forces acting in an element dx of the joint plate-glue-concrete are shown in Fig.6.1. The variation of the longitudinal force is balanced by the bond stress:

$$T + dT = f_{bp} \cdot b' \cdot dx$$

f_{bp} : Bond stress in the external joint

b' : Width of the plate

dT : Variation of the tensile force in the plate

over the distance dx

In the same manner as for the internal bond, the bond stress in the external joint is given by:

$$f_{bp} = \frac{V \cdot A_p \cdot y_p}{b' \cdot I} \quad (6.2)$$

Where :

A_p : Cross sectional area of the plate

I : Second moment of area of the transformed section

y_p : Distance from the plate to the neutral axis

V : Shear force

It can be seen from equations (6.1) and (6.2) that the internal and external bond stresses are proportional to the ratios A_b/P and A_p/b' respectively. Therefore if the amount of steel A_b or A_p is increased by increasing the bar diameter or the plate thickness, the bond stress for the plate f_{bp} will increase more than that for the bars $f_{bb'}$, since the bar perimeter P increases with the bar diameter whereas the plate width b' cannot exceed that of the beam and does not increase with the plate thickness.

6.3 EFFECT OF PLATE CUTOFF ON BOND STRESSES

Equations (6.1) and (6.2) give the internal and external bond stresses in regions of the shear span not affected by the plate cutoff. This cutoff affects the bond stresses over some distance x over which the transfer of tensile forces from the plate to the bars takes place.

Considering the transfer length, the forces acting on the external and internal reinforcements will be as shown in Fig.6.3 where:

S_1 = Section where the plate is stopped and only the bars are active

S_2 = Nearest section where the bars and plate are fully active

The force transfer starts at the section S_2 . At the section S_1 the tensile force is T_1 in the bars and zero in the plate. At the section S_2 the tensile force is T_2 in the bars and T in the plate.

The direction of the bond stress in the external joint is from S_2 to S_1 as shown in the diagram. In the bars however, the direction of the bond stress can be either way depending on the values of T_1 and T_2 . If T_1 is greater than T_2 , the bond stresses will be in the opposite direction to that shown in Fig.6.3.

If l is the distance from the support to the plate cutoff point, then the moment M_1 at section S_1 is $M_1=V.l$. The moment M_2 at section S_2 is $M_2=V(1+x)$. (l is known) (Fig.6.1).

$$T_1 = A_b \frac{y_{b1}}{I_1} V l ; \quad T_2 = A_b \frac{y_b}{I} V (1+x) ; \quad T = A_p \frac{y_p}{I} V (1+x)$$

I_1 : Inertia of transformed section excluding plate (section S_1)

I : Inertia of transformed section including plate (section S_2)

y_p : Distance from the plate to the neutral axis in section S_2

y_b : Distance from the bars to the neutral axis in section S_2

y_{b1} : Distance from the bars to the neutral axis in section S_1

x : Distance over which the force transfer takes place (unknown)

l : Distance from the support to the plate cutoff point

Assuming that the force transfer is linear over the distance x , the bond stress f_{bb} in the bars can be obtained from:

$$f_{bb} \cdot P \cdot x = T_1 - T_2 \quad (\text{or } T_2 - T_1) \quad \text{where } T_1 - T_2 = A_b V \left[1 \frac{y_{b1}}{I_1} - (1+x) \frac{y_b}{I} \right]$$

Therefore:

$$f_{bb} = \frac{V \cdot A_b}{P \cdot x} \left[1 \frac{y_{b1}}{I_1} - (1+x) \frac{y_b}{I} \right] \quad (6.3)$$

The distance from the neutral axis to the bars is greater in section S_1 where there is no plate i.e: $y_{b1} > y_b$. There is a shift in the neutral axis after the plate is stopped. The difference $T_1 - T_2$ can therefore be either positive or negative (Fig.6.2). The external bond stress in the cutoff region is given by:

$$f_{bp} \cdot x \cdot b' = T = A_p \frac{y_p}{I} V(1+x) \quad \text{so} \quad f_{bp} = \frac{V \cdot A_p \cdot y_p}{b' \cdot I} \left[1 + \frac{1}{x} \right] \quad (6.4)$$

Equations (6.3) and (6.4) give the internal and external bond stresses in the region of the plate cutoff (assuming a linear force transfer from the plate to the bars in that region).

Due to the local problem of stress transfer in the cutoff region, failure is prone to develop prematurely and could be a bond or a shear failure or a combination of the two. It can be shown similarly that the plate cutoff has an effect on the shear stresses (89,90). There is an increase in bond and shear stresses due to the sudden change in the transformed section.

The bond stresses resulting from the cutoff can be deduced by subtracting the expressions of equations (6.1) and (6.3) for the bars and (6.2) and (6.4) for the plate.

The direction of the normal bond stresses for the bars and plate is towards the support as shown in Fig.6.1. In the plate cutoff region the longitudinal force in the plate becomes zero and that in the bars increases. For the continuing bars the bond stress resulting from the cutoff is in the opposite direction to the normal bond stress given by equation (6.1). For the stopped plate the two components are additive.

Equations (6.2) and (6.4) show that the fact that the plate is stopped at a distance l from the support results in an increase of $100l/x$ (%) in the external bond stress. Assuming that the distance x over which the force transfer takes place is the same wherever the plate is stopped, the effect of the cutoff on the bond stress can be minimized by stopping the plate as near the support as possible.

Equations (6.3) and (6.4) show that the effect of the cutoff increases with the plate thickness (assuming a constant plate width), for the shift in the neutral axis is higher when thicker plates are stopped.

To avoid premature bond failures, the bond stresses given by equations (6.1) and (6.3) for the bars and (6.2) and (6.4) for the plate must not exceed the ultimate values determined from shear pull out tests. The pull out tests do not however take into account the bending of the beams and the bond stresses in the beams may be lower than those given by pure shear tests (pull out tests).

The CP110 code (79) gives in Table 21 the ultimate local bond stress for plain and deformed steel bars as a function of the grade of concrete used. The ultimate local bond stress for a concrete grade of 50 with deformed bars is $3.4\gamma_m = 5.1 \text{ N/mm}^2$.

γ_m is the CP110 safety factor and is equal to 1.5 for concrete.

The ultimate shear bond stress of the joint steel-epoxy-concrete as determined by the pull out tests described in chapter four is 6.5 N/mm^2 . The same tests also showed that the transfer of forces from the plates to concrete in pure shear is not linear but exponential. This means that the force transfer due to bending in the plate cutoff region is probably not linear as was assumed in equations (6.3) and (6.4).

6.4 PEELING FORCES

It can be seen from Fig.6.1 that unlike in the internal bars where there is total equilibrium between the bond stresses and the tensile stresses in the bars, the eccentricity between the tensile stresses in the plate and the balancing bond stresses will result in normal forces in the joint that will tend to lift the plate. This peeling force F_1 will be higher with a higher eccentricity (thicker plate or joint) as shown in Fig.6.4.

In addition to this force F_1 , there is another peeling force F_2 resulting from the resistance of the plate to bending.

The total peeling force F present in the joint is the combination of the two components F_1 and F_2 . $F = F_1 + F_2$.

Considering the diagram shown in Fig.6.4:

$$F_1 \cdot dx = dT \cdot e \quad \text{so } F_1 = e \cdot \frac{dT}{dx}$$

$$\text{but } dT = A_p \frac{y_p}{I} dM \quad \text{therefore } F_1 = \frac{A_p y_p}{I} V \cdot e$$

The bond stress f_{bp} and the tensile force T are balanced by a system of internal couples which reduces to a single force F_1 at the end of the plate.

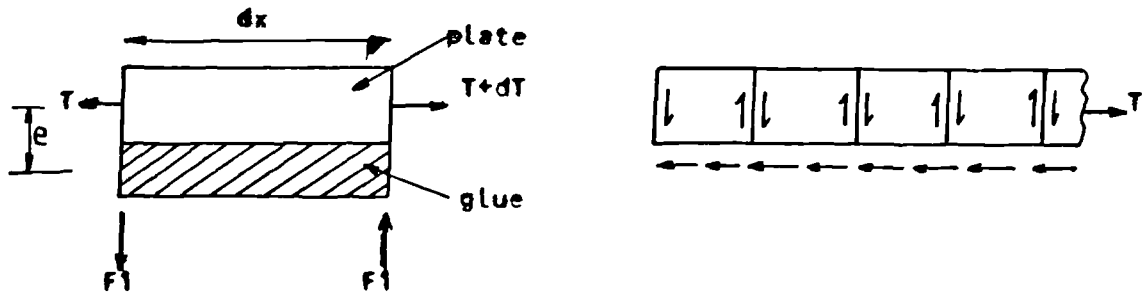


Fig.6.4: System of forces acting in the joint between the plate and the beam

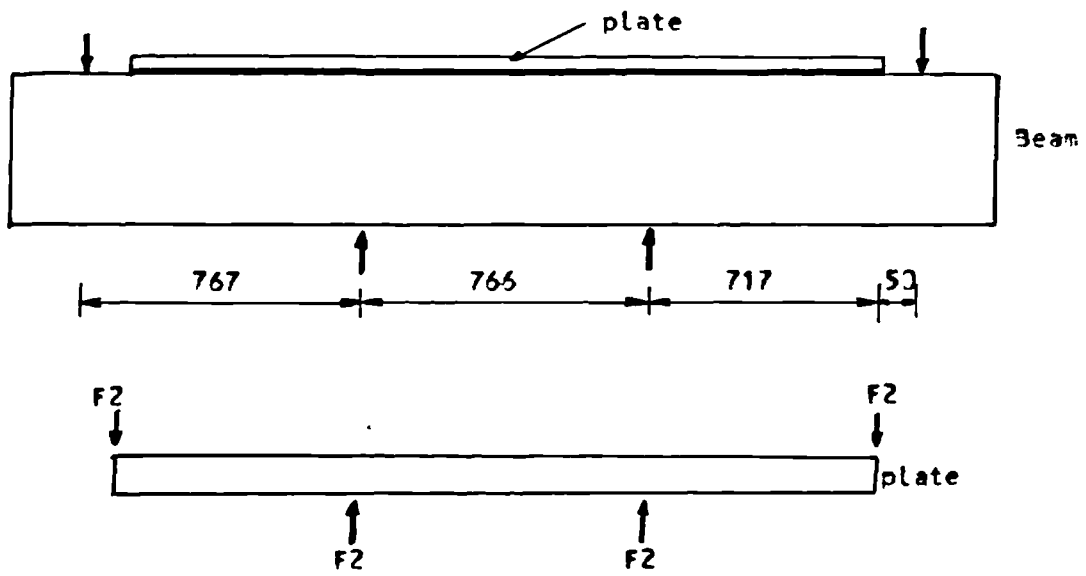


Fig.6.5: Assumed loading system in the plate

$$F_1 dx = f_{bp} \cdot b' \cdot e \cdot dx \quad \text{so } F_1 = f_{bp} \cdot b' \cdot e \quad (6.5)$$

f_{bp} : Bond stress in the joint given by equations (6.2) and (6.4).

b' : Plate width

e : Eccentricity between bond stresses in joint and tensile force in plate.

Jones, Swamy and Ang (66) found the same expression for the peeling force and they assumed that the eccentricity e is equal to half the thickness of the plate.

Assuming that the bond stresses are applied in the middle of the glue joint, then the eccentricity e will be:

$$e = \frac{1}{2}(t_p + t_g) \text{ where } t_p \text{ and } t_g \text{ are the plate and glue thicknesses}$$

respectively. The lifting force F_1 which is proportional to the bond stress f_{bp} is critical at the end of the plate where the bond stress is maximum.

The second component F_2 of the peeling force can be determined from the curvature of the plate. F_2 is the plate resistance to bending. The curvature of the plate is similar to that of the beam, therefore the plate will be assumed to be submitted to a similar loading as shown in Fig.6.5 The load is assumed to be transferred vertically to the plate and the resistance of the plate to bending is assumed to be concentrated at its ends. This is a gross simplification and other models of loading can be possible. The assumed model is however the one giving the highest value for F_2 . Knowing the deflection and the stiffness of the plate, the reaction to bending can be determined by an elastic analysis. The

deflection of the plate is equal to that of the beam. The central deflection is given by:

$$\Delta = \frac{F2 \cdot a \cdot [3 \cdot L^2 - 4 \cdot a^2]}{24 \cdot E_p \cdot I_p}$$

Where $a = 717\text{mm}$, and $L = 2200\text{mm}$

b' = plate width = 125mm , t_p = plate thickness = 6mm

$$E_p = 2.10^5 \text{N/mm}^2 \quad I_p = \frac{b' \cdot (t_p)^3}{12} = 2250\text{mm}^4$$

$\Delta = 0.827 \cdot F2$ therefore $F2 = 1.21\text{N}$ per mm deflection

$$F2 = 1.21\text{N/mm} \quad (6.6)$$

For a deflection of 10mm : $F2 = 12.1\text{N}$ (very small).

The total peeling force F present at the end of the joint is:

$$F = F1 + F2 \approx F1$$

6.5 EXPERIMENTAL INVESTIGATION

6.5.1 INTRODUCTION

The phenomenon of premature bond failures is not unknown in conventionally reinforced concrete. Ferguson and Matloob (89) and Baron (90) reported bond failures of RC beams with splices of bars stopped in the shear span. They found that bending up of the bars solved the problem. Bending up the bars does not affect the total change in the tensile forces but it increases the distance x over which the transfer takes place and makes the shift in the neutral axis position less sudden.

When strengthening existing structures, the plate will always have to be stopped in the shear span. The provision of anchorage lengths is therefore difficult. The solution equivalent to the bending up of the bars may be the tapering of the plate thickness in the shear span but this operation is very difficult and cannot be reliable unless perfectly executed.

6.5.2 EXPERIMENTAL PROGRAMME

The aim of this part of the project was to study the mechanism of premature bond failure and to investigate possible solutions to the problem. The number of beams for this series necessary to find a solution to the bond failure problem and develop the full flexural capacity of the beam was unknown in the beginning. Seven beams in all were eventually tested.

In this section the bond and peel stresses present in the joints are analysed and compared with predictions obtained using expressions presented in the previous sections. The flexural properties of the beams are also studied and compared with those of beam F11 with a 1.5mm plate. Comparison of the behaviour of the unplated beam F01 and the plated beam F11 was described in chapter five.

All the beams in this Series were plated with either one 6mm or two 3mm plates, the epoxy joints between steel and concrete being 1.5mm thick and those between the two plates (beams F32 and F35) being 1mm thick. The internal reinforcement consisted of three Tor bars of 20mm diameter and twelve 6mm mild steel stirrups in each shear span. The beam details are shown in Figs.6.6 and 6.7.

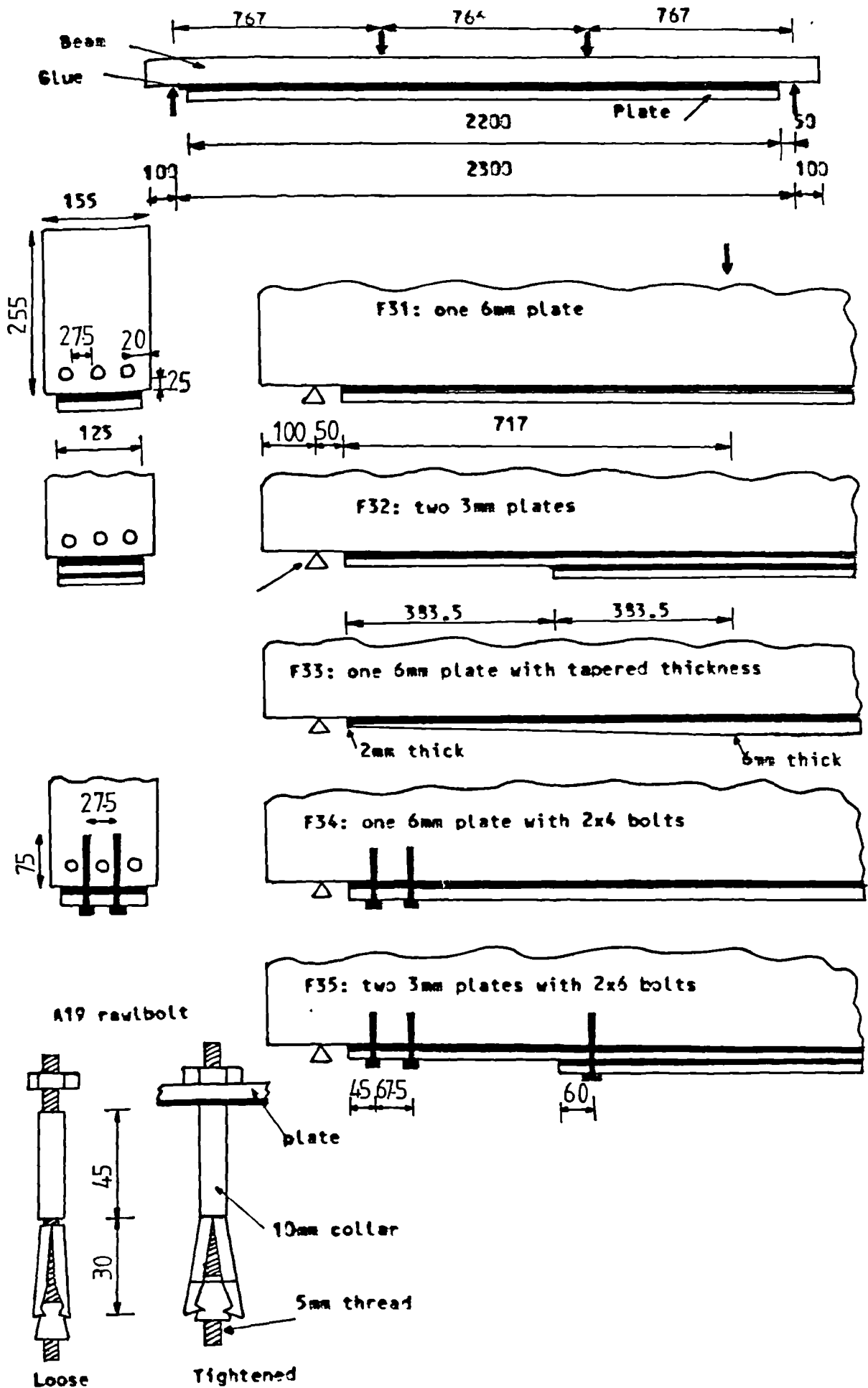


Fig.6.6: Details of bond failure beams

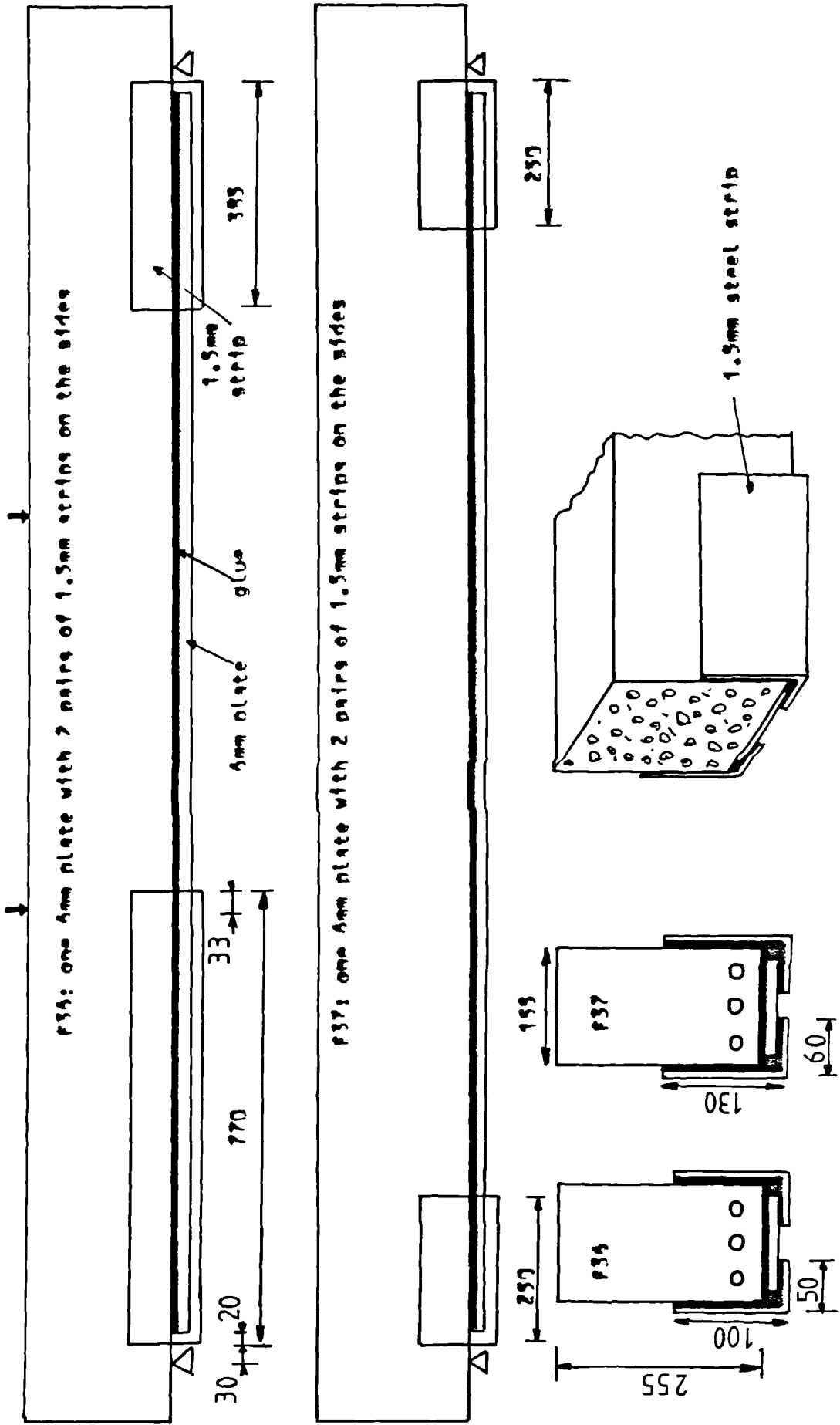


Fig.6.7: Details of panels F34 and F37 with strips

The beams in this Series are as follows;

F31: One 6mm plate

F32: Two 3mm plates, the outer being stopped before the inner.

F33: One 6mm plate with a tapered thickness in the shear span

F34: One 6mm plate with four bolts at each end

F35: Two 3mm plates with four bolts at each end of the inner plate and two bolts at each end of the outer plate

F36: One 6mm plate with side strips at each end

F37: One 6mm plate with side strips at each end

Beam F31 was tested first and was expected to fail in bond by separation of the plate at its end.

The remaining beams F32 to F37 were all designed to have improved performance by reducing the bond stresses or providing anchorages and thus avoiding premature failures and hence developing the full flexural strength.

Beam F32 was strengthened with two 3mm plates. The outer plate was shorter than the inner one and was stopped halfway along the shear span. This device provided the beam with a theoretical flexural strength equal to that of beam F31 but lower values of bond and peel stresses in the region where the inner plate was stopped.

Beam F33 had a 6mm plate with a tapered thickness in the shear spans. It was hoped to achieve an ideal linear tapering of the thickness from 6mm at the load point to zero at the end of the plate. Perfect execution of the tapering proved however to be impractical and the result was a non uniform tapering from 6mm to 2mm. Tapering gradually reduced the cross sectional area of the plate and consequently the bond and peel stresses and was expected to delay (if not avoid) the premature failure.

Beams F34 and F35 were similar to the beams F31 and F32 respectively but after the strengthening operation, the plates were bolted to the beam by A19 rawlbolts (Fig.6.6). The bolts penetrated to a depth of 75mm and were able to sustain a tensile force of 8kN each. The grip was ensured by the enlargement of the base of the bolt when tightened. In addition to this mechanical grip, epoxy glue was poured into the drilled hole (with the bolt) to provide a further bond between concrete and the bolt. These rawlbolts were expected to overcome the peeling force acting at the end of the plate and prevent bond failure.

Beams F36 and F37 were strengthened in flexure with one 6mm plate and subsequently with L shaped 1.5mm thick strips (Fig.6.7). One strip was glued on either face of each shear span. The strips were designed to prevent the peeling of the plate and strengthen the part of the beam where bond failure occurs. The dimensions of the L shaped strips of beam F36 were different: On one shear span the strips covered the whole shear span whereas on the other side they were only 385mm long (Fig.6.7). In both cases the strips were 100mm deep. The strips of beam F37 were all identical and were 250mm long and 130mm deep. The dimensions of the strips and their positions are shown in Fig.6.7.

6.5.3 BEAM DETAILS

The manufacturing of the beams, their section and internal reinforcement, the materials used and the bonding procedure were identical to the ones described in chapter five. The details of the bond failure beams are shown in Figs.6.6 and 6.7.

6.5.4 TEST MEASUREMENTS AND INSTRUMENTATION

The test measurements and the instrumentation used are as described in detail in chapter five. In addition to the central deflections, support rotations, crack widths, concrete strains, central bar and plate strains, the plate and bar strains were measured at different locations along the beams using strain gauges for the bars and 50mm demec gauges for the plate. The strain gauge measurement is described in Appendix A. For the beams with two 3mm plates, the plate strain was measured on the outer plate only in the region where there were two plates and on the inner plate in the other region. The horizontal movement of the end of the 6mm plate and the slip between the two 3mm plates were also measured by means of electrical transducers (LVDT).

6.5.5 TESTING PROCEDURE

The beams were tested in rig 1 (Figs.5.1 and 5.2) except beams F36 and F37 which were tested in rig 2 (Figs.5.3 and 5.4) The testing apparatus and procedure were as described in detail in chapter five.

6.6 TEST RESULTS

The flexural properties (deformations, crack widths, strengths) and the bond stresses present in the beams are discussed separately in the following sections. The analysis of the beams and the methods for computation of the deflections, rotations, strains, crack widths and strengths are similar to those used for the flexural beams of chapter five and are described in Appendices C, D and E. The cube strength and the modulus of rupture varied from 52.0 to 55.8 N/mm² and 4.41 to

4.78 N/mm² respectively (Table 6.1). The use of the value of 53.0 N/mm² as determined in chapter three results in a variation of less than 1% in the ultimate strength of the beams. Furthermore the values of concrete and steel elastic moduli used in the analysis are those determined by the material tests described in chapter three. It was therefore decided to use the same cube strength in the analysis of the beams.

The bond failure beams all had similar transformed sections at midspan and were expected to have similar deformational and cracking properties. The different solutions attempted to overcome bond failure (tapering, bolts and strips) were however expected to increase the ultimate loads. The results show this to be the case. The behaviour of the beams of this Series was similar at low loads but the beams reached different ultimate strengths and the modes of failure were different (Table 6.2). The strength properties, the modes of failure and the effects of the tapering, bolts and strips are discussed in detail in later sections.

6.7 DEFORMATION PROPERTIES

6.7.1 DEFLECTIONS AND ROTATIONS

The methods used for the prediction of the deflections and rotations are the same as those used in chapter five. The theoretical and experimental deflections and rotations at different load levels before and after cracking are given in Tables 6.3 and 6.4. As expected, the stiffnesses of the bond failure beams were similar and greater than that of beam F11 (Figs.6.8 to 6.11). At a load of 100kN, the ratio of measured to predicted deflection was 1.05 for beam F11 and 0.92 for the

Table 6.1: Bond failure beams.

Beam No.	F31	F32	F33	F34	F35	F36	F37
Age (1)	28	28	28	28	28	28	28
(days) (2)	42	42	42	42	42	42	42
Cube strength(N/mm ²)	54.5	55.3	52.9	53.3	52.0	55.8	52.2
Modulus of rupture(N/mm ²)	4.48	4.78	4.54	4.41	4.44	4.55	4.44
Ind.tensile strength(N/mm ²)	3.36	3.68	3.61	3.41	3.57	3.56	3.64
Glue thick.(mm)	1.5	1.5	1.5	1.5	1.5	1.5	1.5
Plate thick.(mm)	6.0	2x3.0	6.0	6.0	2x3.0	6.0	6.0

(1): At strengthening (2): At testing

Table 6.2: Modes of failure and maximum loads carried.

Beam	Max.load (kN)	Mode of failure
F11*	239.0	Flexural crushing of concrete
F31	182.0	Debonding of the plate end
F32	208.0	Debonding of the inner plate end
F33	191.0	Debonding of the plate end
F34	221.0	Flexural crushing of concrete after debonding of the plate
F35	227.0	" " " "
F36	285.1	Flexural crushing of concrete
F37	283.0	" " "

*: Strengthened with a 1.5mm plate

Table 6.3: Experimental and theoretical deflections at different load levels.

Beam No.	Experimental deflections (mm)			Theoretical deflections (mm)						Exp./Theo. (CEB)			
	20kN	100kN	200kN	20kN	100kN			200kN			20kN	100kN	200kN
				(1)	ACI	CEB	CP110	ACI	CEB	CP110			
F11	0.92	4.85	13.34	0.542	3.98	4.60	3.89	8.05	9.98	7.92	1.70	1.05	1.34
F31	0.68	3.34	8.80	0.530	2.81	3.36	2.74	5.64	7.12	5.57	1.28	0.99	1.24
F32	0.43	2.90	9.50	"	"	"	"	"	"	"	0.81	0.86	1.33
F33	0.56	3.00	9.20	"	"	"	"	"	"	"	1.06	0.89	1.29
F34	0.49	2.98	7.90	"	"	"	"	"	"	"	0.93	0.89	1.11
F35	0.65	3.15	8.36	"	"	"	"	"	"	"	1.23	0.94	1.17
F36	0.57	3.34	7.50	"	"	"	"	"	"	"	1.08	0.99	1.05
F37	0.55	2.91	8.50	"	"	"	"	"	"	"	1.04	0.87	1.19

\$: Extrapolated (1): ACI, CEB and CP110

Table 6.4: Measured and predicted rotations at different load levels.

Beam No.	Experimental rotations (min)			Theoretical rotations (min)						Exp./Theo. (CEB)			
	20kN	100kN	200kN	20kN	100kN			200kN			20kN	100kN	200kN
				(1)	ACI	CEB	CP110	ACI	CEB	CP110			
F11	2.83	22.01	63.94	2.43	17.87	20.65	17.47	36.10	44.75	35.54	1.17	1.07	1.43
F31	2.63	13.80	36.4	2.38	12.62	15.06	12.31	25.31	24.97	24.97	1.11	0.92	1.46
F32	2.52	14.69	32.30	"	"	"	"	"	"	"	1.06	0.98	1.29
F33	2.32	14.48	30.29	"	"	"	"	"	"	"	0.98	0.96	1.21
F34	2.25	13.50	30.98	"	"	"	"	"	"	"	0.95	0.90	1.24
F35	2.10	13.55	33.00	"	"	"	"	"	"	"	0.88	0.90	1.32
F36	1.85	13.15	31.07	"	"	"	"	"	"	"	0.78	0.87	1.24
F37	2.15	14.90	35.90	"	"	"	"	"	"	"	0.90	0.99	1.44

\$: Extrapolated (1): ACI, CEB and CP110

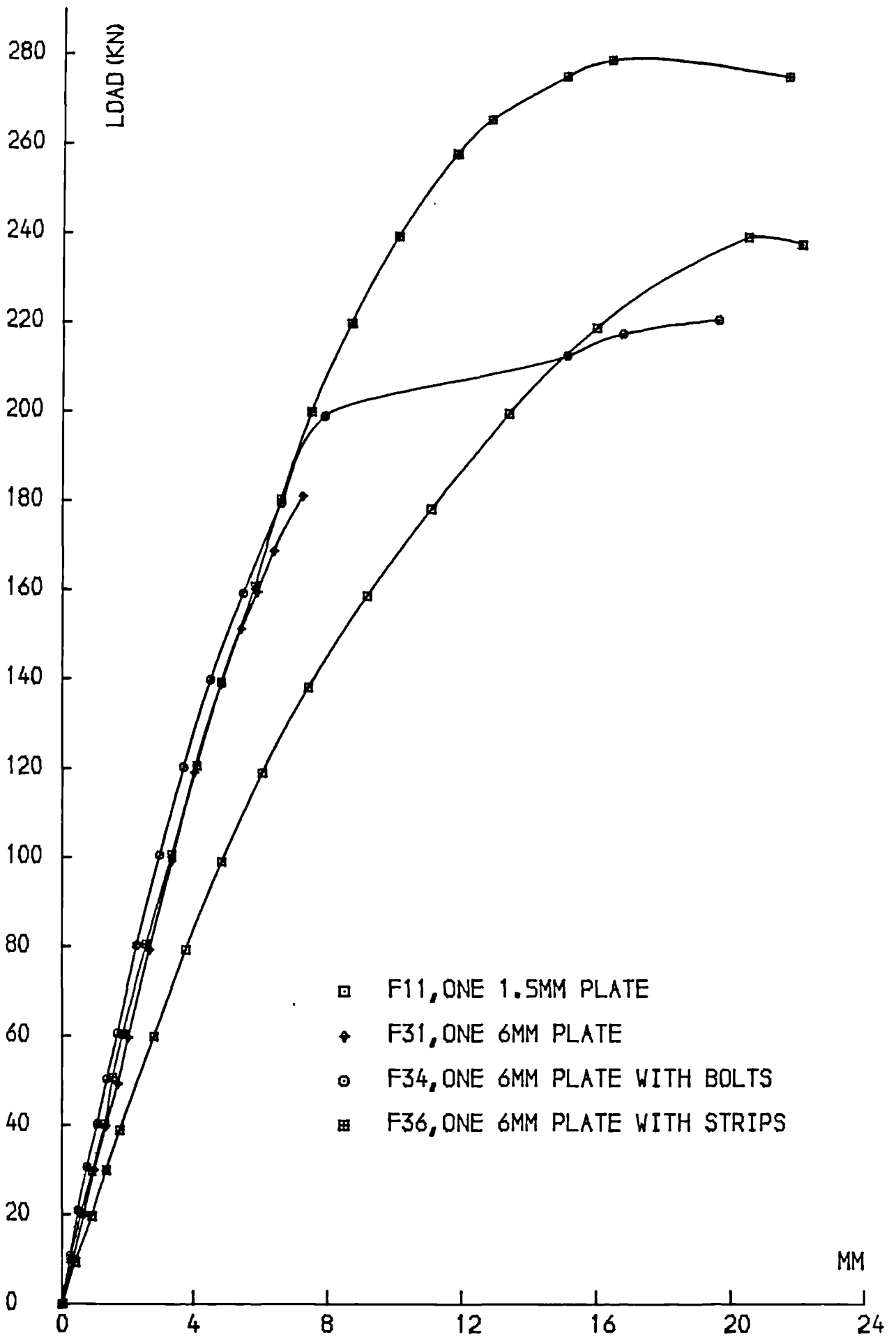


FIG.6.8 ,LOAD-DEFLECTION CURVES

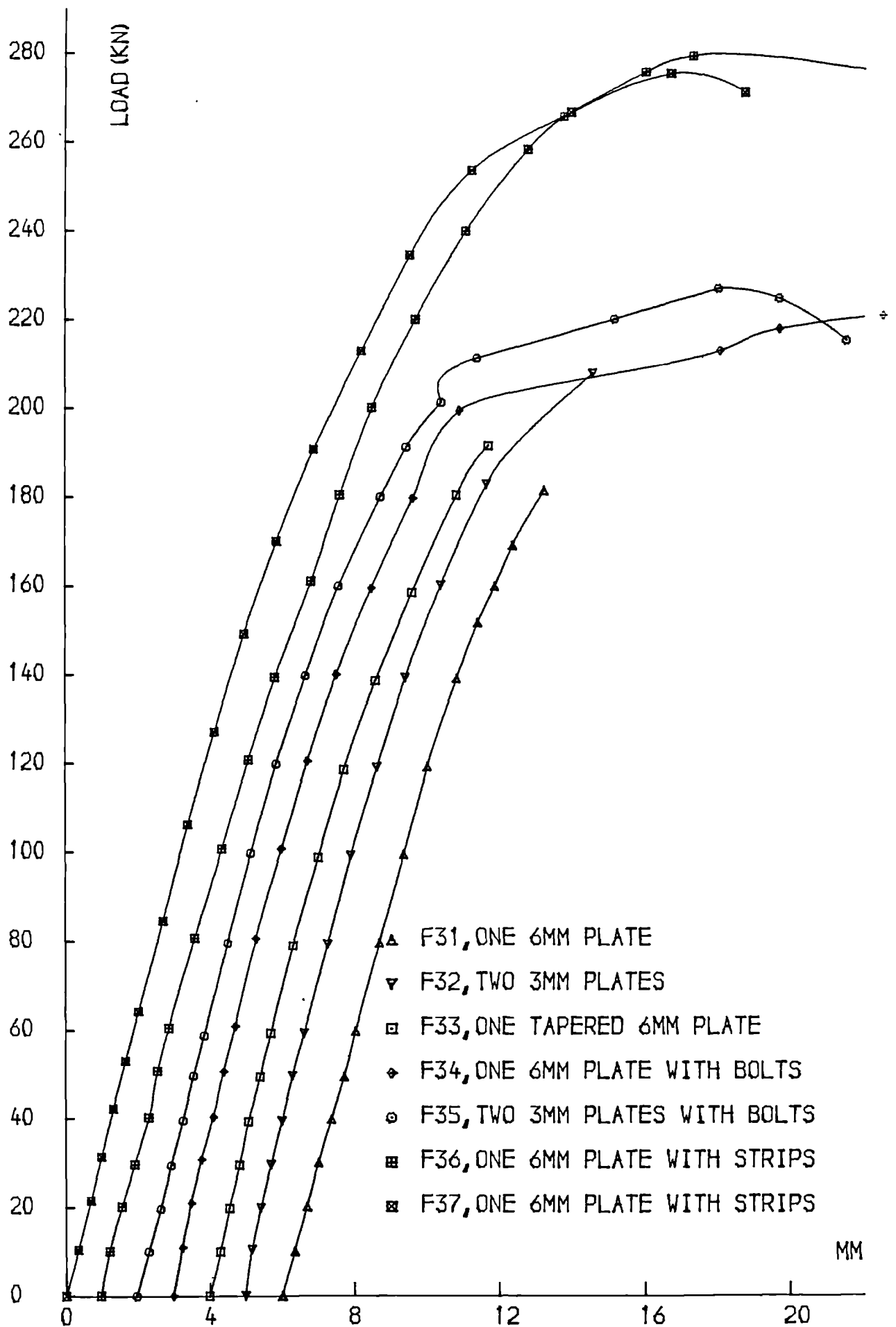


FIG.6.9 ,LOAD-DEFLECTION CURVES

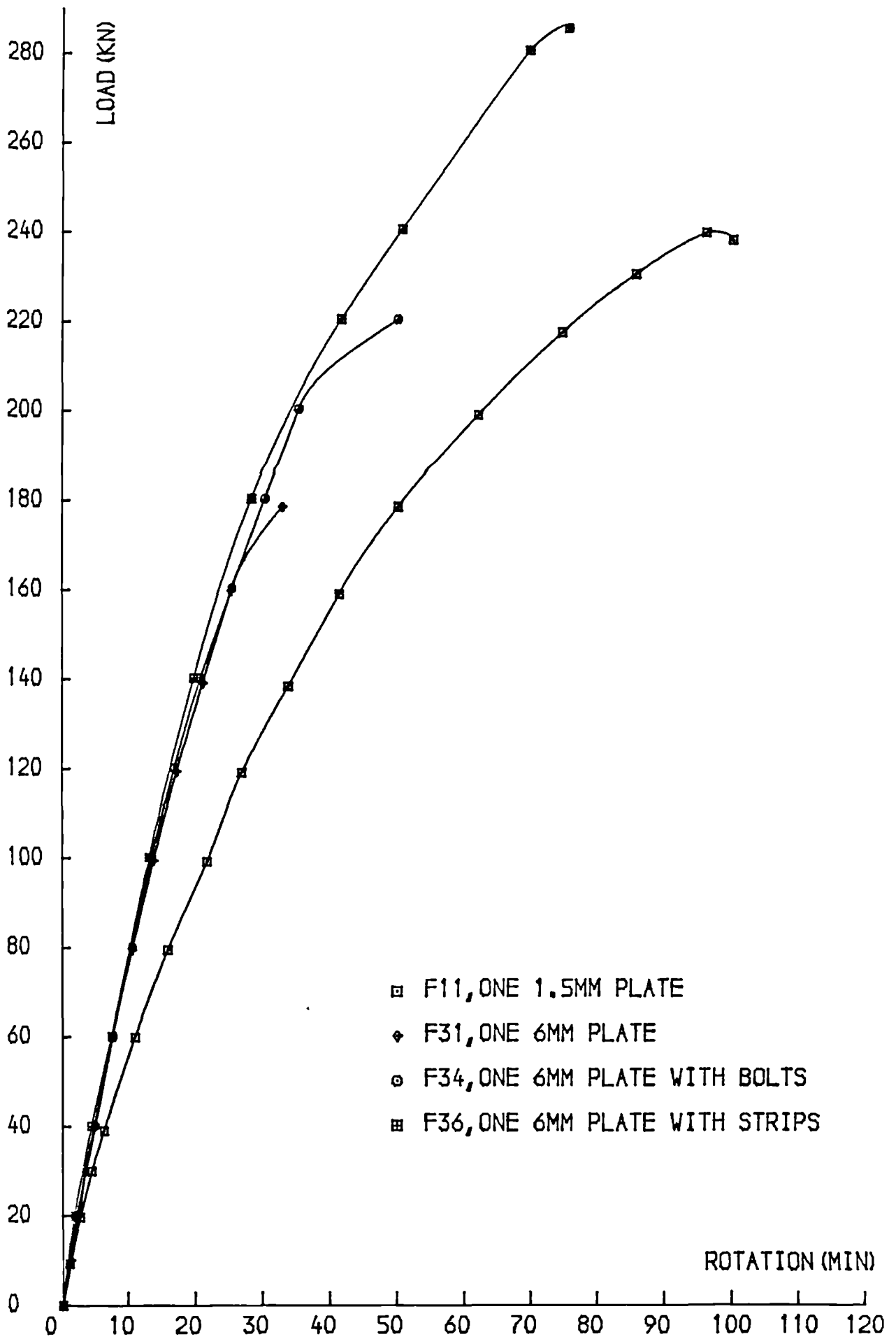


FIG.6.10 ,LOAD-ROTATION CURVES

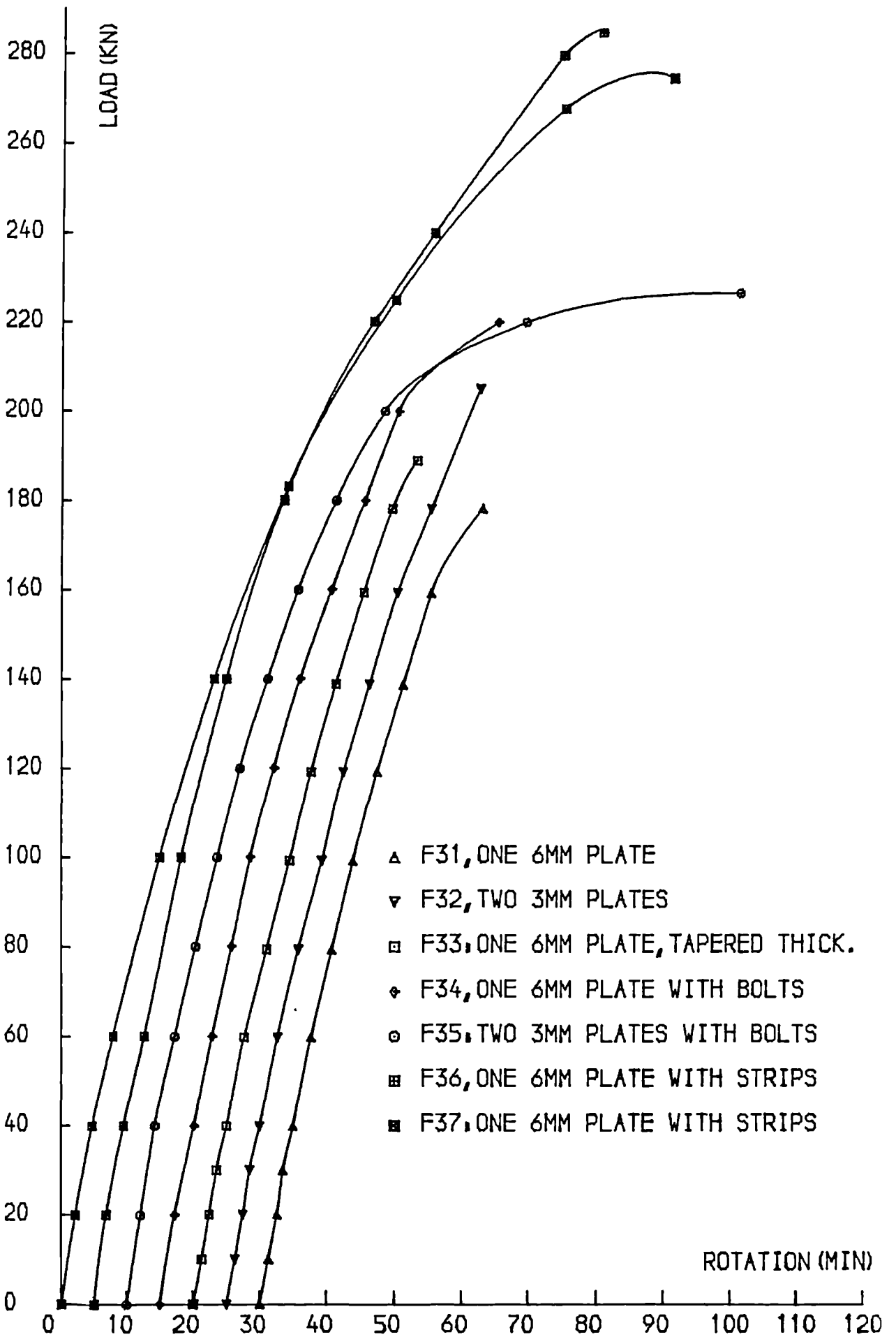


FIG. 6.11 , LOAD-ROTATION CURVES

bond failure beams. The rotation ratios at 100kN were 1.07 and 0.93 respectively. These ratios support the conclusions suggested by the results described in chapter five: The external steel plates seem to perform better than an equivalent amount of internal reinforcement designed to achieve the same result. The above ratios suggest that the improved contribution of concrete in tension in plated beams may be greater with thicker plates. This agrees with Bloxham's results (34) who found that the tensile stresses in concrete increased with the plate thickness.

The beams reached different ultimate strengths. The deformational properties at high load are therefore different. The premature failure in beams F31, F32 and F33 occurred suddenly in the linear part of the load-deflection and load-rotation curves (Figs.6.9 and 6.11).

The deformation properties of beams F34 and F35 with rawbolts were similar to those of the previous beams up to a load of 200kN. The debonding of the plates occurred at 200kN for beam F34 and 210kN for beam F35. The presence of the bolts prevented however the separation of the plates and the beams were able to carry more loads and consequently underwent further deformations. After debonding the deflections and rotations increased considerably until failure of the beams.

Beams F36 and F37 with side strips at the ends of the plates behaved similarly at low loads. The presence of the strips prevented the debonding of the plates and the beams were therefore able to develop their full flexural capacity.

6.7.2 STRAINS

The predicted and measured concrete compressive strains, neutral axis depths, and bar and plate strains at different load levels are given in Tables 6.5, 6.6, 6.7 and 6.8 respectively. The compressive strain of concrete was given by the gauge at 5mm from the compression face of the beam. Unlike the beam F11 where the neutral axis position moves towards the compressive face of the beam at high loads, the variation of the neutral axis position for the bond failure beams is very small. This is due to their higher amount of reinforcement which is near the balanced ratio.

Comparison of the ratios of experimental to theoretical concrete, bar and plate strains for beam F11 and the bond failure beams confirms that the external reinforcement may be performing better than an equivalent internal reinforcement designed to produce the same performance. The additional stiffening effect increases with the plate thickness.

The maximum concrete, bar and plate strains recorded in beams F31, F32 and F33 were less than the ultimate strain of concrete or the yield (proof) strain of steel (Tables 6.5, 6.7 and 6.8; and Figs.6.13, 6.15 and 6.17) due to premature failure by debonding.

The maximum concrete and bar strains recorded in beams F34 and F35 with bolts were higher than the ultimate (proof) strains of concrete and steel respectively (Tables 6.5 and 6.7). The maximum plate strains were however less than the yield value (Table 6.8). After the initiation of the debonding the plate strains started decreasing (Fig.6.17). This suggests that although the bolts prevented the separation of the plates,

Table 6.5: Measured and predicted concrete compressive strains at different service loads.

Beam No.	Experimental concrete compressive strain(10^{-3})				Theor. concrete compressive strain(10^{-3})			Exp./Theo.		
	50kN	100kN	150kN	Max.	50kN	100kN	150kN	50kN	100kN	150kN
F11	.44	.94	1.40	4.50	.41	.81	1.22	1.07	1.16	1.15
F31	.35	.71	1.10	1.46	.40	.79	1.19	.88	.90	0.92
F32	.36	.66	.90	1.63	"	"	"	.90	.84	0.76
F33	.34	.69	1.06	1.57	"	"	"	.85	.87	0.89
F34	.31	.67	1.19	3.35	"	"	"	.78	.85	1.00
F35	.31	.69	1.09	4.16	"	"	"	.78	.87	0.92
F36	.34	.70	1.11	4.26	"	"	"	.85	.89	0.93
F37	.36	.77	1.30	4.11	"	"	"	.90	.97	1.09

Table 6.6: Experimental and theoretical neutral axis depths at different load levels.

Beam No.	Experimental N.A. depth(mm)			Theoretical N.A. depth(mm)					Exp./Theor.				
	20kN	100kN	200kN	20kN	100kN	200kN			20kN	100kN	200kN		
				A	B	C	D	E	A	B	C	D	E
F11	138.2	121.0	115.0	141.5	106.7	102.1	102.0	118.4	.98	1.13	1.13	1.13	.97
F31	148.0	141.0	141.0\$	150.0	125.5	133.1	132.1	154.4	.99	1.12	1.06	1.07	.91
F32	146.5	139.2	140.0	"	"	"	"	"	.98	1.11	1.05	1.06	.91
F33	147.0	132.3	132.0	"	"	"	"	"	.98	1.05	0.99	1.00	.85
F34	149.3	136.5	136.5	"	"	"	"	"	.99	1.09	1.03	1.03	.88
F35	143.0	134.8	134.5	"	"	"	"	"	.95	1.07	1.01	1.02	.87
F36	148.0	135.2	135.0	"	"	"	"	"	.99	1.08	1.01	1.02	.87
F37	147.2	133.0	133.0	"	"	"	"	"	.98	1.06	1.00	1.01	.86

A: Elastic theory, uncracked section

B: " " cracked "

C: Ult.CP110 simplified method

D: CP110-strain compatibility

E: Hognestd-" "

\$: Extrapolated

Table 6.7: Measured and predicted bar strains at different service loads.

Beam No.	Experimental ₃ bar strain(10^{-3})				Theoretical ₃ bar strain(10^{-3})			Exp./Theor.		
	50kN	100kN	150kN	Max.	50kN	100kN	150kN	50kN	100kN	150kN
F11	.26	0.62	1.26	4.35	.432	0.865	1.297	.60	.72	.97
F31	.19	.45	.73	.98	.301	.602	.903	.63	.75	.81
F32	.16	.33	.62	1.25	"	"	"	.53	.55	.69
F33	.19	.40	.69	1.05	"	"	"	.63	.67	.76
F34	.20	.43	.72	4.69	"	"	"	.66	.71	.80
F35	.21	.44	.70	3.97	"	"	"	.70	.73	.78
F36	.18	.37	.64	3.44	"	"	"	.60	.62	.71
F37	.17	.42	.73	3.20	"	"	"	.57	.70	.81

Table 6.8: Measured and predicted plate strains at different load levels.

Beam No.	Experimental ₃ plate strain(10^{-3})				Theoretical ₃ plate strain(10^{-3})			Exp./Theor.		
	50kN	100kN	150kN	Max.	50kN	100kN	150kN	50kN	100kN	150kN
F11	0.44	1.10	1.85	7.10	.573	1.147	1.720	0.77	0.96	1.08
F31	0.28	0.64	1.04	1.43	.418	0.837	1.255	0.67	0.76	0.83
F32	0.28	0.64	1.08	1.60	"	"	"	0.67	0.76	0.86
F33	0.29	0.65	1.12	1.70	"	"	"	0.69	0.78	0.89
F34	0.26	0.62	1.04	1.50	"	"	"	0.62	0.74	0.83
F35	0.27	0.63	1.05	1.43	"	"	"	0.65	0.75	0.84
F36	0.29	0.63	1.04	4.73	"	"	"	0.69	0.75	0.83
F37	0.29	0.70	1.18	4.91	"	"	"	0.69	0.84	0.94

\$: Extrapolated

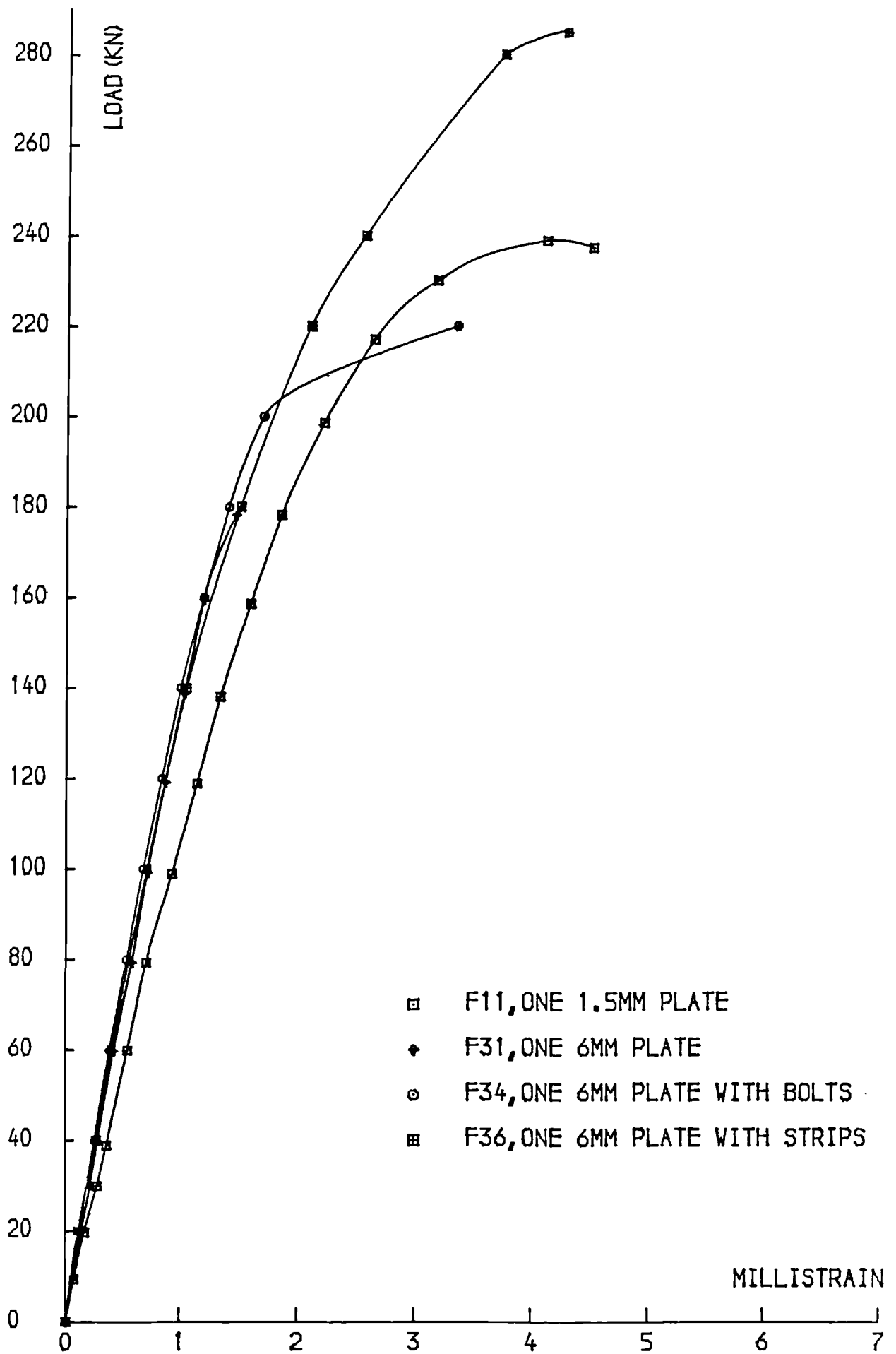


FIG.6.12 ,LOAD-CONC.COMP.STRAIN CURVES

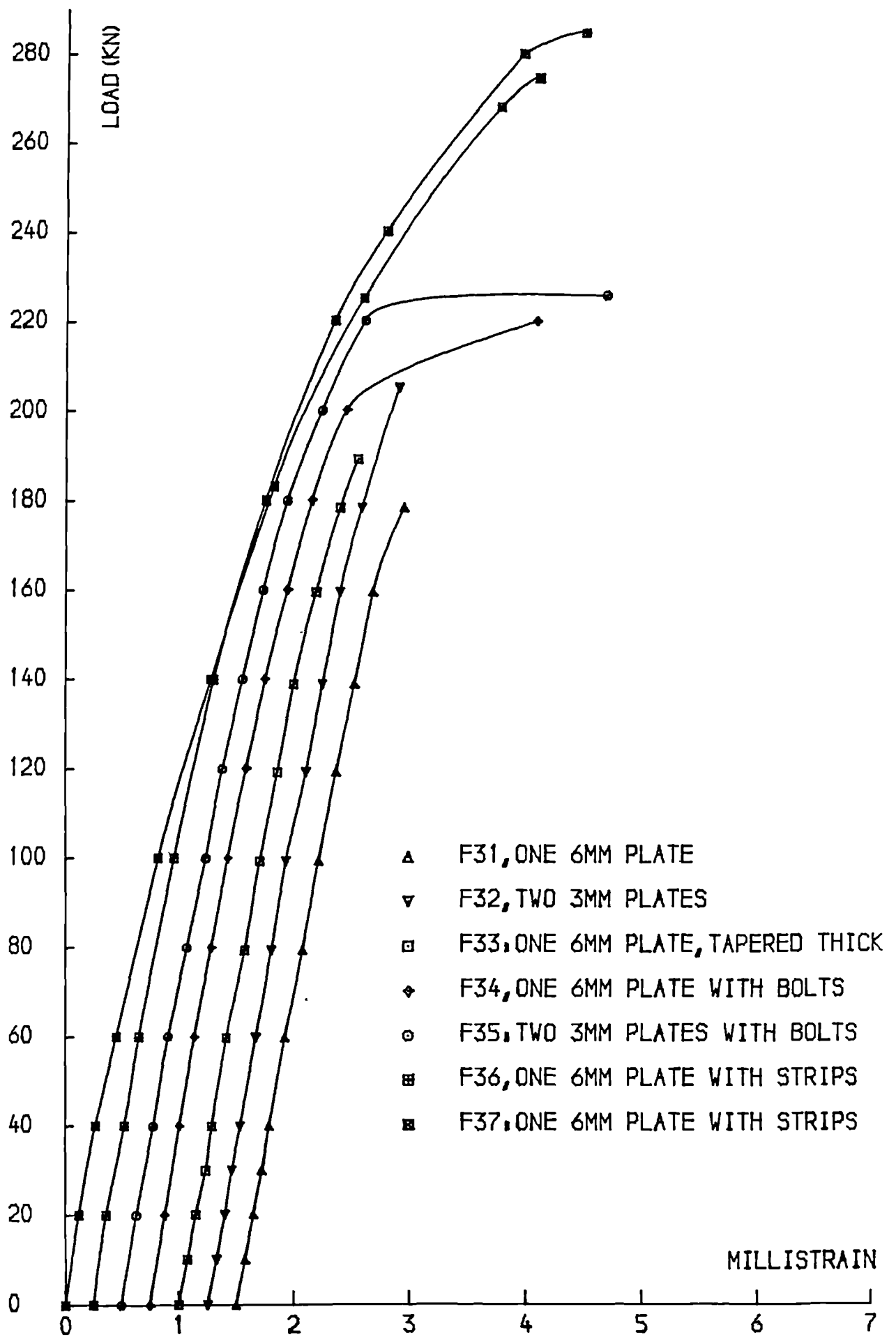


FIG. 6.13 , LOAD-CONC. COMP. STRAIN CURVES

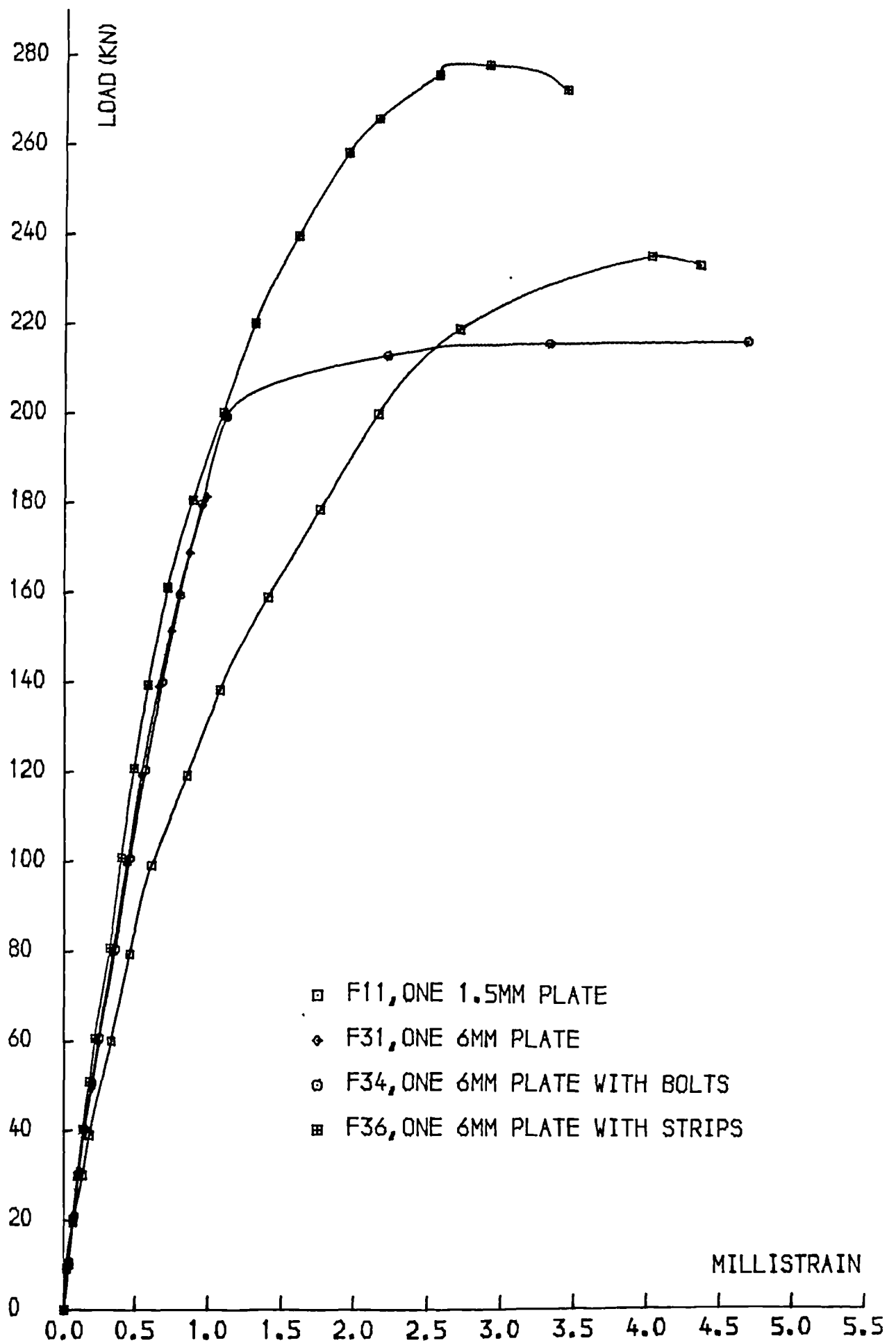


FIG. 6.14 ,LOAD-BAR STRAIN CURVES

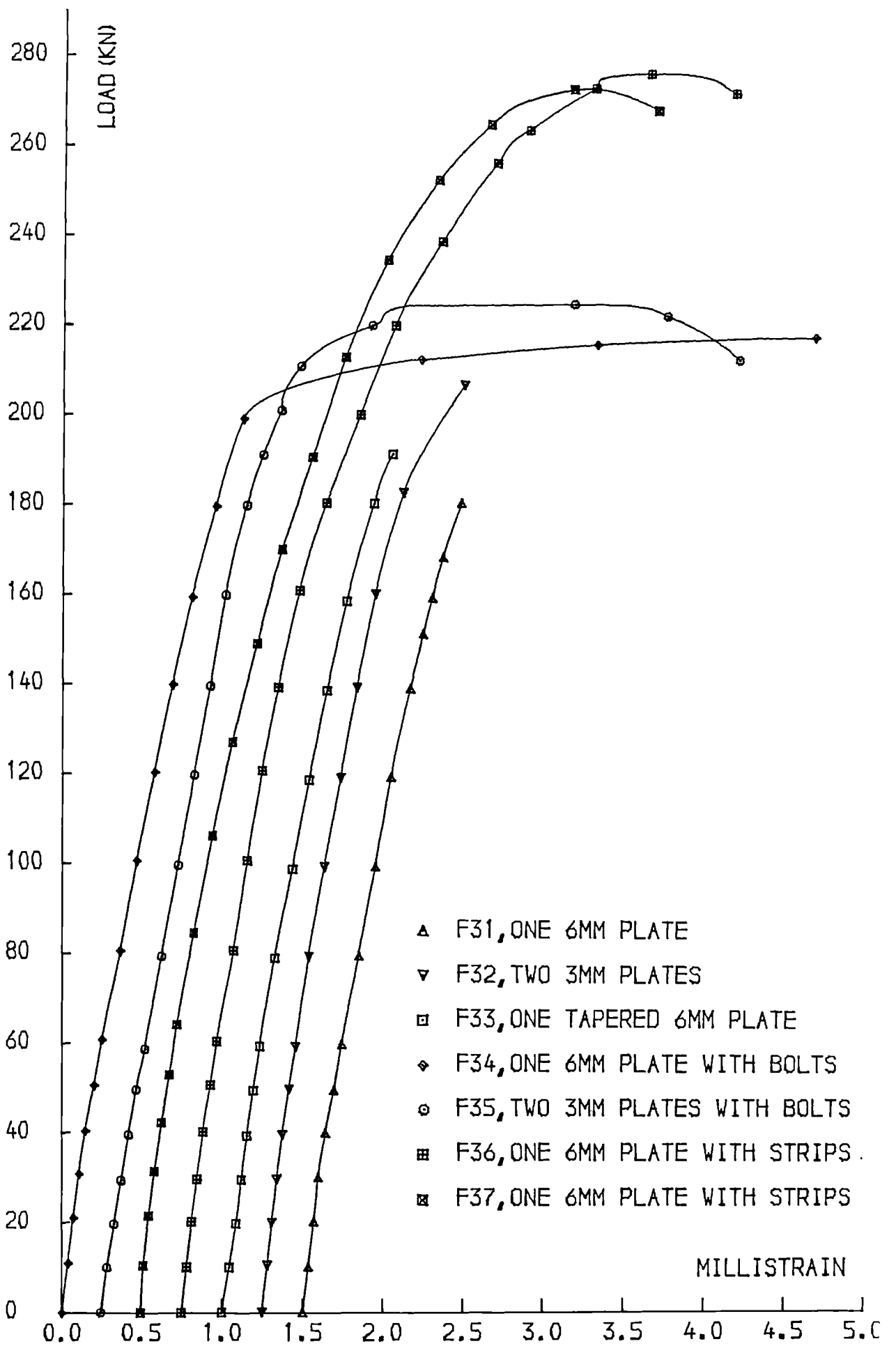


FIG.6.15 ,LOAD-BAR STRAIN CURVES

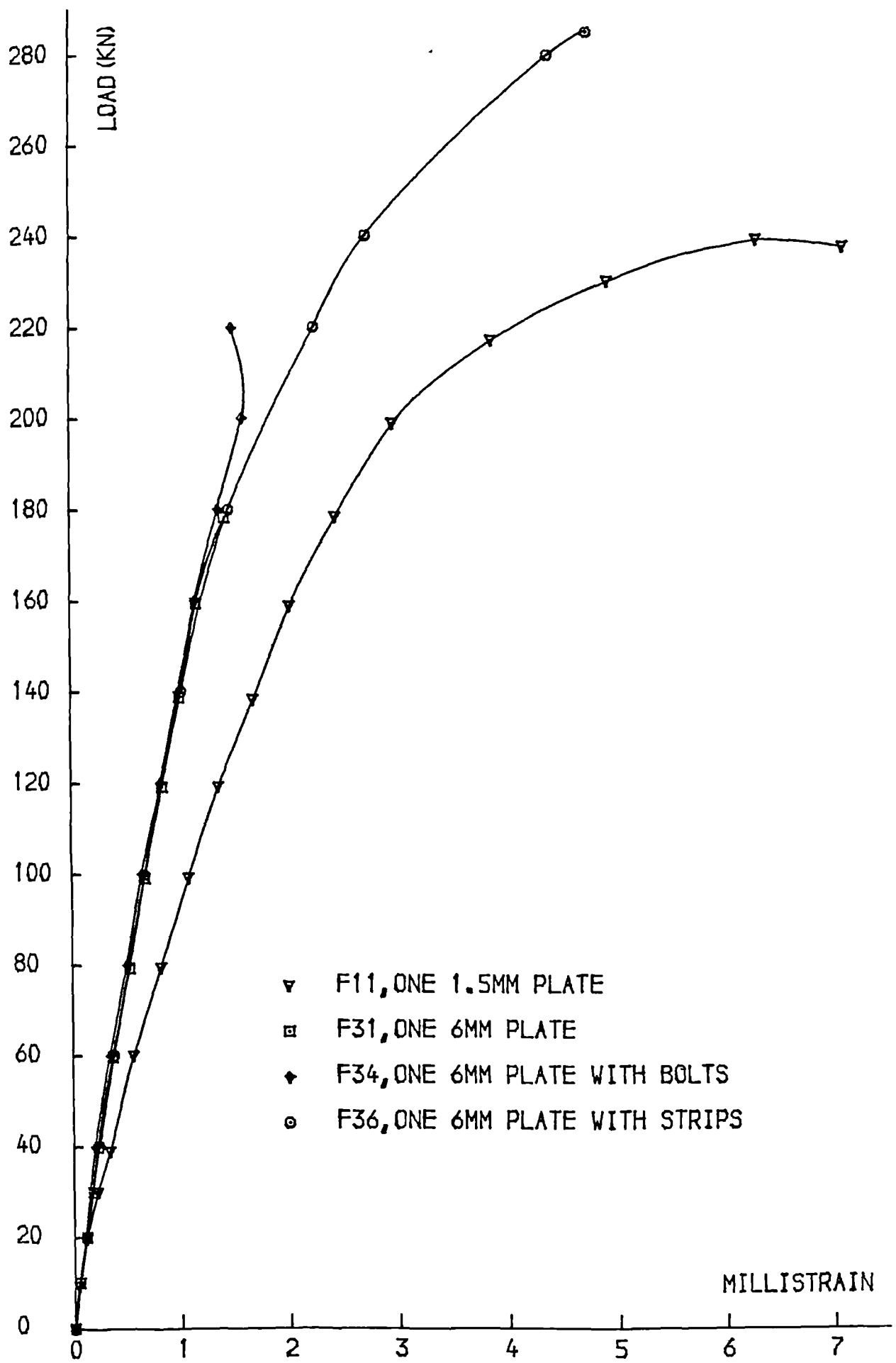


FIG. 6.16 ,LOAD-PLATE STRAIN CURVES

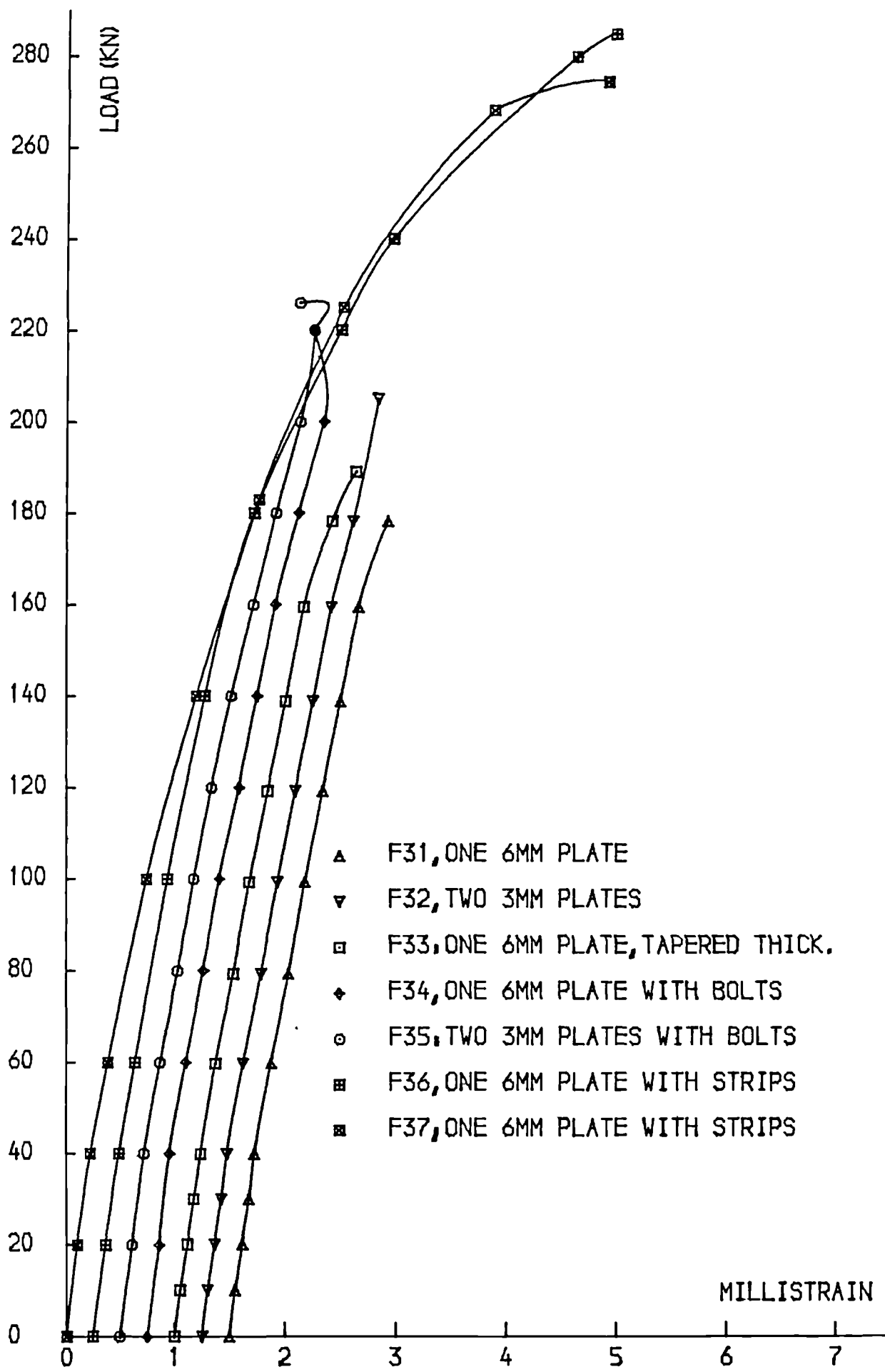


FIG.6.17 ,LOAD-PLATE STRAIN CURVES.

composite action between the beam and the plate was not ensured anymore after the debonding and the beams appeared to have behaved thereafter as unplated beams. The ultimate loads reached confirm this.

The maximum strains in beams F36 and F37 which developed their full flexural capacity were higher than the yield (proof) values (Tables 6.5, 6.7 and 6.8).

6.8 CRACK WIDTHS AND RIGIDITIES

The predicted and measured average crack widths are given in Table 6.9. At 100kN the ratio of experimental to theoretical value was 0.85 for beam F11 and 0.87 for the bond failure beams. The same ratios at 200kN were 1.00 and 0.98 respectively.

The theoretical and experimental rigidities were obtained in the same manner as described in chapter five. The predicted and recorded values before and after cracking are given in Table 6.10. At 20kN (before cracking), the ratio of experimental to theoretical rigidity was 0.76 for beam F11 and 0.91 for the bond failure beams. At 100kN the same ratios were 0.94 and 0.98 respectively. Again these ratios support the previous conclusions that the restraining effect of the plates increased with their thickness.

6.9 TENSILE STRESSES IN CONCRETE

The stiffening effect of concrete in tension was estimated in the same manner as described in chapter five. The contribution of concrete was determined as the difference between the applied moment and the internal moment carried by the bars, glue and plate. The tensile stresses in concrete thus

Table 6.9: Measured and predicted average crack widths at different load levels.

Beam No.	Exper. average crack width(mm)		CP110 average crack width(mm)		Exp./Theo.	
	100kN	200kN	100kN	200kN	100kN	200kN
F11	.046	.115	.054	.115	0.85	1.00
F31	.025	.071\$.029	.064	0.86	1.11
F32	.028	.060	"	"	0.97	0.94
F33	.025	.056	"	"	0.86	0.88
F34	.020	.070	"	"	0.69	1.09
F35	.028	.058	"	"	0.97	0.91
F36	.024	.060	"	"	0.83	0.94
F37	.027	.064	"	"	0.93	1.00

\$: Extrapolated

Table 6.10: Experimental and theoretical rigidities before and after cracking.

Beam No.	Rigidity EI (10^{12} N.mm ²)					
	Exp. EI		Theor. EI		Exp./Theo.	
	20kN	100kN	20kN	100kN	20kN	100kN
F11	6.47	5.02	8.539	5.362	.76	.94
F31	9.04	7.46	9.993	7.655	.91	.98
F32	9.05	7.53	"	"	.91	.98
F33	9.03	7.50	"	"	.90	.98
F34	9.07	7.55	"	"	.91	.99
F35	9.09	7.55	"	"	.91	.99
F36	9.03	7.53	"	"	.90	.98
F37	9.05	7.53	"	"	.91	.98

computed are given in Table 6.11. At 20kN (before cracking) the stress was 2.02 N/mm^2 in beam F11 and 1.93 N/mm^2 in the bond failure beams. At 100kN (in a cracked state), the stresses were 2.67 and 2.96 N/mm^2 . These values confirm the conclusions of chapter five: the presence of the external plates seems to improve the performance of concrete in tension and therefore increase the overall stiffness of the beam. The above results also mean that this improved contribution of concrete in tension may be greater with thicker plates. This agrees again with Bloxham's findings (34) who reported that the tensile stress in concrete in a cracked state was greater in plated beams and increased with the plate thickness.

6.10 STRENGTH PROPERTIES

6.10.1 FIRST CRACK LOADS

The first crack loads were calculated in the same manner as described in chapter five. The predicted and recorded values are given in Table 6.12. The ratio of experimental to theoretical first crack load was 1.39 for beam F11 and 1.51 for the bond failure beams. The ratio of the recorded first crack loads to the CP110 ultimate loads were 0.18 and 0.19 respectively. The tensile strain in concrete at first cracking was 178 microstrains for beam F11 and 181 for the bond failure beams.

The ratios of experimental to theoretical first crack loads and the values of tensile strains in concrete at cracking support the conclusions that the restraining effect of the external plates may be greater than that of conventional reinforcement designed to achieve the same performance and that this stiffening effect increases with the plate thickness.

Table 6.11: Tensile stresses in concrete at the tension face before and after cracking.

Beam No.	Internal moment carried by bars glue and plate (kN.m)		Moment carried by concrete in tension (kN.m)		Tensile stress in concrete (N/mm ²)	
	20kN	100kN	20kN	100kN	20kN	100kN
	F11	4.56	33.64	3.11	4.71	2.02
F31	4.85	33.80	2.82	4.55	2.00	3.03
F32	5.00	33.96	2.67	4.39	1.87	2.88
F33	4.88	33.66	2.79	4.69	1.96	2.90
F34	5.08	33.73	2.59	4.62	1.86	2.96
F35	4.91	33.73	2.76	4.62	1.87	2.92
F36	4.92	33.65	2.75	4.70	1.95	2.98
F37	4.82	33.45	2.86	4.90	2.01	3.05

Table 6.12: Experimental and theoretical strength results. (first crack and ultimate loads).

Beam No.	First crack load(kN)			Maximum load(kN)							1 st crack load over	1 st crack concrete tensile strain
	Exp.	Theo.	Exp.	Theo.ult.flex.			Exp./Theo.			CP110 ult.load	(10 ⁻⁶)	
				A	B	C	A	B	C			
F11	40.0	28.89	1.39	239.0	227.25	227.25	216.99	1.05	1.05	1.10	0.18	178
F31	55.0	36.54	1.51	182.0	284.36	283.08	266.44	0.64	0.64	0.68	0.19	203
F32	"	"	"	208.0	"	"	"	0.73	0.73	0.78	"	178
F33	"	"	"	191.0	"	"	"	0.67	0.67	0.72	"	194
F34	"	"	"	221.0	"	"	"	0.78	0.78	0.83	"	218
F35	"	"	"	227.0	"	"	"	0.80	0.80	0.85	"	194
F36	"	"	"	285.1	"	"	"	1.01	1.01	1.07	"	162
F37	"	"	"	283.0	"	"	"	1.00	1.00	1.06	"	120

A: CP110-simplified method

B: Strain compatibility(rect.stress block)

C: " " (Hognestad et al.)

(the three methods are described in Appendix D)

6.10.2 ULTIMATE STRENGTHS

The ultimate flexural strengths were computed using the three methods described in chapter five and Appendix D. The experimental and theoretical ultimate loads are given in Table 6.12. The detailed results and the effects of the tapering, bolts and strips are discussed in the following sections:

6.10.2.1 BEAM F31

This beam with one 6mm plate failed prematurely as expected by sudden separation of the plate at its end at the level of the internal reinforcement. Fig.6.18 showing the development of the bar strain for each strain gauge position illustrates the initiation of the debonding and also shows that there was some warning before failure. At a load of about 140kN, the slopes of the curves increase considerably. This warning was not however detected visually. The bond failure occurred in the linear part of the load-deformation curves (Figs.6.8 to 6.17) at a load of 182kN equivalent to 64% of the ultimate flexural strength of the beam. The steel bars and plate reached strains of 980 and 1360 microstrains respectively which were less than the bar 0.2% proof strain (2000 microstrains) and the plate yield strain (1400 microstrains).

6.10.2.2 BEAMS F32 AND F33

These beams were designed in such a way that the bond and peel stresses would be lower than those of beam F31 and were expected to perform better. Their flexural behaviours were similar to that of beam F31. The stiffnesses, deflections and cracking were of the same magnitude as those of beam F31 (Tables 6.3 to 6.11). The beams F32 and F33 sustained however

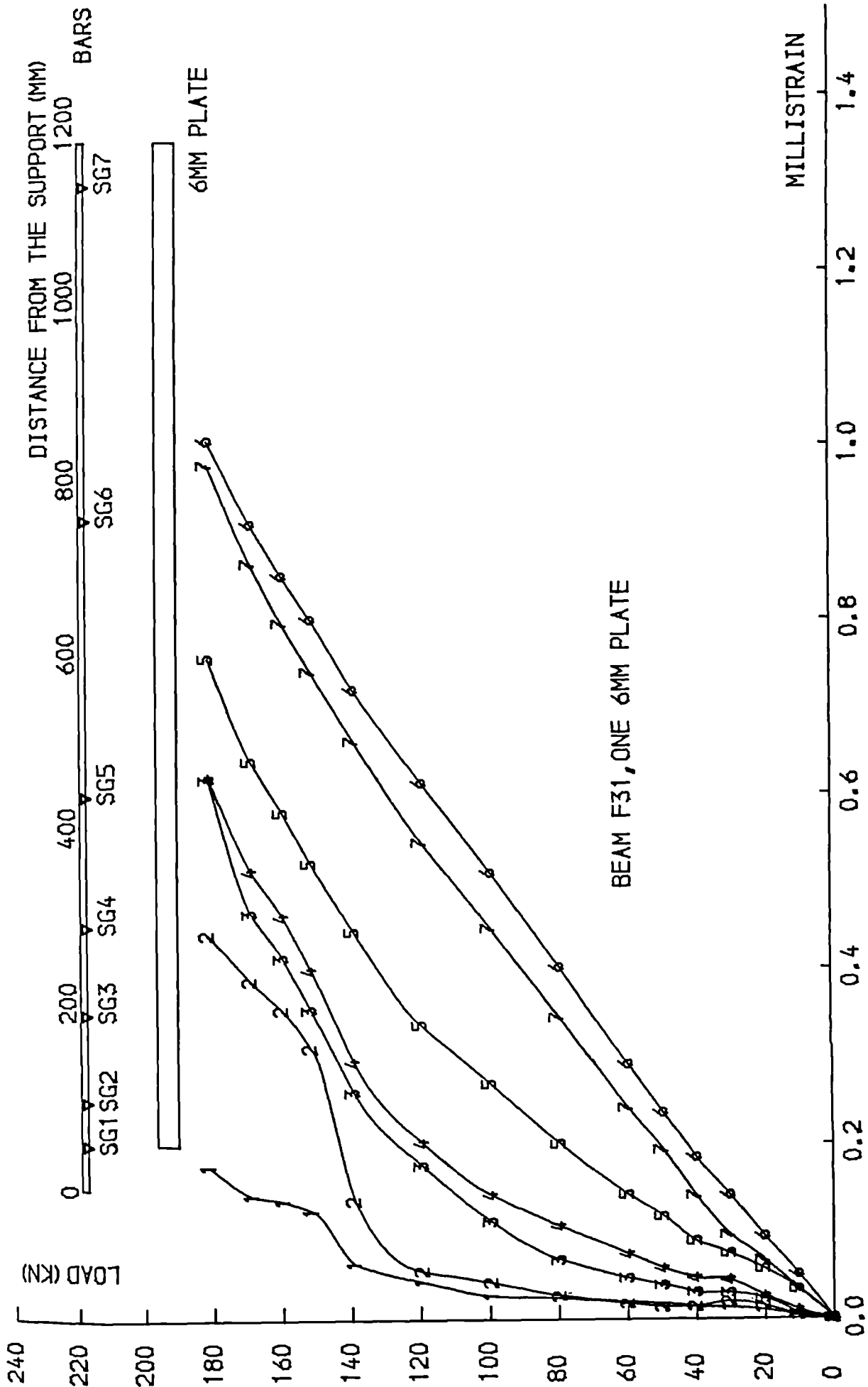
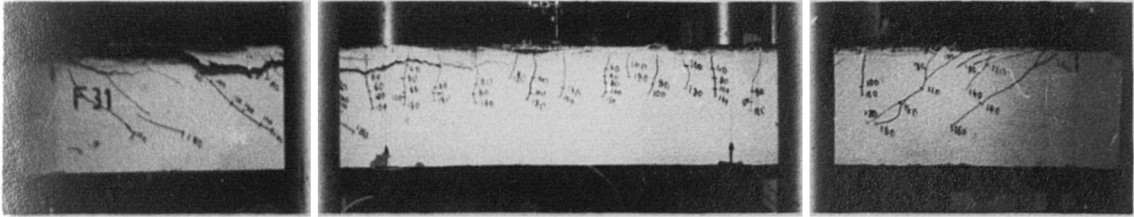
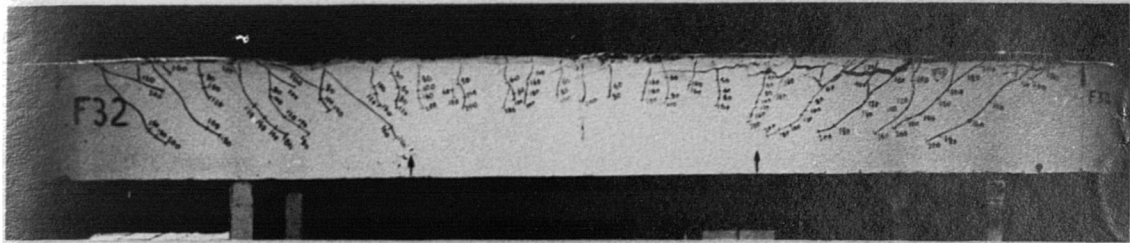


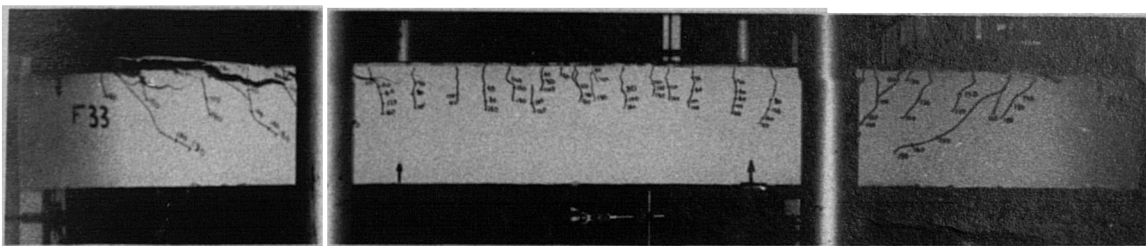
FIG.6.18 LOAD-BAR STRAIN DISTRIBUTION



F31: one 6mm plate



F32: two 3mm plates



F33: one 6mm plate with a tapered thickness in the shear spans

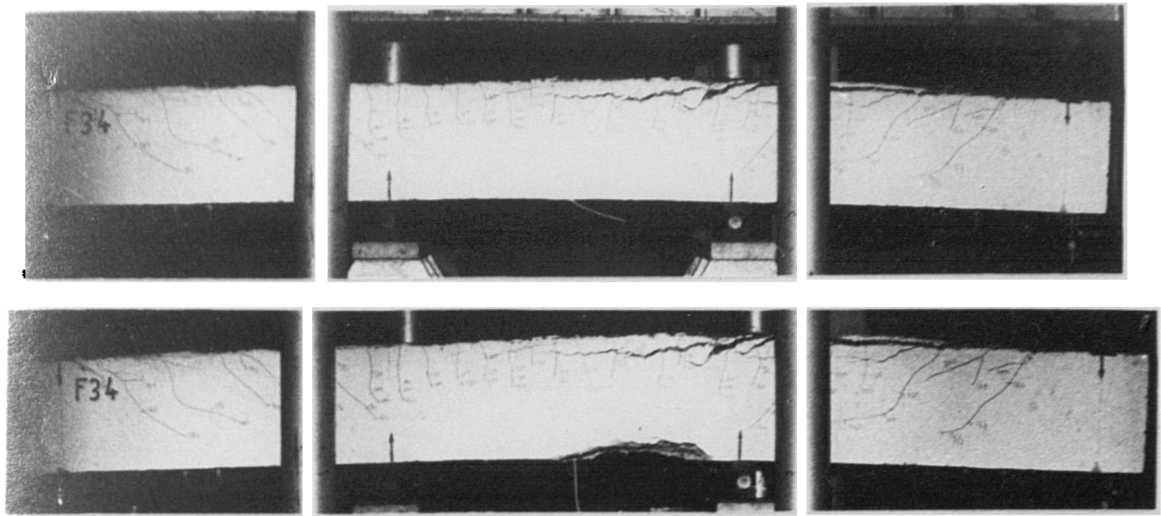
Fig.6.19: Crack patterns and modes of failure of beams F31, F32 and F33

only 26 and 9 kN respectively more than beam F31. They failed at 208 and 191kN respectively or 73 and 67% of their ultimate flexural strength. Failure of beam F33 strengthened with one 6mm plate with a tapered thickness was identical to that of beam F31 (Fig.6.19). Beam F32 failed similarly by separation of the end of the inner plate (Fig.6.19). The maximum bar and plate strains were 1272 and 1510 microstrains for beam F32 and 1020 and 1380 microstrains for beam F33.

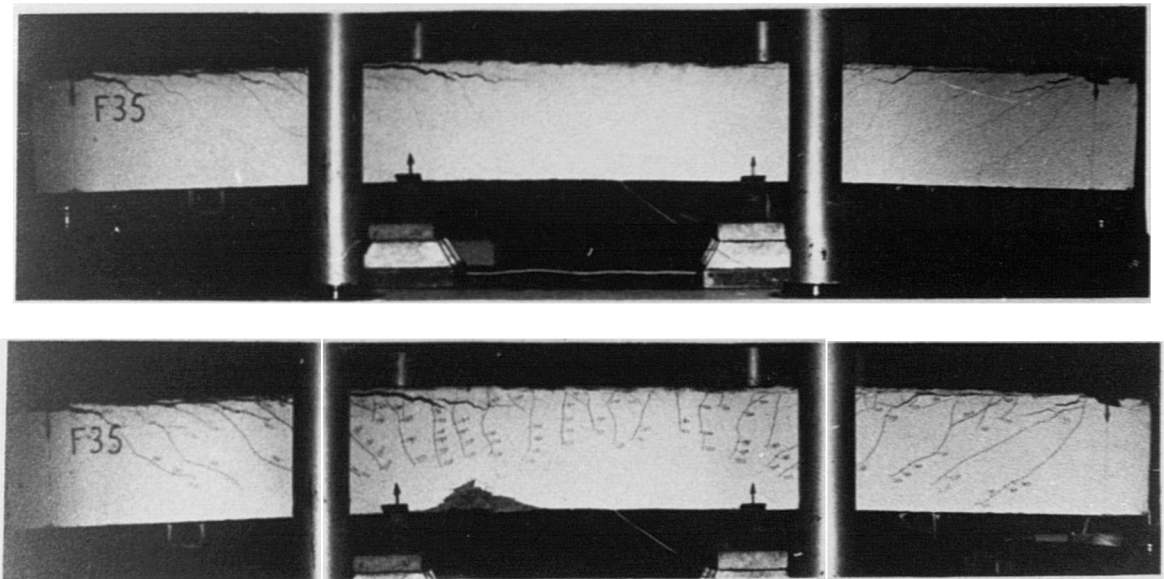
6.10.2.3 BEAMS F34 AND F35 WITH BOLTS

The rawlbolts in these beams were expected to overcome the peeling forces at the ends of the plates and delay (if not avoid) the premature failures. Up to a load of 200kN there was full composite action between the plates and concrete and the beams behaved similarly to the previous ones. However at a load of 200kN for beam F34 and 210kN for beam F35 (70 and 74% of their theoretical flexural strengths respectively), there was a sudden longitudinal debonding of the plate at its end over a length of about 300mm (Figs.6.20 and 6.21).

Despite the debonding however the bolts prevented the separation of the plate and the beams were able to carry more load (Fig.6.20). As the load was increased the plate strains started decreasing (Figs.6.16 and 6.17) and the debonding moved further towards the flexural region. The deflection, rotation, concrete and bar strains increased considerably (Figs.6.8 to 6.17) until the beams failed by compressive crushing of concrete in the constant moment region (Fig.6.20) at loads of 221kN for beam F34 and 227kN for beam F35 or 78 and 80% of the theoretical ultimate strengths respectively.

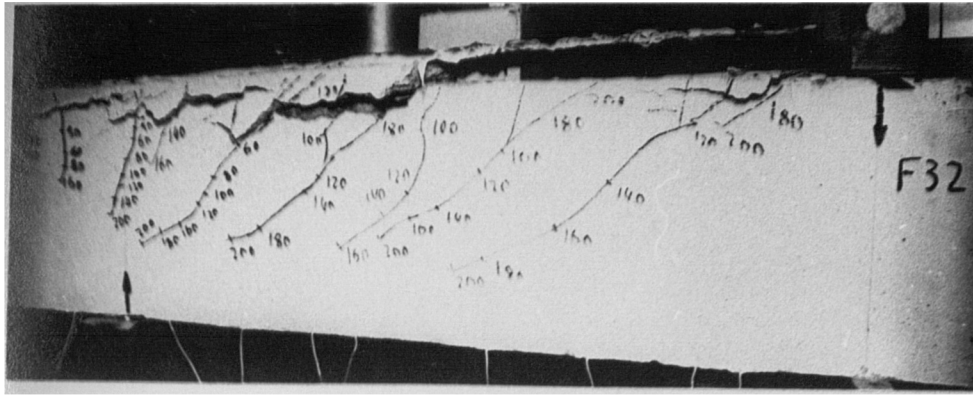


F34: one 6mm plates with bolts

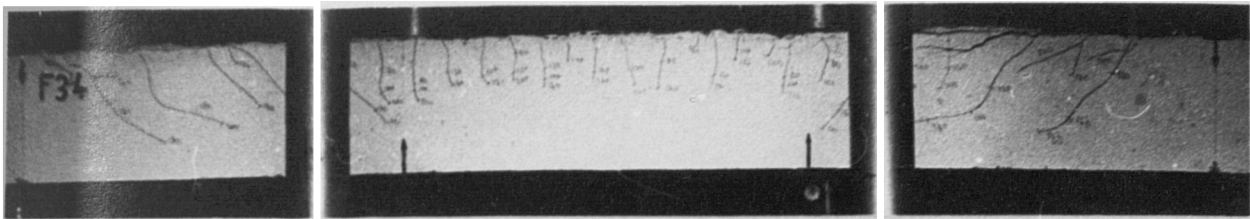


F35: two 3mm plates with bolts

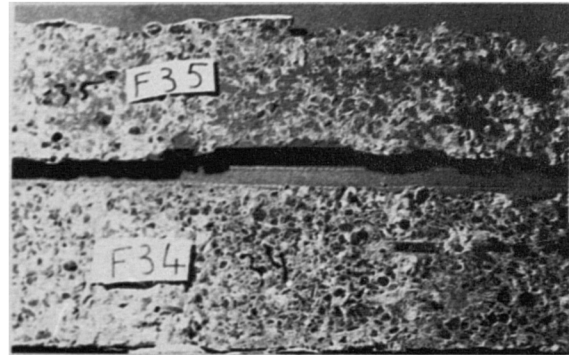
Fig.6.20: Crack patterns and modes of failure of beams
F34 and F35 with bolts
(debonding occurred before crushing of concrete)



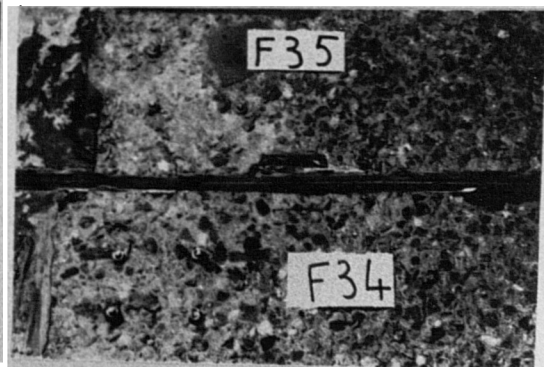
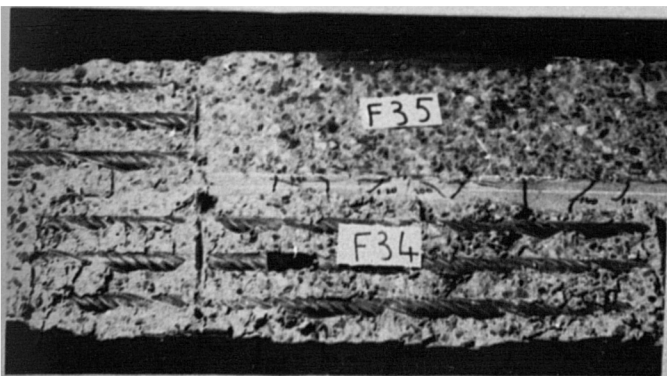
Debonding in a non bolted beam
(free separation of the plate)



Debonding in a bolted beam
(plate held by bolts)



Plates removed from bolted beams



Bolted beams after removal of plates

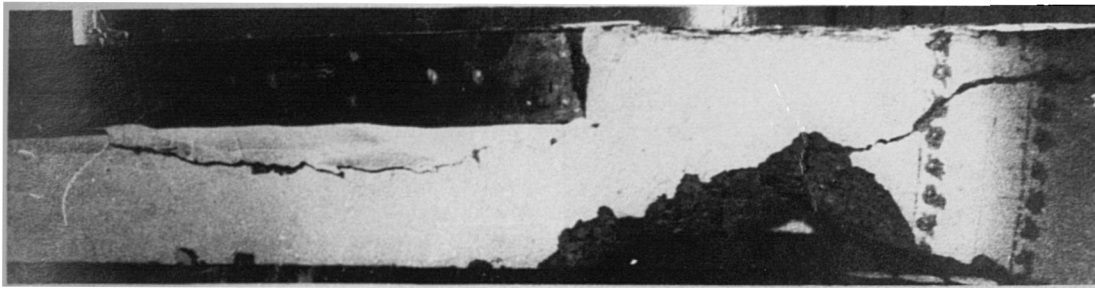
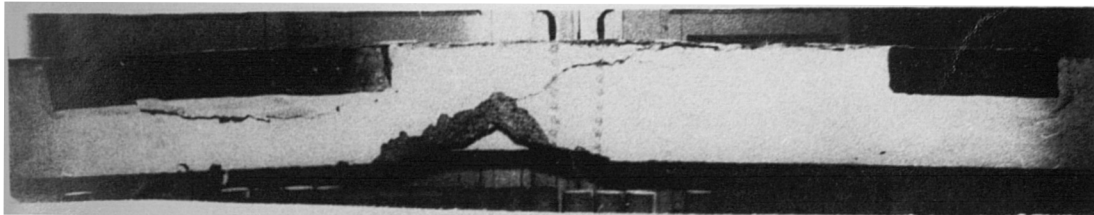
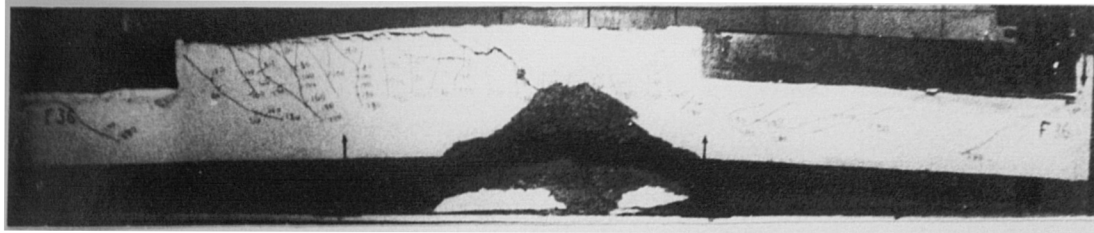
Fig.6.21: Debonding in bolted and non bolted beams

The ultimate strength, maximum deflections, rotations, bar and concrete strains registered were similar to those of the unplated beam F01 described in chapter five. This and the decreasing of the plate strains after the initiation of the debonding suggest that although the bolts overcame the peeling forces, they did not prevent local debonding due to high local bond stresses and the composite action of the plate and concrete was not ensured any longer. The beams behaved thereafter as unplated beams.

6.10.2.4 BEAMS F36 AND F37 WITH SIDE STRIPS

The L shaped steel strips glued at the ends of the plates of these beams were expected to overcome the peeling stresses and hopefully prevent the local debonding which occurred at the level of the internal steel bars. Fig.6.22 shows that in fact the side strips enabled the beams to develop their full flexural strength and full composite action between the beam and the plate was ensured until the beam failed by compressive crushing of concrete (Fig.6.22).

Subsequent observation of the failed beams showed however that the bond between concrete and the longer strip of beam F36 was cracked (Fig.6.22) whereas the shorter strip of beam F36 and the shorter but deeper strips of beam F37 were intact. The recorded strip strains were higher at the ends (Figs.6.23 and 6.24). These higher strip strains in the section where the longitudinal plate was stopped confirm the presence of higher bond and peel stresses in that region.



F36: cracking along long strip



F37: strips intact

Fig.6.22: Crack patterns and modes of failure of beams F36 and F37 with strips

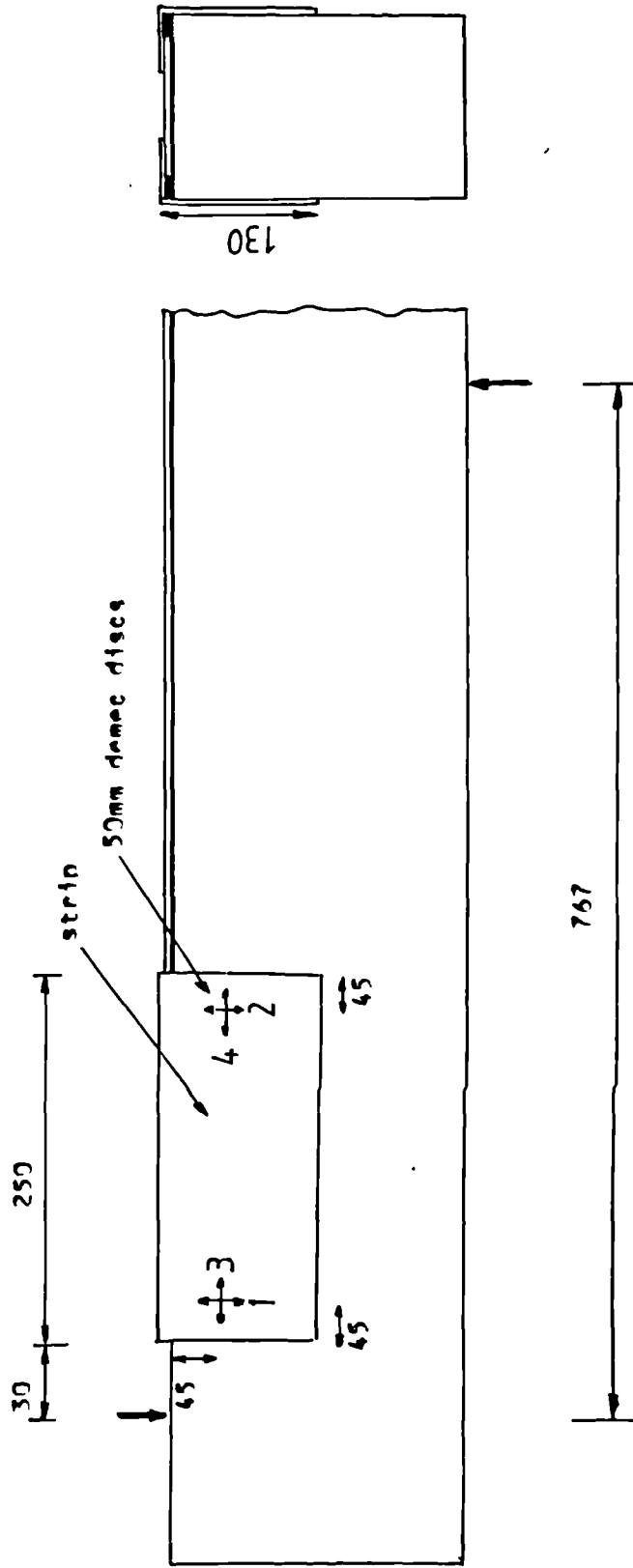


Fig.6.23: Locations of strain strain measurements (beam F37)

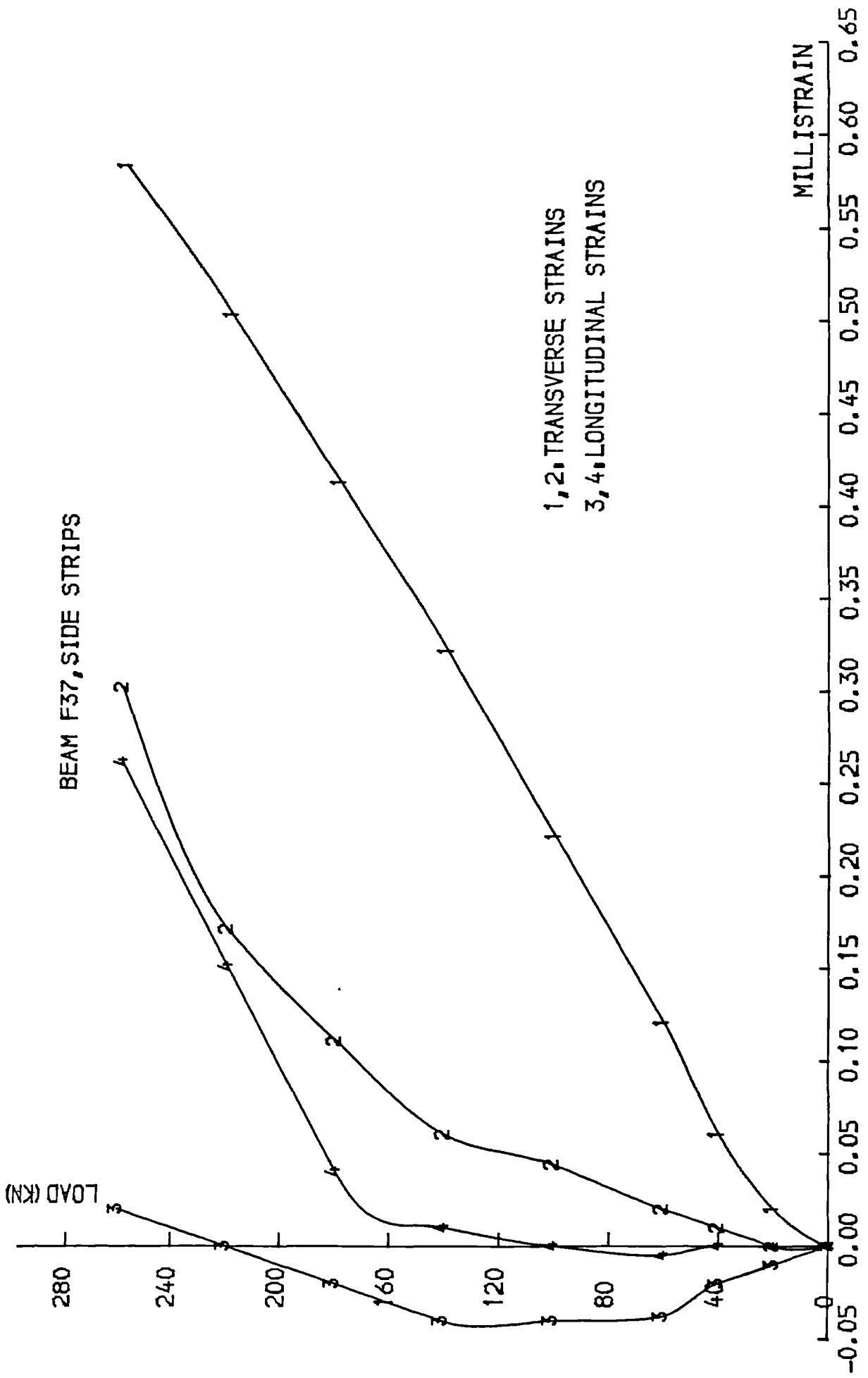


FIG. 6.24 LOAD-STRIP STRAIN CURVES

6.11 BOND STRESSES

6.11.1 EXTERNAL BOND STRESSES (IN EPOXY JOINT)

Figs.6.25 to 6.28 show the distribution of the strains along the plate at different load levels. The positions of the support, load point, bars and plate are shown in Fig.6.29. The broken lines represent the theoretical elastic distribution. It was assumed in the computation of the theoretical strains that the plate remained fully active until its cutoff point. The theoretical distribution was plotted in order to compare its slope to that of the experimental one and investigate the region where the force transfer from the plate to the bars starts. These curves show that beyond a certain distance x from the cutoff point, the theoretical and experimental distributions have similar slopes but within this distance x from the cutoff point, the measured strains decrease rapidly and become smaller than the elastic ones. This proves the existence of a transfer of tensile forces from the plate to the bars over the distance x . This distance x increases slightly at higher loads and the location of the transfer region moves away from the support at higher loads (Figs.6.25 and 6.26).

Figs.6.30 to 6.32 confirm this conclusion: within the same distance x the strains in the bars increase above the theoretical ones as a result of the force transfer from the plate.

The experimental bond stresses are deduced from the strain measurements. The recorded strains on the plates are converted to forces by multiplying by the elastic modulus and the cross-sectional area of the plates. The bond stress between two consecutive locations of demec gauges is equal to the

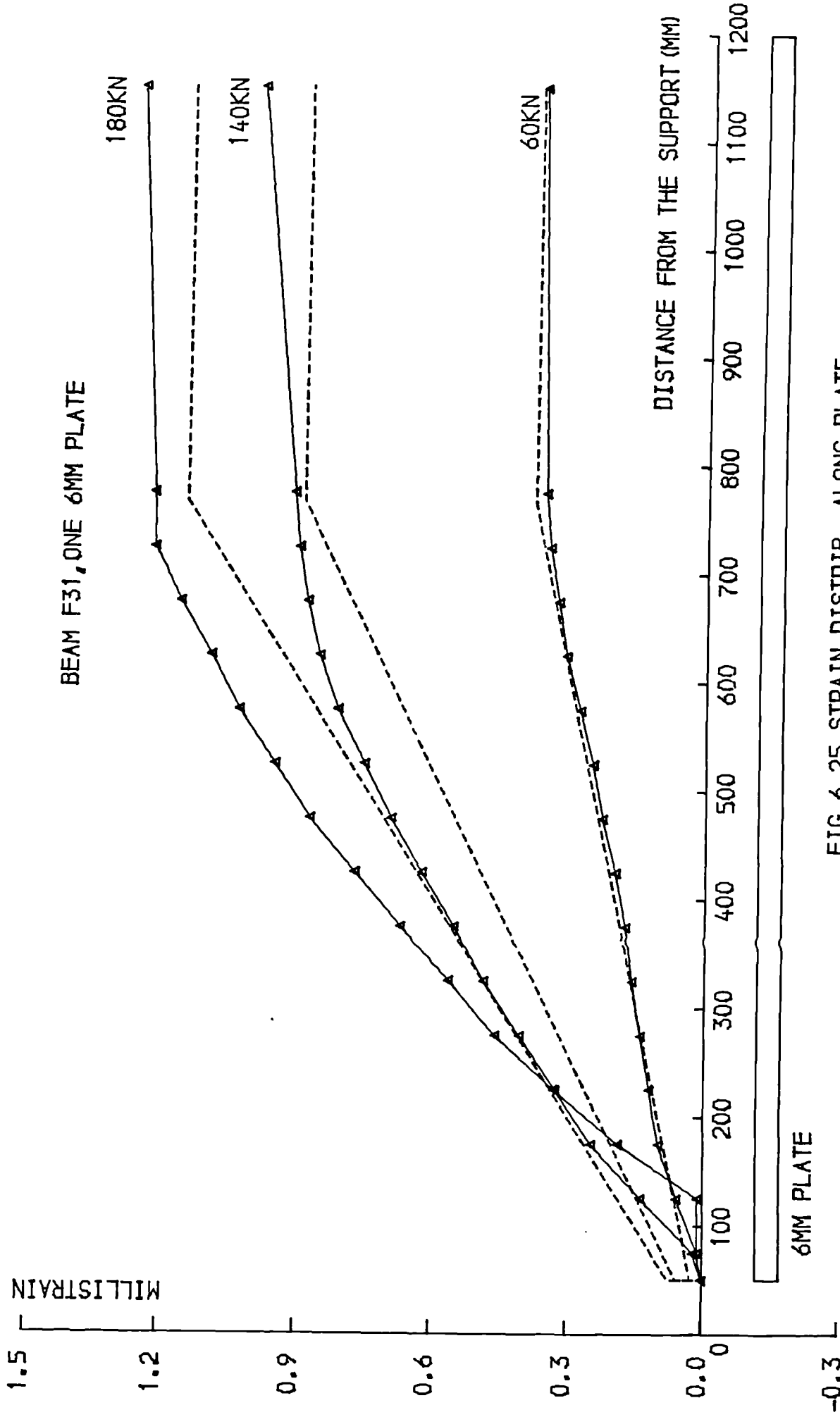


FIG.6.25 STRAIN DISTRIB. ALONG PLATE

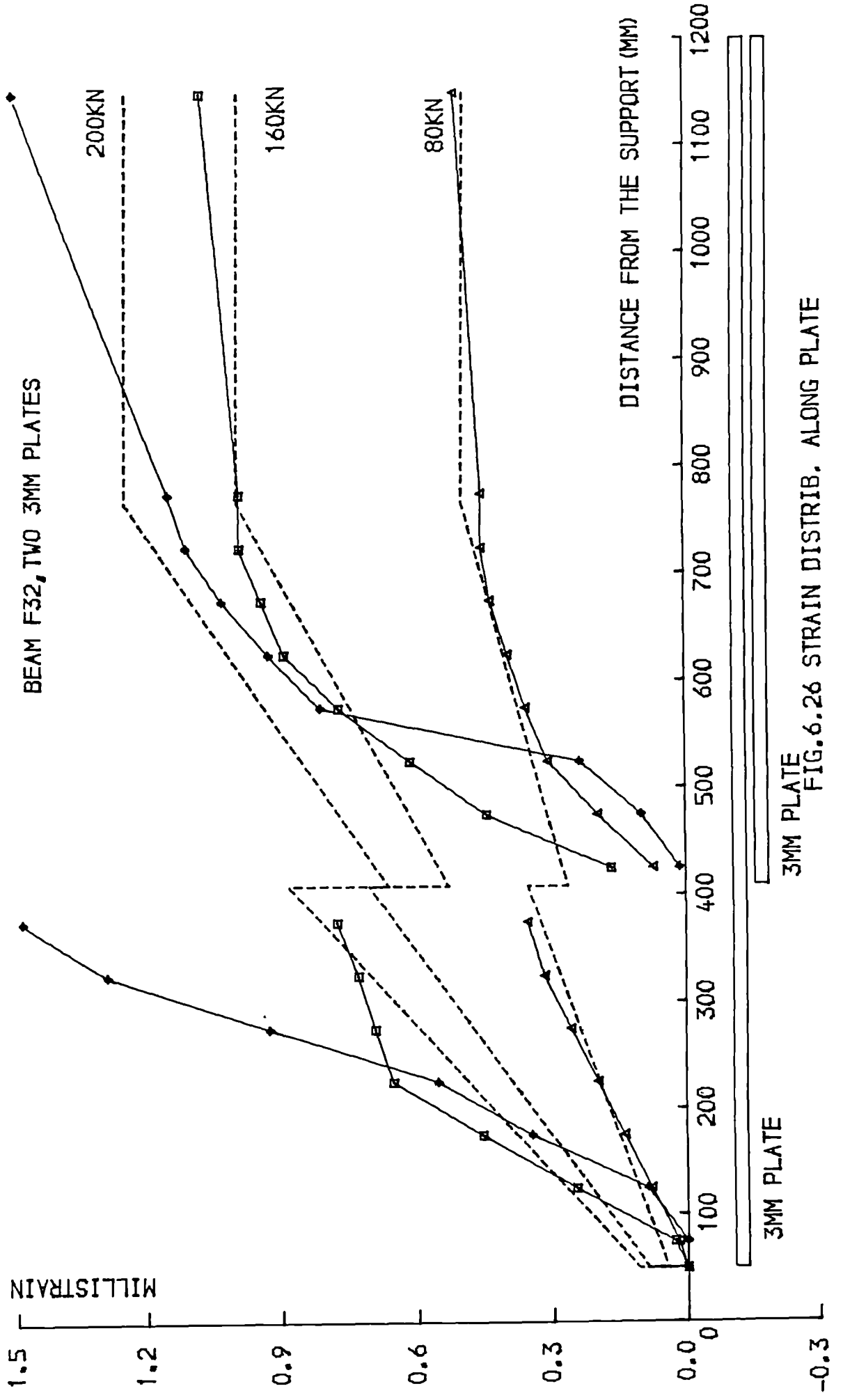


FIG. 6.26 STRAIN DISTRIB. ALONG PLATE

BEAM F33, ONE 6MM PLATE, TAPERED THICK.

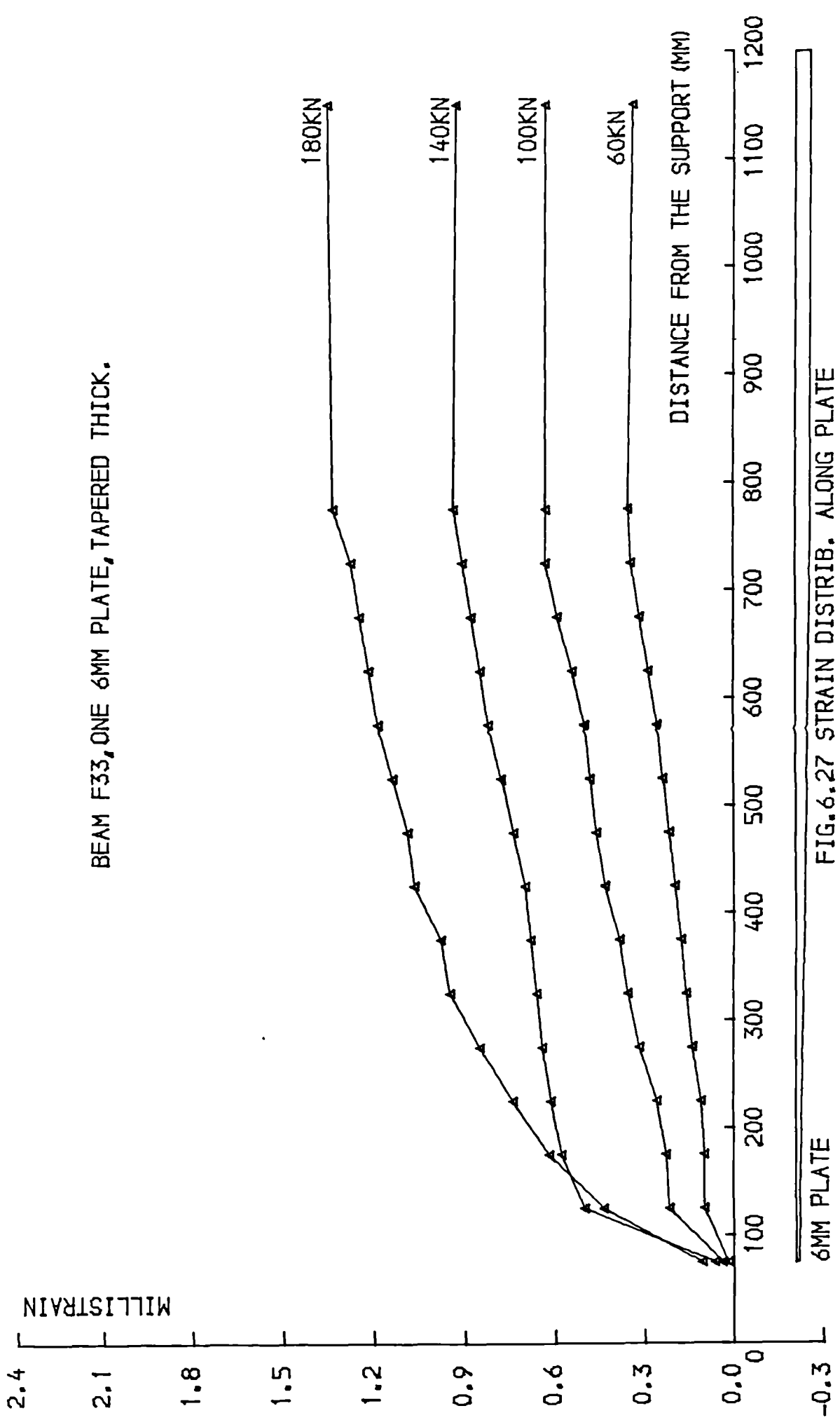


FIG.6.27 STRAIN DISTRIB. ALONG PLATE

BEAM F35, TWO 3MM PLATES, WITH BOLTS

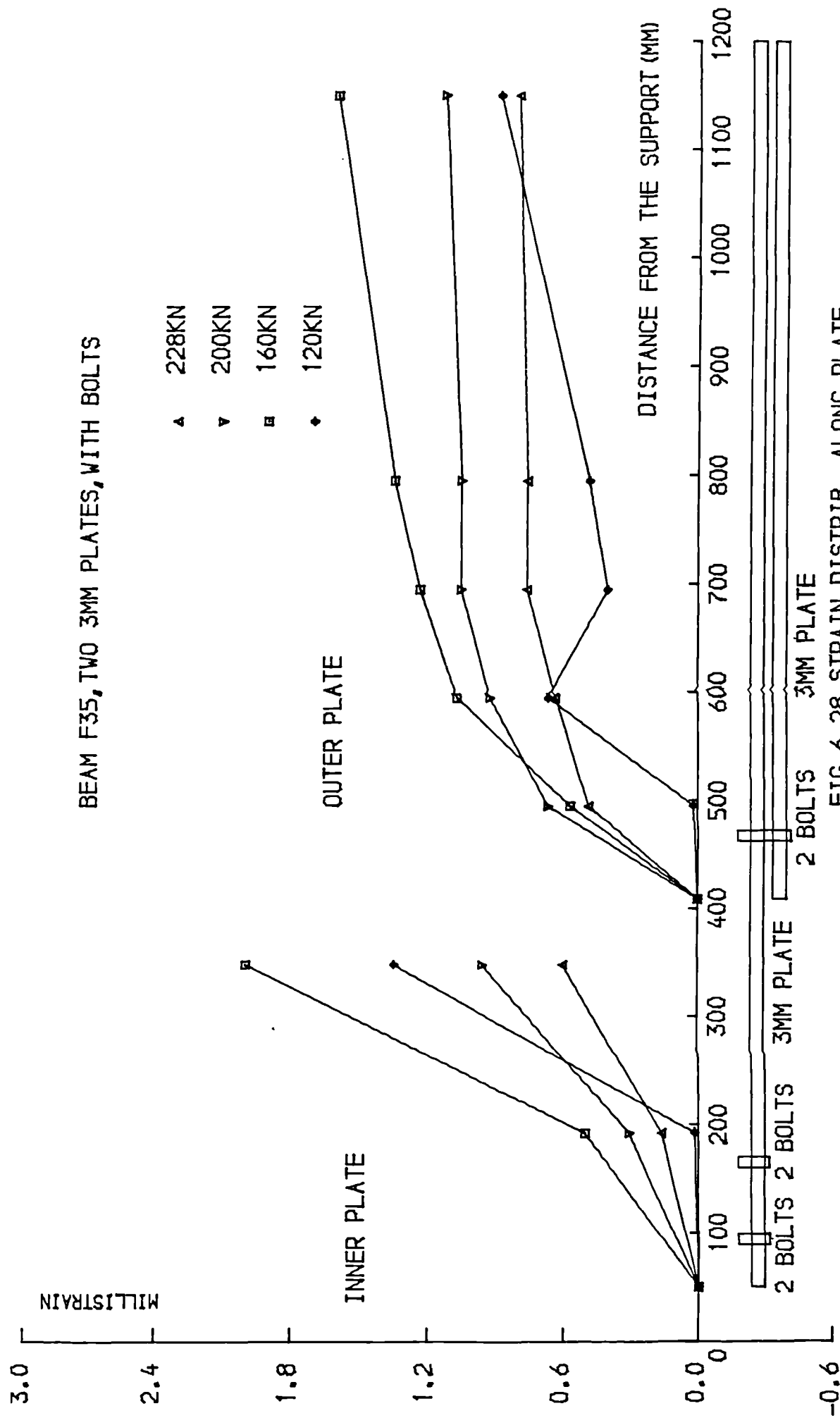


FIG. 6.28 STRAIN DISTRIB. ALONG PLATE

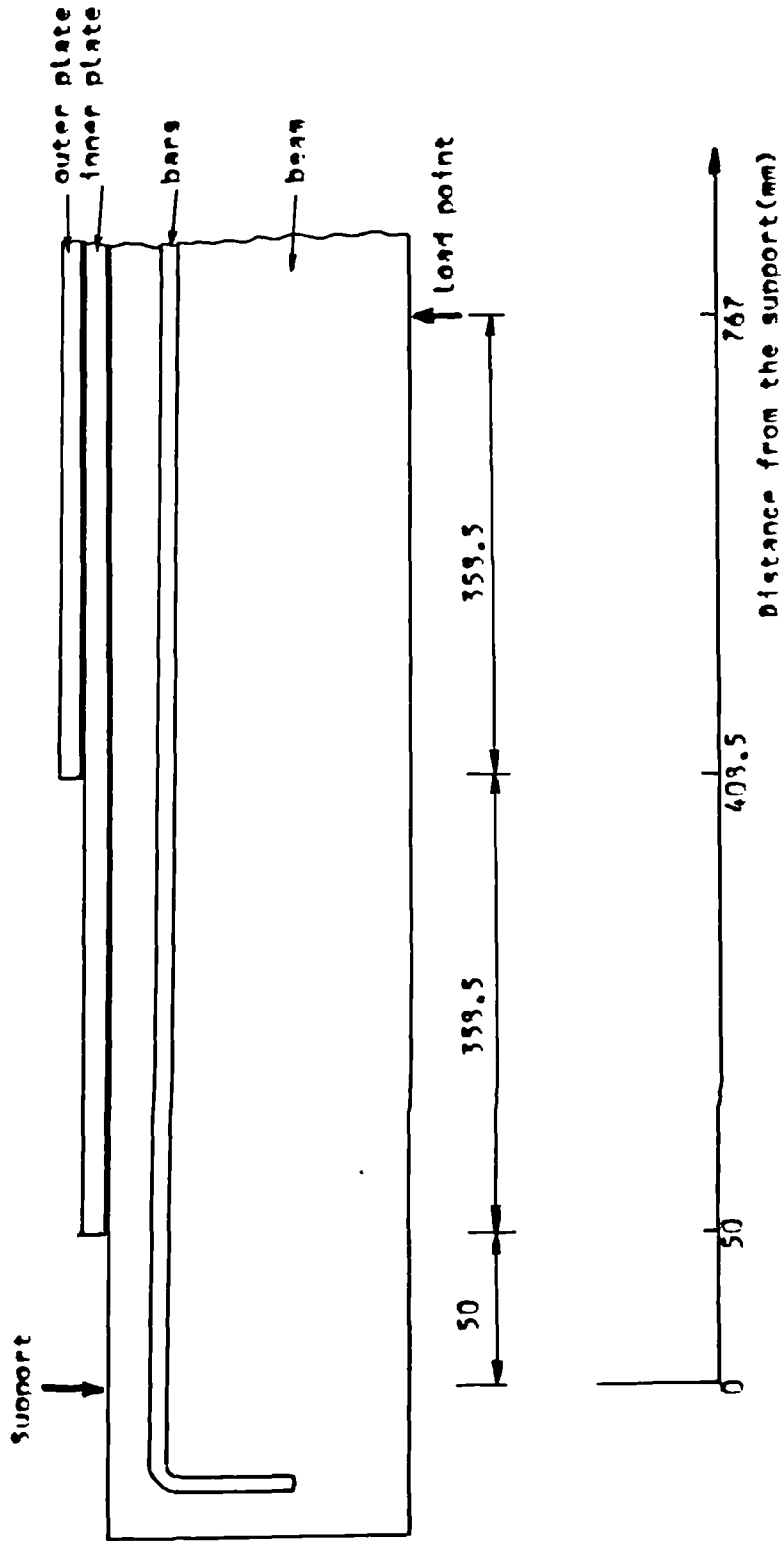


Fig.6.29: Relative distances from the support

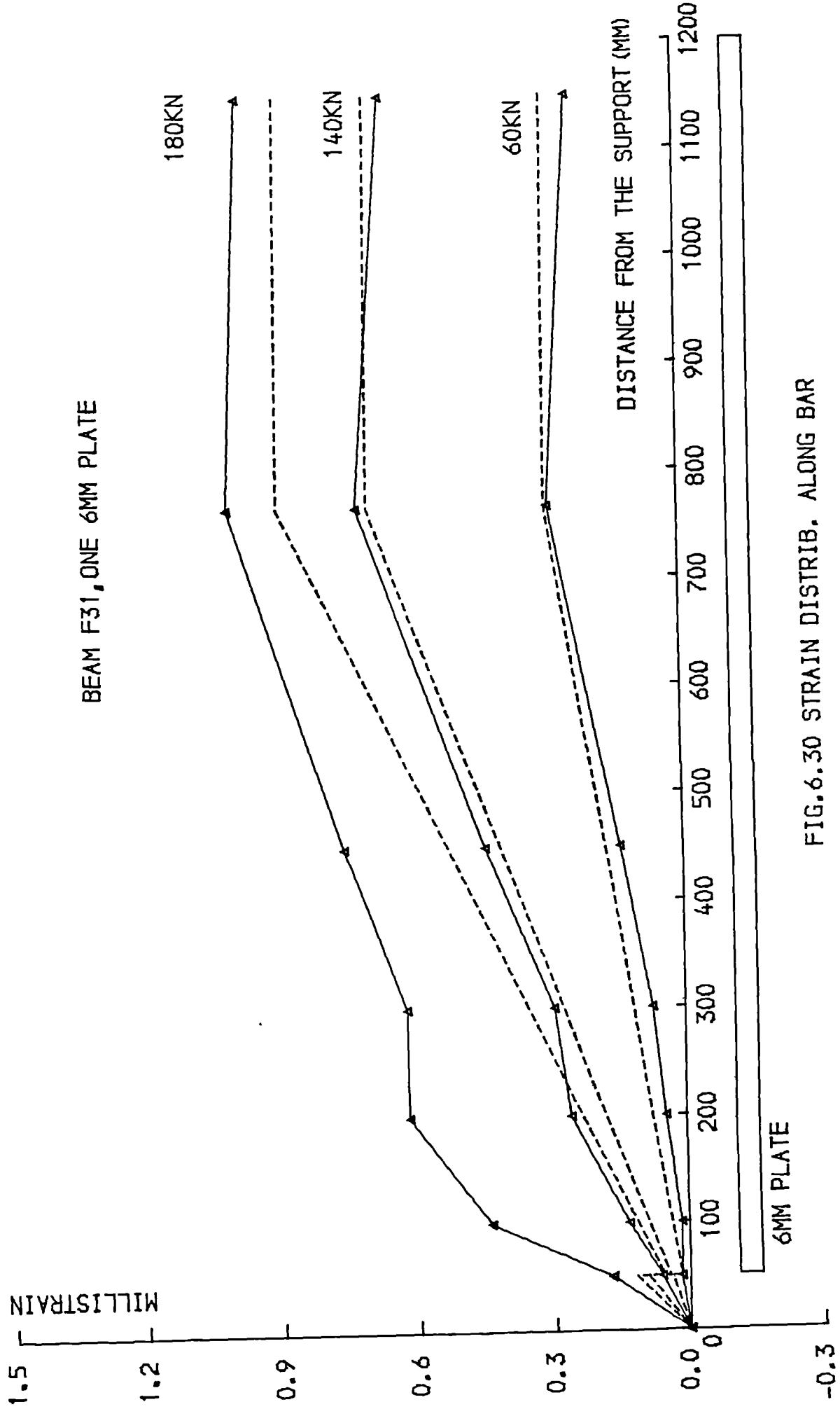


FIG.6.30 STRAIN DISTRIB. ALONG BAR

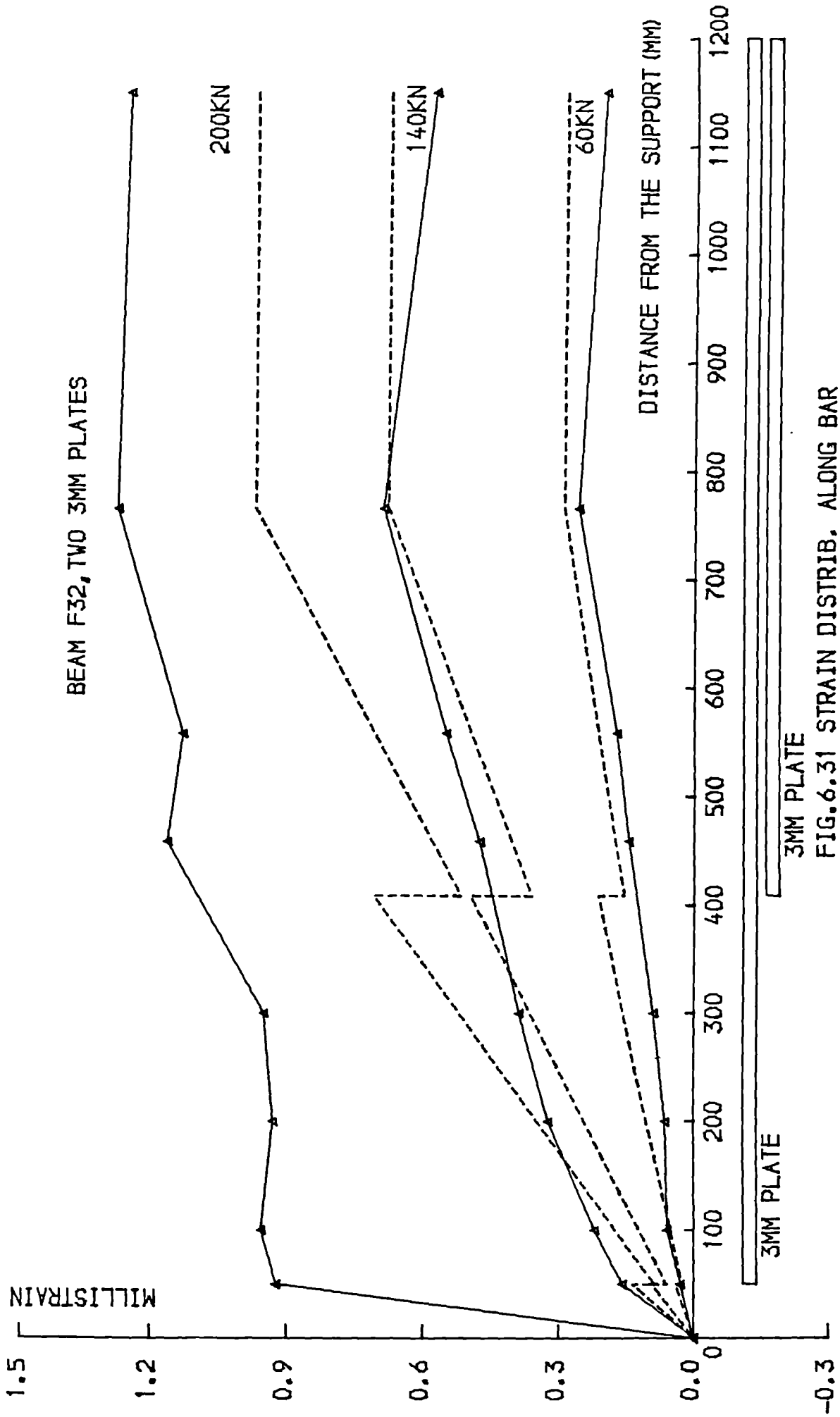


FIG. 6.31 STRAIN DISTRIB. ALONG BAR

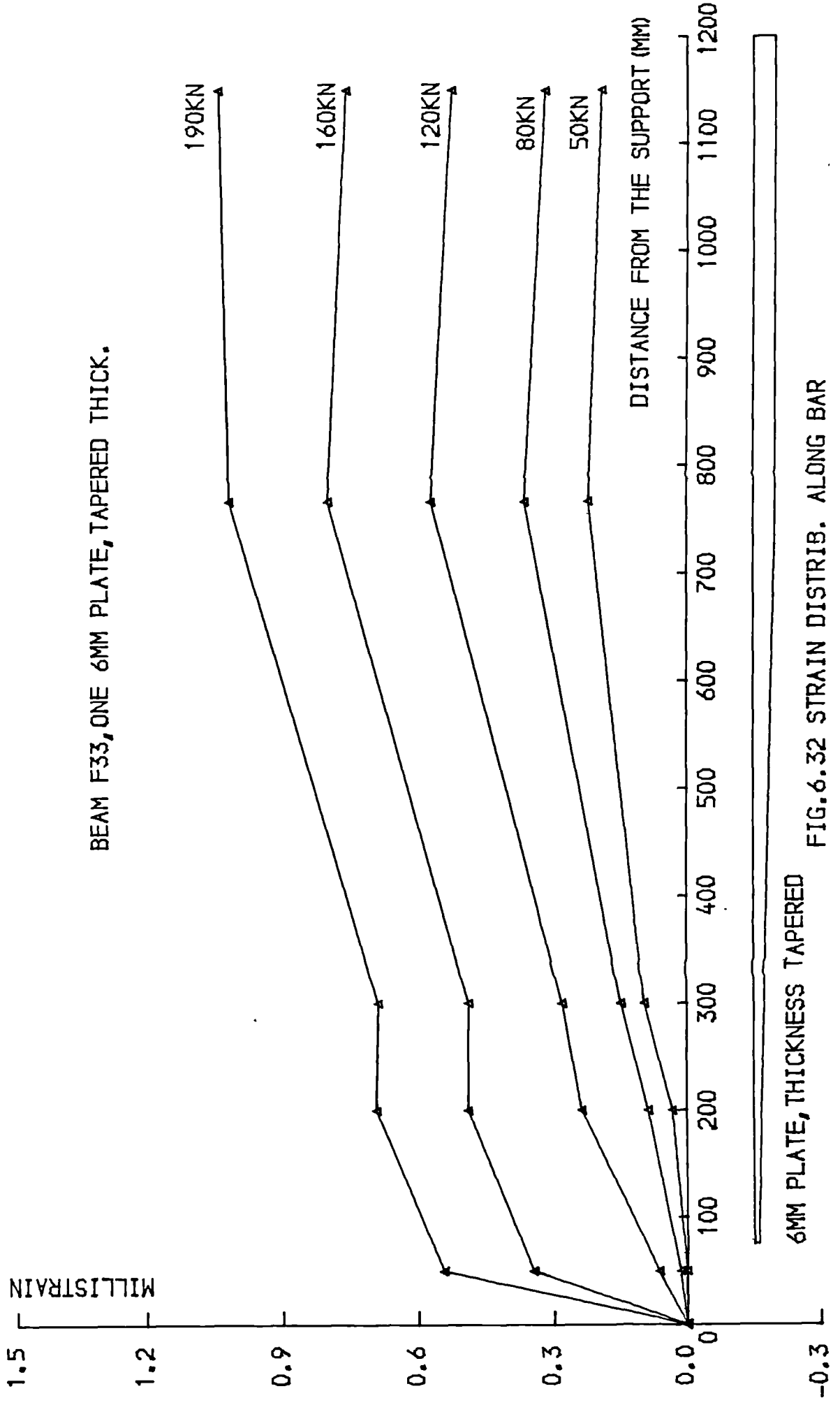


FIG. 6.32 STRAIN DISTRIB. ALONG BAR

difference between the two recorded forces divided by the bond area between the two locations, this bond area being equal to the product of the plate width b' by the distance ΔL between the two locations:

$$\text{Bond stress } f_{bp} = \frac{\Delta \epsilon \cdot A_p \cdot E_p}{b' \cdot \Delta L} \quad (6.7)$$

where ΔL is the distance between the two considered locations, $\Delta \epsilon$ the difference between the recorded strains, A_p , E_p and b' are the cross-sectional area, the elastic modulus and the width of the plate. But $A_p = b' \cdot t_p$ where t_p is the plate thickness. Equation (6.7) becomes therefore:

$$f_{bp} = \frac{\Delta \epsilon \cdot t_p \cdot E_p}{\Delta L} \quad (6.8)$$

The distribution of the interface shear bond stresses along the plate thus obtained are shown in Figs.6.33 to 6.36. these figures confirm that the location of the transfer region tends to move away from the support at higher loads.

For the beams with two 3mm plate (F32 and F35), it was assumed in the computation of the bond stresses that there was no relative slip between the two plates and that they behaved as one 6mm plate. The bond stresses were deduced from the strains measured on the outer plate (in the region where there were two plates) and on the inner plate elsewhere (Figs.6.34 and 6.36). The bond failure occurred at the end of the inner plate, yet the deduced bond stresses were higher in the region where there were two plates (Figs.6.34 and 6.36). This means that the assumption that the two plates behaved as a single one was not justified. Fig.6.37 showing the plate end movements and

BEAM F31, ONE 6MM PLATE

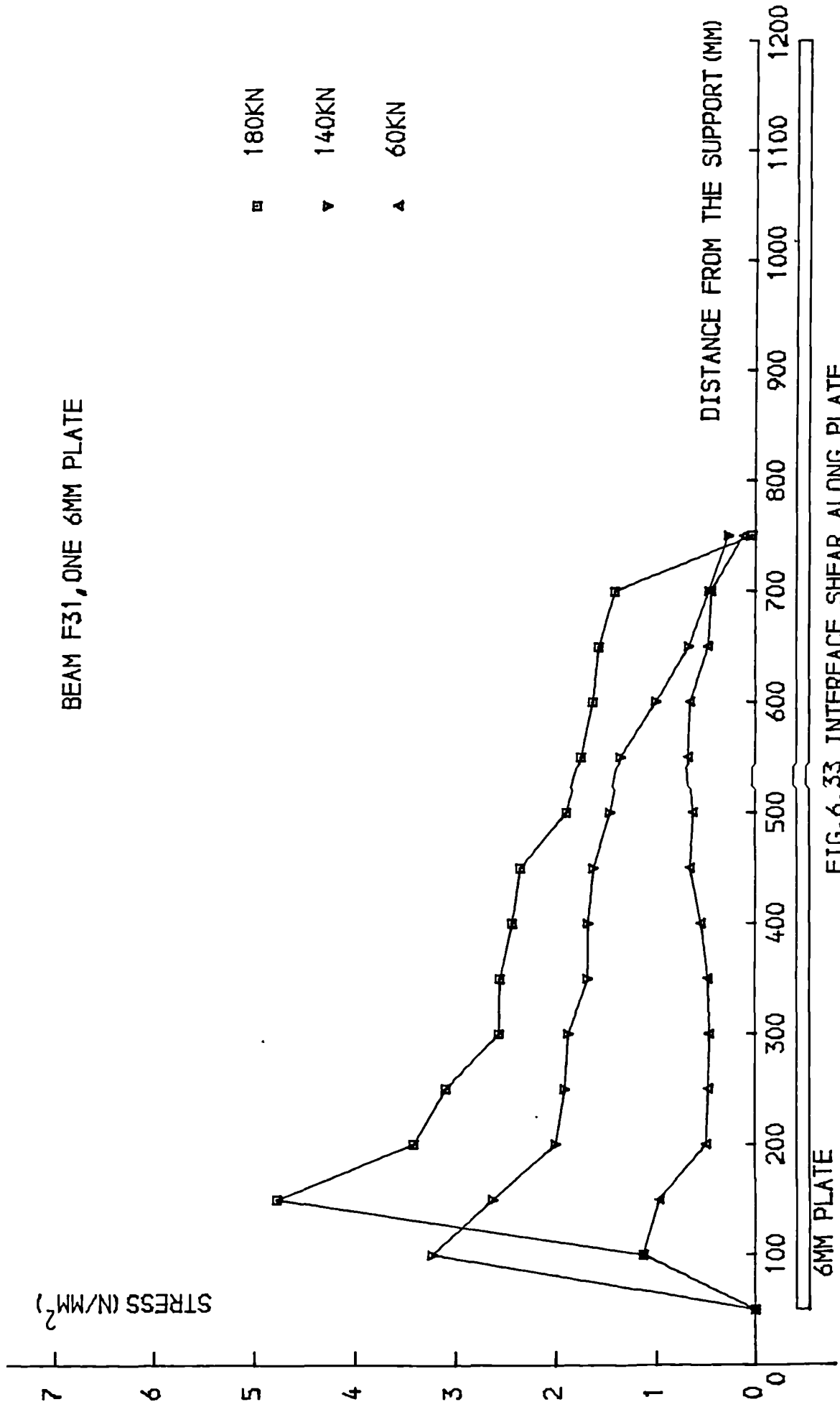


FIG.6.33 INTERFACE SHEAR ALONG PLATE

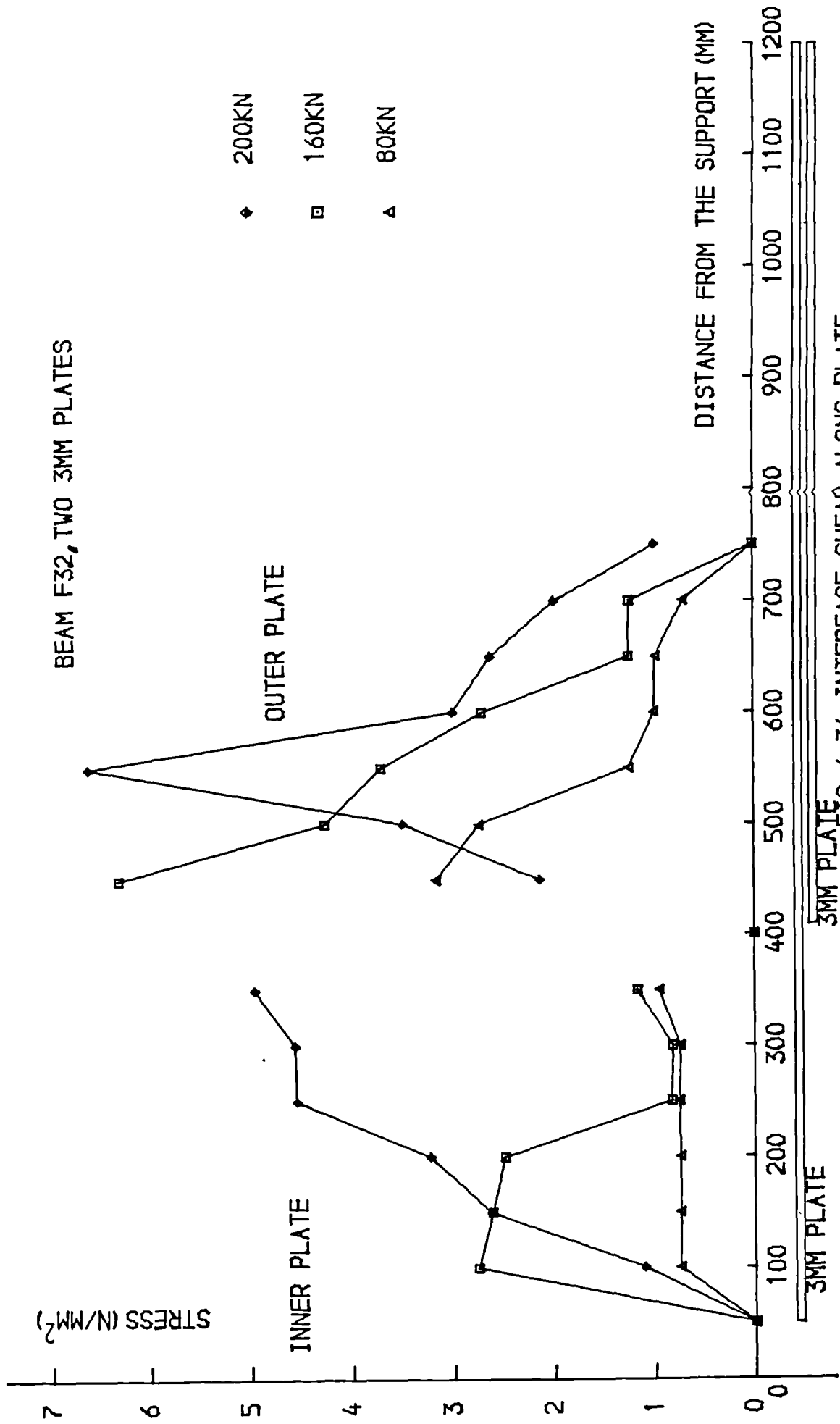


FIG. 6.34 INTERFACE SHEAR ALONG PLATE

BEAM F33, ONE 6MM PLATE, TAPERED THICK.

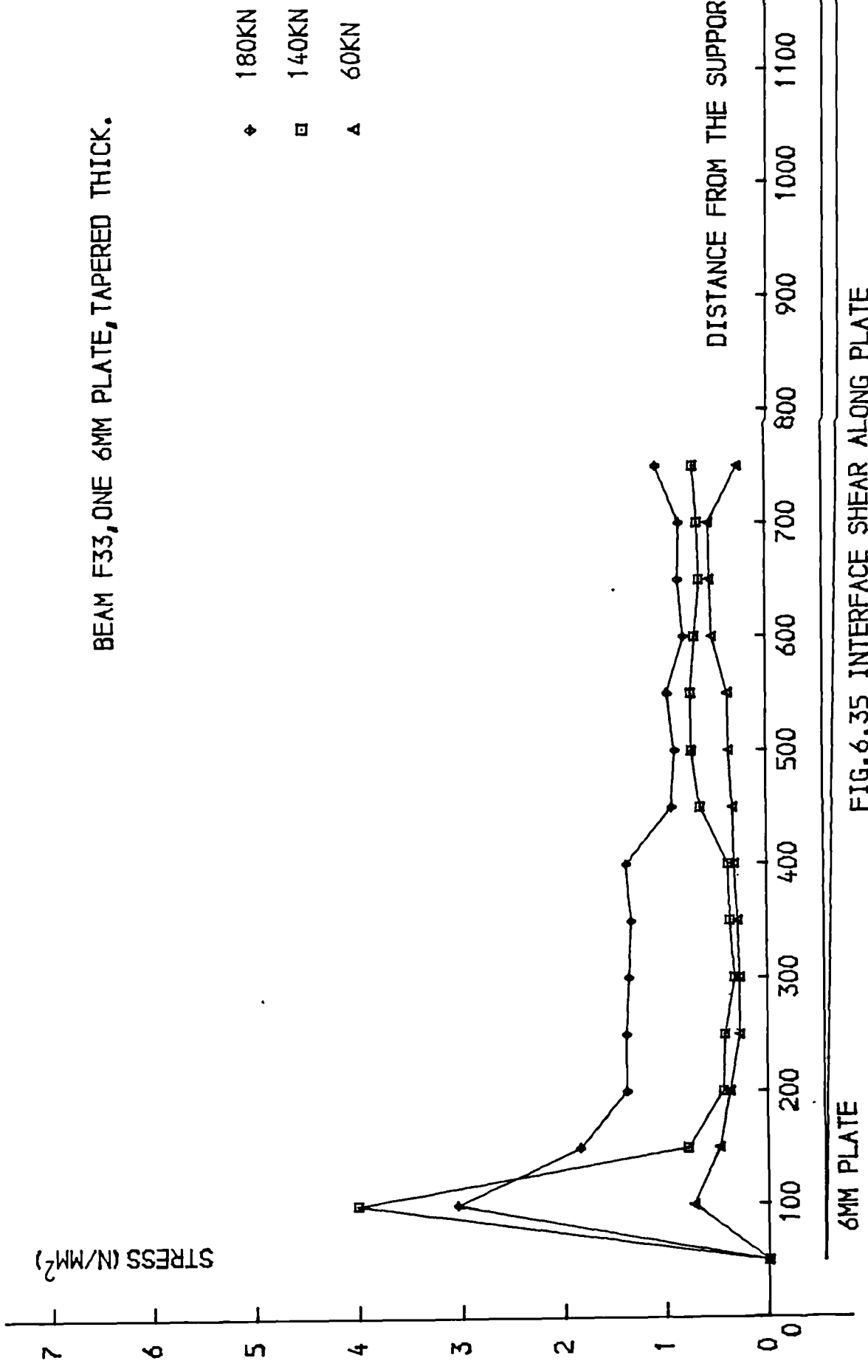


FIG. 6.35 INTERFACE SHEAR ALONG PLATE

6MM PLATE

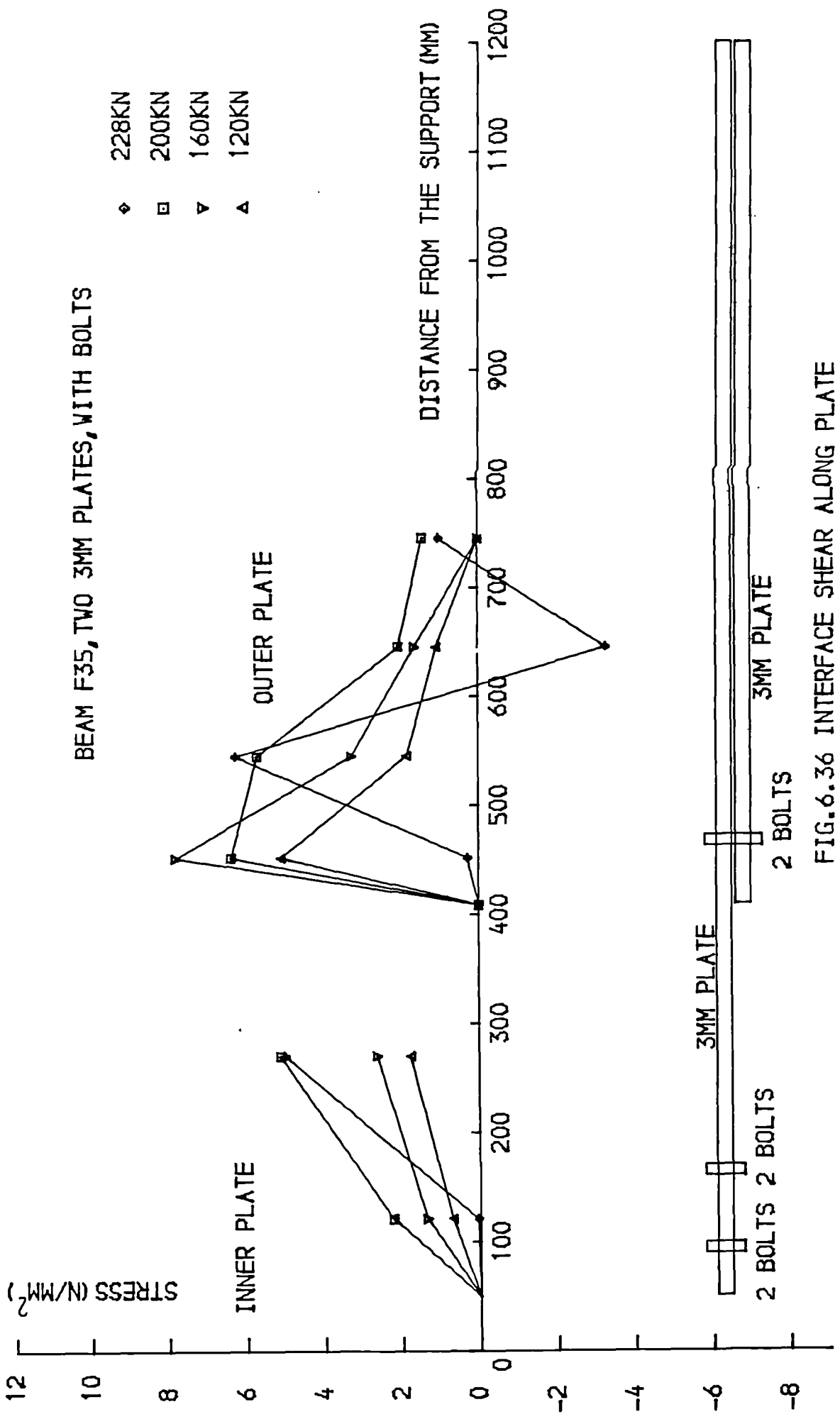


FIG.6.36 INTERFACE SHEAR ALONG PLATE

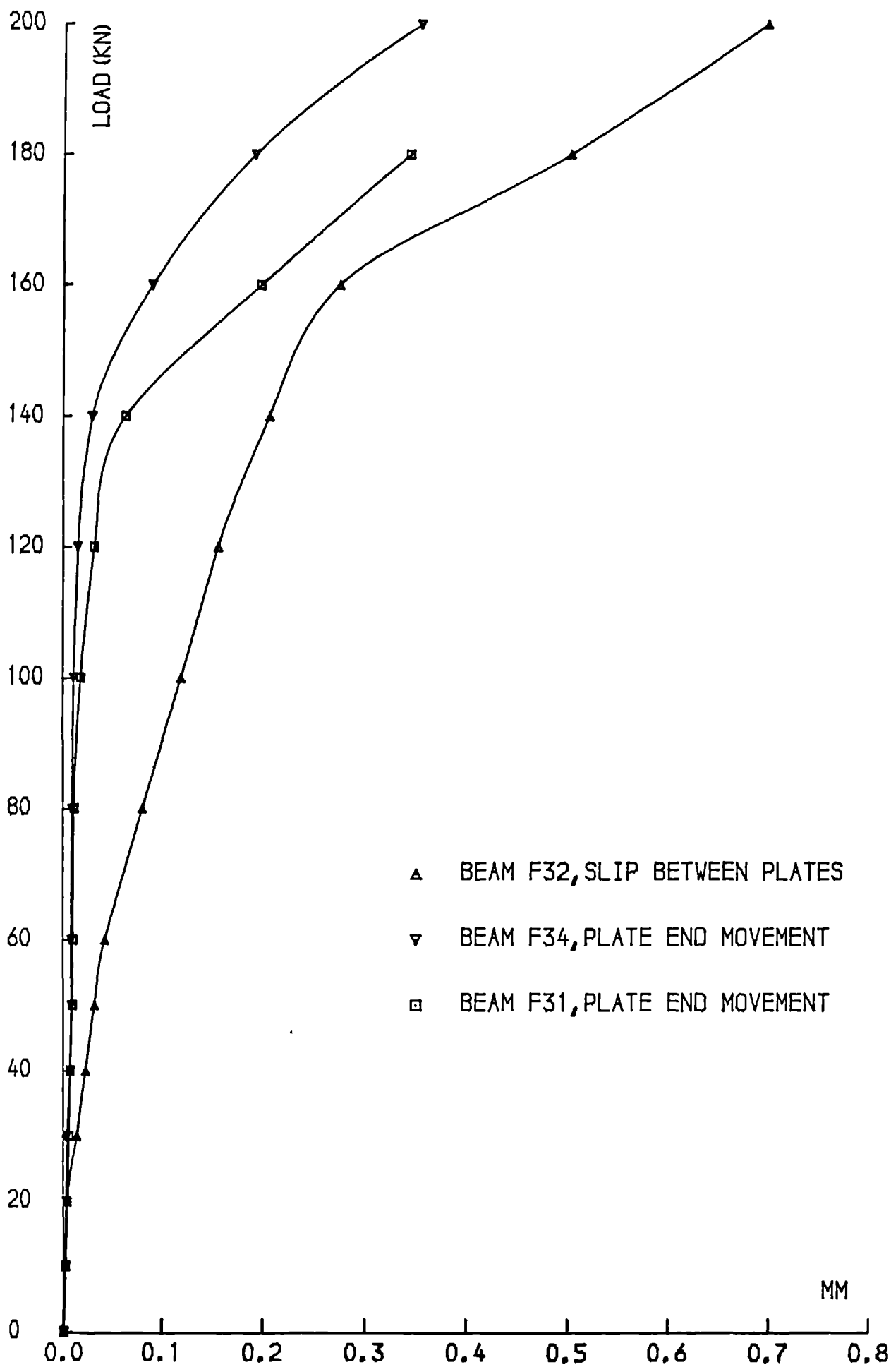


FIG. 6.37 LOAD-PLATE MOVEMENT CURVES

the relative slip between the two 3mm plates supports the conclusion that the two plates did not act as a single one. The deduced bond stresses at the end of the outer plate (where there are two plates) cannot therefore be reliable. For this reason, the maximum values of bond stresses to be considered will be those registered in the region of one plate only.

The maximum interface bond stresses registered (for the beams that did not reach their full flexural strength) were:

Beam F31: 5.02 N/mm²
 Beam F32: 4.95 N/mm²
 Beam F33: 4.22 N/mm²
 Beam F34: 4.82 N/mm² (just prior to debonding)
 Beam F35: 4.90 N/mm² " " "

After the initiation of debonding in beams F34 and F35, the plate strains decreased and the bond stresses deduced from the registered strains became insignificant (Fig.6.36) as there was no composite action of concrete and the plate anymore.

The theoretical bond stresses in regions not affected by the plate cutoff given by equation (6.2) are:

Beam F31: 1.99 N/mm²
 Beam F32: 2.30 N/mm²
 Beam F33: 2.07 N/mm²
 Beam F34: 2.17 N/mm² (at debonding)
 Beam F35: 2.32 N/mm² " "

These values compare satisfactorily with the critical value of 2.15 N/mm² found by Jones, Swamy and Ang (66) but are less than half the measured ones. This is due to the fact that equation (6.2) does not take into account the plate cutoff effect.

The interface bond stresses given by equation (6.4) which accounts for the plate cutoff effect depend on the transfer length x . The distance l from the support to the cutoff point is 50mm. It was seen before in equation (6.4) that stopping the plate at a distance l from the support results in an increase of $100l/x$ (%) in the interface bond stress, x being the distance over which the stress transfer takes place. Comparison of the distributions of the theoretical elastic and experimental strains along the plate (Figs.6.25 to 6.28) shows that the value of x is about 50 to 100mm. Although the transfer region moves away from the support at higher loads (Fig.6.31), the peak in the shear stress distribution remains over a distance of 50 to 100mm. These figures show the distance x over which the force transfer from the plate to the bars takes place and show that this transfer is not completely linear as was assumed in equation (6.4). The plate strain measurements were carried out by means of 50mm demec gauges and an accurate determination of the variation of the strains in the cutoff region requires a better strain measurement such as electrical strain gauges fixed along the plate at very small spacings. Assuming a value of 50mm for this transfer length, and since the distance l from the plate cutoff to the support is equal to 50mm, the values of bond stresses given by equation (6.4) will be double those given by equation (6.2) i.e:

Beam F31: 3.98 N/mm²

Beam F32: 4.60 N/mm²

Beam F33: 4.14 N/mm²

Beam F34: 4.34 N/mm²

Beam F35: 4.64 N/mm²

Assuming that the transfer of forces from the plate to the bars in the plate cutoff region is linear over a distance of 50mm, the values predicted by equation (6.4) agree satisfactorily with the recorded ones.

The maximum bond stress registered was 5.02 N/mm² (beam F31). Beams F32 and F33 had slightly lower bond stresses than those of beam F31. This was expected as the beams had lower cross section area of plates at the cutoff region. The reduction in bond stresses in beam F33 would have been more pronounced had the tapering of the thickness been perfectly executed. The actual thickness varied from 2 to 6mm in the shear span and this resulted in a reduction of about 25% in the bond stresses but an increase of only 5% in the failure load.

The rawbolts fixed in beams F34 and F35 prevented complete separation of the plate and reduced the plate end movement (Figs.6.20 and 6.37) but did not prevent the local longitudinal debonding at the level of the internal bars which stopped the composite action of the plate and the beam.

6.11.2 INTERNAL BOND STRESSES

The strain distribution (Figs.6.30 to 6.32) and the deduced bond stress distribution along the bars (Figs.6.38 to 6.40) confirm the existence of the force transfer from the external to the internal reinforcement.

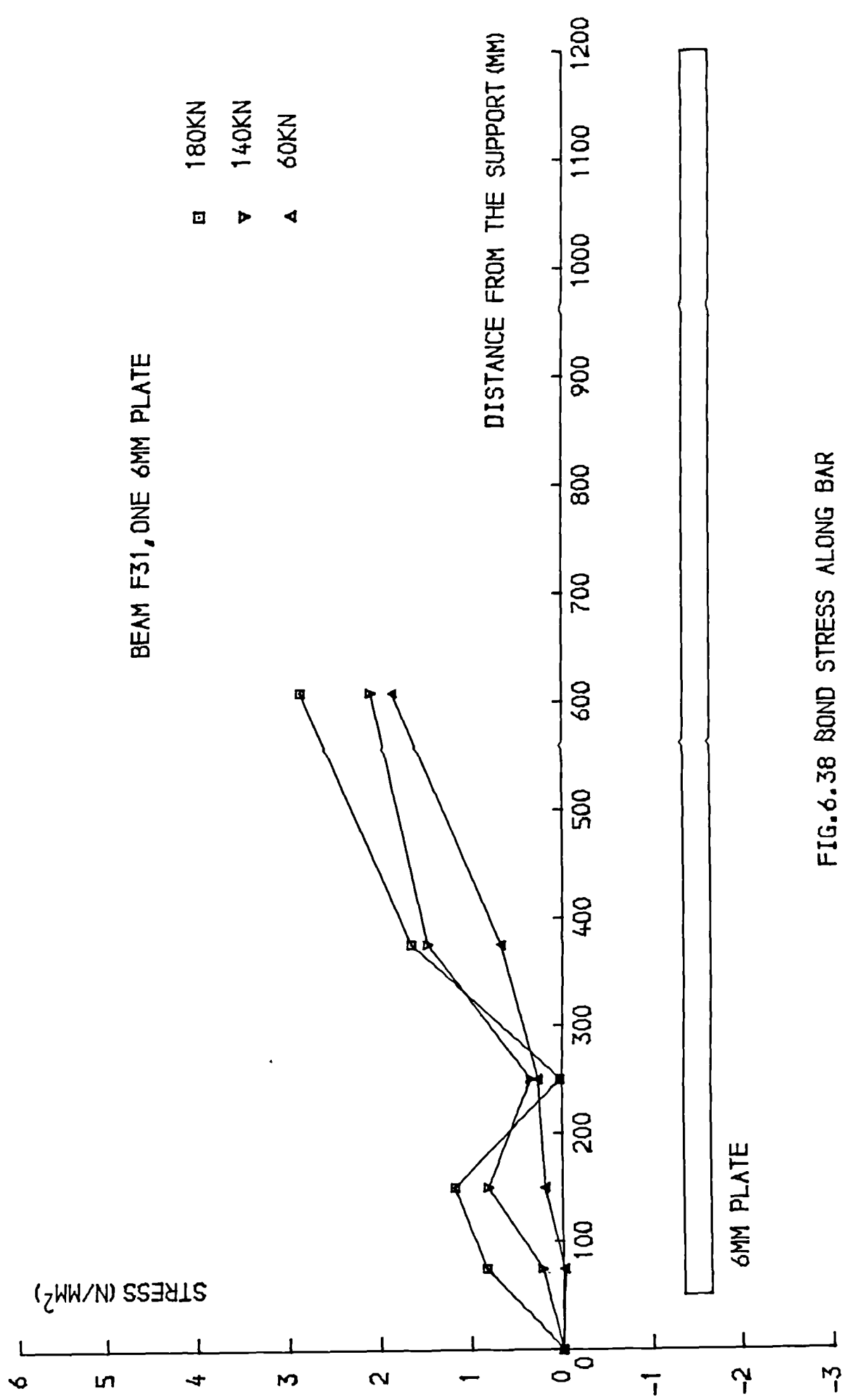


FIG. 6.38 BOND STRESS ALONG BAR

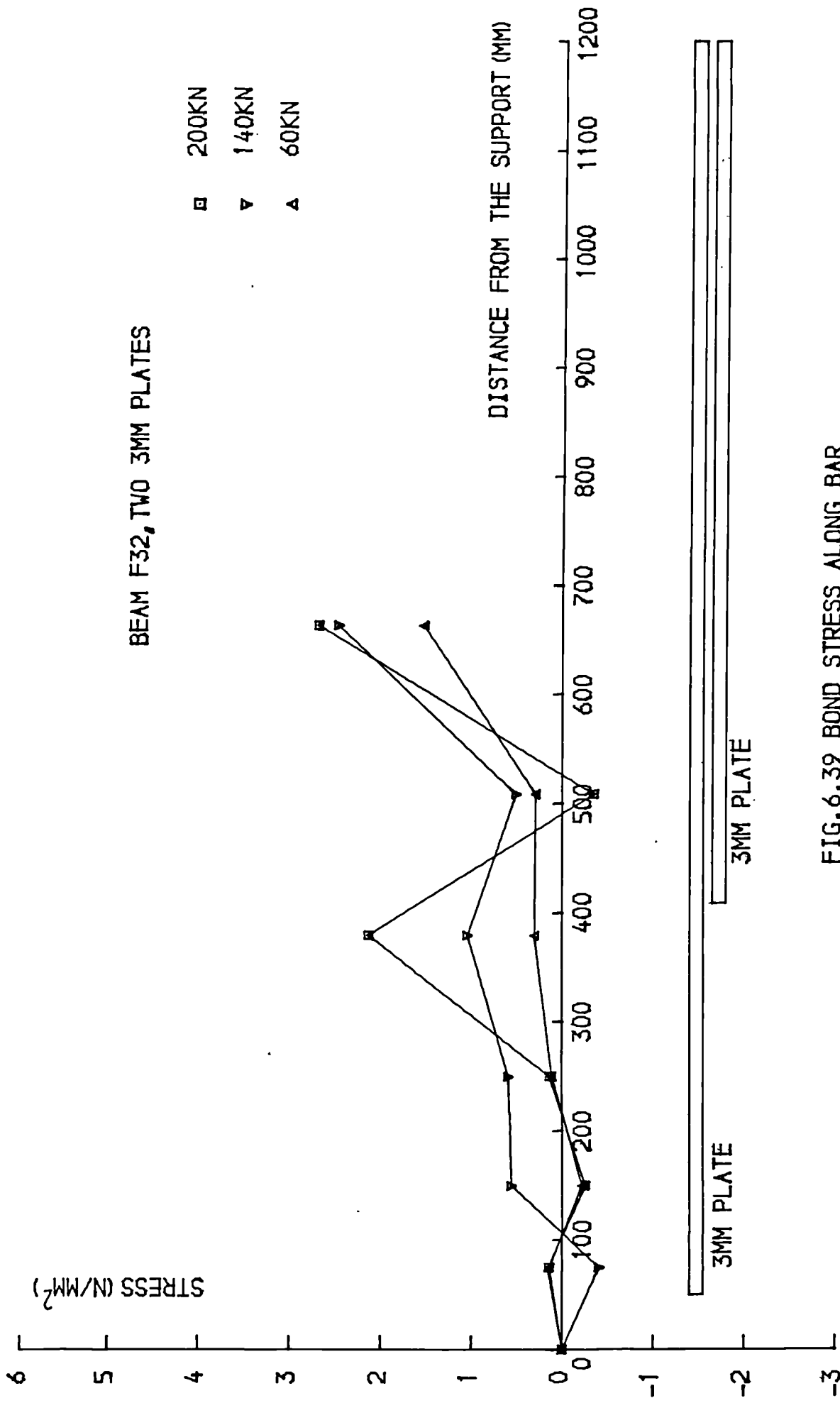


FIG. 6.39 BOND STRESS ALONG BAR

BEAM F33, ONE 6MM PLATE, TAPERED THICK.

- 190KN
- ▽ 120KN
- ▲ 50KN

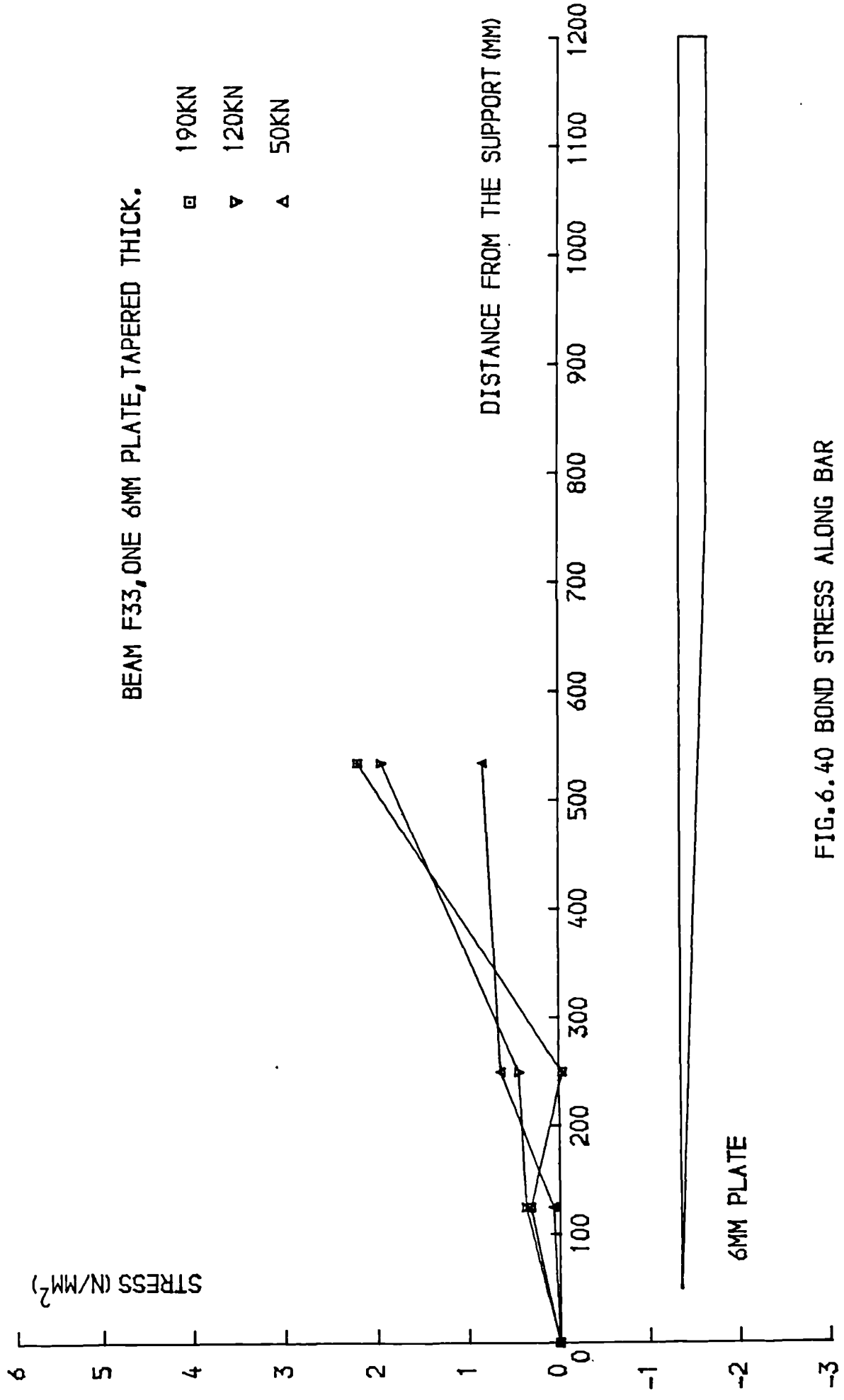


FIG. 6.40 BOND STRESS ALONG BAR

For the beams with two 3mm plates (F32 and F35), the transfer takes place twice: where the outer plate is stopped and at the end of the inner plate (Figs.6.31 and 6.39). This results in a total stress opposite to the local bond stress (Fig.6.39) confirming the predictions of equation (6.3).

The maximum internal bond stresses recorded were 2.88 N/mm² for beams F31 and F32 and 2.20 N/mm² for beam F33.

6.12 PEELING FORCES

The theoretical peeling forces are computed using equations (6.5) and (6.6).

6.12.1 COMPONENT F1

The values of the peeling force F1 as given by equation (6.5) are proportional to the bond stresses and depend on the eccentricity considered. Depending on whether the plate cutoff effect is taken into account, the value of the bond stress will be the one given by equations (6.2) or (6.4).

(a) The eccentricity e is taken as equal to the distance between the plate and the bars e=39.5mm:

NO CUTOFF EFFECT

Beam F31: F1=9.7kN

Beam F32: F1=11.4kN

Beam F33: F1=10.2kN

Beam F34: F1=10.7kN

Beam F35: F1=11.5kN

CUTOFF EFFECT

F1=21.8kN

F1=22.8kN

F1=20.4kN

F1=21.4kN

F1=23.0kN

(b) The eccentricity is taken as equal to the distance between the plate and the epoxy joint $e=3.75\text{mm}$:

NO CUTOFF EFFECT

CUTOFF EFFECT

Beam F31: $F_1=0.92\text{kN}$

$F_1=2.07\text{kN}$

Beam F32: $F_1=1.08\text{kN}$

$F_1=2.16\text{kN}$

Beam F33: $F_1=0.97\text{kN}$

$F_1=1.94\text{kN}$

Beam F34: $F_1=1.02\text{kN}$

$F_1=2.04\text{kN}$

Beam F35: $F_1=1.09\text{kN}$

$F_1=2.18\text{kN}$

The peeling forces were not directly measured but if equation (6.5) is applied to the measured bond stresses, the experimental peeling forces for an eccentricity $e=3.75\text{mm}$ will be:

Beam F31: $F_1=2.35\text{kN}$

Beam F32: $F_1=2.32\text{kN}$ (The force F_1 is proportional to the bond stress).

Beam F33: $F_1=1.98\text{kN}$

Beam F34: $F_1=2.30\text{kN}$

Beam F35; $F_1=2.30\text{kN}$

6.12.2 COMPONENT F2

The second component F_2 of the peeling force is the resistance of the plate to undergoing bending. It was seen in equation (6.6) that $F_2=1.21\text{N}$ per mm central deflection. The ultimate central deflections recorded for the bond failure beams were about 10.0mm (except for beams F34 and F35 which deflected further after local debonding and beams F36 and F37 which did not fail by bond).

The total resistance F_2 of the plate to bending after a deflection of 10.0mm is therefore $F_2=12.1\text{N}$.

The total peeling force F present at the end of the joint is the sum of the two components F_1 and F_2 :

$$F = F_1 + F_2 \approx 2000 + 12 \approx F_1 \text{ (Newtons)}.$$

6.13 CONCLUSIONS

The following conclusions can be drawn from the theoretical and experimental investigations into the premature bond failures of the plated beams:

(1) The epoxy glue ensures full composite action between the plates and concrete at low loads thus increasing the stiffness of the beam. The study of the flexural behaviour of the beams also showed that the plates improved the contribution of concrete in tension and resulted in an overall increase in the beam stiffness. This restraining effect was greater with thicker plates.

(2) Stopping the external plate in the shear span increases the bond stresses considerably and creates a critical section where premature bond failure is prone to occur.

(3) The predicted values of bond stresses in the plate cutoff region agree satisfactorily with the experimental results although the theoretical model assumed a linear force transfer from the plate to the bars over a distance of 50mm. The experimental bond stresses varied between 4.22 and 5.02 N/mm² and the predicted ones between 3.98 and 4.64 N/mm². A better instrumentation is however needed to assess the distribution and the length of the transfer.

(4) The bond stresses registered were all slightly lower than the ultimate shear bond stress of 6.5 N/mm² (determined by the pull out tests described in chapter four) supporting the conclusion that the premature failure was a combination of bond and peel stresses.

(5) Tapering of the plate thickness in the shear spans and the use of two 3mm plates instead of one 6mm plate (the second being stopped before the first) reduced the bond stresses and improved slightly the beam performance but did not enable the beams to reach their full strengths.

(6) The deduced peeling forces from the theoretical and experimental bond stresses were of the same magnitude.

(7) The bolts prevented the free separation of the plates but did not delay the local debonding occurring at the level of the internal bars nor did they ensure full composite action of the plate and concrete. This undermines the confident use of bolts with thick plates in practical applications of structural repair of bridges (71) and more research in this area is therefore needed.

(8) Bonding of external steel strips at the plate ends seems to be the only adequate solution to the problem of premature bond failures. The strips resist the bond and peel forces and strengthen the part of the beam where the debonding occurs.

CHAPTER SEVEN

SHEAR BEHAVIOUR OF PLATED BEAMS

7.1 INTRODUCTION

The possible reasons for structural repair and the different strengthening techniques commonly used have been reviewed before. In practice, structures may need additional stiffness and/or strength in flexure or shear. The additional reinforcement required could then be either longitudinal to increase the ultimate flexural capacity and reduce the deformations or transverse to increase the shear capacity of the member or a combination of the two.

Shear failures are often brittle and premature and prevent full development of flexural strength and full exploitation of longitudinal steel. This lack of ductility leads to a sudden and sometimes dangerous failure.

Whilst the main characteristics, mechanisms, principles and modes of shear failure and the different parameters affecting it have been recognized for many years (91-116), no satisfactory analytical method, for an adequate prediction of shear forces, has been developed as yet. Nevertheless various safe design formulae have been derived over the years.

The main types of shear transfer are:

- (a) Shear in uncracked concrete
- (b) Interface shear or 'Aggregate interlock'
- (c) Dowel action
- (d) Arch action (in members loaded close to supports)
- (e) Shear reinforcement

Most modern design codes assign the total shear strength to the compressive zone (uncracked concrete) and the web reinforcement.

Many parameters such as beam dimensions, web and longitudinal steel, concrete strength and load distribution affect the shear strength of a beam but the shear mode of failure depends mainly on the shear span to effective depth ratio, a/d . There exists a region bounded by limiting values of a/d inside which diagonal failure is generally produced and outside which full flexural strength is usually attained (98).

The use of the ratio of ultimate moment at failure to ultimate flexural moment, M_u/M_{flex} , as an indicator of diagonal failure is more convenient than the ultimate shear strength V_u which can vary considerably with a/d . The minimum ratio of ultimate moment to full flexural moment is about 0.5 (98) and occurs at a shear span to effective depth ratio of about 2.5. The critical value of a/d at which there is a change from a shear mode of failure to a flexural failure depends on the amount of reinforcement and the concrete strength.

In conventional reinforced concrete if a reinforcing bar crosses a shear crack, the shearing displacement along the crack will be resisted partly by the dowelling force in the bar. This dowel action depends on the tensile strength of concrete, the cover and bending resistance of the bar (104). These dowel forces decrease at ultimate loads and are not allowed for in design code formulae.

One of the objectives of this project was to study the effect of externally bonded steel on the shear capacity of the beams. The aim was to detect the existence of any dowel action

in the longitudinal plates and investigate the possibilities of using externally bonded steel in the form of strips or channels as web reinforcement. The test variable was the shear span to effective depth ratio, a/d .

7.2 LITERATURE REVIEW

There is little information about the shear behaviour of plated beams. The main review of past research into the shear behaviour of reinforced concrete beams strengthened with externally bonded reinforcement was presented in chapter two.

Shear failures of sandwich beams (beams without internal reinforcement and with steel plates on both compression and tension faces) were brittle (26,41,68) and the ultimate interface shear stress between steel and concrete was much higher than the value predicted by the ACI code. Bouderbalah (65) reported tests on two beams in shear (one unplated and the other plated) and he found that the longitudinal steel plate did not improve the shear capacity of the beam. External shear reinforcement in the form of steel strips glued to the web of a beam has however been used successfully to increase shear strength (50,55-57,69). Apart from the reported increase in shear capacity there is however little information about the behaviour of the external web reinforcement as compared to internal stirrups.

The possible existence of dowel action in the external longitudinal reinforcement and the use of epoxy bonded steel as web reinforcement are both areas worthy of further investigation.

7.3 EXPERIMENTAL PROGRAMME

A total of eight beams were tested in this series. The beams were manufactured in the same way as described in chapter five. The same concrete and internal longitudinal reinforcement were used. The bonding procedure, testing apparatus, instrumentation and the test measurements were identical to those used for the flexural beams. The beams were tested in rig 1 described in chapter five. The central deflections, support rotations, concrete strains across the depth, bar and plate strains were all measured. The deflections were measured at the central section of the beams using Linear Variable Displacement Transducers (LVDT). The rotations were recorded at the supports using an inclinometer over a length of 150mm. The concrete strains across the beam depth and the plate strains were measured at the middle section with a 100mm demec gauge. The bar strains were measured at the central section with electrical strain gauges. The different measuring instruments were described in detail in chapter five.

Six of the beams (three unplated and three plated) were tested to investigate the possible existence of dowel action in the external plates, the variable being the shear span. The shear span to effective depth ratios used were: 1.5, 3.0 and 4.5. The beams with a ratio $a/d=4.5$ were loaded at the middle section and had no constant moment region. For each value of the shear span, two beams were tested: one unplated and the other with a 1.5mm plate bonded to its tensile face. The glue thickness in the plated beams was 1.5mm. The six beams had no shear reinforcement except for three stirrups at each support to prevent bearing failure (Fig.7.1).

The two remaining beams were tested to study the possible use of externally bonded steel as shear reinforcement. The two beams S61 and S62 had the same internal longitudinal reinforcement as the previous ones and no external longitudinal plates. The external shear reinforcement was glued on one shear span only to save steel plates and epoxy adhesive. Internal stirrups were provided on the other shear span (Figs.7.2 and 7.3). The geometry, size and placing of the external plate reinforcement are shown in Fig.7.2. Beams S61 and S62 had the same amount of internal and external shear reinforcement. The external web reinforcement was in the form of strips for beam S61 and channels for beam S62 (Fig.7.2).

The details of the shear beams are summarized in Table 7.1.

7.4 DISCUSSION OF RESULTS

The deformation, cracking and strength results of the shear beams are presented separately in the following sections.

7.4.1 DEFORMATION PROPERTIES

The deformational behaviour of the unplated and plated shear beams were similar to those of the flexural beams reviewed in chapter five. Typical curves of deflections, rotations concrete and steel strains are shown in Figs.7.4 to 7.14. These curves illustrate the brittle nature of shear failures. Beams S61 and S62 were more ductile as a result of having shear reinforcement in both spans.

At a load of 100kN, the longitudinal plates increased the beam stiffness and reduced the deflections by 29.5, 20.3 and 25.4% for shear span to effective depth ratios of 1.5, 3.0 and 4.5 respectively (Fig.7.4). The reductions in the

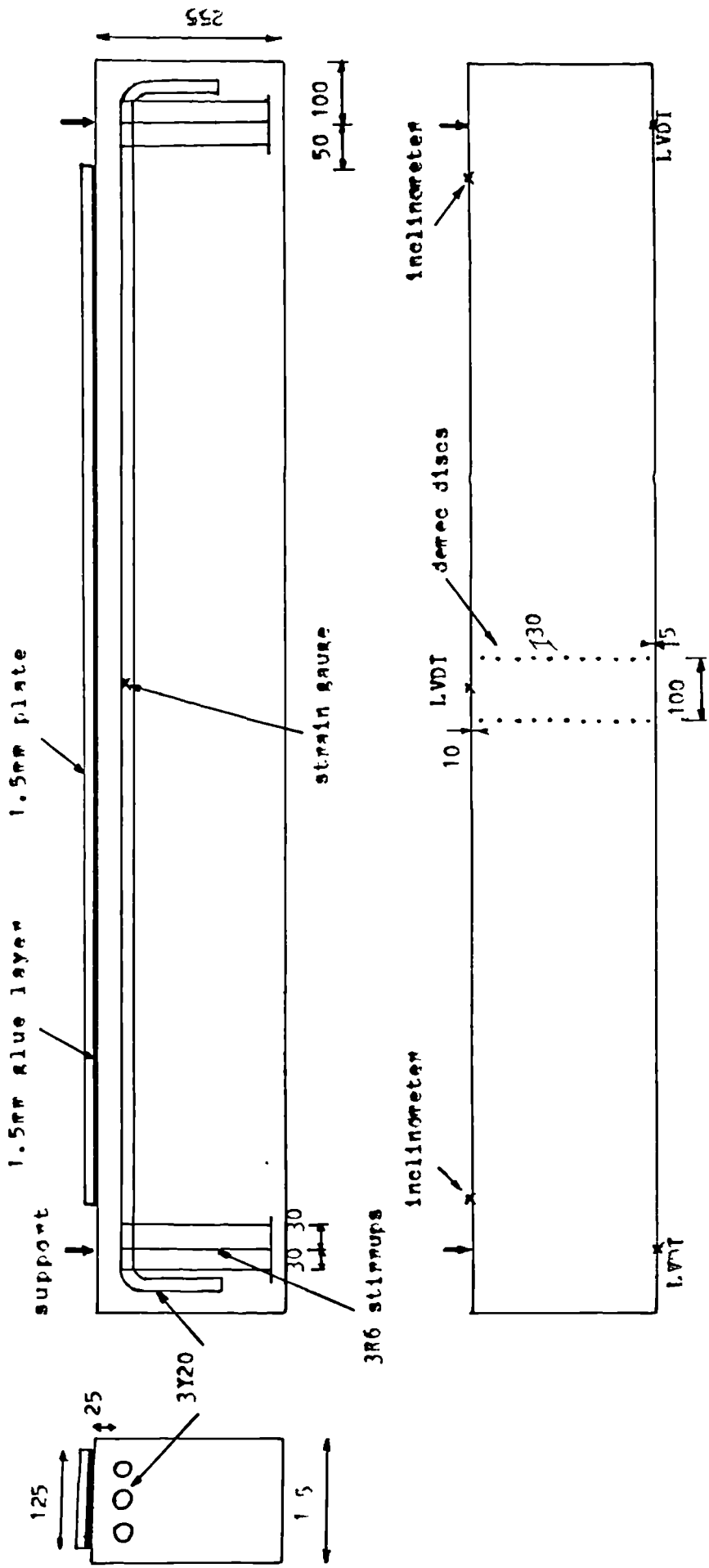


Fig.7.1: Details of shear beams and instrumentation

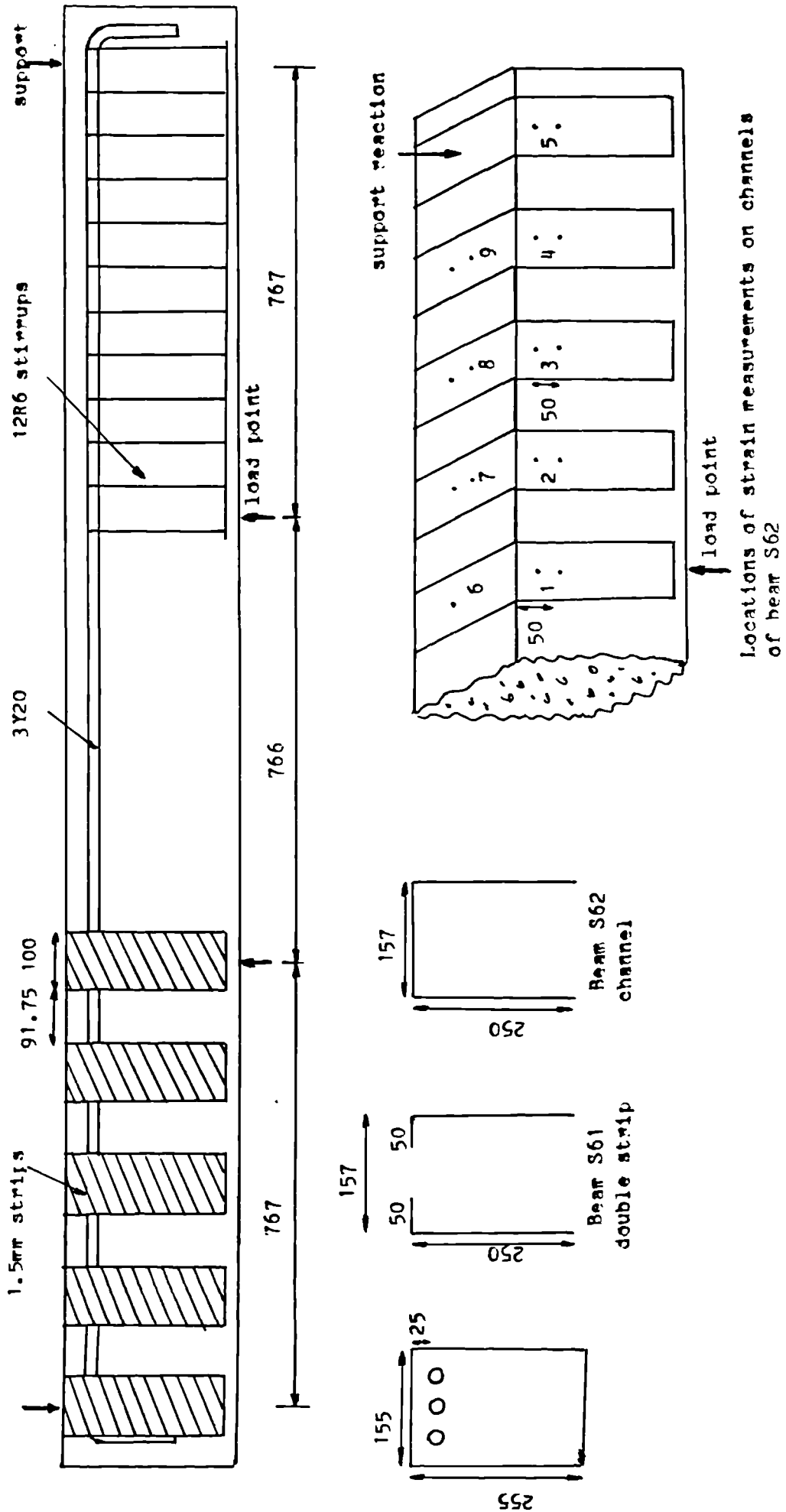


Fig.7.2: Details of beams S61 and S62 with external web steel

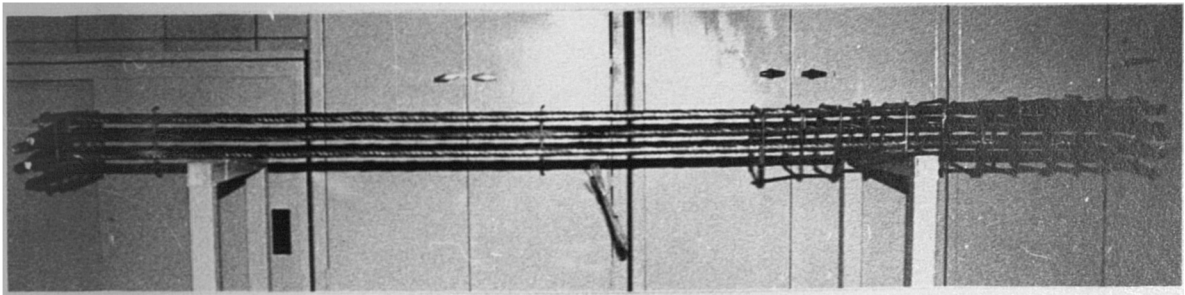
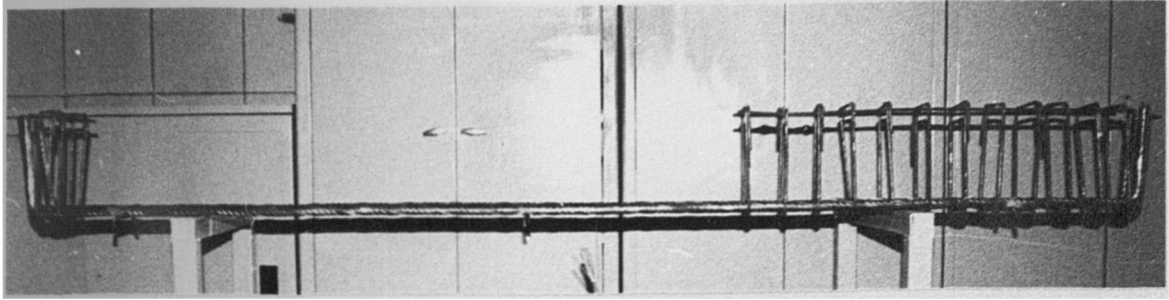


Fig.7.3: Internal reinforcement in beams S61 and S62

Table 7.1: Details of shear beams.

Beam	Shear span to depth ratio a/d	Internal web steel	Longitudinal steel plate	External web steel	Cube strength (N/mm^2)	Mod. of rupt. (N/mm^2)	Ind. ten. strength (N/mm^2)	Observations
S43	1.5	none	none	none	52.4	4.98	4.03	3 stirrups at supports
S41	3.0	"	"	"	55.6	4.93	3.37	" " "
S42	4.5	"	"	"	53.1	4.87	3.58	" " "
S53	1.5	"	1.5mm plate	"	52.0	4.41	3.44	" " "
S51	3.0	"	"	"	55.4	4.88	3.78	" " "
S52	4.5	"	"	"	55.2	4.46	3.37	" " "
S61	3.0	side A	none	side B	54.5	4.60	3.33	stirrups on one shear span and 1.5mm strips glued on the other
S62	3.0	"	"	"	52.7	4.74	3.56	stirrups on one shear span and 1.5mm channels glued on the other

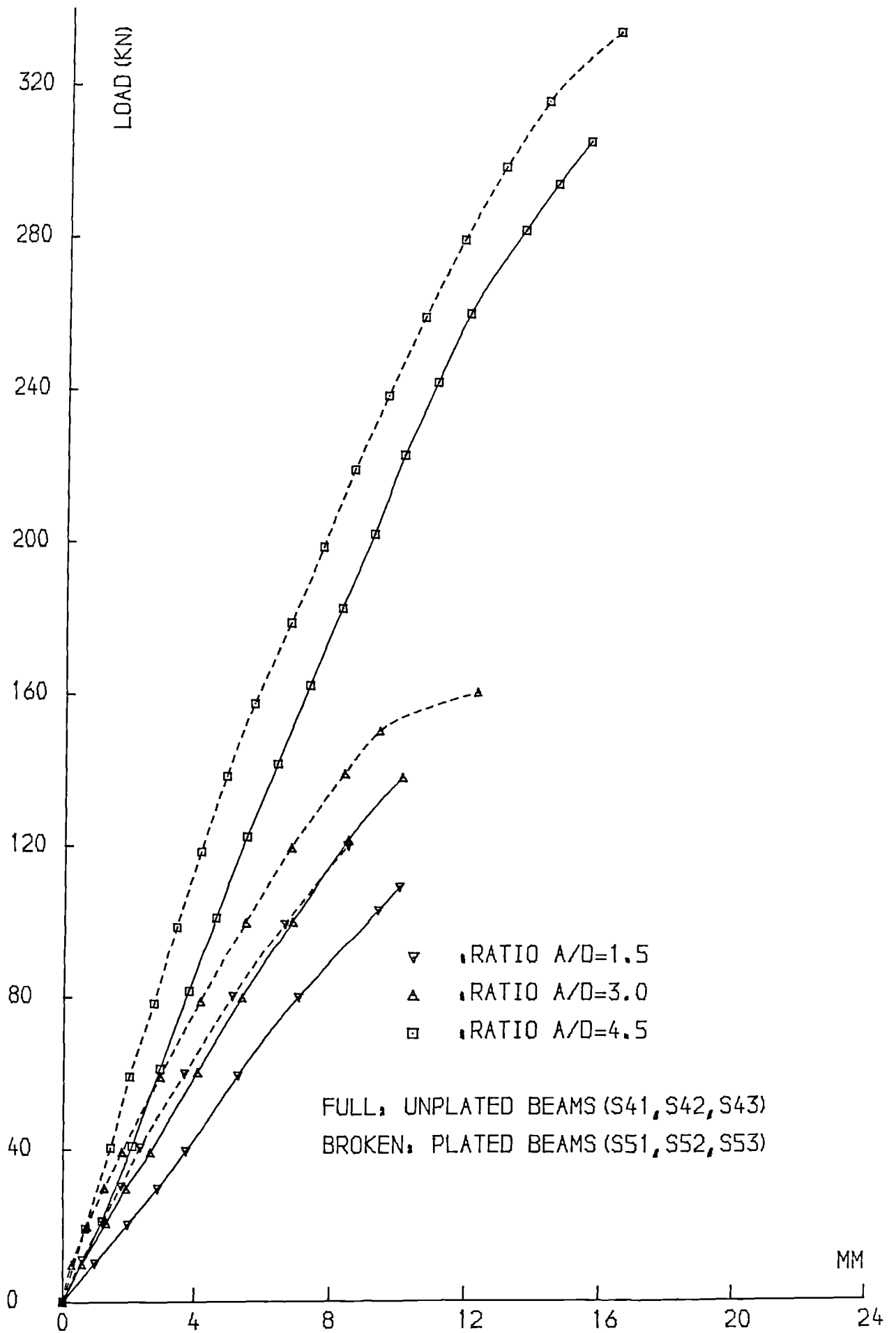


FIG.7.4 ,LOAD-DEFLECTION CURVES

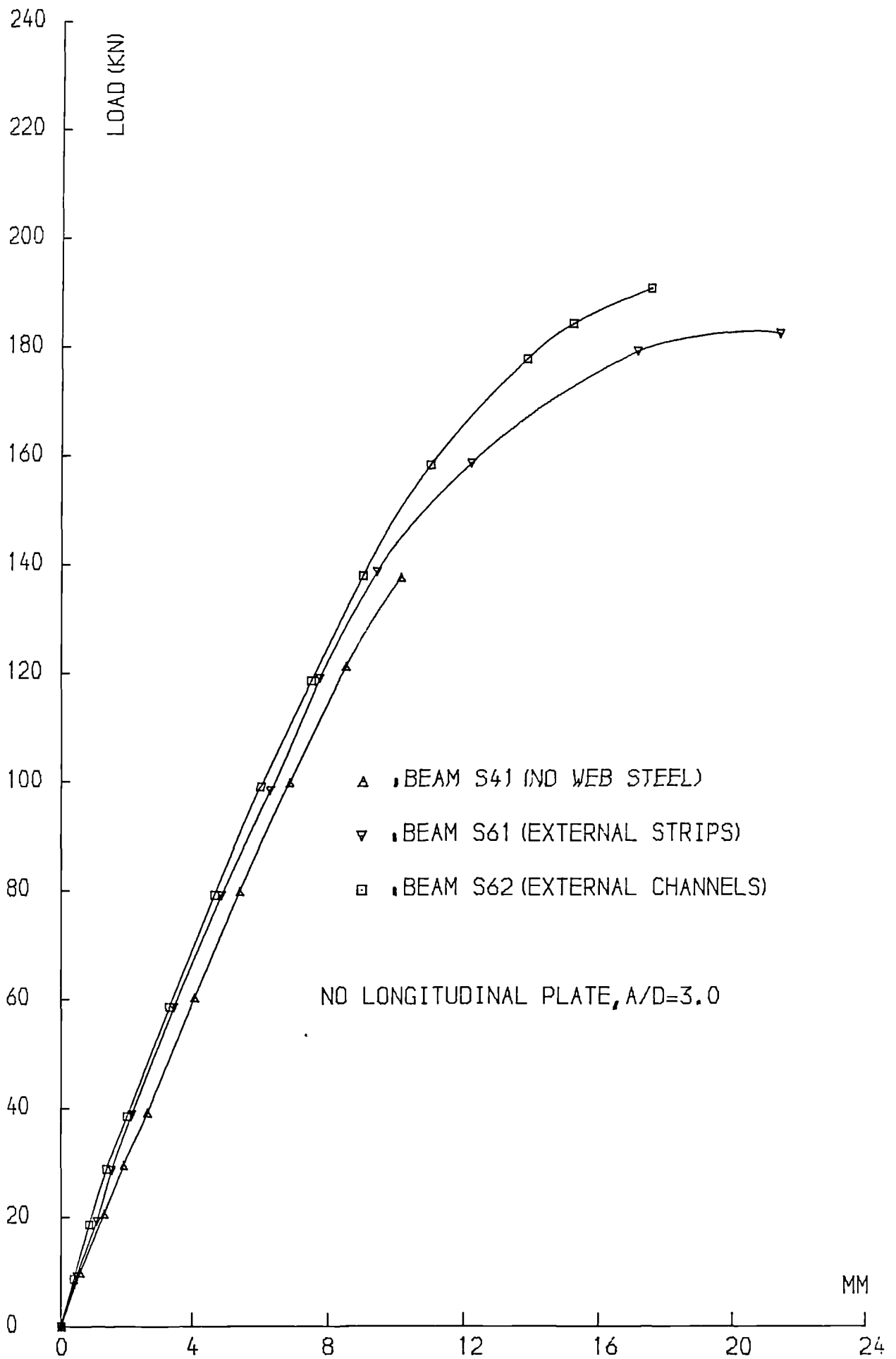


FIG. 7.5 , LOAD-DEFLECTION CURVES

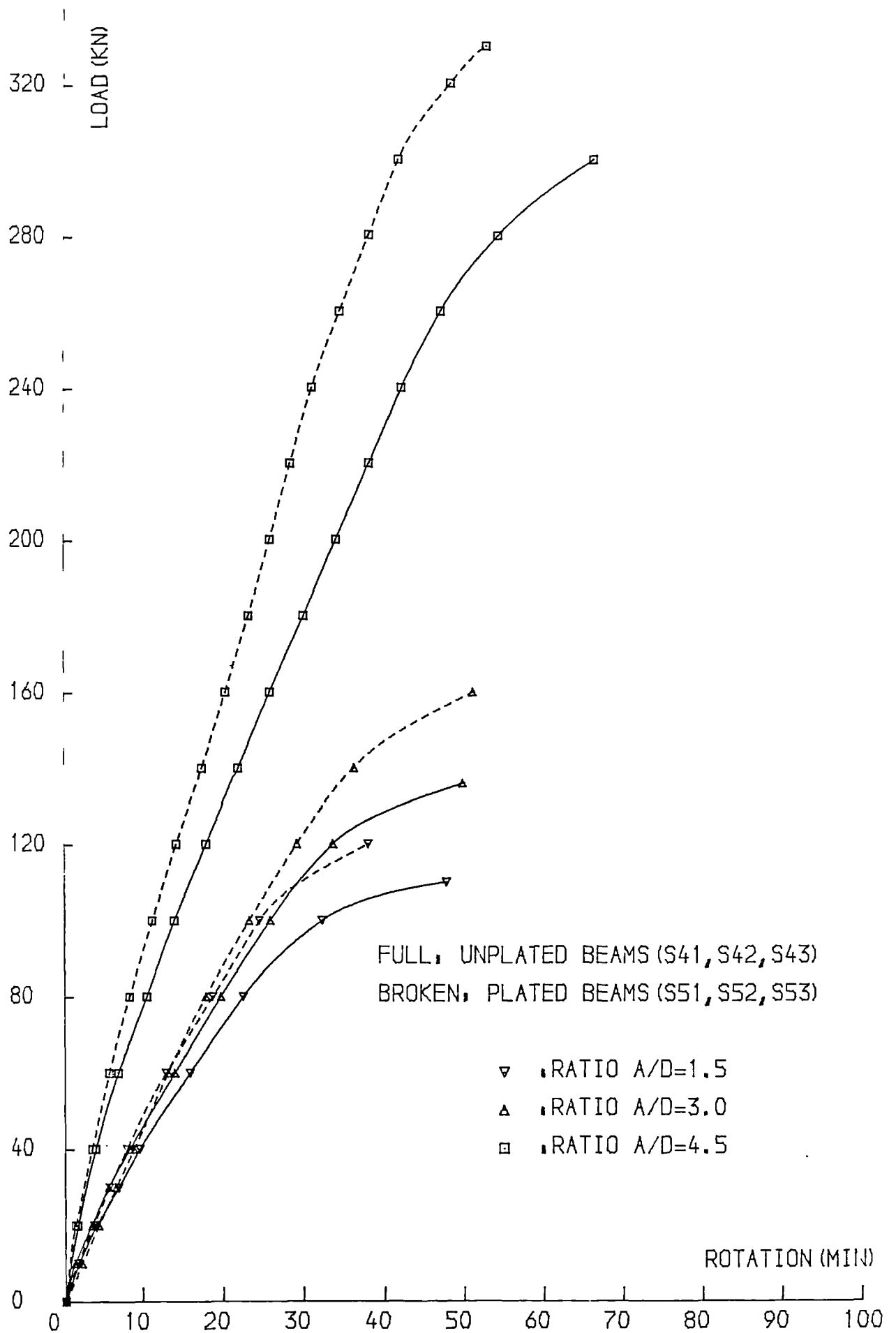


FIG.7.6 ,LOAD-ROTATION CURVES

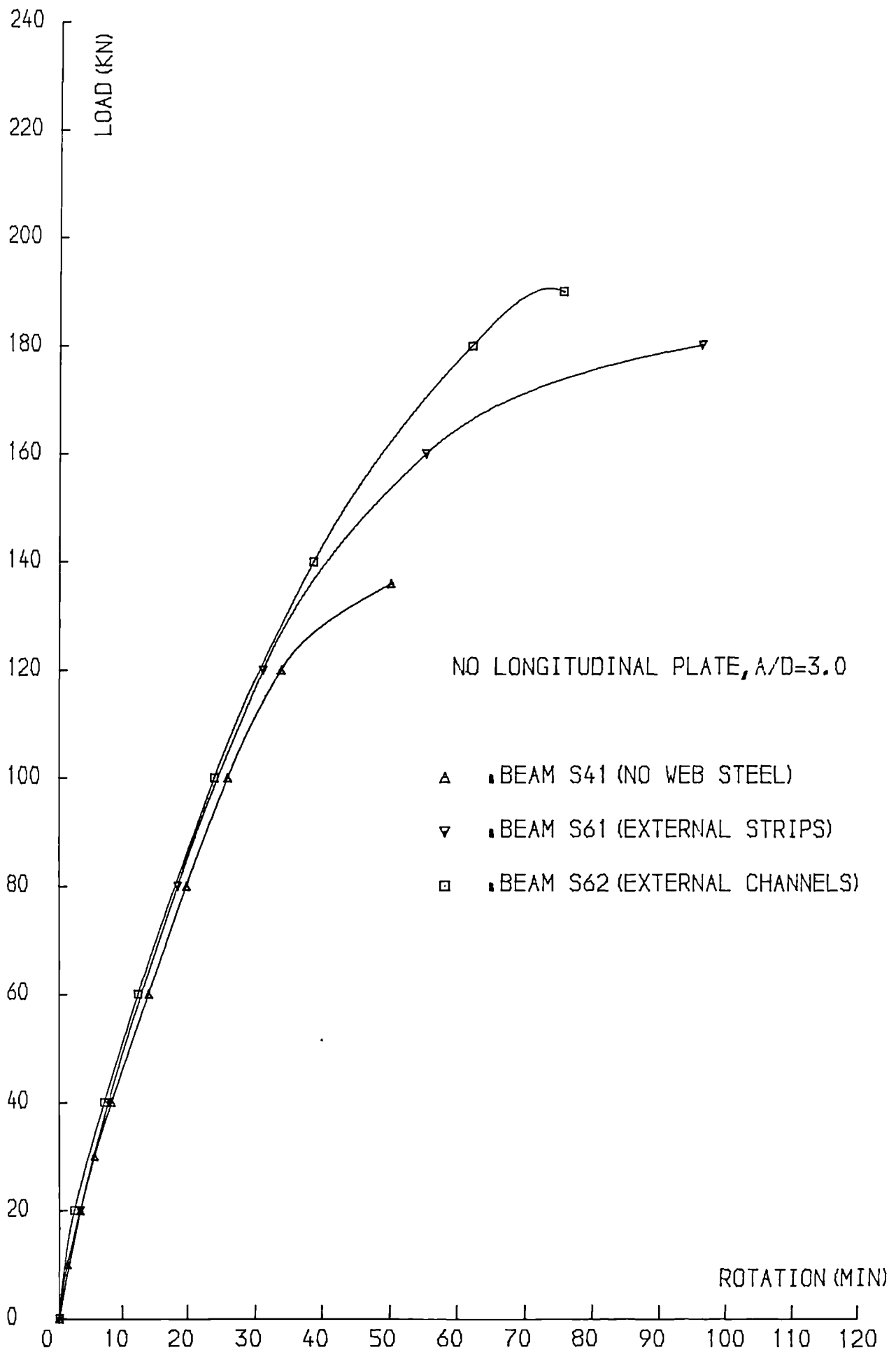


FIG. 7.7 ,LOAD-ROTATION CURVES

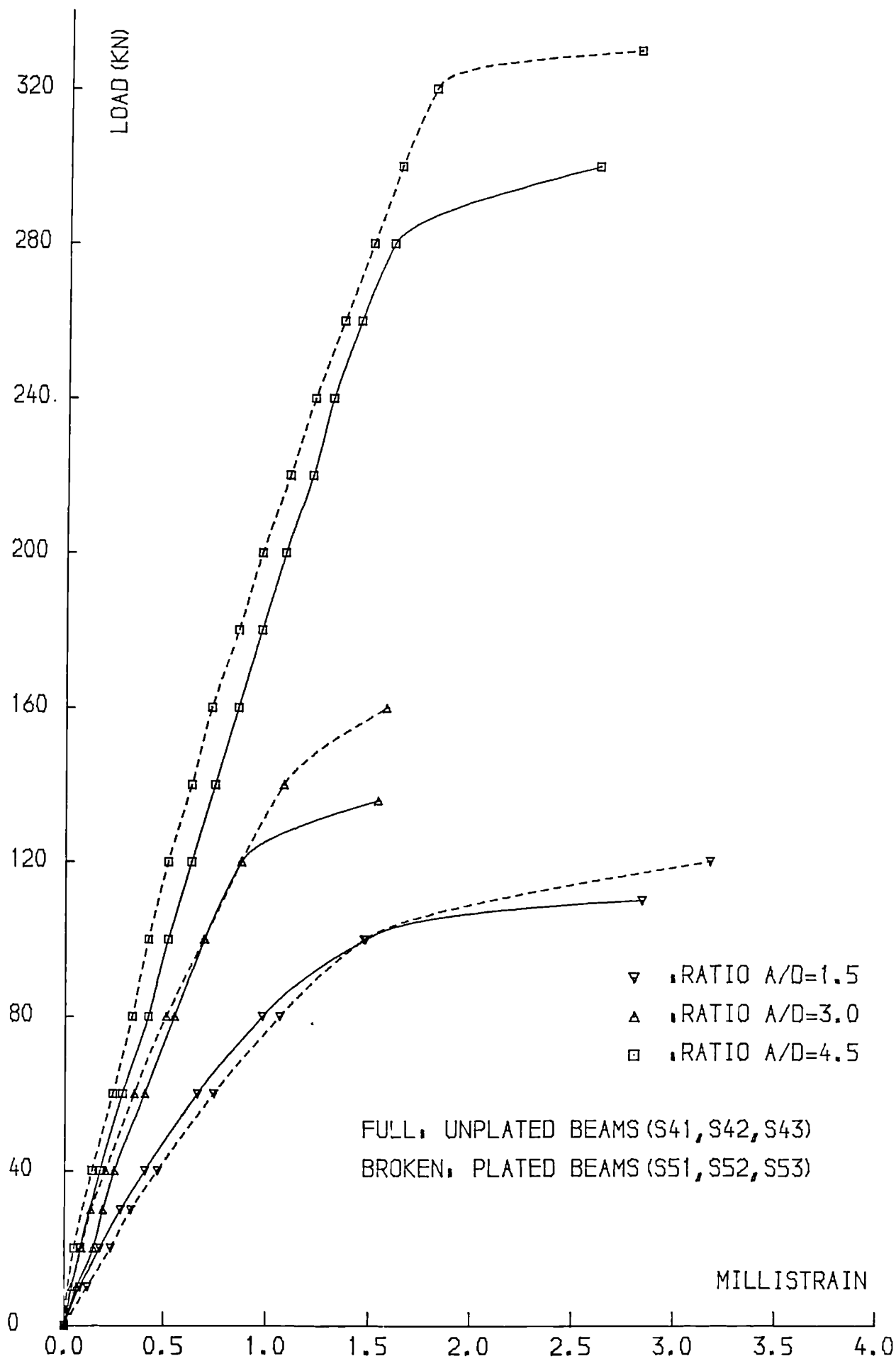


FIG. 7.8 ,LOAD-CONC.COMP.STRAIN CURVES

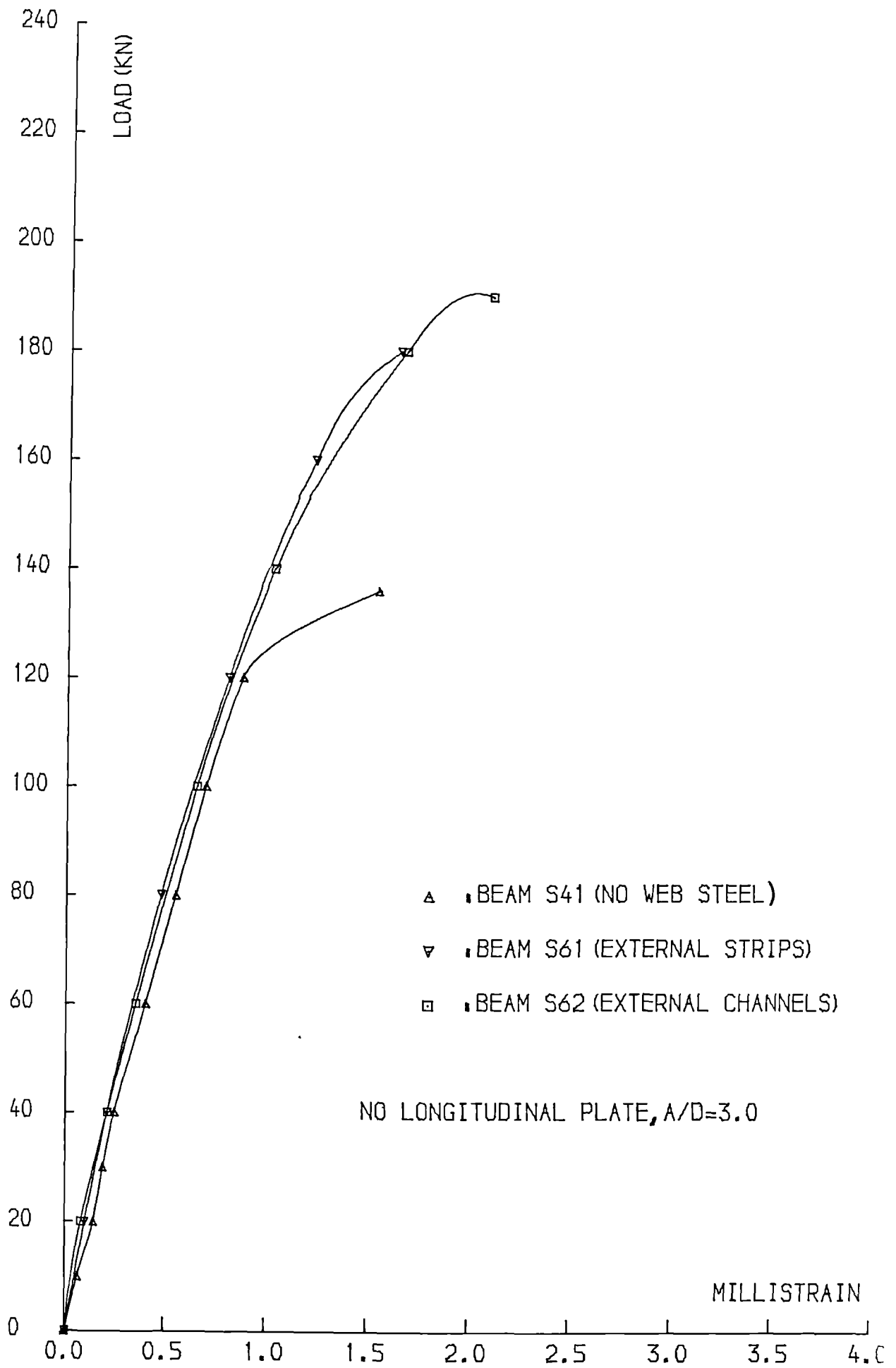


FIG.7.9 ,LOAD-CONC.COMP.STRAIN CURVES

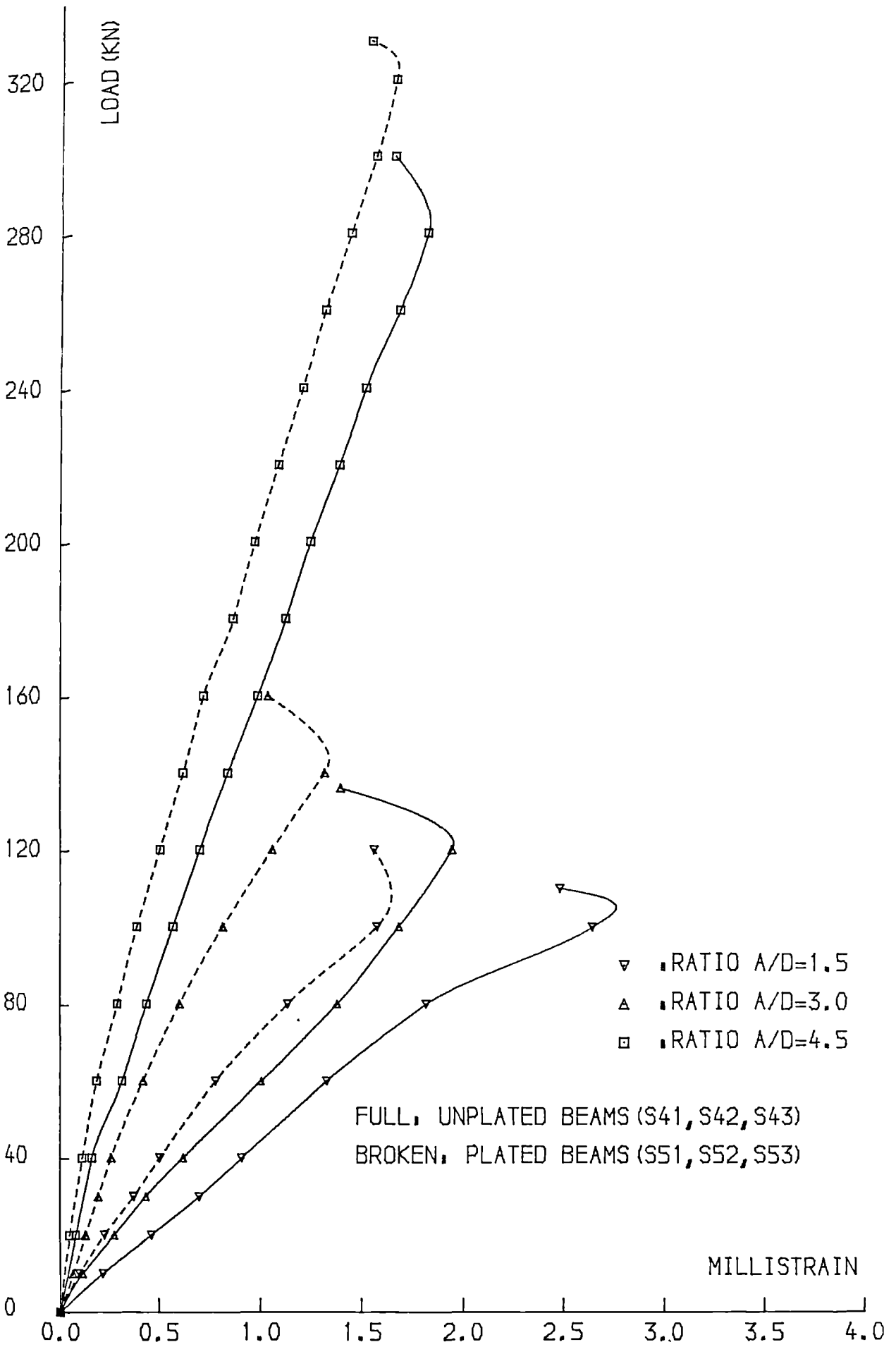


FIG. 7.10 , LOAD-CONC. TENS. STRAIN CURVES

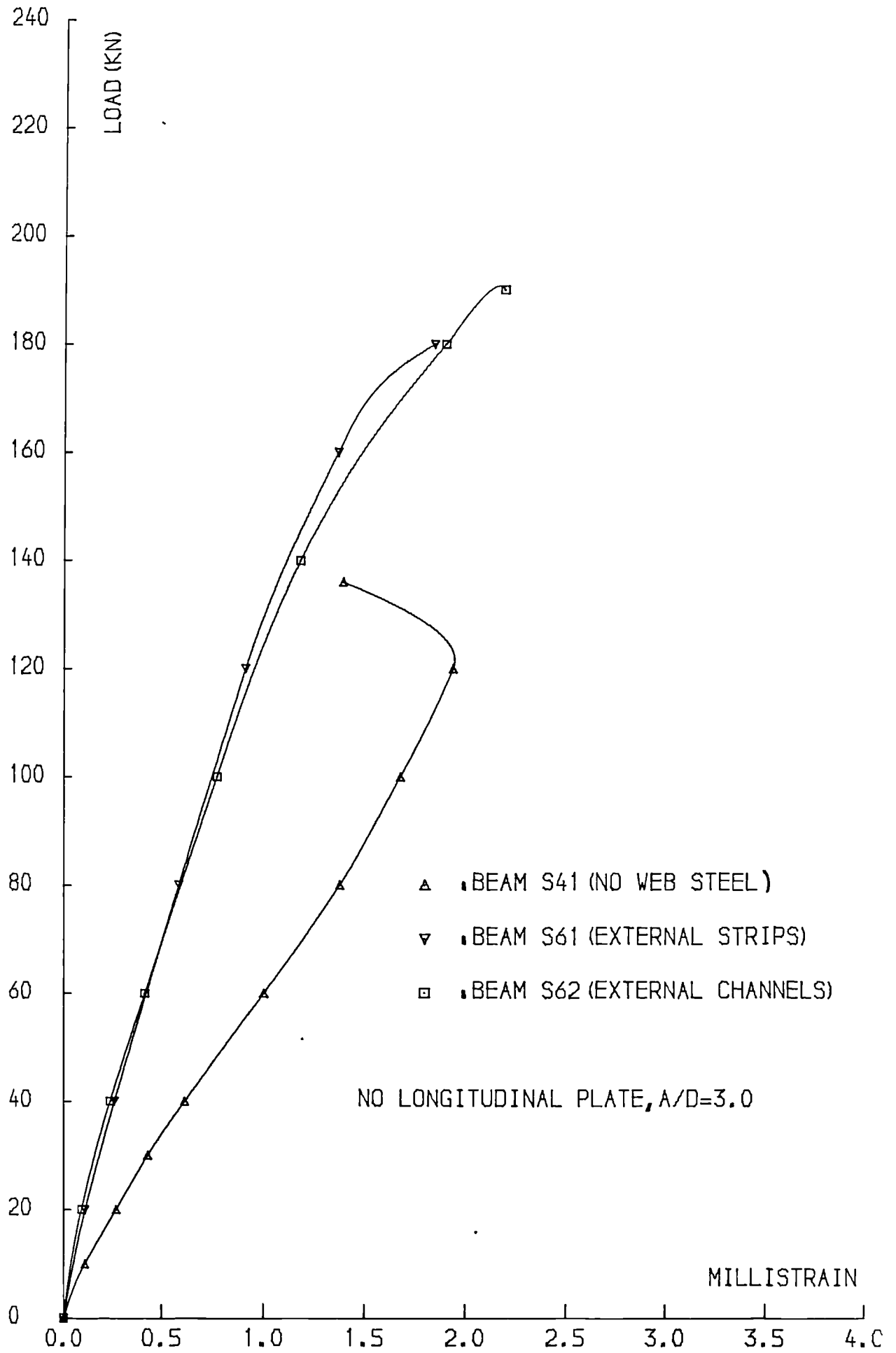


FIG.7.11 ,LOAD-CONC.TENS.STRAIN CURVES

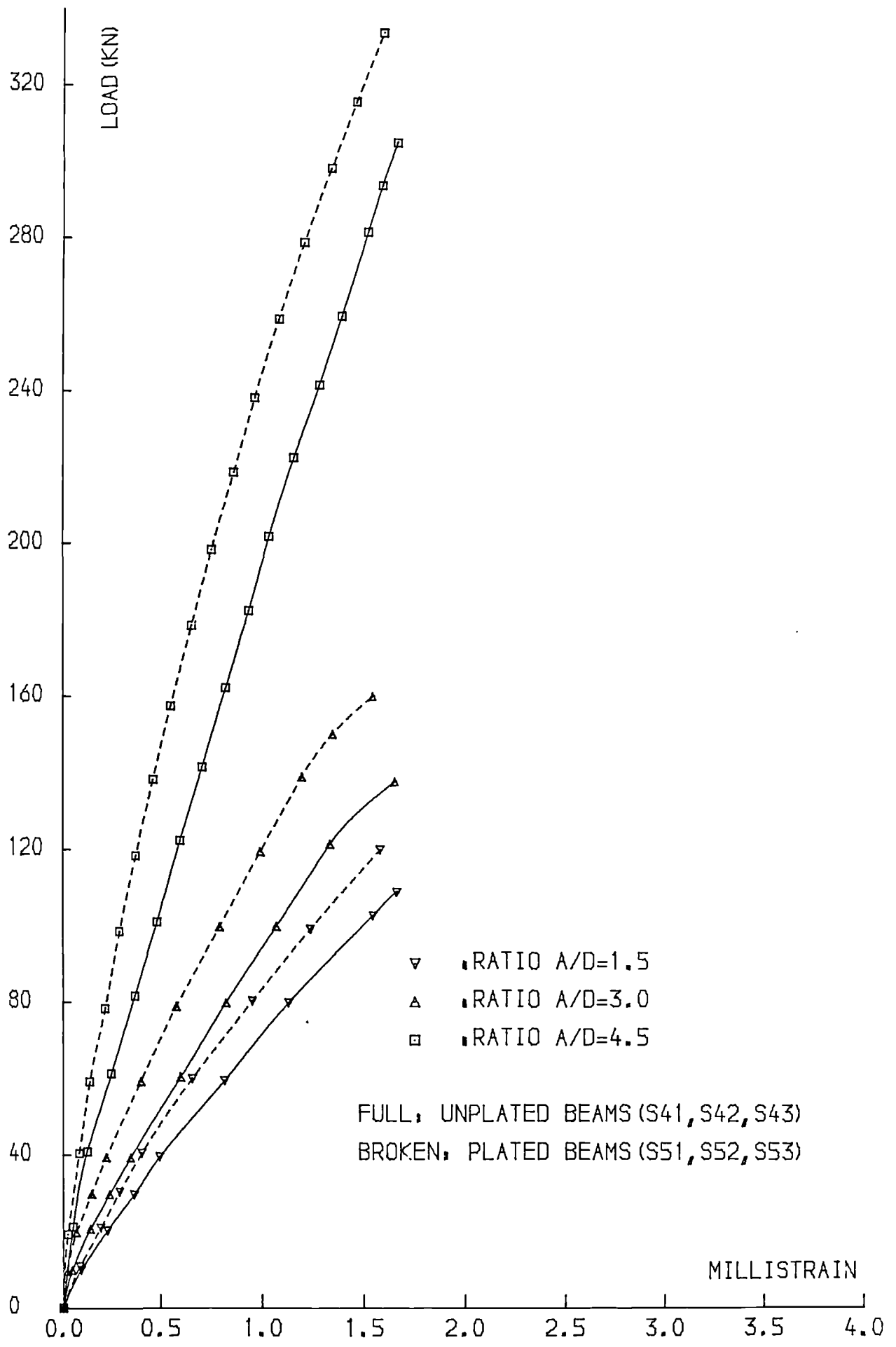


FIG. 7.12 ,LOAD-BAR STRAIN CURVES

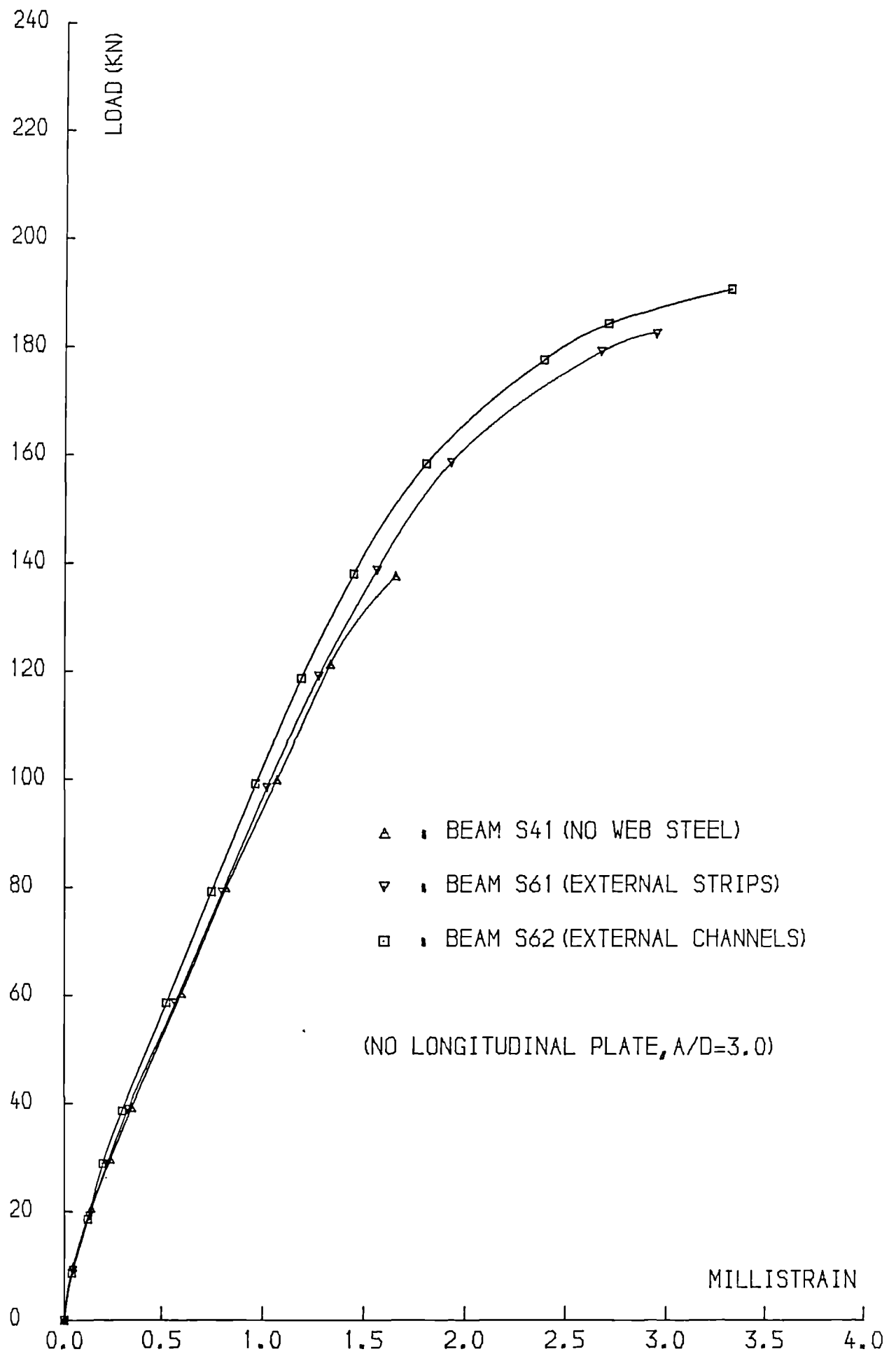


FIG.7.13 ,LOAD-BAR STRAIN CURVES

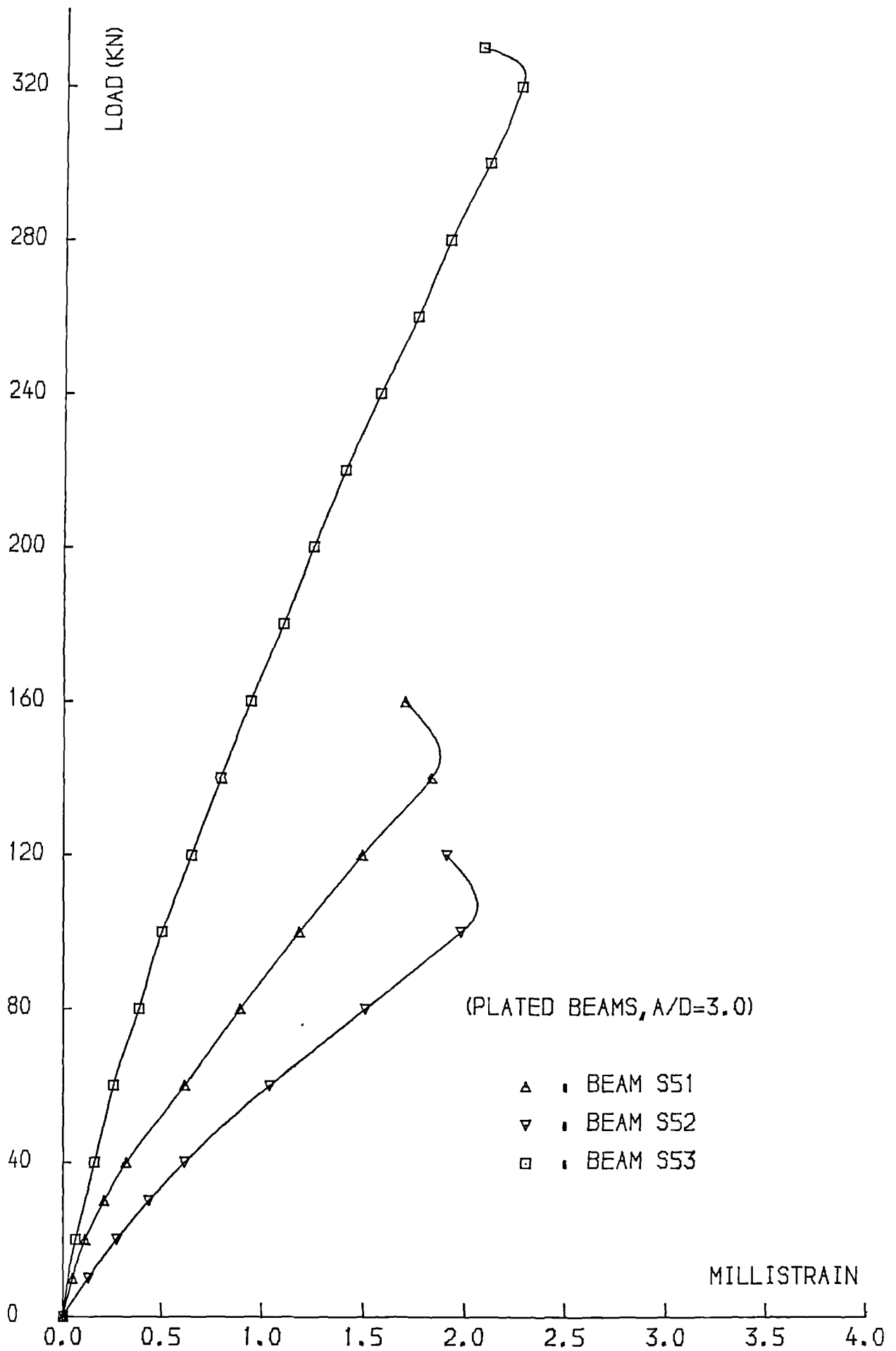


FIG.7.14 , LOAD-PLATE STRAIN CURVES

rotations, concrete and bar strains were 24.1, 10.0, 19.6% (Fig.7.6); 9.6, 16.4, 19.1% (Figs.7.8 and 7.10) and 19.5, 26.2, 37.5% (Fig.7.12) respectively. The concrete strains were measured on the vertical face across the beam depth. The compressive strain was recorded at a distance of 5mm from the compressive face and the tensile strain at 10mm from the tensile face (Fig.7.1). The tensile strain included the widths of the cracks present within the 100mm length over which the measurement was made.

The deflections, rotations, concrete and bar strains in beams S61 and S62 with shear reinforcement at a load of 100kN were 8.0 and 11.7%; 3.0 and 7.5%; 8.6 and 5.7%; and 4.7 and 9.3% lower than those of beam S41 respectively (Figs.7.5, 7.7, 7.9, 7.11 and 7.13). This increase in the flexural stiffness probably resulted from the combination of internal and external shear reinforcement effects.

The load-concrete tensile strain and load-plate strain curves (Figs.7.10, 7.11 and 7.14) show that there was a decrease in the concrete and plate tensile strains near failure. This relaxation of the tensile face of the beam was probably the result of the instability caused by the shear tensile splitting along the steel bars. This was not observed on beams S61 and S62 which had external shear reinforcement.

The maximum bar strain recorded in the beams without external web reinforcement (S41, S42, S43, S51, S52, S53) was less than the 0.2% proof value of 2000 microstrains. The maximum strain in the longitudinal steel plates (S51, S52, S53) was however greater than the yield value of 1400 microstrains. Despite a premature shear failure the bars in beams S61 and S62

reached strains of 2930 and 3350 microstrains which are greater than the proof value.

The strains measured on the external steel channels are shown in Fig.7.15. The strains were recorded by means of a 50mm demec gauge and the locations of the measurements are shown in Fig.7.2. The strains on the vertical face of the strips were similar to those recorded on the vertical face of the channels (Fig.7.15). The channels and strips did not reach their yield strain. The maximum strains recorded on the tensile face of the channels varied between 60 and 530 microstrains (Fig.7.15). The last value is much greater than the tensile strain of 100-150 microstrains at which concrete generally cracks. These high tensile strains were probably the cause of the splitting in two of the tensile face of beam S61.

7.4.1 CRACKING PROPERTIES

7.4.2.1 FLEXURAL CRACKING

The first cracks were observed visually within load increments of 5kN. The first flexural crack moments are given in Table 7.2. As for the flexural beam series (chapter five), the flexural cracking in the shear beams was initiated in the constant moment region except beams S42 and S52 with a ratio $a/d=4.5$ where the first vertical cracks appeared below the central load point. The widths, heights, spacings and propagation of these cracks were similar to those described in chapter five. The difference between the cracking of the unplated beams S41, S42, S43 and that of the plated beams S51, S52, S53 is similar to the one described in chapter five. The plates delayed the flexural cracks and reduced their size.

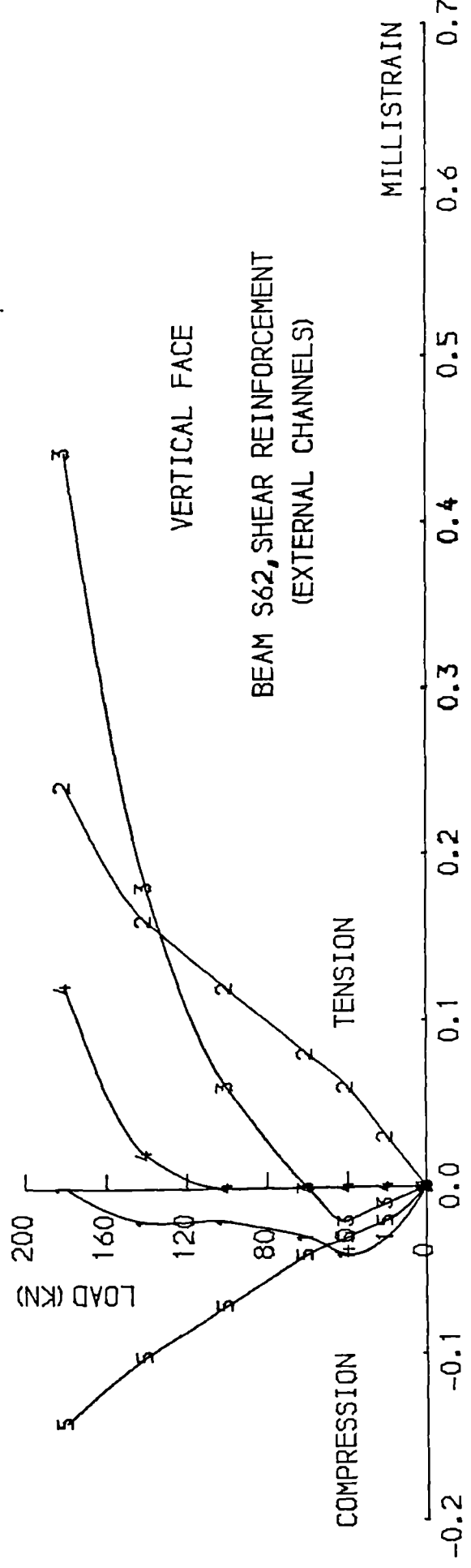
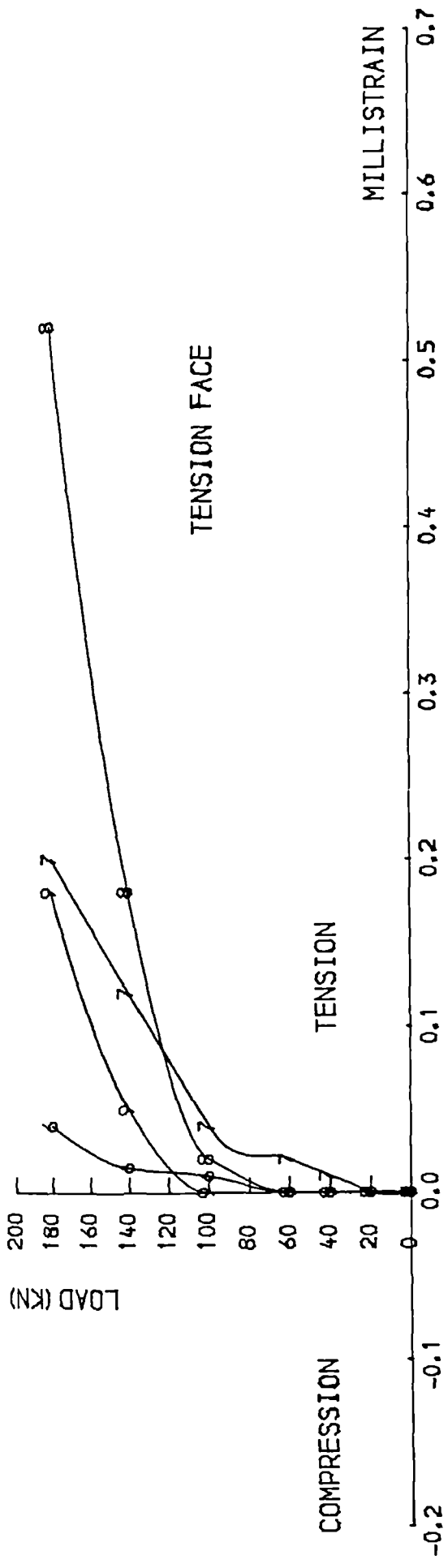


FIG.7.15 , LOAD-CHANNEL STRAIN CURVES

Table 7.2: Strength results of shear beams.

Beam	Ratio a/d	First flex.crack mnt (kNm)	First diag.crack mnt (kNm)	Exp. ult.mnt (kNm)	1 st diag. mnt over max.mnt	theor.ult. flex.mnt (kNm)	Exp/theor.	Mode of failure
S43	1.5	23.01	46.02	116.97	0.39	155.09	0.75	Diag.tens.split.and conc.crush.at load pt.
S53	1.5	30.68	46.02	128.47	0.36	174.53	0.74	" " "
S41	3.0	23.01	92.04	105.85	0.87	155.09	0.68	Diag.tens.split.and conc.crush.at load pt.
S51	3.0	30.68	92.04	105.85	0.75	155.09	0.70	" " "
S42	4.5	28.76	115.05	125.41	0.92	155.09	0.81	Diag.tens.splitting
S52	4.5	34.52	126.56	138.06	0.92	174.53	0.79	" " "
S61	3.0	23.01	107.38	141.13	0.76	155.09	0.91	Split.of tens.face between strips
S62	3.0	23.01	107.38	149.57	0.72	155.09	0.96	Diag.split.after debonding of channel

7.4.2.2 DIAGONAL CRACKING

The diagonal cracks are defined as non-vertical cracks or cracks inclined at an angle greater than 20° to the vertical. The first diagonal crack loads are given in Table 7.2. For a shear span to depth ratio $a/d=1.5$ (beams S43 and S53), the diagonal cracks formed at mid-height in the web independent of any flexural cracks. For a ratio $a/d=4.5$ (beams S42 and S52), the diagonal cracking was an extension of the vertical cracks. In beams S41 and S51 with a ratio $a/d=3.0$, the diagonal cracking was a combination of the previous two: near the load points the diagonal cracks extended from vertical ones and near the supports the diagonal cracks were initiated in the web independent of flexural cracks.

In the beams with a ratio $a/d=4.5$ failure occurred very soon after the appearance of first diagonal cracks, whereas the beams with a smaller ratio ($a/d=3.0$ and $a/d=1.5$) were able to sustain higher loading after the formation of diagonal cracks (Table 7.2). The longitudinal steel plates did not delay diagonal cracking.

In the beams with external shear reinforcement (S61 and S62), flexural cracking was similar to that of the other beams but reduced in the shear span where the external strips or channels were bonded. In beam S61, two diagonal cracks appeared in the web between the strips near the load point. As the load increased the nearest crack to the load point progressed upwards adjacent to the second strip until it reached the tensile face of the beam. There the crack moved towards the supports through the the part of the beam uncovered by the strips.

The formation of the first diagonal crack in beam S62 occurred between the second and third channels and as the load increased the crack extended and reappeared between the first and second channels.

Unlike the flexural cracks, the propagation of diagonal cracks in all beams was slow and steady at first but became rapid at high loads.

7.4.3 STRENGTH PROPERTIES

Three methods were used to compute the shear capacities of the beams. The experimental maximum shear stress, v , was calculated by dividing the recorded shear force, V , by the cross section, $b.d$, of the beam. The theoretical and experimental ultimate shear stresses thus determined are shown in Table 7.3. The values predicted by the CP110, ACI and CEB-FIP codes were multiplied by their respective safety factors. Although the ratio of cross-sectional area of shear reinforcement, A_{sv} , to the spacing, S_v , (A_{sv}/S_v) was less for the internal stirrups than for the external strips or channels, the value of A_{sv}/S_v taken into account in the equations for beams S61 and S62 was that of the external strips or channels (failure occurred in the spans with external shear steel). The cross-sectional area A_{sv} was taken equal to the product of the width of the strips or channels by their thickness. The spacing S_v was taken equal to the distance between the vertical central lines of the strips or channels.

Table 7.3: Experimental and theoretical ultimate shear stresses.

Beam	Ratio a/d	Exper.max. shear force V (kN)	Ultimate shear stress (N/mm ²)				Exp./theor.		
			Exper. v=V/bd (1)	Theoretical			(1) CP110	(1) CEB-FIP	(1) ACI
S43	1.5	152.5	3.86	1.95	2.26	1.52	1.98	1.71	2.54
S53	1.5	167.5	4.24	1.95 2.00*	2.26	1.59	2.17 2.12*	1.88	2.67
S41	3.0	69.0	1.75	1.46	1.70	1.36	1.20	1.03	1.29
S51	3.0	80.0	2.02	1.46 1.50*	1.70	1.40	1.38 1.35*	1.19	1.44
S42	4.5	54.5	1.38	1.46	1.70	1.31	0.95	0.81	1.05
S52	4.5	60.0	1.52	1.46 1.50*	1.70	1.33	1.04 1.01*	0.89	1.14
S61	3.0	92.0	2.33	4.70 2.64£	4.15 2.52£	4.14 2.40£	0.50 0.88£	0.56 0.93£	0.56 0.97£
S62	3.0	97.5	2.47	4.70 2.64£	4.15 2.52£	4.14 2.40£	0.53 0.94£	0.60 0.98£	0.60 1.03£

*: Taking into account the plate (Table 5 of CP110).

£: Using the recorded strain in the equations instead of the yield strain

7.4.3.1 CP110 CODE

Table 5 of the CP110 code (79) gives the ultimate shear stress v_u for reinforced concrete beams without web reinforcement. This value depends on the concrete grade and the amount of longitudinal reinforcement which continues at least an effective depth beyond the section considered. The code stipulates that if the shear span a is less than the twice the depth d , the ultimate shear stress v_u may be increased by a factor $2d/a$. The code also gives the requirement for shear reinforcement:

$$\frac{A_{sv}}{S_v} > \frac{b(v-v_u)}{0.87f_{yv}}$$

A_{sv} : Cross section area of web reinforcement

S_v : Spacing of shear reinforcement (S_v should not exceed $0.75d$)

v : Shear stress = V/bd (V being the shear force)

v_u : Ultimate shear stress given in Table 5 of the code

f_{yv} : Characteristic strength of shear reinforcement.

Table 6 of the code gives limit values of shear stress not to be exceeded in beams with web reinforcement.

7.4.3.2 ACI CODE

The ACI code (81) revised in 1977, proposes the following formula for the prediction of ultimate shear stresses in beams without web steel:

$$v_u = \left[1.9 \sqrt{f'_c} + 2500 \rho \frac{Vd}{M} \right] \quad (\text{psi}) \quad (Vd/M=d/a) \quad (f'_c=0.8f_{cu})$$

The code specifies that the quantity Vd/M should not exceed 1.0 and that the ultimate shear stress should be less than $3.5 \sqrt{f'_c}$.

For the beams with web reinforcement, the US code proposes the following equation:

$$v_u = \left[1.9 \sqrt{f'_c} + 2550 \rho \frac{Vd}{M} \right] + A_{sv} \frac{f_{yv}}{b \cdot S_v} \quad (\text{psi})$$

ρ is the ratio of the longitudinal reinforcement = $A_s/b \cdot d$

The quantity Vd/M should not exceed 1.0 and the ultimate shear stress should be less than $8 \sqrt{f'_c}$.

7.4.3.3 CEB-FIP CODE

The CEB-FIP model code (80) gives the following formula for calculating ultimate shear stresses in beams without web steel:

$$v_u = \tau_{Rd} k \cdot (1 + 50 \rho)$$

τ_{Rd} is a function of the concrete compressive strength and is given in Table 11.1 of the code.

$k = 1.6 - d$, d : beam depth in meters, k should be greater than 1.0

ρ is the ratio of longitudinal steel and should be less than 0.02

The ultimate shear stress may be increased by a factor $2d/a$ for beams with a shear span a less than $2d$.

The CEB-FIP ultimate shear stress for beams with web reinforcement is given

$$\text{by:} \quad v_u = \frac{A_{sv}}{b \cdot S_v} 0.9 f_{yv} + 2.5 \tau_{Rd}$$

7.4.3.4 EFFECT OF THE LONGITUDINAL PLATE

Fig.7.16 and Table 7.3 show the variation of the ultimate shear stress with the shear span to effective depth ratio a/d . The variation is similar for plated and unplated beams. The longitudinal plates increased the shear capacity of the beams by 9.8, 10.1 and 15.4% for ratios a/d of 1.5, 3.0 and 4.5 respectively.

For the beams without shear reinforcement (S41, S42, S43, S51, S52, S53), the ratio of measured to theoretical strength decreases when the ratio a/d increases and the precision of the predicting formulae of the three codes appears to vary with the shear span. The CEB-FIP code generally gave higher predictions than those of CP110 and ACI. For $a/d=1.5$ the three codes underestimated the shear capacity of the beams. For $a/d=3.0$ the predictions were more satisfactory and the CEB-FIP values were only 3% out. The CEB-FIP code however overestimated the shear strength for a ratio $a/d=4.5$ where the CP110 and ACI equations gave better results (Table 7.3).

The CEB-FIP formula does not take into account all the longitudinal steel. The amount allowed for in the equation was limited to 2%. The cross sectional area of the internal steel bars of the shear beams was equivalent to 2.38%. The formula could not therefore predict the effect of the longitudinal plate.

The ACI equation predicted an increase in the shear strength by the plate of 4.6, 2.94 and 1.53% for a/d equal to 1.5, 3.0 and 4.5 respectively.

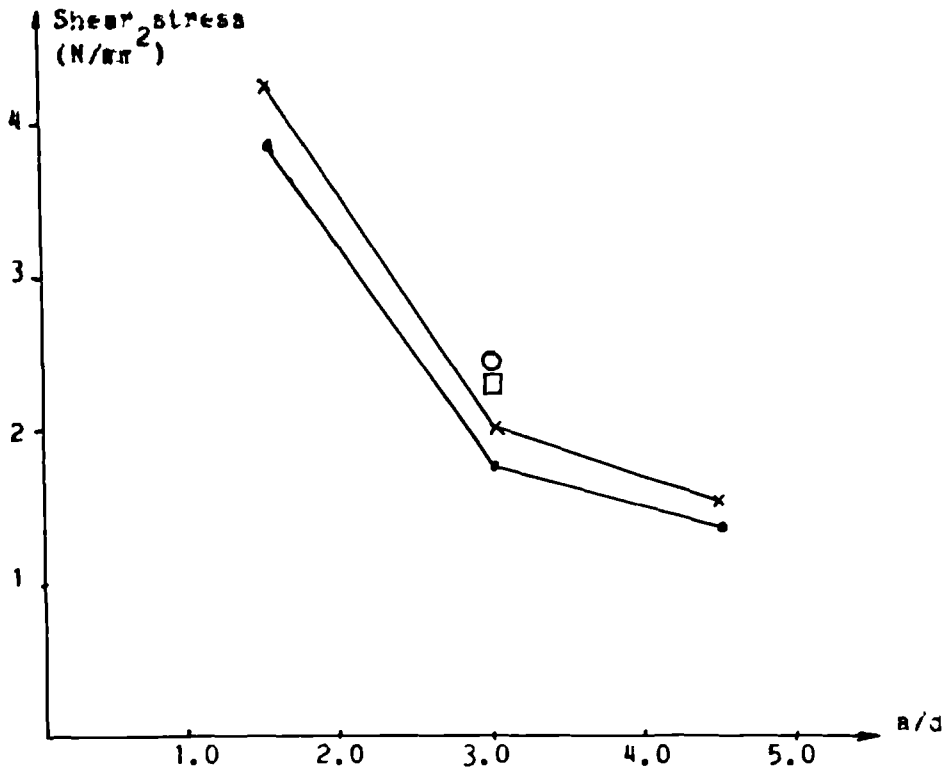


Fig.7.16: Variation of shear stress with shear span

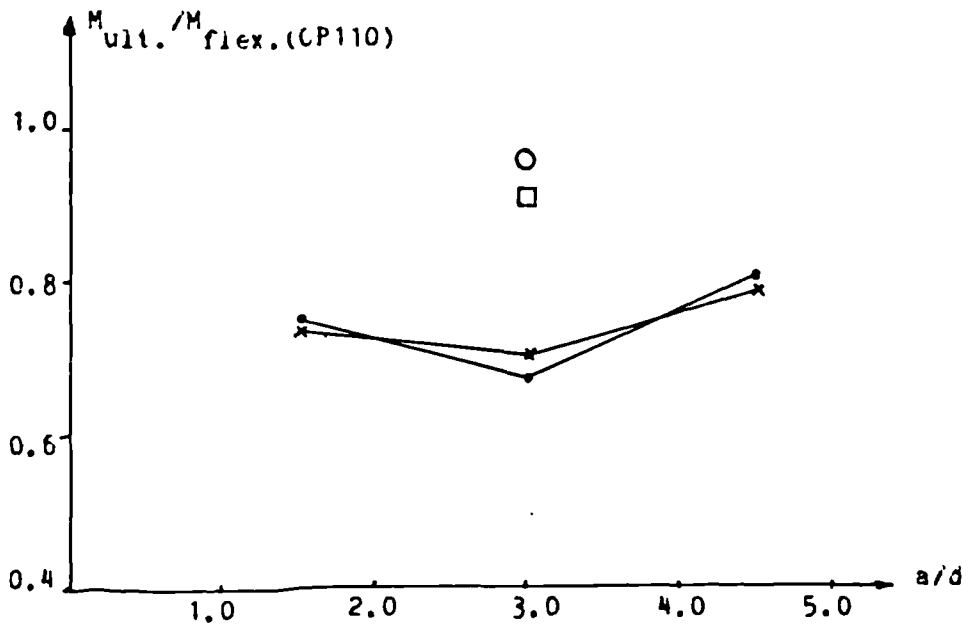


Fig.7.17: Variation of ratio of maximum to flexural moment with shear span

•: Unplated beams | without shear reinforcement
 x: Plated beams
 □: Beam S61 | with shear reinforcement
 ○: Beam S62

The same increase predicted by the CP110 code were 2.56, 2.74 and 2.74%. The code specifies however that only the longitudinal steel that continues at least an effective depth beyond the considered section should be taken into account.

The three codes underestimated, if at all, the effect of the longitudinal plates on the shear capacity of the beams. Although they did not delay the appearance of first diagonal cracks, the plates increased the shear strength of the beams by 9.8 to 15.4%, more than the codes predicted. This may be due to the presence of a dowelling action in the external steel that could be higher than that of an equivalent internal reinforcement. More tests are obviously needed to confirm such a conclusion but if the dowel action of the external plates is greater than that of an equivalent internal reinforcement (as suggested by the present results), it may be due to the greater contact area between the plates and concrete preventing the relative vertical slippage which usually follows diagonal cracking.

7.4.3.5 EFFECT OF SHEAR SPAN

The shear strength and the ultimate flexural capacity of a beam depend on the length of the shear span. The use of the ratio of maximum moment to ultimate flexural moment to study the shear behaviour of a member is a better indicator than the maximum shear strength V_u which can vary considerably with a/d (98). Fig.7.17 shows that the variation of this ratio is similar for plated or unplated beams and confirms the observations of Kani (98) who found that there was a region bounded by limiting values of ρ and a/d inside which shear failures occur and outside which full flexural strength is

attained. It was beyond the scope of this project to investigate these limiting values. The ratio of maximum moment to flexural moment for the unplated beams was 0.75, 0.68 and 0.81 for $a/d=1.5$, 3.0 and 4.5 respectively. The same ratios were 0.74, 0.70 and 0.79 for the plated beams.

7.4.3.6 EFFECT OF EXTERNAL SHEAR STEEL

The external web reinforcement of beams S61 and S62 was designed to enable the beams to reach their full flexural strength but premature failures occurred at 91 and 96% of the ultimate flexural capacities respectively before yielding of the strips and channels. The maximum shear stresses recorded in beams S61 and S62 varied between 50 and 60% of those predicted by the CP110, ACI and CEB-FIP codes (Table 7.3). This suggests that the strips and channels did not perform as well as an equivalent cross-sectional area of internal stirrups. The predicting formulae of the codes are based on the assumption that the shear reinforcement reaches 87% (CP110), 100% (ACI) or 90% (CEB-FIP) of its characteristic strength. The actual maximum strains recorded on the channels were only 37% of the yield strain. The use of the actual strains in the code equations resulted in better predictions (Table 7.3). This apparent premature failure of the external shear reinforcement as compared to internal stirrups may be due to the presence of peel forces in the joints. The external strips and channels nevertheless increased the strength of the beams by 33.3 and 41.3% respectively (as compared with beam S41). This shows that external web reinforcement can increase the shear capacity of a member but its confident use is still premature and further research is needed to determine the appropriate size, location

and spacing of the external web steel.

7.4.4 MODES OF FAILURE

All the eight beams failed in shear before reaching their ultimate flexural strength (Figs.7.18 to 7.23).

The beams with an a/d ratio of 4.5 failed by diagonal tension soon after the appearance of inclined cracks. Failure was characterized by tensile splitting along the level of the main internal reinforcement (Fig.7.20) and subsequent instability in the compression zone as the critical crack moved at an angle of about 45° towards the load point.

In the beams with a/d ratios of 3.0 and 1.5, failure occurred as a combination of diagonal tensile splitting along the main steel bars and compressive crushing of concrete near the load points (Fig.7.21). The diagonal part of the critical crack was at a distance of $1.0d$ to $1.3d$ from the load points.

Beam S61 with external strips failed by splitting of concrete cover in the tensile face between the strips (Fig.7.22). Beam S62 with external channels failed by diagonal tensile splitting resulting from the debonding of the second channel from the load point (Fig.7.23). Subsequent examination of the beam showed that the debonded channel had not been fully glued to the beam.

Failures in beams S61 and S62 were less sudden than in other beams. This ductility was the result of the presence of internal stirrups on one shear span and external web reinforcement on the other.

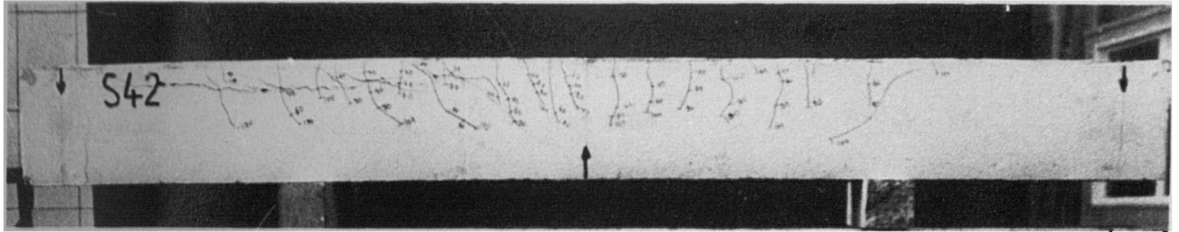
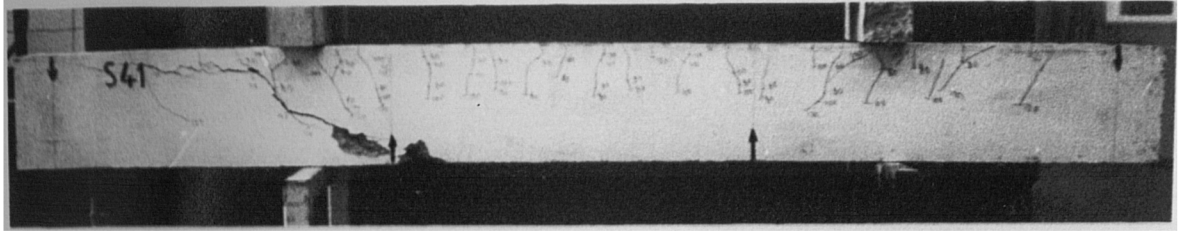


Fig.7.18: Failure of unplated beams without shear reinforcement

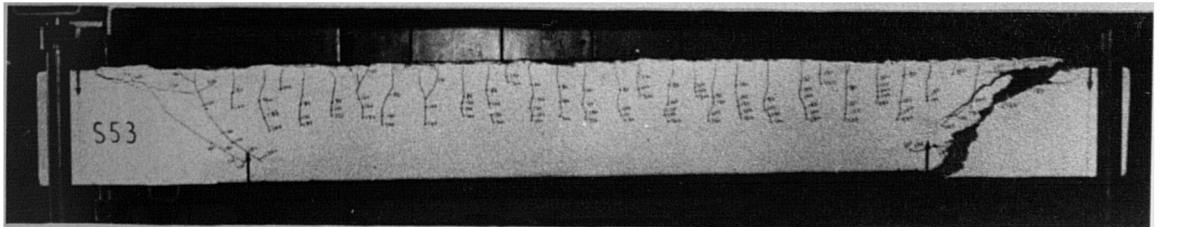
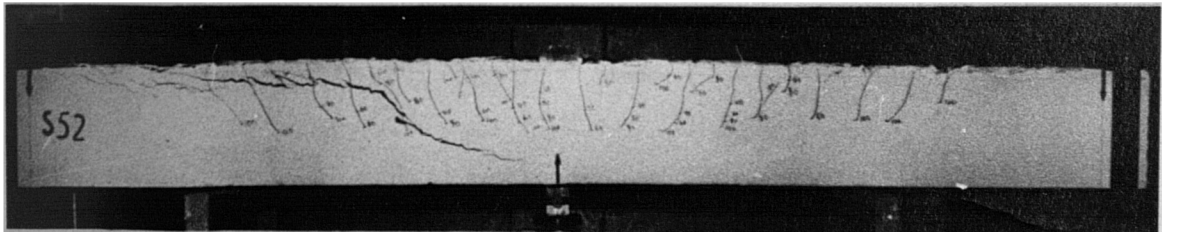
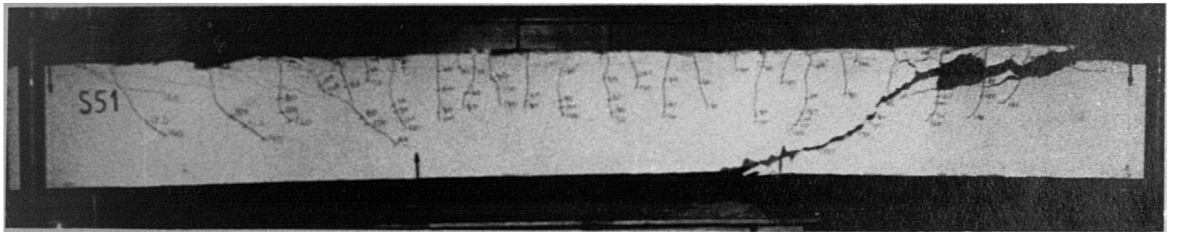
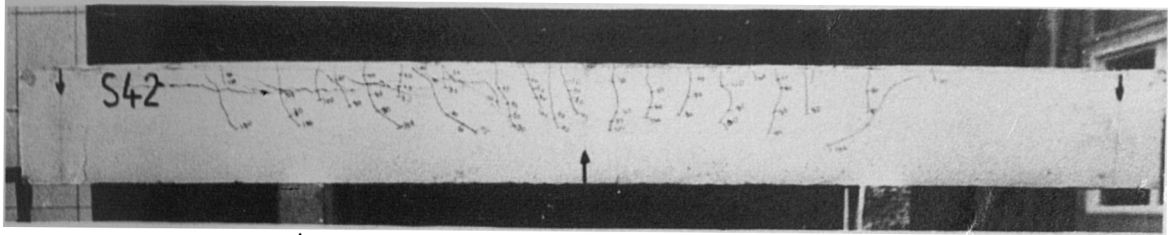
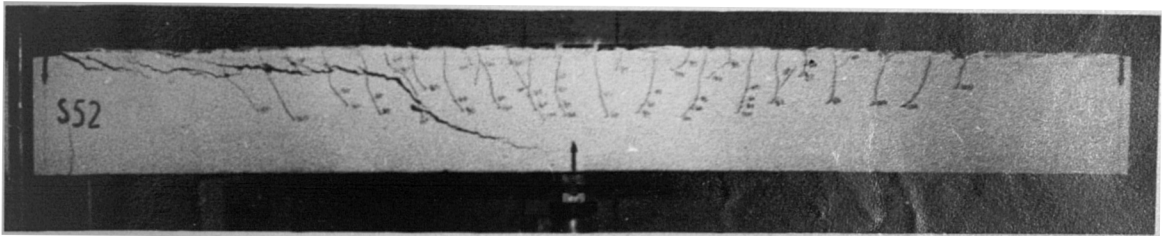


Fig.7.19: Failure of plated beams without shear reinforcement



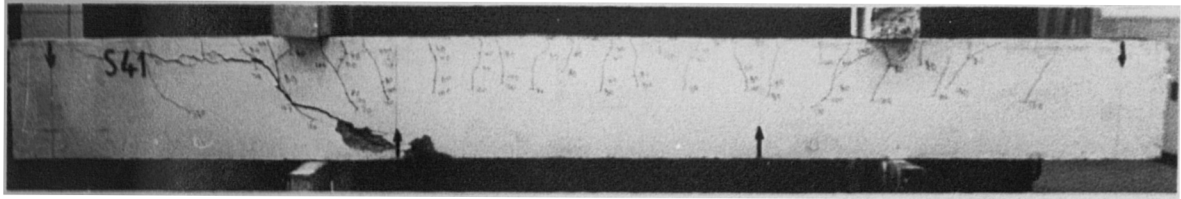
Beam S42: Unplated



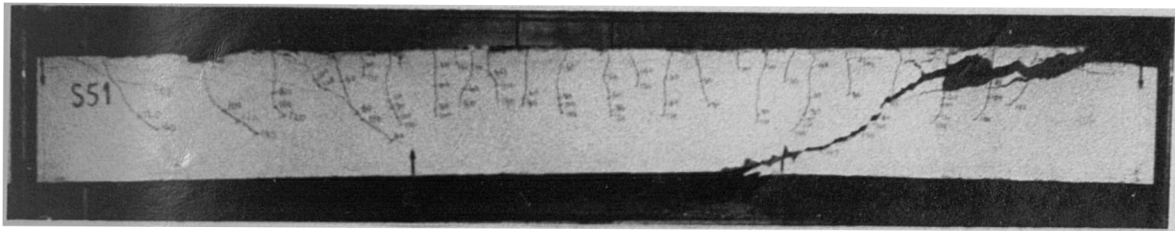
Beam S52: Plated



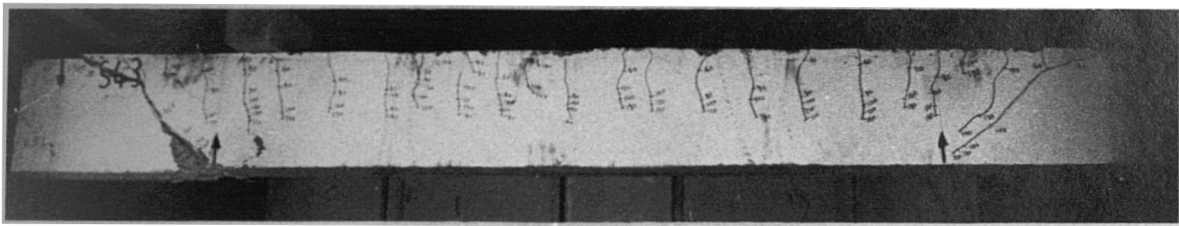
Fig.7.20: Tensile splitting along steel bars in beams with a shear span to depth ratio $a/d = 4.5$



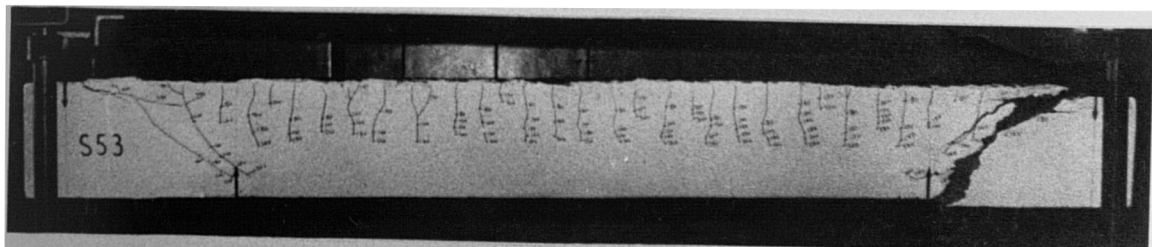
Beam S41: Unplated



Beam S51: Plated



Beam S43: Unplated



Beam S53: Plated

Fig.7.21: Combination of tensile splitting along bars and crushing of concrete near the load point in beams with a shear span to depth ratio of 1.5 or 3.0

7.5 CONCLUSIONS

As a result of composite action between steel and concrete ensured by epoxy resin, the plates bonded on the tensile face of the beams delayed the first flexural cracks, increased the stiffnesses of the beams and reduced their deformations and flexural crack propagation; and although they did not delay the appearance of diagonal cracks, they increased the shear capacity of the beams by 9.8 to 15.4%. This may be due to dowelling action from the plates opposing relative diagonal movement which usually follows inclined cracking and is partly responsible for the subsequent shear failure. This dowel force is underestimated by the CP110, CEB-FIP and ACI codes. The force may result from a larger contact area present in the external bond between the plates and concrete (when compared to conventional RC beams for which the equations were initially derived).

The external steel strips and channels glued in the shear spans of the beams as web reinforcement did not delay the appearance of first flexural cracks but reduced the deflections, rotations, concrete and bar strains by 9, 5, 7 and 7% respectively. This increase in stiffness was probably the result of a combined effect of the internal and external shear reinforcement. The strips and channels however delayed the first diagonal cracks, reduced their propagation, affected the crack pattern in the shear span and increased the shear capacity of the beams by 33 and 41% respectively. Although designed to develop full flexural strength, the beams with external web steel failed prematurely at 91 and 96% of their ultimate flexural capacities. The strips and channels reached

37% only of their characteristic strength. The use of the recorded strains in the equations of the CP110, ACI and CEB-FIP codes gave satisfactory predictions of the ultimate shear stresses.

From the limited number of shear tests in this series the following conclusions may be drawn:

1- Dowel action in the external plates may be more important than in an equivalent internal reinforcement. The plates did not delay the diagonal cracking but increased the shear capacity.

2- Shear reinforcement in the form of externally bonded steel strips or channels can improve the shear strength of the beams but may cause premature failures as compared with an equivalent internal web reinforcement in the form of stirrups. More research is therefore needed to investigate the desirable geometry of the strips and their optimum thickness and spacings.

CHAPTER EIGHT
LONG TERM BEHAVIOUR OF PLATED BEAMS

8.1 INTRODUCTION

All reinforced concrete structures are subject to time dependent deformations due to creep and shrinkage. Creep and shrinkage are long term deformations influenced by many parameters (117-127) and greatly affected by the amount and fineness of cement paste and the relative humidity of the environment. While creep is a deformation directly resulting from the application of a sustained load on the specimen and is usually proportional to the applied stress (117), shrinkage is a deformation caused by the contraction of the material. Shrinkage is a feature of all paste composites and results from the loss of moisture as the specimen dries out and matures. Drying shrinkage depends on the amount of material used, the ambient temperature, the humidity of the atmosphere and other environmental conditions. Alternative wetting and drying of a concrete member will cause a 'moisture movement' and result in corresponding expansions and contractions. The total deformation in a structure sustaining a constant load includes the instant elastic strain (directly resulting from the application of the load), creep, and shrinkage. While the recording of the instant elastic strain is a straightforward operation, the isolation of the other components requires careful attention. To deduce the creep strain from the total deformation, the shrinkage and total deformations must be measured separately on similar members of the same age and

exposed to the same environmental conditions.

Creep and shrinkage deformations in concrete are generally accelerated at high temperatures at any age up to fifty years (125) and are lower with larger specimens (126). Creep is reduced if the specimen is older at loading.

These long term deformations increase almost linearly with the logarithm of time (119,120,123) and may become critical to the serviceability and safety of the structure. Furthermore, the thermal movement due to cement hydration could cause cracking of the members.

In the case of reinforced concrete structures strengthened by externally epoxy bonded steel plates, the risk to the serviceability and safety of the structure is increased further by the presence of the external joint concrete-epoxy-steel. Epoxy resins are visco-elastic materials where the time dependent deformations under a sustained stress can be considerable. In addition, the moisture movement may cause migration of humidity from concrete through the joint to the external steel and could result in metal corrosion or loss of adhesion and subsequent loss of bond strength.

This chapter describes the time dependent deformations recorded in plated beams after a period of 47 months and the effects of exposure to severe environmental conditions on the beams and the concrete-epoxy-steel joints. It is an extension of the study reported by Bloxham (34) who started the programme.

8.2 EXPERIMENTAL INVESTIGATIONS

8.2.1 EXPERIMENTAL PROGRAMME

The long term behaviour of plated beams was first investigated by Bloxham (34) and was part of his study programme. This part of the present project is only an extension of the recorded time dependent deformations over a longer period of time.

The experimental programme included eight beams subjected to sustained loading, sixteen unloaded beams and twenty four 100x100x500mm prisms. All the beams were plated with one or two 1.5mm thick plates (Table 8.1). Unfortunately, no shrinkage beam and no unplated beams were included in the original programme. The deduction of the creep deformations from the total deformations would be very difficult as no shrinkage deformations were measured at the same time and the assessment of the long term performance of the plated beams is limited as no unplated beams were studied for comparison.

The concrete used was that of mix 5 as described in chapter three. The weight ratios of the mix are:

1 : 1.04 : 2.44 : 0.39 : 0.28

Cement : Sand : Gravel : Water : Febflow

Rapid hardening cement and 19mm maximum size uncrushed gravel were used.

The manufacturing of the beams, their dimensions, internal reinforcement, the glue, steel plates and the bonding procedure were all identical to those described in chapter five.

Table 8.1: Details of long term beams

Beam	101	102	103	104	105	106	107	108	109	110	111	112	113	114	115	116	117	118	119	120	121	122	123	124
Glue thick. (mm)	3	6	(1) 2-8	(2) 3	3	3	3	3	3	6	(1) 2-8	(2) 3	3	3	3	3	3	6	(1) 2-8	(2) 3	3	3	3	3
Plate thick. (mm)	1.5	1.5	1.5	1.5	1.5	1.5	1.5	1.5	1.5	1.5	1.5	1.5	1.5	1.5	1.5	1.5	1.5	1.5	1.5	1.5	1.5	1.5	1.5	1.5
No. of plates	1	1	1	1	1	1	2	2	1	1	1	1	1	1	2	2	1	1	1	1	1	1	2	2
Lap						cen.	cen.	l.p.					cen.	l.p.	cen.	l.p.					cen.	l.p.	cen.	l.p.
Age (5 months)	18	18						18																
Cube strength (N/mm ²)	66.4	63.2	68.5	65.5	76.8	76.4	65.0	77.0	70.5	69.2	78.5	73.3	73.0	74.5	72.2	80.2	80.4	71.2	81.2	80.6	69.2	79.1	79.1	81.1
Mod. rup. (N/mm ²)	80.0	76.6	78.3	78.3	80.3	81.7	78.3	80.6	77.8	83.0	86.0	78.4	78.4	82.2	86.4	85.3	83.2	82.2	86.8	83.4	77.7	79.4	81.5	86.9
	86.3	89.0					86.6																	
	5.85	5.92					5.73																	

(1): Glue thickness varies along the joint from 2 to 8mm

(2): V notches cut in tension face of the beam at load points

(3): At 28 days

(4): At strengthening

(5): At testing

UL: Unloaded

L: Loaded

cen.: Lap in the center

l.p.: Lap in the left half

The prism tests were designed to study the effects of various sealing agents on the durability of the concrete-epoxy-steel joints under dry and moist conditions.

8.2.2 LOADING APPARATUS AND TEST MEASUREMENTS

The beams sustaining constant stress were loaded at 28 days and then kept in the laboratory for a further four months. The loaded and unloaded beams were then transported to their sites where they were left exposed to severe external weathering conditions at a sewage treatment works.

The details of the long term beams are summarized in Table 8.1. The beams were loaded by means of steel frames made up by Macalloy tie bars and a spreader beam. The beams were placed in rigs as shown in Figs.8.1 and 8.2. Each loading frame was designed to take two beams. The total load applied on each beam was 100kN and was determined to be equivalent to a maximum stress in the concrete equal to one third of the 28 day cube strength. Control cubes and prisms were kept exposed under the same conditions. The load was monitored by means of a hydraulic jack positioned at one end of the loading frame (Fig.8.1). To ensure that the total load was applied symmetrically and correctly, the extensions of the Macalloy steel bars were controlled by mechanical measurements by means of a 300mm demountable demec gauge extensometer. However, as a result of corrosion in the unprotected steel tie bars, the demec points fell off after a few months. The accuracy of the load given by the pressure gauge attached to the pump operating the loading jack was affected further by the friction in the bolts caused by corrosion.

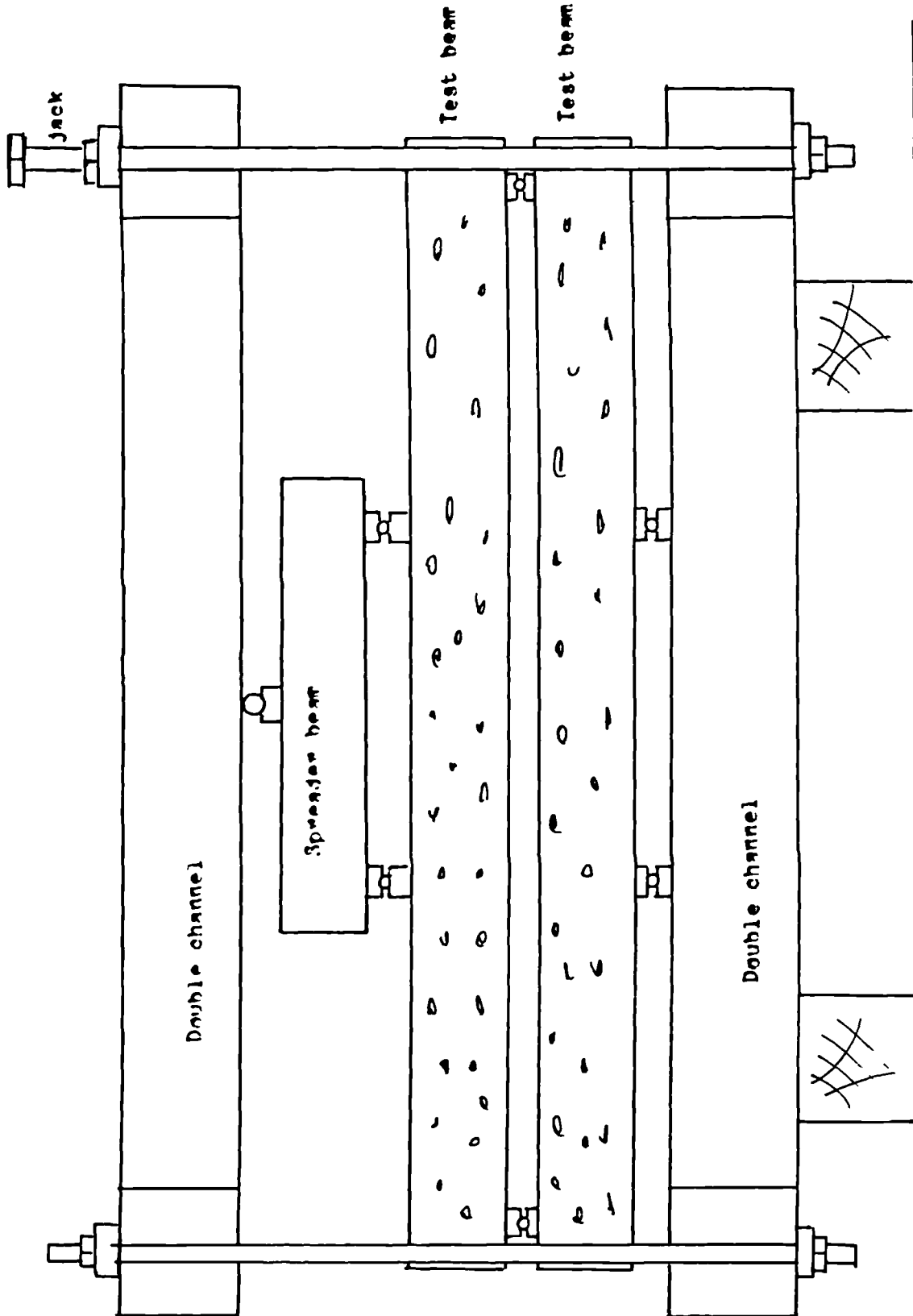
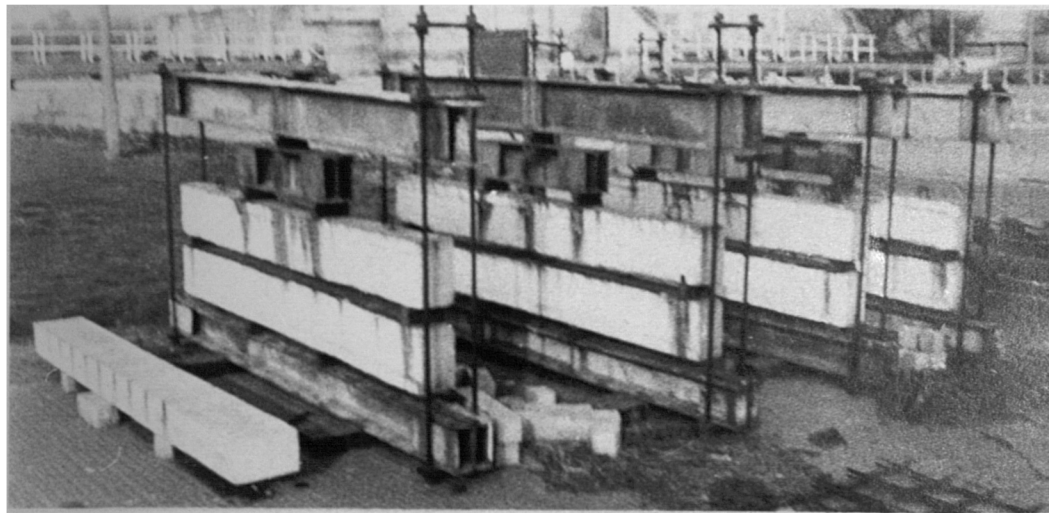
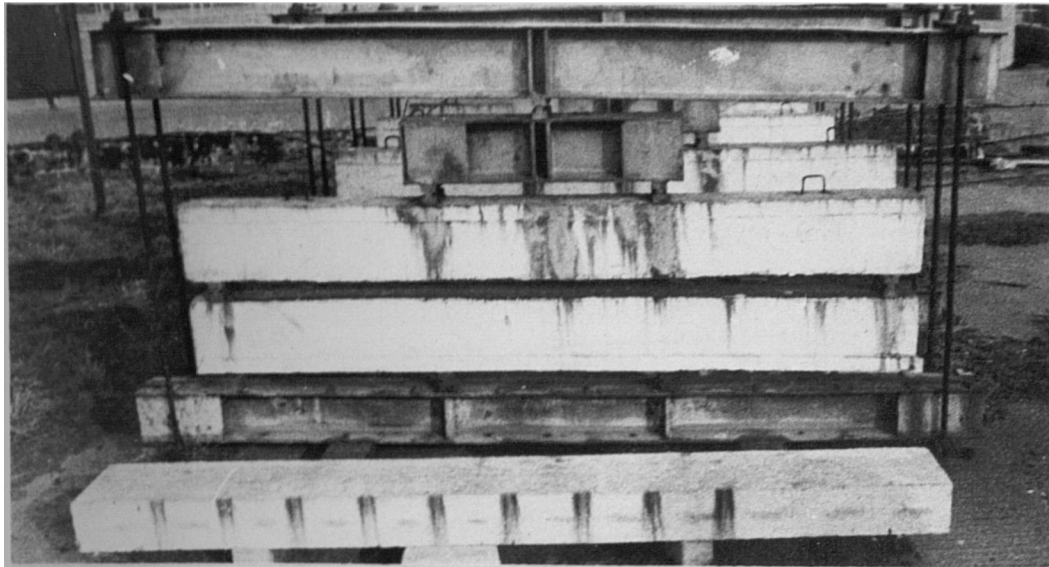
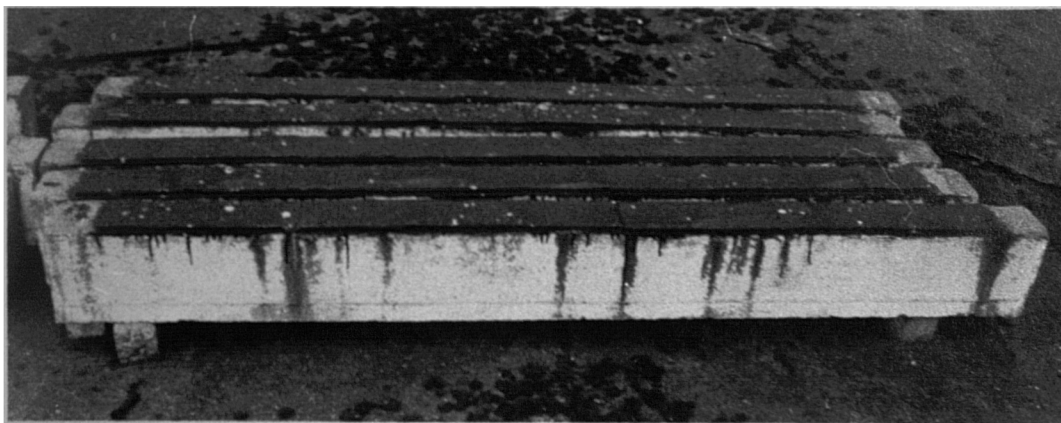


Fig. 8.1: Long beam loading rig



Shrinkage and creep beams



Unloaded beams

Fig.8.2: Long term beams

The concrete strains at different locations in the middle section across the beam depth were measured at regular time intervals using a demec extensometer of 203.2mm (8 inches) gauge length. The deflections, rotations, steel bar and plate strains were not measured.

Shrinkage deformations were initially measured on 100x100x500mm prisms (34) but it was subsequently decided to cast another beam to take into account the effects of the reinforcement and the specimen size on the shrinkage. The time scale was unavoidably different from that of the creep beams. The strains on the shrinkage beam were measured throughout the length on the compressive and tensile faces and across the beam depth.

For the various reasons mentioned before, the information yielded by these tests will be considerably restricted. The shortcomings of the tests are:

(1) Loading:

The load was not adjusted regularly before each strain reading in the first few weeks and the recorded deformations cannot be very reliable. The accuracy and symmetry of the loading was affected by the corrosion and subsequent friction in the unprotected metal elements of the apparatus.

(2) Test measurements:

Only concrete strains across the beam depth were recorded. No bar or plate strains and no deflections, rotations or crack widths were measured.

(3) Shrinkage beam:

The shrinkage beam was not cast at the same time with the creep beams. Although the variation of shrinkage and total deformations with time can be determined separately, it will be practically impossible to deduce the creep deformations as the beams did not have the same environmental history. The environmental conditions that the creep and shrinkage beams were exposed to at the same age were different. The deformations caused by the moisture movement (due to the variation of the humidity of the atmosphere and other environmental conditions) were therefore different.

(4) Unplated beam:

The consequences of the previous negligences would have been minimized had the experimental programme included unplated beams. The total deformations of unplated and plated beams sustaining constant load and exposed to the same conditions would have produced some useful comparative information between the long term performance of plated and unplated beams.

As a consequence of these unfortunate negligences, valuable information was lost and the usefulness of the results was therefore very limited.

8.3 DISCUSSION OF RESULTS

The results of the long term investigations including a summary of those of Bloxham are presented in the following sections.

8.3.1 DURABILITY

The durability of concrete-epoxy-steel joints was investigated by long term tests on unloaded and plated prisms and beams.

8.3.1.1 PRISM TESTS (BLCXHAM'S RESULTS)

Twenty four 100x100x500mm concrete prisms were strengthened with 1.5mm steel plates and kept in the mist room for 20 months. The joints were protected with different sealing agents. It was found (34) that after 20 months in the mist room, all the coatings used proved to be effective and no corrosion or loss of strength was observed.

8.3.1.2 BEAM TESTS

After 18 months of exposure to severe weathering conditions, three of the sixteen unloaded and plated beams were tested and no loss of bond or strength was observed (34). However, carbonation of concrete had occurred on all surfaces of the beams (over a depth of 2 to 3mm) except the bottom (tensile) face on which the steel plates were glued. The concrete-epoxy-steel joints seemed to have therefore withstood satisfactorily the effects of 18 months of exposure to environmental conditions and even acted as a protection against concrete carbonation. The remaining thirteen unloaded and eight loaded beams and the concrete-epoxy-steel joints were closely observed at regular time intervals and after 47 months of exposure, no adverse effect was observed. It was subsequently decided to leave these beams for a longer period before testing by others.

8.3.2 LONG TERM DEFORMATIONS

The shrinkage and total deformations measured on the beams over a period of 32 and 47 months respectively are presented in the following sections. The recorded shrinkage results in the laboratory are compared to those predicted by Brooks and Neville's simplified equations (119,120).

8.3.2.1 SHRINKAGE

The shrinkage beam was manufactured with the same materials and internal reinforcement as the creep beams but was unplated. Although the shrinkage beam was manufactured sixteen months after the creep ones, it was, like the previous beams, kept in the laboratory for five months before being taken to the exposure site. Fig.8.3 and Table 8.2 show the development of shrinkage deformations that occurred during the first 32 months and illustrates the 'moisture movement' which resulted from the intermittent dry and wet weather conditions after the beam was transported out of the laboratory. The deformations shown in Fig.8.3 are those recorded on the compression and tension faces of the beam. For convenience, the face with the longitudinal steel bars was defined as the tension face and the opposite face as the compression face. The restraining effect of the reinforcement on the shrinkage contractions is also illustrated in Fig.8.3 and Table 8.2. The deformation in the tension face at 28 days was only 27% of that in the compression face. The variation of the shrinkage deformations with time is similar to that of a logarithmic function when the beam was kept in the laboratory in fairly constant conditions (Fig.8.3). This agrees with the observations of others (119,120,123). The deformations were however greatly affected by the variable

environmental conditions after it was taken to the exposure site. The relative expansions and contractions illustrated by Fig.8.3 and Table 8.2 were caused by the daily and seasonal variation of the humidity and other conditions of the environment.

At 28 days, the shrinkage contraction was equivalent to 375 microstrains in the compression face and 100 microstrains in the tension face. The increase in shrinkage at two and four months (while the beam was still in the laboratory) over that at 28 days was 49.3% and 78.6% respectively in the compression face and 60.0% and 70.0% respectively in the tension face. The variation of shrinkage with time is similar to a logarithmic function as suggested by Brooks and Neville (119,120) who proposed the following formula for the prediction of the long term shrinkage from the value measured at 28 days:

$$Sh_t = B.(Sh_{28})^b \quad (8.1)$$

$$\text{Where } B = (-4.17 + 1.53\text{Log}_e t)^2 \quad (8.2)$$

$$\text{and } b = \frac{100}{2.90 + 29.2\text{Log}_e t} \quad (8.3)$$

Sh_t is the shrinkage deformation at the time t (in days).

The predicted increase in shrinkage over that at 28 days from the above equation is 48.0% at 2 months and 70.0% at 4 months in the compression face. These values agree satisfactorily with the recorded ones.

In the tension face the same predicted increases were 88.0% and 150.0% respectively. These values are rather greater than the recorded ones. This difference is probably due to the fact the

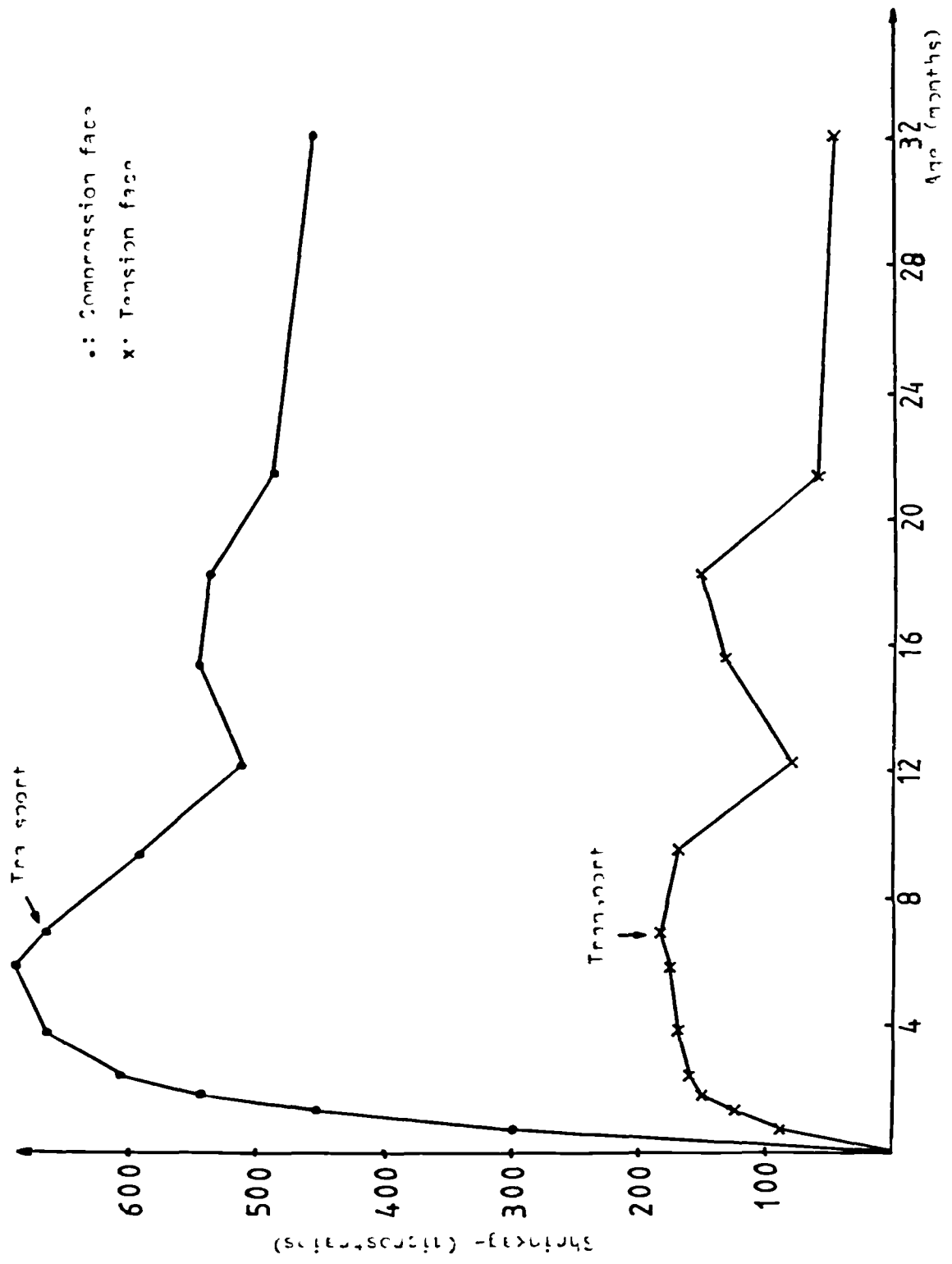


Fig.3.3: Shrinkage variation with time

Table 8.2: Shrinkage deformations (microstrains)

Date	Age (days)	Compression face	Tension face
13/08/80	21	300	90
02/09/80	41	455	125
15/09/80	54	545	150
03/10/80	72	610	160
13/11/80	113	670	170
12/01/81	173	695	175
10/02/81	202	670	185
28/04/81	279	595	170
21/07/81	363	515	80
28/10/81	463	550	135
21/01/82	547	540	150
16/04/82	632	490	60
10/03/83	960	460	45

Shrinkage beam: Casting: 23/07/80
 Transported to site: 15/01/81

Table 8.3: Elastic deformations in creep beams (microstrains)

Beam No.	Compressive strain	Tensile strain
117	440	880
118	470	840
119	430	780
120	520	540
121	510	310
122	600	520
123	420	380
124	410	720

theoretical predictions of Brooks and Neville (119,120) were derived for plain concrete and not for reinforced concrete. Nevertheless their formula gave a satisfactory prediction in the compression face where there was no reinforcement. Comparison of the recorded and predicted increases in the tension face suggests that the restraining effect of the reinforcement on the shrinkage contractions was greater after 28 days.

8.3.2.2 TOTAL DEFORMATIONS

The creep deformation of a material is obtained by deducting the arithmetic values of the shrinkage and short term elastic deformations from the total deformation. In absolute values, the shrinkage deformation must be subtracted from the total deformation in compression whereas in tension however the two components must be added together. The short term elastic deformation are the ones registered immediately after the application of the load and are given in Table 8.3. For the reasons mentioned before, it was impossible to separate the shrinkage and creep deformations in the loaded beams. The total concrete strain (excluding the elastic strain) variations with time are shown in Tables 8.4 and 8.5 and Figs.8.4 to 8.8. The compressive and tensile strains are the ones recorded on the vertical face of the beam at distances of 10mm from the compression and tension faces respectively. The recorded tensile strain included the width of all the cracks present within the gauge of 203.2mm over which the measurement was made. Figs.8.4 and 8.5 show that the total compressive strain increased with time when the beams were kept in the laboratory but decreased considerably when they were transported to the

Table 8.4: Shrinkage and creep deformations
in compression (microstrains)

Date	Age (days)	Beam 117	Beam 118	Beam 119	Beam 120	Beam 121	Beam 122	Beam 123	Beam 124
10/04/79	7	50	40	40	30	20	10	50	40
17/04/79	14*	80	50	100	60	120	20	60	70
01/05/79	28*	300	250	250	250	310	210	230	280
29/05/79	56*	350	330	310	300	380	280	330	380
12/07/79	100	10	30	10	20	120	10	40	120
25/08/79	144	160	120	100	70	280	130	140	270
18/01/80	290	230	230	140	140	360	170	190	330
11/03/80	343	370	300	310	330	460	220	240	430
25/05/80	422	420	330	330	350	520	290	300	500
17/11/80	594	400	370	370	410	520	300	330	510
10/02/81	679	480	450	430	460	610	350	370	590
28/04/81	756	520	450	470	540	600	370	400	620
21/07/81	840	400	360	420	630	560	420	380	550
28/10/81	939	520	490	520	750	660	410	460	680
21/01/82	1024	540	480	520	760	770	410	450	690
16/04/82	1109	450	430	490	730	610	370	400	650
10/03/83	1437	470	450	500	580	610	390	420	670

Creep beams: Casting: 06/03/79

Loaded: 03/04/79

Transported: 12/07/79

*: Load not adjusted before strain reading

Table 8.5: Creep and shrinkage deformations
in tension (microstrains)

Date	Age (days)	Beam 117	Beam 118	Beam 119	Beam 120	Beam 121	Beam 122	Beam 123	Beam 124
10/04/79	7	160	90	110	60	80	100	70	60
17/04/79	14*	210	110	90	90	10	40	50	50
01/05/79	28*	-70	-100	-120	-130	-170	-150	-120	-130
29/05/79	56*	-90	-170	-170	10	-220	-200	-170	-180
12/07/79	100	200	180	160	140	0	120	180	110
25/08/79	144	560	430	300	250	90	350	320	410
18/01/80	290	680	560	430	310	210	360	300	450
11/03/80	343	790	700	690	520	280	410	460	500
25/05/80	422	940	840	780	590	440	510	680	850
17/11/80	594	710	570	760	660	280	390	540	640
10/02/81	679	630	420	720	640	160	250	530	630
28/04/81	756	710	430	700	620	190	290	510	620
21/07/81	840	840	540	820	710	330	370	590	750
28/10/81	939	730	490	730	630	240	290	510	670
21/01/82	1024	740	480	720	630	230	310	510	640
16/04/82	1109	860	560	840	720	350	380	570	770
10/03/83	1437	910	570	870	740	330	360	610	800

Creep beams: Casting: 06/03/79

Loading: 03/04/79

Transported: 12/07/79

*: Load not adjusted before strain reading

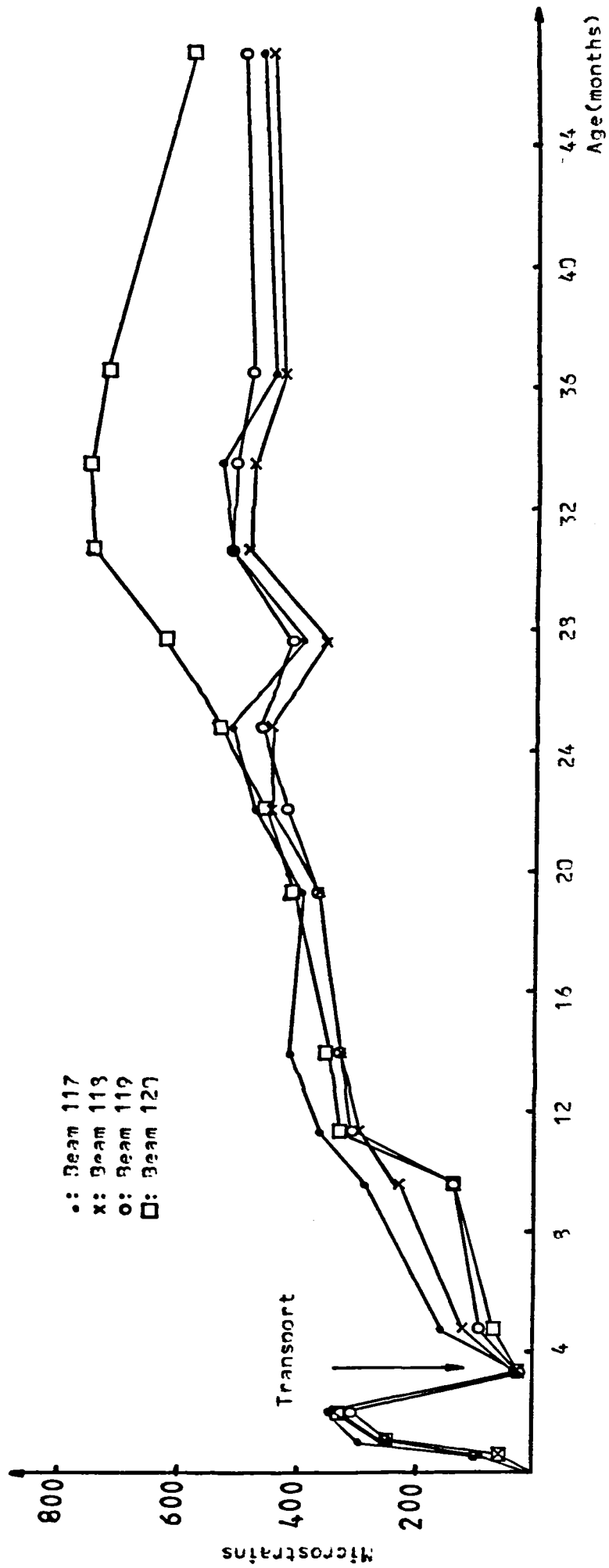


Fig. 3.4: Total strain variation in compression *

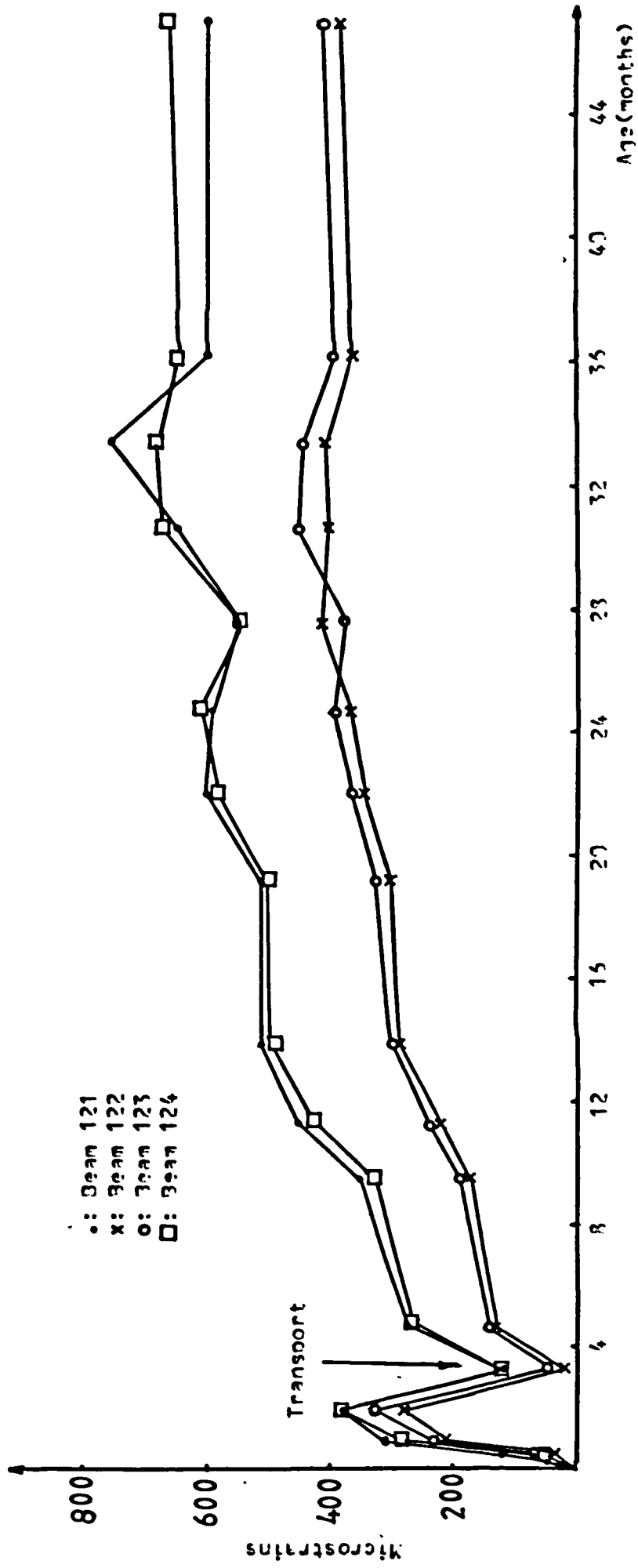


Fig.3.5: Total strain variation in compression

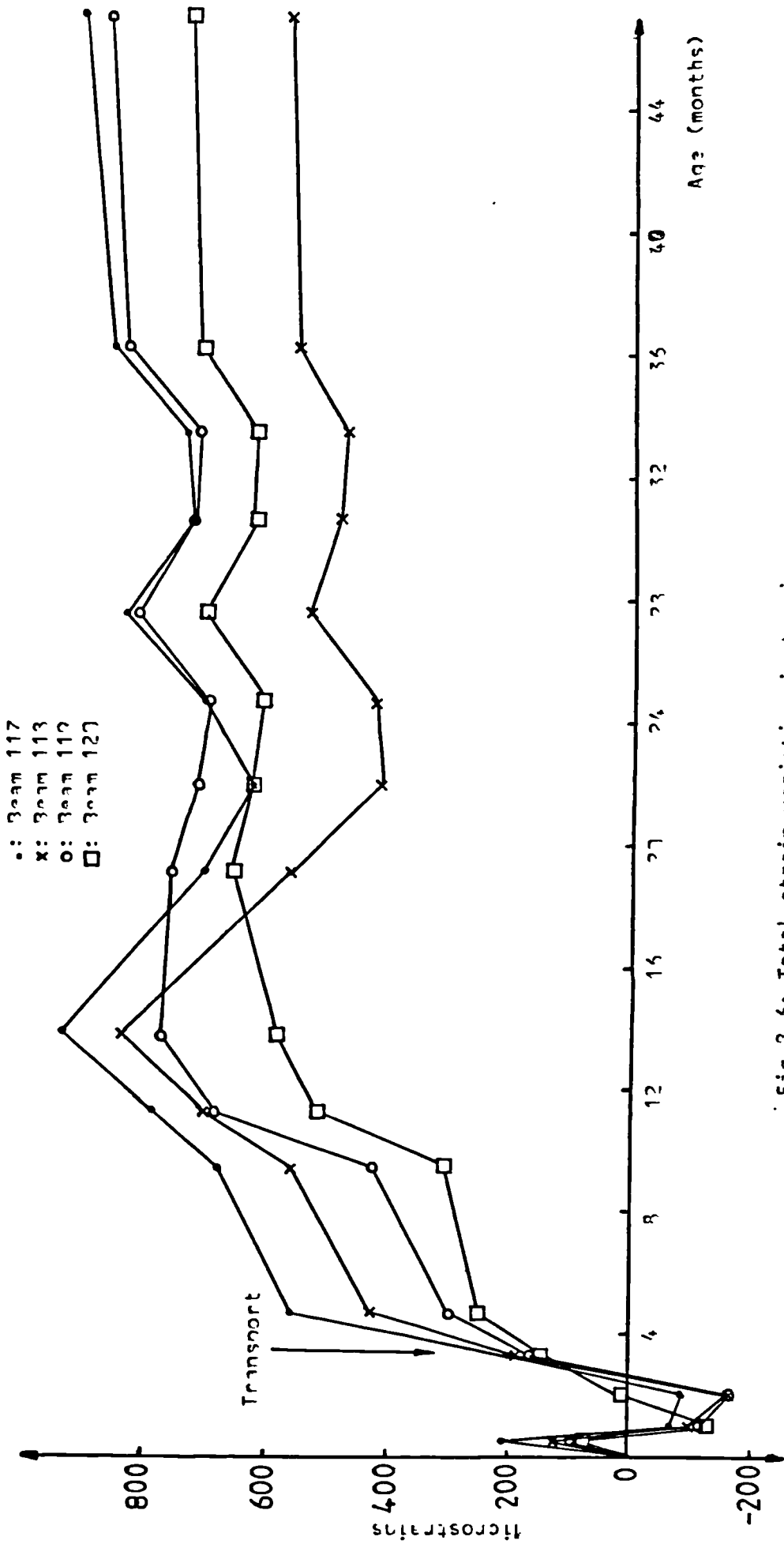


Fig.3.6: Total strain variation in tension

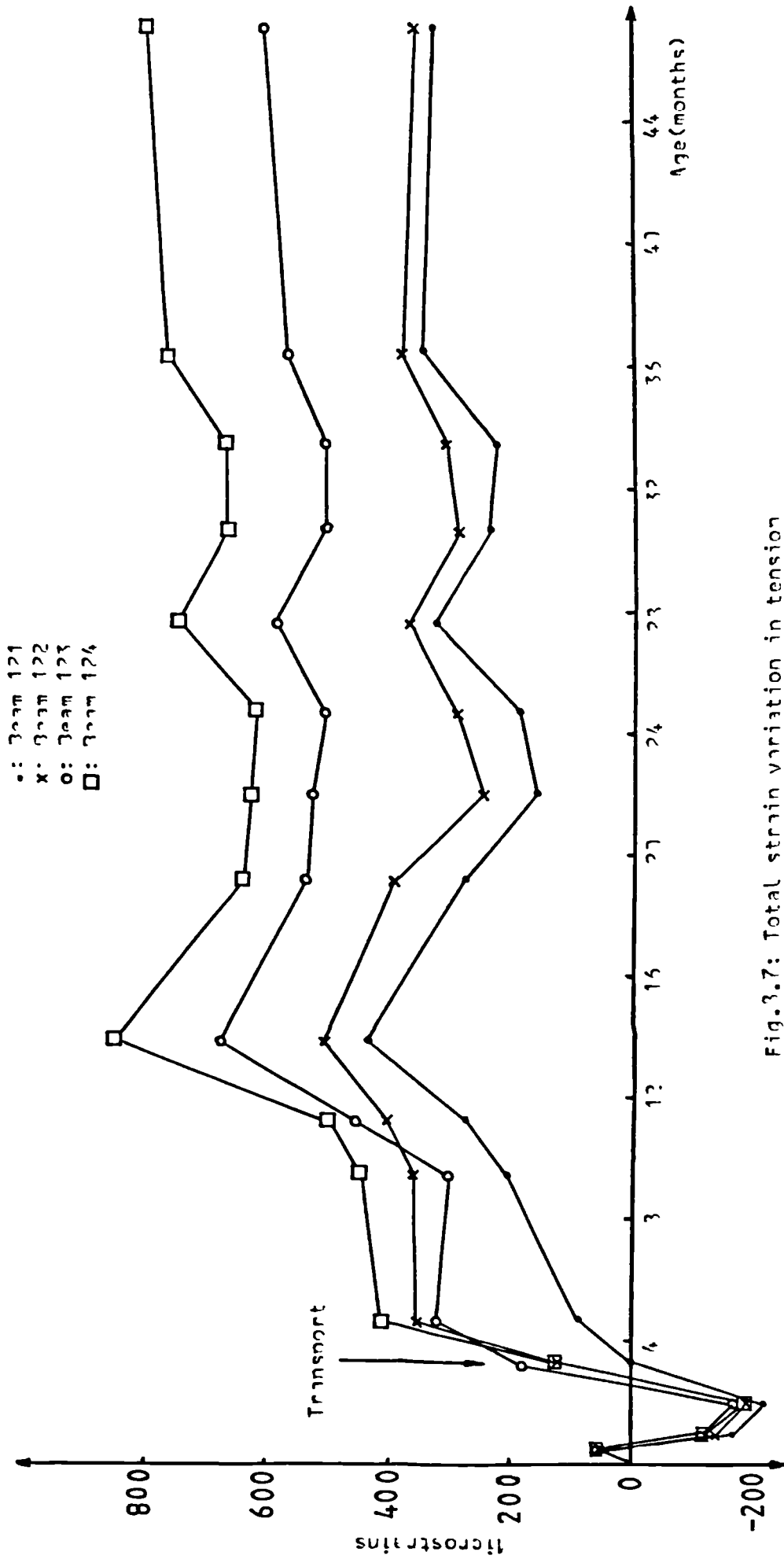


Fig.3.7: Total strain variation in tension

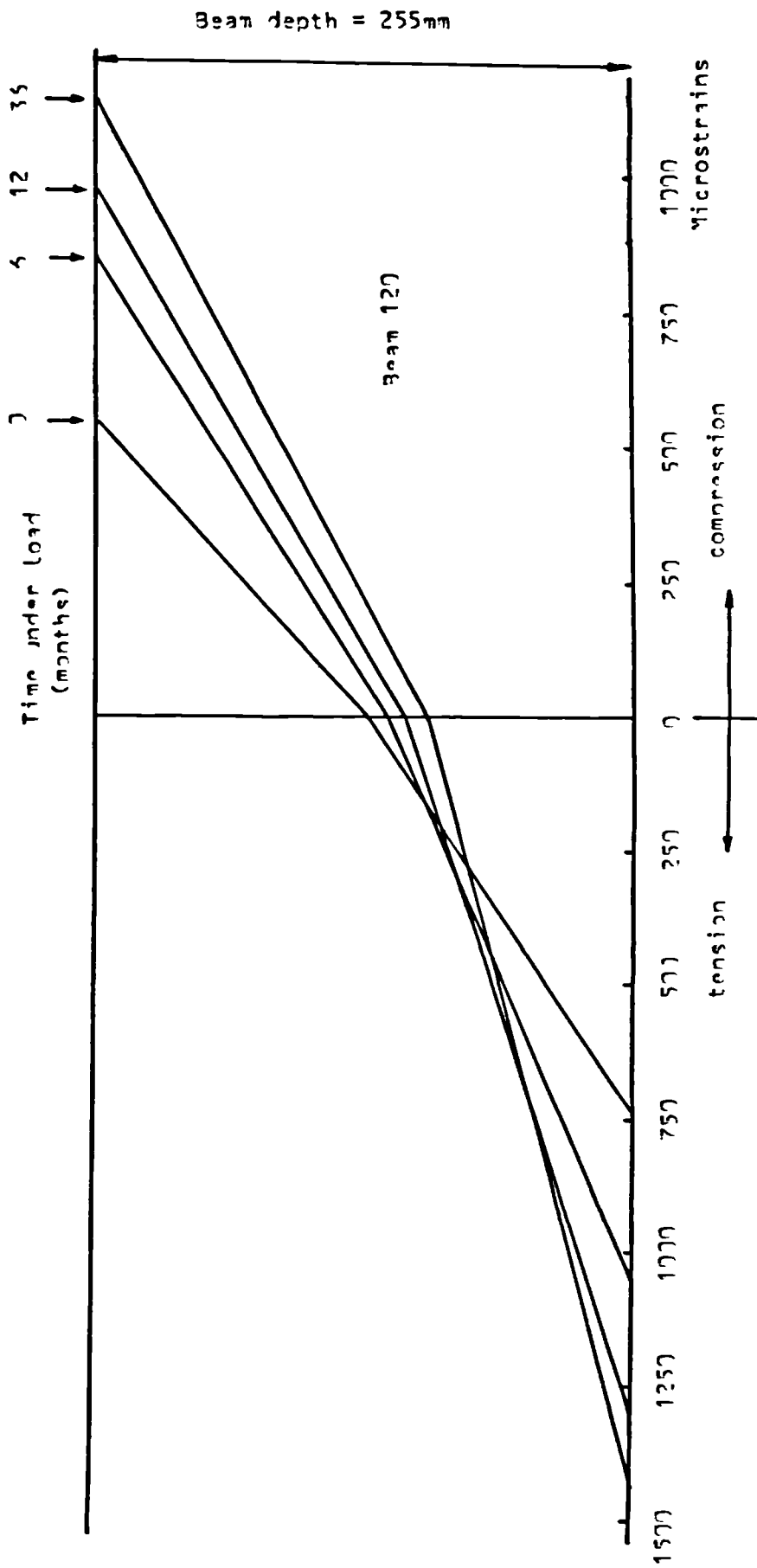


Fig. 3.3: Variation of concrete strain distribution across the beam depth with time

exposure site. The subsequent variations were greatly dependent on the environmental conditions. The variation of the total tensile strains in the laboratory was however different. (Figs.8.6 and 8.7). The negative total tensile strain (which is equivalent to a compressive strain) can only be the result of high shrinkage contractions during that period of time. The addition of the shrinkage contraction recorded on the shrinkage beam for the same interval of time but at different dates does not however result in a positive tensile creep deformation. This may be due partly to the fact that the load was not adjusted before the recording of those strains (Table 8.5). The other possible explanation to this may be a considerable difference in the temperature and humidity in the laboratory between the two periods of time in question. Table 8.6 shows that the average outside temperatures for the two periods (May 1979 and October 1980) were 15.6 and 8.3 degrees Celsius respectively.

Fig.8.8 shows a typical variation of the concrete strains across the beam depth and the neutral axis position with time. The neutral axis position moves towards the tensile face of the beam. This is probably the result of the reduction in the effective modulus of elasticity of concrete with time.

8.4 CONCLUSIONS

As there is no available accepted theory predicting the long term deformations as a function of the member characteristics, it is not easy to assess the long term behaviour of reinforced concrete beams and therefore difficult to compare the long term deformational results of plated beams to those of unplated ones without the availability of both sets

Table 8.6: Weather summary
Weston Park Meteorological Centre

Month	Max. Temp. °C	Min. Temp. °C	Mean Temp. °C	Rain mm	Rain days	Sun Hours
Apr. 79	18.8	-0.7	7.8	83.1	20	106.0
May 79	25.8	3.7	15.6	75.5	13	168.8
Jun. 79	27.3	5.7	16.8	34.9	11	190.0
Jul. 79	26.4	8.3	16.3	13.0	7	169.8
Aug. 79	24.3	6.7	15.5	79.0	15	171.2
Sep. 79	22.6	3.2	13.7	19.0	7	167.1
Oct. 79	21.1	1.6	11.0	66.4	15	82.5
Nov. 79	16.8	-3.5	6.7	96.9	22	54.9
Dec. 79	13.5	-0.9	5.5	137.7	25	42.5
Jan. 80	9.2	-3.2	2.4	70.9	21	47.4
Feb. 80	13.0	-2.6	5.4	117.1	18	28.4
Mar. 80	11.5	-2.2	4.8	100.1	19	87.8
Apr. 80	21.4	-0.6	9.2	10.6	6	149.3
May 80	24.3	2.1	11.1	20.5	7	213.6
Jun. 80	28.5	7.2	14.1	132.8	22	114.8
Jul. 80	27.2	7.8	14.7	66.9	15	130.0
Aug. 80	23.7	7.2	15.9	79.0	16	155.9
Sep. 80	22.9	6.7	15.0	33.2	14	151.5
Oct. 80	17.0	0.1	8.3	117.7	24	93.7
Nov. 80	14.2	-1.4	6.5	81.8	21	41.6
Dec. 80	13.0	-2.2	6.1	51.7	19	48.9
Jan. 81	11.7	-2.2	4.9	56.4	17	47.8
Feb. 81	12.1	-3.3	2.9	89.4	15	55.6
Mar. 81	15.4	0.0	7.4	149.9	25	48.3
Apr. 81	19.0	-0.7	7.4	110.5	14	112.6
May 81	20.7	0.1	11.6	65.3	19	149.0
Jun. 81	23.2	5.1	13.6	33.4	14	163.7
Jul. 81	24.0	9.1	15.9	18.8	15	172.6
Aug. 81	27.1	8.0	16.4	57.2	7	174.4
Sep. 81	24.5	7.4	15.0	107.8	12	162.2
Oct. 81	17.6	0.0	8.3	87.9	20	112.0
Nov. 81	15.1	0.2	7.7	70.4	17	41.1
Dec. 81	11.2	-9.1	0.1	102.2	17	37.4
Jan. 82	11.1	-9.2	2.8	39.9	16	48.2
Feb. 82	13.4	-3.1	4.6	20.4	13	33.0
Mar. 82	19.1	-0.1	6.2	100.1	21	131.7
Apr. 82	20.7	-0.8	9.1	17.3	7	167.1
May 82	24.2	0.7	11.9	23.6	7	238.9
Jun. 82	28.9	7.2	15.0	225.0	24	120.7
Jul. 82	27.6	9.8	16.7	14.7	6	173.0
Aug. 82	28.3	7.7	15.8	83.5	18	172.7
Sep. 82	26.4	4.8	14.6	56.4	11	148.5
Oct. 82	17.0	1.5	10.1	54.7	15	55.3
Nov. 82	16.8	-1.2	7.7	117.5	25	38.6
Dec. 82	14.2	-2.9	4.4	78.7	16	22.6
Jan. 83	13.4	-0.2	6.6	98.7	24	42.8
Feb. 83	8.4	-5.0	1.4	39.9	13	35.3
Mar. 83	14.3	0.4	6.7	65.7	22	85.4
Apr. 83	15.3	-0.9	6.6	121.2	21	115.3

of results.

As for conventional concrete, the long term deformations (shrinkage and creep) of plated beams are considerably affected by the conditions of their environment. The reinforcement resulted in lower shrinkage deformations in the tension face of the beam. More tests are obviously needed to assess the long term deformations separately.

Observation of the loaded and unloaded plated beams showed that despite 47 months exposure to severe environmental conditions, the joints concrete-epoxy-steel were unaffected and there was no apparent reason why the long term behaviour of the plated beams should be different from that of conventionally reinforced beams. However, a study over a longer period of time is necessary to confirm this conclusion.

CHAPTER NINE

LIMITATIONS OF PRESENT WORK, OVERALL CONCLUSIONS AND RECOMMENDATIONS FOR FUTURE WORK

9.1 LIMITATIONS OF PRESENT WORK

It is hoped that the present work has given a clear insight and yielded some useful information about the use of epoxy resins for bonding structural materials together in general and strengthening of reinforced concrete beams by bonding external steel plates in particular. It is also hoped that our knowledge about the mechanical and adhesion properties of epoxy resins and the structural behaviour of plated beams is enhanced.

The assessment of all the important parameters of study was however beyond the scope of this work and beyond the limitations of the project. There are numerous variables involved in the different areas investigated and the programme of study included many of the most important parameters. The limited number of tests could not however cover all the different variables. The limitations of the project are:

- (1) Only one type of epoxy resin was used throughout the project.
- (2) The range of the variables studied in the properties of epoxy was limited. The effects of the specimen thickness and loading rate on epoxy properties was studied over limited ranges. Only mild steel and one plate thickness were used in the pull out and double lap tests.
- (3) The dimensions of the beams were not varied.

- (4) The internal steel bar reinforcement was not varied.
- (5) The same concrete mix was used in all the beam tests.
- (6) Only one type of loading was used in the flexural tests.
- (7) The steel plate width and length were the same in the beam tests. The plates used were of mild steel.
- (8) The long term studies covered limited periods of time. Only concrete strains were measured in the plated beams sustaining constant load. The shrinkage deformations were not measured at the same time. Creep deformations could not therefore be deduced from the total deformations. The plate strains were not measured and the composite action between the beam and plate could only be observed visually.

9.2 OVERALL CONCLUSIONS

The following general conclusions are extracted from the more detailed conclusions presented at the end of each chapter and are valid within the limitations mentioned earlier:

(a) Epoxy properties:

- (1) The mechanical properties of epoxy resin depended closely on the dimensions of the test specimen and the rate of loading.
- (2) The behaviour of concrete-epoxy-steel joints in shear agreed with the theoretical predictions.
- (3) Epoxy resin offered a bond stronger than concrete in shear.
- (4) The mechanical and adhesion properties of epoxy were not affected by 6 month immersion in water or exposure to environmental conditions.
- (5) Because of the presence of peeling stresses, the single lap test is not a reliable method of studying shear adhesion of epoxy to metals.

(b) Flexural behaviour of plated beams:

(1) Epoxy resin did not crack with the concrete in flexure and acted as a participant in the structural resistance of the beam.

(2) Epoxy resin ensured full composite action between the beams and the external steel plates and resulted in increased stiffnesses and strengths as compared to unplated beams.

(3) The general flexural behaviour of plated beams was similar to that of conventionally reinforced concrete beams and could be predicted satisfactorily by existing theories.

(4) The greater bond area between the steel plates and concrete, as compared to internal reinforcement, seemed to have an additional restraining effect on the beams. This improved performance is thought to be the result of a better contribution of concrete in tension in plated beams.

(5) Loading of up to 70% of the ultimate load of the unplated beams and unloading them did not have any adverse effect on the behaviour of the subsequently plated beams.

(6) Loading of up to 70% of the ultimate load of unplated beams and bonding of the steel plates whilst the beams were still under load did not prevent the full exploitation of the added strength from the plates. The beams failed at loads similar to that of a beam plated without preloading. This was due to the lower yield strain of plates (mild steel) as compared to the 0.2% proof strain of the bars (high yield steel) and to the plastic properties of the reinforcement.

(c) Bond failure beams:

(1) Stopping the steel plate in the shear span short of the support created a critical section where premature failure was prone to occur by debonding of the plate. Failure was due to high bond and peeling forces caused by the high transfer of tensile forces from the plate to the continuing bars where the plate was stopped. These bond and peel stresses were higher with thicker plates and produced premature bond failure beyond a certain plate thickness (6mm in the present tests).

(2) The use of bolts did not prevent bond failure and their use in practice to strengthen bridges with thick plates requires more investigation.

(3) The use of externally bonded steel strips was successfully used to avoid premature bond failures. The strips overcame the peeling and bond forces and strengthened the part of the beam where debonding occurs.

(d) Shear behaviour:

(1) Bonding of the steel plates on the tension face of the beams increased their shear capacity by 9 to 15%, more than the CP110, ACI and CEB code equations (derived for conventional reinforcement) predicted. This may have been due to the fact that the equations are conservative. The dowel action in the external plates may also be greater than that of an equivalent amount of internal reinforcement. This may be due to the greater bond area in the external plates which prevents relative slippage after diagonal cracking.

(2) The use of externally bonded steel strips or channels as web reinforcement was shown to be effective. More research is however needed to determine the appropriate size, location and

spacing of the strips.

(e) Long term behaviour

The conclusions from this part of the project are limited because of the shortcomings described before.

(1) The total deformations (creep and shrinkage) in plated beams are highly affected by the variations of the conditions of their environment.

(2) 47 month exposure to severe environmental conditions of plated beams did not affect the concrete-epoxy-steel joint and no visual deterioration was observed.

9.3 RECOMMENDATIONS FOR FUTURE WORK

The confident use of epoxy resins to strengthen structures by bonding steel plates requires further investigation. The following areas are thought to be of particular interest:

(1) Long term mechanical and adhesion properties of epoxy resin. Creep is particularly worth investigating (epoxy is a viscous material and creep is very important).

(2) Testing beams with less longitudinal reinforcement to investigate whether epoxy cracks with concrete in flexure and if so at what strain. Epoxy resin may crack before failure in very under reinforced beams and the concrete-epoxy-plate joint may be affected.

(3) Use of mild steel internal bars or high yield steel plates with beams preloaded and strengthened whilst under their preloads should be investigated. The difference in the total strains of the internal bars and external plates (which are active only when the load is increased beyond the preload) may

lead to failure of the beams before yielding of the plates and without full exploitation of the added strength.

(4) The bond and peeling stresses depend on the amount of reinforcement and the bond areas of the two reinforcements. The effects of varying the amount of internal reinforcement, and the ratio of plate width to its thickness (keeping the same amount of external steel), on the bond and peel stresses are worth investigating.

(5) The bond and peel stresses are also affected by the plate cutoff. The plate cutoff effect on the stresses depends on the distance over which the transfer of tensile forces from the plate to the bars takes place, and on the distance from the cutoff point to the support. A better test instrumentation, such as electrical strain gauges fixed on the plate at small spacings, will be needed to assess the nature of the distribution of bond stresses over the transfer length.

(6) More tests are needed to investigate the existence and the nature of dowel action in the externally bonded plates on the tension face. The use of external steel as shear reinforcement is also worth studying. The optimum form of the external web steel should be investigated.

(7) Most of the research carried out so far was concerned with short term tests. Little is known about the long term behaviour of reinforced concrete structures strengthened by epoxy bonded steel plates. If the technique is to be confidently used in practice, more long term tests are therefore needed.

(8) The strengthening of prestressed concrete beams is also an area worthy of further research as many bridges and other structures which need strengthening are prestressed.

APPENDIX A

STRAIN GAUGE INSTRUMENTATION

A1 STRAIN GAUGE

A strain gauge consists of a conductor well cemented (by an appropriate adhesive) to the test object so that the strains in the specimen are transmitted to the conductor without relative slippage. Application of external loads cause deformations in the specimen which in turn result in changes in the gauge length of the conductor. The change in gauge resistance is related to the change in gauge length by the gauge factor K:

$$K = \frac{dR}{R} \frac{dl}{l} = \frac{dR}{\epsilon R} \quad \text{so} \quad \epsilon = \frac{dR}{R} \frac{l}{K}$$

R: Resistance dR: Variation of the resistance

l: Gauge length dl: Variation in gauge length $\frac{dl}{l} = \epsilon$: strain

A2 MEASURING CIRCUIT (WHEATSTONE BRIDGE)

The Wheatstone measuring circuit is shown in Fig.A1:

R: Resistance (Ω)

i: Current (Amp.)

V: Voltage output (volts)

E: Excitation voltage (input) (volts)

If the resistances R_{ij} are identical, the bridge is balanced: $V=0$.

$$V_{24} = i_1 R_{24} = V_{23} = i_2 R_{23} \quad V_{14} = i_1 R_{14} = V_{13} = i_2 R_{13}$$

$$E = (R_{24} + R_{14}) i_1 = (R_{13} + R_{23}) i_2 \quad \text{therefore} \quad \frac{R_{24}}{R_{14}} = \frac{R_{23}}{R_{13}} \quad \text{so} \quad R_{24} = \frac{R_{23} R_{14}}{R_{13}}$$

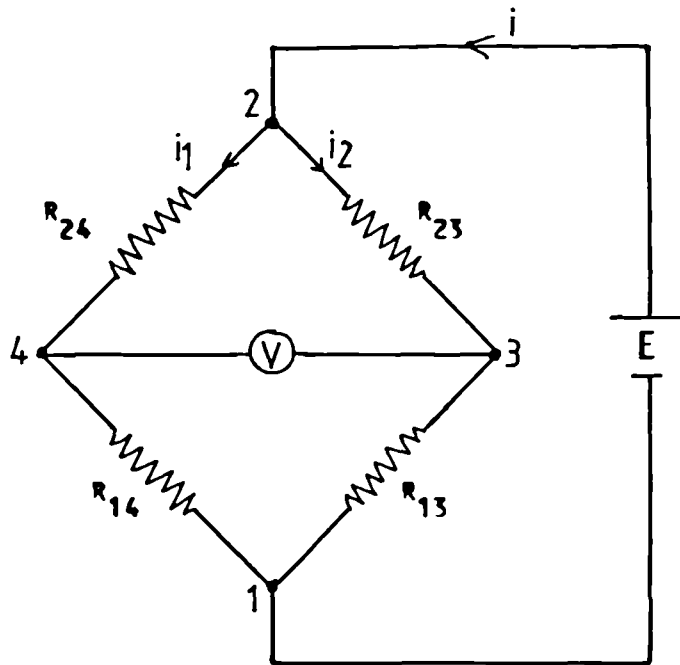


Fig.A1: Wheatstone strain gauge bridge

A2.1 QUARTER BRIDGE

Suppose $R_{13}=R_{23}=R_{14}=R_{24}=R$ but only R_{24} is active (R_{24} becomes $R+dR$):

$$i_1 = \frac{E}{2R+dR} \quad i_2 = \frac{E}{2R}$$

$$V_{24} = i_1 R_{24} = \frac{E}{2R+dR} (R+dR) = \frac{E(R+dR)}{2R+dR} \quad V_{23} = i_2 R_{23} = \frac{ER}{2R} = \frac{E}{2}$$

$$V = V_{23} - V_{24} = \frac{E}{2} - \frac{E(R+dR)}{2R+dR} \quad \text{so} \quad V = \frac{EdR}{4R+2dR}$$

$$\text{If } dR \text{ is very small: } V = \frac{EdR}{4R} \quad \text{so} \quad \epsilon = \frac{4V}{EK}$$

A2.2 HALF BRIDGE

The voltage output can be amplified by using two active strain gauges. If R_{24} and R_{13} are active the voltage output will become: $V=EdR/2R$

The half bridge can also be used in pure bending or combined bending and axial force (one strain gauge fixed on the compression face and the other on the tensile face) and the connections arranged to separate the effects of the two components (138).

A2.3 FULL BRIDGE

The sensitivity of the circuit is improved further by using four active strain gauges (two in the longitudinal direction and two in the transverse direction). The full bridge is used when the Poisson's ratio of the material tested is known (138).

A3 SOURCES OF ERROR

The most common sources of errors are electrical-supply leads-bridge non linearity and variations in ambient conditions. These different sources of error are described in detail in reference 138.

Although the strain gauges used in this project allow self compensation of the variation of resistance due to temperature effects, all the inactive strain gauges of the measuring bridges were 'dummy' strain gauges, i.e., strain gauges similar to the active ones and fixed on similar materials to balance the ambient conditions effects (138).

APPENDIX B

THEORETICAL MODELS FOR PULL OUT AND DOUBLE LAP TESTS

B1: PULL OUT TEST

The test rig is shown in Figs.4.11 and 4.12. The theoretical model was proposed by Bresson (25) using the following assumptions:

- 1- The materials (glue, steel and concrete) obey Hook's law.
- 2- The glue carries shear stresses only.
- 3- The normal stresses are uniformly distributed in the adherents.

As the specimen is symmetrical, only one half is considered as is shown in Fig.B1.

t_p : Thickness of steel plate=3.0mm

t_g : Thickness of glue:variable

t_c : Half thickness of concrete prism=30.0mm

p: Load per unit of concrete width

At a distance x from the free end, the concrete is submitted to a compressive force P_2 and the steel plate to a tensile force $P_1=-P_2$. Under the forces P_1 and P_2 , the points C and Q occupy new positions C_1 and Q_1 .

$QQ_1=u_1$: displacement of a point in the steel plate.

$CC_1=u_2$: displacement of a point in the concrete prism.

The shear strain in the glue is $\gamma=(u_1-u_2)/t_g$ and the shear stress is:

$\tau=G.(u_1-u_2)/t_g$ where G is the shear modulus of the glue.

$$\frac{d\tau}{dx} = \frac{G}{t_g} \left[\frac{du_1}{dx} - \frac{du_2}{dx} \right] = \frac{G}{t_g} \left[\frac{P_1}{E_p t_p} - \frac{P_2}{E_c t_c} \right] = \frac{P_1.G}{t_g} \left[\frac{1}{E_p t_p} + \frac{1}{E_c t_c} \right]$$

$$\frac{d\tau}{dx} = P_1.u^2 \quad \text{where} \quad u^2 = \frac{G}{t_g} \left[\frac{1}{E_p t_p} + \frac{1}{E_c t_c} \right] \quad \text{The unit of } u \text{ is } \text{mm}^{-1}$$

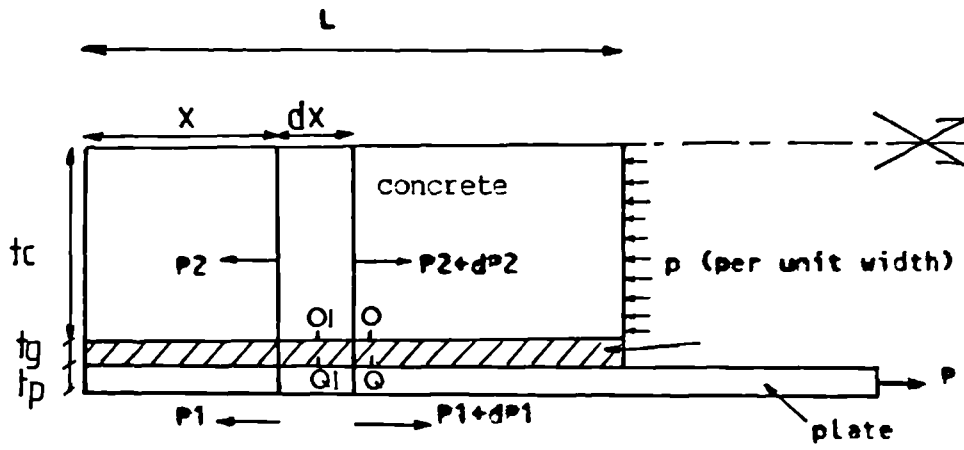


Fig.B1: Forces acting in pull out specimen

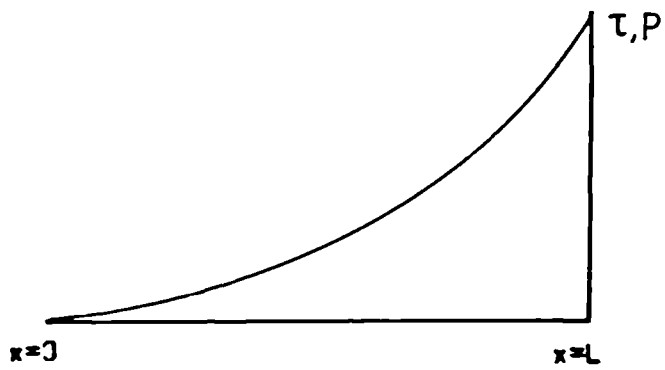


Fig.B2: Distribution of longitudinal force and shear stress along pull out joint

$$\frac{d^2\tau}{dx^2} = w^2 \frac{dPl}{dx}, \text{ but } \frac{dPl}{dx} \text{ is the interface shear stress.}$$

$$\text{Therefore } \frac{dPl}{dx} = \tau \quad \text{so } \frac{d^2\tau}{dx^2} = w^2 \tau$$

The solution of this differential equation after applying the boundary conditions is:

$$\tau(x) = Pw \cdot \frac{\cosh.w x}{\sinh.w L} = Pw \frac{e^{wx} + e^{-wx}}{e^{wL} - e^{-wL}}$$

The interface shear stress is maximum at the end where the load is applied ($x=L$) and minimum at the other end ($x=0$). The variation is exponential (Fig.B2)

$$\tau_{\max} = \tau(L) = Pw \frac{\cosh.w L}{\sinh.w L}$$

$$P(x) = \int \tau(x) dx = P \frac{\sinh.w x}{\sinh.w L}$$

The variation of the longitudinal force along the plate is exponential as well. $P_{\max} = P(L) = P$ The longitudinal force and shear stress are maximum at the end where the load is applied (Fig.B2).

B2: DOUBLE LAP TEST

The rig is shown in Fig.4.14. The same approach and assumptions are used. Only one half of the specimen is considered as is shown in Fig.B3.

E_1 :Elastic modulus of inner plate

E_2 :Elastic modulus of outer plate $E_1=E_2=2.10^5 \text{ N/mm}^2$

t_1 :Half thickness of inner plate $t_1=t_2=3.0\text{mm}$

t_2 :Thickness of outer plate

t_g :Thickness of glue

At a distance x the inner plate is submitted to a force P_1 and the outer plate to a force P_2 . $P_1+P_2=P=\text{constant}$.

Under these forces the points O and Q occupy new positions O1 and Q1.

u_2 :displacement of a point in the outer plate

u_1 :displacement of a point in the inner plate.

The shear stress in the glue is:

$$\tau = \frac{G}{t_g} (u_1 - u_2) \quad \text{so} \quad \frac{d\tau}{dx} = \frac{G}{t_g} \left[\frac{du_1}{dx} - \frac{du_2}{dx} \right] = \frac{G}{t_g} \left[\frac{P_1}{E_1 t_1} - \frac{P_2}{E_2 t_2} \right]$$

$$\frac{d^2\tau}{dx^2} = \frac{G}{t_g} \left[\frac{1}{E_1 t_1} \frac{dP_1}{dx} - \frac{1}{E_2 t_2} \frac{dP_2}{dx} \right] \quad \text{but} \quad \frac{dP_1}{dx} = - \frac{dP_2}{dx} = \tau$$

$$\text{so} \quad \frac{d^2\tau}{dx^2} = w^2 \tau \quad \text{where} \quad w^2 = \frac{G}{t_g} \left[\frac{1}{E_1 t_1} + \frac{1}{E_2 t_2} \right]$$

The solution is: $\tau(x) = A \cdot \sinh.wx + B \cdot \cosh.wx$

$$\frac{d\tau}{dx} = \frac{G}{t_g} \left[\frac{P_1}{E_1 t_1} - \frac{P_2}{E_2 t_2} \right] = Aw \cosh.wx + Bw \sinh.wx$$

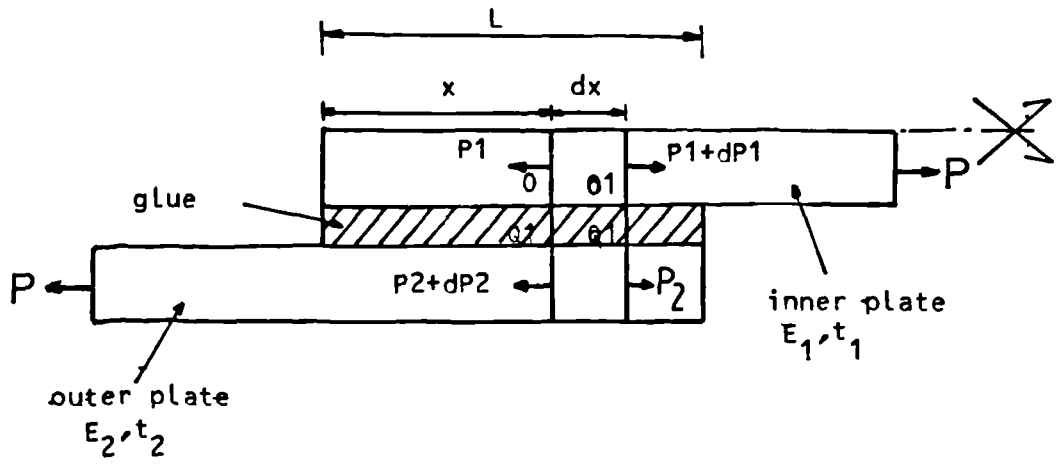


Fig.B3: Forces acting in a double lap specimen

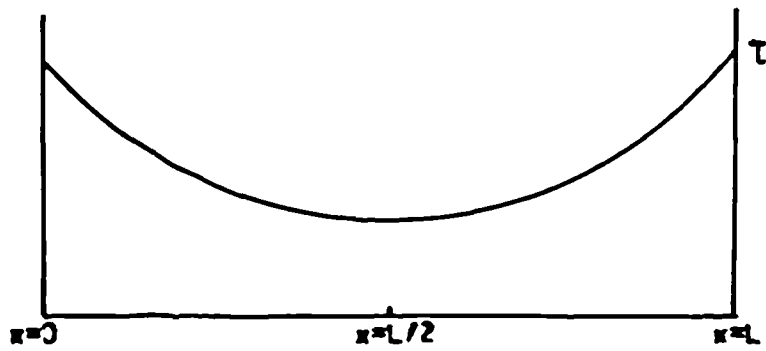


Fig.B4: Distribution of shear stress along double lap joint

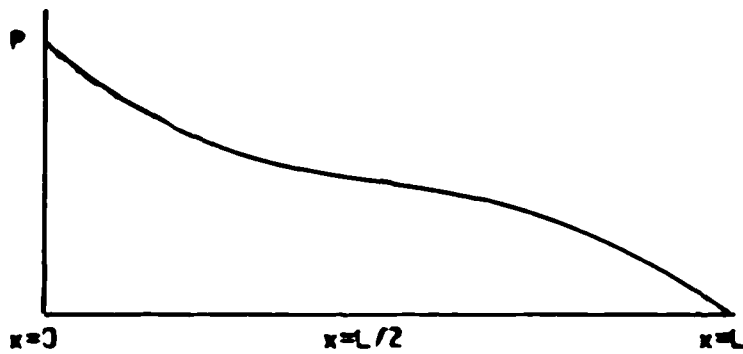


Fig.B5: Distribution of longitudinal force along the outer plate of double lap joint

for $x=0$ $P_1=0$ and $P_2=P$ so $Au = \frac{-G}{t_g} \frac{P}{E_2 t_2}$ therefore $A = \frac{-G}{t_g u} \frac{P}{E_2 t_2}$

for $x=L$ $P_1=P$ and $P_2=0$ so $B = \frac{G}{t_g u \sinh. uL} \left[\frac{1}{E_1 t_1} + \frac{\cosh. uL}{E_2 t_2} \right]$

so $\tau(x) = \frac{G}{u t_g} \frac{P}{\sinh. uL} \left[\frac{\cosh. ux}{E_1 t_1} + \frac{\cosh. u(L-x)}{E_2 t_2} \right]$

But $E_1=E_2=E_p$ and $t_1=t_2=t_p$

Therefore $\tau(x) = \frac{G.P}{u t_g E_p t_p \sinh. uL} \left[\cosh. ux + \cosh. u(L-x) \right]$

where $u^2 = \frac{2G}{t_g E_p t_p}$

The curve is symmetrical about the axis $x=L/2$. The shear stress is minimum at the middle of the joint ($x=L/2$) and maximum at the ends ($x=0$ and $x=L$) (Fig.B4). The variation is exponential.

$\tau_{\min} = \tau(L/2) = \frac{G.P}{u t_g E_p t_p \sinh. uL} 2 \cosh. \left(\frac{uL}{2} \right)$

$\tau_{\max} = \tau(0) = \tau(L) = \frac{G.P}{u t_g E_p t_p \sinh. uL} \left[\cosh. uL + 1 \right]$

The longitudinal forces in the plates are:

$P_1(x) = \int \tau(x) dx + C_1$ $P_2(x) = \int \tau(x) dx + C_2$

After integration and applying the boundary conditions:

$$P_1(x) = \frac{P}{2} \left[\frac{\sinh.ux - \sinh.u(L-x)}{\sinh.uL} + 1 \right]$$

$$P_2(x) = \frac{P}{2} \left[\frac{\sinh.u(L-x) - \sinh.ux}{\sinh.uL} + 1 \right]$$

The variation of the longitudinal forces along the inner and outer plates is exponential (Fig.B5). The point $x=L/2$ is a point of contraflexure.

APPENDIX C
BEAM ANALYSIS

C1: UNCRACKED SECTION (ELASTIC THEORY)

The materials (concrete, steel and glue) are assumed to obey Hook's law. Considering the diagram shown in Fig.C1:

If ϵ_b , ϵ_g and ϵ_p are the tensile strains in the bars, glue and plate, and ϵ_c and ϵ_c' are the compressive and tensile strains in concrete:

The compressive and tensile forces are: $C = \frac{b \cdot x \cdot \epsilon_c' E_c}{2}$

and $T = A_b \epsilon_b E_b + A_g \epsilon_g E_g + A_p \epsilon_p E_p + E_c \left[\epsilon_c' \frac{b(d-x)}{2} - \epsilon_b A_b \right]$

$\epsilon_b = \epsilon_c \left[\frac{d_b - x}{x} \right]$; $\epsilon_g = \epsilon_c \left[\frac{d_g - x}{x} \right]$; $\epsilon_p = \epsilon_c \left[\frac{d_p - x}{x} \right]$

so $T = E_c \left[A_b (E_b - E_c) \frac{d_b - x}{x} + A_g E_g \frac{d_g - x}{x} + A_p E_p \frac{d_p - x}{x} + E_c b \frac{(d-x)^2}{2x} \right]$

$T = C$ so $\frac{b \cdot x \cdot E_c}{2} = \frac{1}{x} \left[A_b (E_b - E_c) (d_b - x) + A_g E_g (d_g - x) + A_p E_p (d_p - x) + E_c b \frac{(d-x)^2}{2} \right]$

$x^2 \left(\frac{b E_c}{2} - \frac{b E_c}{2} \right) = A_b (E_b - E_c) d_b + A_g E_g d_g + A_p E_p d_p + E_c b \frac{d^2}{2} - x \left[A_b (E_b - E_c) + A_g E_g + A_p E_p + E_c b d \right]$

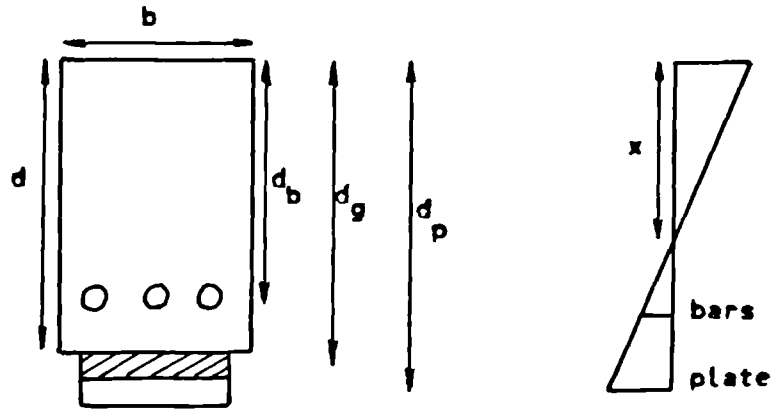


Fig.C1: Section details

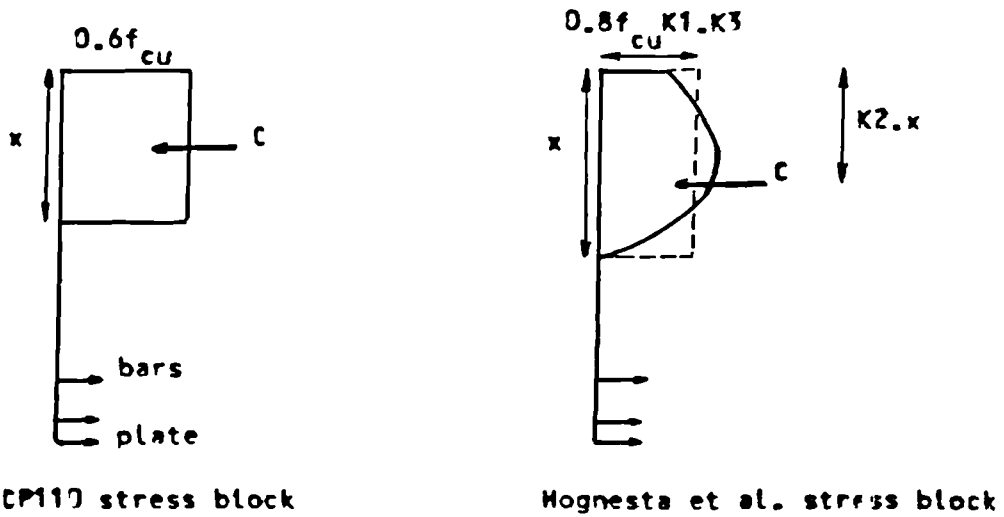


Fig.D1: Stress blocks at ultimate state

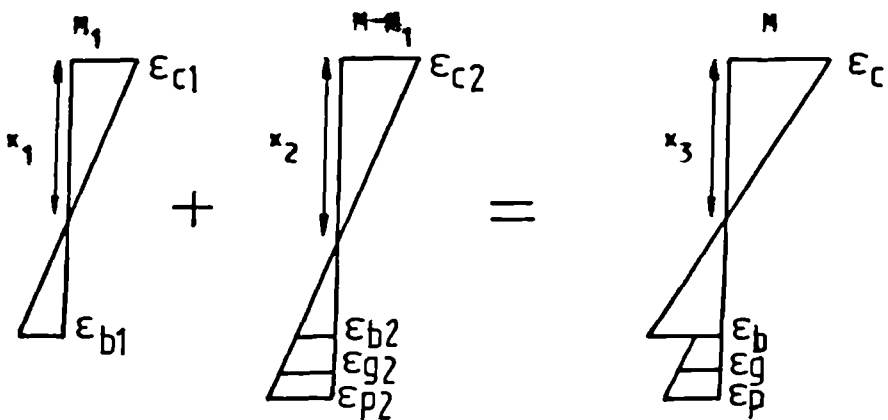


Fig.D2: Strain model for preloaded beams of Series III

The solution is:
$$x = \frac{A_b (E_b - E_c) d_b + A_g E_g d_g + A_p E_p d_p + E_c b \frac{d^2}{2}}{A_b (E_b - E_c) + A_g E_g + A_p E_p + E_c b d}$$

x is the neutral axis depth of uncracked section.

The second moment of area of the uncracked section is :

$$I_{\text{uncr}} = \left[\frac{b \cdot x^3}{12} + b \cdot x \cdot \frac{x^2}{2} \right] + \left[b \frac{(d-x)^3}{12} + b(d-x) \frac{d-x^2}{2} - A_b (d_b - x)^2 \right] : \text{concrete}$$

$$+ \frac{1}{E_c} \left[A_b E_b (d_b - x)^2 + A_g E_g (d_g - x)^2 + A_p E_p (d_p - x)^2 \right] : \text{bars, glue, plate}$$

The inertias of the epoxy layer and steel bars and plate about their own axes are neglected.

$$I_{\text{uncr}} = \frac{b}{3} \left[x^3 + (d-x)^3 \right] + \frac{1}{E_c} \left[A_b (E_b - E_c) (d_b - x)^2 + A_g E_g (d_g - x)^2 + A_p E_p (d_p - x)^2 \right]$$

The first crack moment is:

$$M_{\text{cr}} = \epsilon'_c E_c b \frac{(d-x)}{2} \frac{2}{3} d - \epsilon_b E_b A_b \left(d_b - \frac{x}{3} \right) : \text{concrete in tension}$$

$$+ \epsilon_b E_b A_b \left(d_b - \frac{x}{3} \right) + \epsilon_g E_g A_g \left(d_g - \frac{x}{3} \right) + \epsilon_p E_p A_p \left(d_p - \frac{x}{3} \right)$$

The first crack moment is reached when the stress in the tensile face of concrete is equal to the modulus of rupture f_b determined by the prism tests described in chapter three. At first cracking the compressive and tensile strains in concrete are therefore:

$$\epsilon'_{\text{cr}} = \epsilon_{\text{cr}} \frac{d-x}{x} = \frac{f_b}{E_c} \quad \text{so} \quad \epsilon_{\text{cr}} = \frac{f_b \cdot x}{E_c (d-x)}$$

The first crack moment becomes therefore:

$$M_{cr} = \frac{f_b}{E_c(d-x)} \left[A_b (E_b - E_c) (d_b - x) \left(d_b - \frac{x}{3} \right) + A_g E_g (d_g - x) \left(d_g - \frac{x}{3} \right) \right] \\ + \frac{f_b}{E_c(d-x)} \left[A_p E_p (d_p - x) \left(d_p - \frac{x}{3} \right) + E_c b d \frac{(d-x)^2}{3} \right]$$

For a third point loading, the maximum moment is:

$$M = (P/2) \cdot (L/3) = PL/6 \text{ so } P = 6M/L.$$

The first crack load is therefore $P_{cr} = 6M_{cr}/L$

C2: CRACKED SECTION (ELASTIC THEORY)

Immediately after cracking, the materials are still assumed to be elastic but the concrete in tension is ignored.

$$C=T \text{ so } \epsilon_c E_c \frac{b \cdot x}{2} = \epsilon_b E_b A_b + \epsilon_g E_g A_g + \epsilon_p E_p A_p \text{ But } \frac{\epsilon_c}{x} = \frac{\epsilon_b}{d_b - x} = \frac{\epsilon_g}{d_g - x} = \frac{\epsilon_p}{d_p - x}$$

$$\text{therefore } \epsilon_c E_c \frac{b \cdot x}{2} = \epsilon_c \left[A_b E_b \frac{d_b - x}{x} + A_g E_g \frac{d_g - x}{x} + A_p E_p \frac{d_p - x}{x} \right]$$

$$E_c \frac{b}{2} \cdot x^2 + \left[A_b E_b + A_g E_g + A_p E_p \right] x - (A_b E_b d_b + A_g E_g d_g + A_p E_p d_p) = 0$$

Equation of second degree, the solution of which is:

$$x = \frac{-(A_b E_b + A_g E_g + A_p E_p) + \sqrt{(A_b E_b + A_g E_g + A_p E_p)^2 + 2bE_c (A_b E_b d_b + A_g E_g d_g + A_p E_p d_p)}}{bE_c}$$

x is the neutral axis depth after cracking. The inertia of the section is:

$$I_{cr} = b \frac{x^3}{3} + \frac{1}{E_c} \left[A_b E_b (d_b - x)^2 + A_g E_g (d_g - x)^2 + A_p E_p (d_p - x)^2 \right]$$

APPENDIX D
ULTIMATE FLEXURAL STRENGTH

Three methods are used for the determination of the theoretical flexural capacities of the beams. The three methods are based on the following assumptions:

- 1- Plane sections before loading remain plane up to failure. In other words the strain distribution across the beam depth is linear at all load levels.
- 2- Concrete in tension is ignored.
- 3- Epoxy resin and the steel bars and plates are assumed to have elasto-plastic stress strain relationships. The plastic stresses are the 0.2% proof stresses or yield stresses as described in chapter three for the steel bars and plates. Epoxy resin was considered to have an average elastic modulus of 1200 N/mm^2 and a plastic stress of 10 N/mm^2 (although the actual stress strain relationship varies with the geometry of the specimen and the rate of loading as seen in chapter four). The contribution of the glue was limited to 10 N/mm^2 up to failure (testing of the beam F02 showed that the adhesive remained uncracked up to breaking point).

D1: CP110 SIMPLIFIED METHOD (79)

The CP110 simplified method is based on the assumptions that:

- (a) The concrete stress distribution is rectangular over the entire compression zone and is equal to $0.6 f_{cu}$.
- (b) The ultimate compressive strain of concrete is 0.0035.
- (c) The centroid is at half the depth of the compression zone.

The material safety factors are taken equal to unity. The CP110 stress block is shown in Fig.D1. At failure, the bars, glue and plate reach their 0.2% proof(yield) stresses f_{bo} , f_{go} and f_{po} respectively, (the beams are under reinforced).

$$C = 0.6 \cdot b \cdot x \cdot f_{cu} \quad \text{and} \quad T = A_b f_{bo} + A_g f_{go} + A_p f_{po} \quad C=T \quad \text{so} \quad x = \frac{A_b f_{bo} + A_g f_{go} + A_p f_{po}}{0.6 b f_{cu}}$$

The ultimate moment is:

$$M_u = A_b f_{bo} \left(d_b - \frac{x}{2}\right) + A_g f_{go} \left(d_g - \frac{x}{2}\right) + A_p f_{po} \left(d_p - \frac{x}{2}\right)$$

If the beam is first preloaded, then plated while the load is maintained, and finally tested to failure after two weeks of bond curing, then this simplified method cannot take into account the difference that might exist. The diagram of Fig.D2 showing the strain distribution illustrates this.

$$\epsilon_c = \epsilon_{c1} + \epsilon_{c2} \quad \epsilon_b = \epsilon_{b1} + \epsilon_{b2} \quad \epsilon_g = \epsilon_{g2} \quad \epsilon_p = \epsilon_{p2}$$

The CP110 simplified method assumes that the bars plate and glue reach their respective 0.2% proof (yield) strains at failure. The diagram in Fig.D2 shows however that the final bar and concrete strains could be so much greater than the the glue and plate strains (depending on the preloading load) that the bars may reach their proof strain long before the plate and glue.

D2: CP110 STRAIN COMPATIBILITY METHOD

The same stress block and ultimate concrete strain are assumed. At the preloading stage, the section is cracked (the preloading load is higher than the first crack load) but the materials are assumed to be elastic.

$$x_1 = \frac{-A_b E_b + \sqrt{(A_b E_b)^2 + 2A_b E_b d_b b E_c}}{b E_c}$$

$$e_{cl} = \frac{M_1 \cdot x_1}{A_b E_b (d_b - x_1) (d_b - \frac{x_1}{3})}, \quad M_1 \text{ is the preloading moment.} \quad e_{bl} = e_{cl} \frac{d_b - x_1}{x_1}$$

The strain compatibility method uses the actual stress strain of the materials and takes into account their plastic properties. The steel bars and plate are assumed to have ideal elasto-plastic stress-strain curves. The method is adopted by successive iterations:

Assume an initial neutral axis depth x ; deduce the strains in the bars, glue and plate; deduce the tensile and compressive forces. If the two forces are different, correct the value of the neutral axis depth x and start all over again. The correction method of the value of x should be carefully chosen to obtain convergence towards the exact solution.

The successive iterations were carried out by means of a computer with the following flowcharts:

$$1) \quad \epsilon_{cu} = 0.0035$$

$$2) \quad x = 100.0$$

$$3) \quad \epsilon_b = \epsilon_{cu} \frac{d_b - x}{x}$$

$$4) \quad \epsilon_g = (\epsilon_b - \epsilon_{bl}) \frac{d_g - x}{x}$$

$$5) \quad \epsilon_p = (\epsilon_b - \epsilon_{bl}) \frac{d_p - x}{x}$$

$$6) \quad \text{If } \epsilon_b > \epsilon_{bo} \text{ then } \epsilon_b = \epsilon_{bo}$$

$$7) \quad \text{If } \epsilon_g > \epsilon_{go} \text{ then } \epsilon_g = \epsilon_{go}$$

$$8) \quad \text{If } \epsilon_p > \epsilon_{po} \text{ then } \epsilon_p = \epsilon_{po}$$

$$9) \quad T = A_b E_b \epsilon_b + A_g E_g \epsilon_g + A_p E_p \epsilon_p$$

$$10) \quad C = 0.6b \cdot x \cdot f_{cu}$$

$$11) \quad \text{If } \frac{C}{T} > 1.001 \text{ or } \frac{C}{T} < 0.999 \text{ then } x = \frac{T+C}{2(0.6bf_{cu})} \text{ goto 66}$$

$$12) \quad M_u = A_b E_b \epsilon_b \left(d_b - \frac{x}{2}\right) + A_g E_g \epsilon_g \left(d_g - \frac{x}{2}\right) + A_p E_p \epsilon_p \left(d_p - \frac{x}{2}\right)$$

$$13) \quad \text{Print } x \text{ and } M_u$$

For the beams which are not preloaded, the preloading moment M_1 is taken equal to zero.

D3: HOGNESTAD ET AL. STRAIN COMPATIBILITY METHOD

This is a more refined method using the stress block suggested by Hognestad et al. (82) and shown in Fig.D1.

K1: Factor related to the shape of the stress block

K2: Factor related to the depth of the neutral axis

K3: Factor related to the maximum stress in concrete

After converting to metric units and using the cube strength $f_{cu} = 1.25f'_{cu}$ (f'_{cu} being the cylinder strength), the ultimate concrete strain is :

$$\epsilon_{cu} = 0.004 - \frac{f_{cu}}{56000}$$

The coefficients K1K3 and K2 are given by:

$$K1K3 = \frac{3900 + 40.5f_{cu}}{3200 + 116f_{cu}}, \quad K2 = 0.5 - \frac{f_{cu}}{690}$$

The same flowcharts as before were used with the following differences:

$$\epsilon_{cu} = 0.004 - \frac{f_{cu}}{56000} \quad C = 0.8f_{cu} b \cdot x \cdot K1K3$$

$$\text{The correcting formula for } x \text{ is } x = \frac{(C+T)}{2(0.8f_{cu} b \cdot K1K3)}$$

$$M_u = A_b E_b \epsilon_b (d_b - K2 \cdot x) + A_g E_g \epsilon_g (d_g - K2 \cdot x) + A_p E_p \epsilon_p (d_p - K2 \cdot x)$$

APPENDIX E

CALCULATION OF DEFLECTIONS, ROTATIONS AND CRACK WIDTHS

E1: DEFLECTIONS AND ROTATIONS

Three methods are used for the computation of the theoretical deflections and rotations. The same assumptions are made:

- 1- Plane sections before loading remain plane up to failure.
- 2- Epoxy resin and the steel bars and plates are elastic.
- 3- Concrete is elastic before cracking.

E1.1: UNCRACKED SECTION

Before cracking the three codes CP110, ACI and CEB adopt the same elastic analysis using the short term elastic modulus of concrete and the inertia of the uncracked section.

The curvature is given by the simple bending theory $1/r = M/EI$ where $M=PL/6$ (third point loading).

Assuming a constant stiffness of the beam, the rotation is given by the first integration of the curvature of the beam. After applying boundary conditions the rotation of a point at a distance a from the support is:

$$\theta = \frac{PL}{6EI} \left[\frac{L}{3} - \frac{3a^2}{2L} \right] = \frac{M}{EI} \left[\frac{L}{3} - \frac{3a^2}{2L} \right] \quad \theta = \left[\frac{L}{3} - \frac{3a^2}{2L} \right] \frac{1}{r} \quad (a < \frac{L}{3})$$

The central deflection Δ is given by the second integration of the

$$\text{curvature:} \quad \Delta = \frac{23PL^3}{1296EI} = \frac{23ML^2}{216EI} \quad \Delta = \frac{23L^2}{216} \frac{1}{r}$$

The short term elastic modulus of concrete and the inertia of the uncracked section were used. The central deflection and the rotation at a distance a from the support are:

$$\Delta = \frac{23ML^2}{216E_c I_{uncr}} \quad \theta = \frac{M}{E_c I_{uncr}} \left(\frac{L}{3} - \frac{3a^2}{2L} \right)$$

The rotations were measured at a distance $a=220.0\text{mm}$ from the supports.

E1.2: CRACKED SECTION

After cracking the three codes propose different stiffnesses:

E1.2.1: CP110 RECOMMENDATIONS (79)

To allow for the stiffening effect of concrete in tension, the CP110 code recommends the assumption of a triangular tensile stress distribution in concrete having a value of zero at the neutral axis and a value of 1N/mm^2 at the centroid of the tension steel.

For the cracked section the neutral axis depth is first calculated on the basis of zero stress in the concrete in tension. The curvature is then calculated by deducting the resisting moment of concrete in tension from the applied moment and using the inertia of the cracked section.

$$\frac{1}{r} = \frac{M - M_c}{E_c I_{cr}} \quad M_c = 1 \cdot \frac{(d_b - x) b}{2} \frac{2}{3} d_b = b d_b \frac{(d_b - x)}{3}$$

M_c is the resisting moment of concrete in tension. The deflection and rotation

are given by:
$$\Delta = \frac{23L^2}{216} \frac{1}{r} = \frac{23L^2}{216} \frac{M - M_c}{E_c I_{cr}} \quad \theta = \frac{M - M_c}{E_c I_{cr}} \left[\frac{L}{3} - \frac{3a^2}{2L} \right]$$

E1.2.2: ACI RECOMMENDATIONS (81)

The ACI code proposes an effective inertia depending on the inertias of the uncracked and cracked sections and the first crack moment:

$$I_e = \left[\frac{M_{cr}}{M} \right]^3 I_{un-cr} + \left[1 - \left[\frac{M_{cr}}{M} \right]^3 \right] I_{cr}$$

The deflection and rotation become:

$$\Delta = \frac{23ML^2}{216E_c I_e} \quad \theta = \frac{M}{E_c I_e} \left[\frac{L}{3} - \frac{3a^2}{L} \right]$$

E1.2.3: CEB RECOMMENDATIONS (80)

After cracking the CEB code divides the curvature in two:

- (a) Uncracked state: $1/r_1 = M_{cr}/(E_c I_{un-cr})$
- (b) In the cracked state the code assumes that the effective stiffness of the beam is:

$$(EI)_e = \frac{4}{3} \left[E_b A_b (d_b - x) \left(d_b - \frac{x}{3} \right) + E_g A_g (d_g - x) \left(d_g - \frac{x}{3} \right) + E_p A_p (d_p - x) \left(d_p - \frac{x}{3} \right) \right]$$

The curvature in the cracked state is then calculated by deducting the first crack moment: $1/r_2 = (M - M_{cr}) / (EI)_e$. The deflection and rotation become:

$$\Delta = \frac{23L^2}{216} \left[\frac{1}{r_1} + \frac{1}{r_2} \right] = \frac{23L^2}{216} \left[\frac{M_{cr}}{E_c I_{un-cr}} + \frac{M - M_{cr}}{(EI)_e} \right] \quad \theta = \left[\frac{L}{3} - \frac{3a^2}{2L} \right] \left[\frac{M_{cr}}{E_c I_{un-cr}} + \frac{M - M_{cr}}{(EI)_e} \right]$$

E1.2.4: PRELOADED BEAMS

The sectional properties of the preloaded beams F22-F23-F24 are changed after the plating has been applied. The deflections and rotations are calculated as superpositions of two components:

- Deflection and rotation before plating.
- Deflection and rotation after plating.

For the three beams tested, the first crack loads occurred during the preloading stage.

At a moment M greater than the preloading moment $M_{1'}$, the deflections and

rotations of the beams F22-F23-F24 are given by:

(1) CPL10 CODE

$$\Delta = \frac{23L^2}{216E_c} \left[\frac{M_1 - M_{c1}}{I_{cr1}} + \frac{M - M_1 - M_{c2}}{I_{cr2}} \right] \quad \theta = \left(\frac{L}{3} - \frac{3a^2}{2L} \right) \left[\frac{M - M_{c1}}{I_{cr1}} + \frac{M - M_1 - M_{c2}}{I_{cr2}} \right]$$

M: Moment at which the deflections and rotations are computed.

M₁: Preloading moment (M₁=0 for beams not preloaded).

M_{c1}: Resisting moment of concrete in tension before plating.

I_{cr1}: Inertia of the beam before plating (cracked section).

M_{c2}: Resisting moment of concrete in tension after plating.

I_{cr2}: Inertia of the beam after plating.

(2) ACI CODE

The effective inertias before and after plating are:

$$I_{e1} = \left[\frac{M_{cr1}}{M_1} \right]^3 I_{un-cr1} + \left[1 - \left[\frac{M_{cr1}}{M_1} \right]^3 \right] I_{cr1}, \quad I_{e2} = \left[\frac{M_{cr2}}{M} \right]^3 I_{un-cr2} + \left[1 - \left[\frac{M_{cr2}}{M} \right]^3 \right] I_{cr2}$$

I_{un-cr1}: Inertia of uncracked section of unplated beam.

I_{un-cr2}: Inertia of uncracked section of plated beam.

M_{cr1}: First crack moment of unplated beam.

M_{cr2}: First crack moment of plated beam. The deflections and rotations are then given by:

$$\Delta = \frac{23L^2}{216E_c} \left[\frac{M}{I_{e1}} + \frac{M - M_1}{I_{e2}} \right] \quad \theta = \left(\frac{L}{3} - \frac{3a^2}{2L} \right) \left[\frac{M_1}{I_{e1}} + \frac{M - M_1}{I_{e2}} \right]$$

(3) CEB CODE

The effective stiffnesses of the unplated and plated beams in the

cracked state are:
$$(EI)_{e1} = \frac{4}{3} \left[E_b A_b (d_b - x_1) \left(d_b - \frac{x_1}{3} \right) \right]$$

$$(EI)_{e2} = \frac{4}{3} \left[E_b A_b (d_b - x_2) \left(d_b - \frac{x_2}{3} \right) + E_g A_g (d_g - x_2) \left(d_g - \frac{x_2}{3} \right) + E_p A_p (d_p - x_2) \left(d_g - \frac{x_2}{3} \right) \right]$$

x_1 : Neutral axis depth of the cracked section of unplated beam.

x_2 : Neutral axis depth of the cracked section of plated beam.

Before plating the deflections and rotations are divided into two components: ie. before and after cracking.

The total deflections and rotations are given by:

$$\Delta = \frac{23L^2}{216} \left[\frac{M_{cr1}}{E_c I_{uncr1}} + \frac{M_1 - M_{cr1}}{(EI)_{e1}} + \frac{M - M_1 - M_{cr2}}{(EI)_{e2}} \right]$$

$$\theta = \left(\frac{L}{3} - \frac{3a^2}{2L} \right) \left[\frac{M_{cr1}}{E_c I_{uncr1}} + \frac{M_1 - M_{cr1}}{(EI)_{e1}} + \frac{M - M_1 - M_{cr2}}{(EI)_{e2}} \right]$$

E2: CALCULATION OF CRACK WIDTHS

The CP110 method is used for the computation of the average crack widths.

$$w_{cr} = \frac{3a_{cr} \epsilon_m}{1 + 2 \left[\frac{a_{cr} - c_{min}}{d - x} \right]} \quad (\text{equation 61 of CP110})$$

a_{cr} is the distance from point considered to the surface of the nearest reinforcing bar and c_{min} the minimum cover to the main reinforcing bars.

At the level of the steel bars $a_{cr} = c_{min}$, so $w_{cr} = 3a_{cr} \epsilon_m$ and the average

strain ϵ_m is related to the bar strain ϵ_b , which is determined ignoring the concrete in tension, by:

$$\epsilon_m = \epsilon_b - \frac{1.2bd(d_b - x)10^{-3}}{(d-x)(A_s f_{ys})} \quad (\text{equation 62 of CP110})$$

Where A_s is the cross section of the reinforcement and f_{ys} its yield stress

$$\text{In our case: } A_s f_{ys} = A_b f_{yb} + A_g f_{yg} + A_p f_{yp}$$

Where f_{yb} , f_{yg} and f_{yp} are the yield (proof) stresses of the bars, glue and plate respectively. As in the ultimate state analysis, the glue is assumed to have elasto-plastic properties with a yield stress of 10N/mm^2 . The CP110 code specifies that the formula is limited to cases where the strain in the tension reinforcement is less than 80% of the yield strain.

For the preloaded beams, the principle of superposition is again applied (Fig.D2).

$$w_{cr} = 3a_{cr}(\epsilon_{m1} + \epsilon_{m2})$$

$$\epsilon_{m1} = \epsilon_{b1} - \frac{1.2bd(d_b - x_1)10^{-3}}{(d-x_1)A_b f_{yb}} \quad \epsilon_{m2} = \epsilon_{b2} - \frac{1.2bd(d_b - x_2)10^{-3}}{(d-x_2)A_s f_{ys}}$$

x_1 : Neutral axis depth of cracked section of unplated beam.

x_2 : Neutral axis depth of cracked section of plated beam.

$$\epsilon_{c1} = \frac{M_1 \cdot x_1}{A_b E_b (d_b - x_1) \left(d_b - \frac{x_1}{3}\right)} \quad \epsilon_{b1} = \epsilon_{c1} \frac{d_b - x_{b1}}{x_{b1}} \quad (\text{see Appendix B})$$

$$\epsilon_{c2} = \frac{(M-M_1) \cdot x_2}{A_b E_b (d_b - x_2) \left(d_b - \frac{x_2}{3}\right) + A_g E_g (d_g - x_2) \left(d_g - \frac{x_2}{3}\right) + A_p E_p (d_p - x_2) \left(d_p - \frac{x_2}{3}\right)}$$

$$\epsilon_{b2} = \epsilon_{c2} \frac{d_b - x_2}{x_2}$$

$$\epsilon_{g2} = \epsilon_{c2} \frac{d_g - x_2}{x_2}$$

$$\epsilon_{p2} = \epsilon_{c2} \frac{d_p - x_2}{x_2}$$

REFERENCES

- 1- D.F.Evans
"Problems of assessing buildings for strength."
The Structural Engineer.Feb.78,Vol.6A,No.2,pp.43-45.
- 2- R.H.Berger et al.
"Extending the service life of existing bridges."
Transport Research Record 664. Bridge Engineering.
Vol.1,pp.47-55.
- 3- L.G.Byrd
"Highway maintenance management."
Civil Engineering.Apr.82,pp.23-25.
- 4- R.Taylor
"Strengthening of reinforced and prestressed beams."
Concrete Jnl.,Dec.76,Vol.10,No.12,pp.28-29.
- 5- A.O.Kaeding
"Structural use of polymers in concrete."
Second International Congress on Polymers in Concrete.
University of Texas,Austin,Oct.78,pp.9-23
- 6- A.O.Kaeding
"Building structural restoration using monomer
impregnation."
International Symposium on Polymers in Concrete.
Detroit 79, A.C.I. SP58, pp.281-298.
- 7- M.Steinberg
"Concrete polymer materials and its worldwide
development."
Polymers in Concrete.A.C.I. SP40,PP.1-14.
- 8- J.Bresson
"Renforcement par collage d'armatures du passage
inferieur du CD 126 sous l'autouroute du sud."
Annales de l'I.T.B.T.P., serie beton, beton arme,
suppl.297, Sept.72, pp.3-24
- 9- T.Sommerard
"Swanley's steel plate patch up."
New Civil Engineer.No.247,Jun.77,pp.18-19.
- 10- ACI Committee 503
"Use of epoxy compounds with concrete."
ACI Jnl.,Sept.73,pp.614-645.
- 11- G.N.Harding,B.U.Duvall
"Epoxies with concrete- Applications- Specifications-
Guidelines."
ACI SP21,1968,PP.119-135.

- 12- RILEM
 "Experimental research on new developments brought by synthetic resins to building techniques."
 RILEM International Symposium. Paris Sept. 67, Mater. and Struct., May-Jun. 68, pp. 187-296.
- 13- P.C. Hewlett, J.G. Morgan
 "Static and cyclic response of RC beams repaired by resin injection."
 Mag. of Conc. Research, Vol. 34, No. 118, Mar. 82, pp. 5-17
- 14- L.J. Tabor
 "Effective use of epoxy and polyester resins in civil engineering structures."
 Construction Industry Research and Information Association, Report 69, Jan. 78, 70p.
- 15- J. Warner
 "Epoxyes-Miracle materials don't always give miracle results."
 ASCE Civ. Eng., Feb. 78, pp. 48-55.
- 16- COLEBRAND
 "Comparison of mechanical properties of CXL 83 and CXL 194."
 Private communication.
- 17- R. Cirodde
 "Caracteristiques generales des colles de structures."
 Annales de l'ITBTP, No. 349, Apr. 77.
- 18- A.C. Meeks
 "Fracture testing and toughening of epoxy resins."
 British Polymer Jnl., Vol. 7, No. 1, Jan. 75, pp. 1-10.
- 19- W.L. Ettel et al.
 "Contribution à la resistance chimique des resines epoxydes chargees et leur controle."
 Mat. and Struct., Vol. 9, No. 53, Sep-Oct. 76, pp. 315-323.
- 20- J.M. Plecnik
 "Temperature effects on epoxy adhesives."
 ASCE Struct. Div., Vol. 106, No. ST1, Jan. 80, pp. 99-114.
- 21- U. Carputi et al.
 "Assemblages colles dans les structures composites."
 Mat. and Struct., No. 79, Jan-Feb. 81, pp. 3-12.
- 22- ACI Committee 503
 "Standard specifications for bonding hardened concrete, steel, wood, brick and other materials to hardened concrete with a multi component epoxy adhesive."
 Proposed ACI Standard 503.1

- 23- J.Bresson
 "L'application du beton plaque."
 Annales de l'ITBTP, No.349, Apr.77.
- 24- J.D.Kriegh
 "Arizona slant shear test: a method to determine epoxy bond strength."
 ACI Jnl., Vol.73, No.7, Jul.76, pp.372-373.
- 25- J.Bresson
 "Nouvelles recherches et applications concernant l'utilisation des collages dans les structures. Beton plaque."
 Annales de l'ITBTP serie beton, beton arme, Suppl.278, Feb.71, PP.23-54.
- 26- S.K.Solomon
 "Steel-concrete-steel sandwich beams."
 Report WBRU/IR2, university of Dundee, Sept.75.
- 27- D.Van gemert
 "Force transfer in epoxy bonded steel-concrete joints."
 Internat. Jnl. of Adhesion and Adhesives, Vol.1, No.2, Oct.80, pp.67-72.
- 28- P.Burkhardt et al.
 "Experiences sur les poutres mixtes en acier-beton liees à l'aide d'adhesifs epoxydes."
 Mat. and Struct., Jul-Aug75, pp.261-278.
- 29- A.R.Cusens, D.W.Smith
 "A study in epoxy adhesive joints in shear."
 The Struct. Eng., Vol.58A, No.1, Jan.80, pp.13-18.
- 30- G.C.Mays, D.Smith
 "Adhesive bonded steel- concrete composite construction."
 Internat.Jnl. of Adhesion and Adhesives, Apr.82, pp.103-107.
- 31- R.S.Utam
 "Durability of epoxy adhesive joints in concrete, steel and aluminium."
 Report WBRU-IR24, university of Dundee, Jun.79.
- 32- A.J.J.Calder
 "Exposure tests on externally reinforced concrete beams-First two years."
 TRRL suppl. rep.529, 1979.
- 33- G.O.Lloyd, A.J.J.Calder
 "The microstructure of epoxy bonded steel-to-concrete joints."
 TRRL suppl. rep.705, 1982.

- 34- J.W.Bloxham
 "Investigation of the flexural properties of RC beams strengthened by externally bonded steel plates."
 Ph.D thesis,Sheffield university,Sept.80.
- 35- C.Hill
 "Testing of structural adhesives."
 Technical report,Sheffield polytechnic.
- 36- T.R.Guess,R.E.Allred
 "Comparison of lap shear test specimens."
 Jnl. of Testing and Evaluation, Vol.5,
 No.2,Mar.77,pp.84-93.
- 37- U.Yuceoglu,D.P.Updike
 "Adhesive bonded stiffener plates and double joints."
 ASCE Advances in civ. eng. through engineering
 mechanics. 1977, pp.479-482.
- 38- Y.Gilibert,C.Collot
 "Contribution à l'etude de l'adhesivite colle-acier en
 fonction des etats micro-geometriques des surfaces
 rectifiees et rectifiees sablees."
 Mat. and Struct.,Nov-Dec.75,pp.425-436.
- 39- Y.Gilibert et al.
 "Mesure des deformations et des contraintes engendrees
 lors d'un essai de cisaillement en traction à la
 surface des plaques d'acier collees."
 Mat. and Struct., Vol.9, No.52, Jul-Aug.76,pp.255-260.
- 40- Y.Gilibert et al.
 "Etude de la resistance mecanique des plaques d'acier
 collees en fonction de la rugosite et de l'epaisseur de
 l'adhesif."
 Mat. and Struct.,Vol.9,No.54,Nov-Dec.76,pp.419-424.
- 41- E.B.Ramel
 "Analytical and experimental studies of adhesive bonded
 beams and plates."
 Ph.D thesis,Dundee university,Sept.76.
- 42- U.Yuceoglu,D.P.Updike
 "The effect of bending on the stresses in adhesive
 joints."
 Leigh university report IFSM-75-68, NASA-NGR 39-
 007-011, Mar.75.
- 43- W.A.Dukes,R.W.Bryant
 "The effect of adhesive thickness on joint strength."
 Jnl.of Adhesion,Vol.1,part 1,1969,pp.48-53.
- 44- N.L.Harrison,W.J.Harrison
 "The stresses in an adhesive layer."
 Jnl. of Adhesion,Vol.3,part 3,1972,pp.195-212.

- 45- J.Pirvics
 "Two dimensional displacement stress distribution in adhesive bonded composite structures."
 Jnl. of Adhesion, Vol.6, part 3, 1974, pp.207-229.
- 46- G.C.Mays, G.P.Tilly
 "Long endurance fatigue performance of bonded structural joints."
 Internat. Jnl. of Adhesion and Adhesives, Apr.82, pp.109-113.
- 47- G.C.Mays, W.J.Harvey
 "Fatigue performance of adhesive bonded joints for bridge deck construction."
 IABSE colloquium, Lausanne 1982.
- 48- A.J.J.Calder
 "Strength of bonded shear joints subjected to movement during cure."
 TRRL report 1981
- 49- W.Luhowiak et al.
 "Essai de fatigue de choc sur des assemblages colles par l'intermediaire d'une resine epoxydique."
 Mat. and Struct., No.86, Mar-Apr.82, pp.135-140.
- 50- R.L'hermite, J.Bresson
 "Beton arme par collage des armatures."
 RILEM symposium, part 2, Paris 1967, pp.175-203.
- 51- H.Lerchental
 "Bonded sheet metal reinforcement for concrete slabs."
 RILEM symposium, Paris 1967, pp.165-173.
- 52- H.Lerchental, I.Rosenthal
 "Flexural behaviour of concrete slabs reinforced with steel sheet."
 Mat. and Struct., No.88, Jul-Aug.82, pp.279-282.
- 53- S.Kajfasz
 "Concrete beams with external reinforcement bonded by glueing."
 RILEM symposium- Synthetic resins in building construction, part 2, Paris 1967, pp.142-151.
- 54- M.D.Mac Donald
 "The flexural performance of 3.5m concrete beams with various bonded external reinforcements."
 TRRL suppl. report 728, Crowthorne 1982.
- 55- C.G.Fleming, G.E.M.King
 "The development of structural adhesives for three original uses in South Africa."
 RILEM symposium, part 2, Paris 1967, pp.75-92.

- 56- R.L'hermite
 "Use of bonding techniques for reinforcing concrete and masonry structures."
 Mat. and Struct., Vol.10, No.56, Mar-Apr.77, pp.85-89.
- 57- R.L'hermite
 "Renforcement des ouvrages en beton et en maconnerie par collage."
 Annales ITBTP, No.349, Apr.77.
- 58- S.K.Solomon, L.K.Gopalani
 "Flexural tests on concrete beams externally reinforced by steel sheet."
 The Indian Concrete Jnl. , Vol.53, No.9, Sept.79, pp.249-253.
- 59- T.H.Eng
 "The effect of bonded mild steel plates in the strengthening and repairing of RC beams."
 Jnl. of Institution of Engineers, Malaysia, Jun-Dec.79, pp.31-37.
- 60- R.Jones, R.N.Swamy, J.Bloxham, A.Bouderbalah
 "Composite behaviour of concrete beams with epoxy bonded external reinforcement."
 Intern. Jnl. of Cem. Comp. and Lightw. Conc., Vol.2, No.2, May 80, pp.91-107.
- 61- M.Ladner
 "Field measurements on subsequently strengthened slabs."
 Douglas Mc Henry Internat. Symposium on Concrete and Concrete Structures. pp.481-492.
- 62- T.H.Ang
 "The strengthening of RC beams using glued steel plates."
 Msc thesis, Sheffield university, Sept.79.
- 63- M.D.Mac Donald
 "The flexural behaviour of concrete beams with bonded external reinforcement."
 TRRL suppl. rep.415, Crowthorne 1978.
- 64- C.A.K.Irwin
 "The strengthening of concrete beams by bonded steel plates."
 TRRL suppl. rep.160uc, Crowthorne 1975.
- 65- A.Bouderbalah
 "Strengthening of existing concrete beams by use of glued steel plates."
 Msc thesis, Sheffield university, Sept.78.

- 66- R.Jones,R.N.Swamy,T.H.Ang
 "Under and over reinforced concrete beams with glued steel plates."
 Internat. Jnl. of Cement Composites and Lightweight Concrete. Vol.4, No.1, Feb.82, pp.19-32.
- 67- G.C.Mays,C.D.Smith
 "Reinforced slab of the future."
 Jnl. of Concrete,Vol.14,No.6,Jun.80,pp.13-15.
- 68- S.K.Solomon,D.W.Smith,A.R.Cusens
 "Flexural tests on steel-concrete-steel sandwiches."
 Mag. of Conc. Research,Vol.28,No.94,Mar.76,pp.13-20.
- 69- D.A.Van gemert
 "Repairing of concrete structures by externally bonded steel plates."
 Internat. sympos.: Plastics in materials and structural engineering. pp.519-526.
- 70- J.Bresson
 "Realisation pratique d'un renforcement par collage d'armatures."
 Annales de l'ITBTP,suppl.278,Feb.71,pp.50-52.
- 71- K.D.Raithby
 "External strengthening of concrete bridges with bonded steel plates."
 TRRL suppl. rep.612,1980.
- 72- M.Ryback
 "Renforcement des ponts par collage de l'armature."
 Mat.and Struct.No.91,Jan/Feb.83,pp.13-17.
- 73- British Standards Institution (BSI)
 "Portland cement-Ordinary and Rapid Hardening."
 BS12:1958
- 74- BSI
 "Aggregates from natural sources for concrete."
 BS882,part 2,London 1973,16p.
- 75- BSI
 "Methods of sampling and testing of mineral aggregates, sands and fillers."
 BS812,4 parts,London 1975.
- 76- BSI
 "Methods for tensile testing of metals."
 BS18,3 parts,1971.
- 77- D.C.Teychenéⁿ et al.
 "Design of concrete mixes."
 Dept. of the Environment, Building Research Establishment, TRRL, 1975.

- 78- BSI
 "Methods of testing concrete."
 BS1881,6 parts,London 1970.
- 79- BSI
 "Code of practice for structural use of concrete."
 CP110,part 1,1972.
- 80- CEB
 "Common unified rules for different types of
 construction and material- CEB-FIP code for concrete
 structures."
 CEB Bulletin d'information No.124/125E,2 parts,1978.
- 81- ACI
 "Building code requirements for reinforced concrete."
 ACI-318-77,1977.
- 82- Hognestad et al.
 "Concrete stress distribution in ultimate strength
 design."
 ACI Jnl.,Vol.52,Dec.55,pp.455-479.
- 83- A.Hillerborg
 Private communication
 (Seminar on fracture mechanics of concrete).
- 84- ACI Committee 408
 "Bond stress-The state of the art."
 ACI Jnl.,Vol.63,No.11,1966,pp.1161-1188.
- 85- ACI
 "Interaction between steel and concrete."
 ACI symposium, ACI Jnl., Vol.76, No.2, Feb.79, pp.227-
 356, 6 papers.
- 86- R.M.Mains
 "Bond stresses along reinforcing bars."
 ACI Jnl.,Vol.48,No.11,Nov.52,pp.225-252.
- 87- E.L.Kemp,W.J.Wilhelm
 "Influence of the parameters influencing bond
 cracking."
 ACI Jnl.,Vol.76,No.1,Jan.79,pp.47-72.
- 88- M.Betzle
 "Bond slip and strength of lapped bar splices."
 Douglas Mc Henry Internat. Symposium,pp.493-514.
- 89- P.M.Ferguson,F.N.Matloob
 "Effect of bar cutoff on shear and bond strength of RC
 beams."
 ACI Jnl.,Vol.56 part 1,Jan.59,pp.5-24.

- 90- M.J. Baron
"Shear strength of RC beams at points of bar cutoff."
ACI Jnl., Vol. 63 part 1, Jan. 66, pp. 127-133.
- 91- B. Bresler, J.C. Gregor
"Review of concrete beams failing in shear."
ASCE Struct. Div., Vol. 93, No. ST1, Feb. 67, pp. 343-732.
- 92- A. Placas, P.E. Regan
"Shear failures of RC beams."
ACI Jnl., Vol. 68, No. 10, Oct. 71, pp. 763-773.
- 93- Joint ASCE-ACI Task Committee 426
"The shear strength of RC members."
ASCE Struct. Div., Vol. 99, No. ST6, Jun. 73, pp. 1091-1187.
- 94- ASCE-ACI Committee 326
"Shear and diagonal tension-Part 1: General principles."
ACI Jnl. Vol. 59, No. 1, Jan. 62, pp. 3-30.
- 95- R.C. Fenwick, T. Paulay
Mechanisms of shear resistance of concrete beams."
ASCE Struct. Div., Vol. 94, No. ST10, Oct. 68, pp. 2325-2350.
- 96- Shear Study Group
"The shear strength of RC beams."
Instit. of Struct. Eng., London 1969.
- 97- CEB
"Shear and torsion."
Bulletin d'information No. 126, Jun. 78.
- 98- G.N.J. Kani
"Basic facts concerning shear failure."
ACI Jnl., Vol. 63, No. 6, part 1, Jun. 66, pp. 675-690.
- 99- P. Kumar
"Collapse load of deep RC beams."
Mag. of Conc. Resear., Vol. 28, No. 94, Mar. 76, pp. 30-36.
- 100- W.J. Kreffeld, C.W. Thurston
"Contribution of longitudinal steel to shear resistance
of RC beams."
ACI Jnl., Vol. 63, No. 3, part 1, Mar. 66, pp. 325-343.
- 101- W.J. Kreffeld, C.W. Thurston
"Studies of the shear and diagonal tension strength of
simply supported RC beams."
ACI Jnl., Vol. 63, No. 4, part 1, Apr. 66, pp. 451-475
- 102- R.N. Swamy, A.M. Bahia
"Influence of fiber reinforcement on the dowel
resistance to shear."
ACI Jnl. Vol. 76, No. 7, Feb. 79, pp. 327-355.

- 103- D.W.Johnston,P.Zia
 "Analysis of dowel action."
 ASCE Struct. Div.,Vol.97,No.ST5,May 71,pp.1611-1636.
- 104- R.G.Mathey,D.Watstein
 "Strains in beams having diagonal tension cracks."
 ACI Jnl.,Vol.55,No.6,Dec.58,pp.717-728.
- 105- R.G.Mathey,D.Watstein
 "Shear strength of beams without web reinforcement
 containing deformed bars of different yield strength."
 ACI Jnl.,Vol.60,No.2,Feb.63,pp.183-205.
- 106- R.N.Swamy,A.Andriopoulos
 "Arch action and bond in concrete shear failures."
 ASCE Struct. Div.,Vol.96,No.ST6,Jun.70,pp.1069-1091.
- 107- J.A.Hofbeck,I.C.Ibrahim,A.H.Mattock
 "Shear transfer in reinforced concrete."
 ACI Jnl.,Vol.66,No.2,Feb.69,pp.119-128.
- 108- A.H.Mattock,N.W.Hawkins
 "Shear transfer in reinforced concrete-Recent
 research."
 Jnl. of Prestressed Concrete Institute, Vol.17, No.2,
 1972, pp.55-75.
- 109- R.Taylor,R.S.Brewer
 "The effect of type of aggregate on the diagonal
 cracking of RC beams."
 Mag. of Conc. Resear.,Vol.15,No.44,Jul.63,pp.87-92.
- 110- H.P.J.Taylor
 "The shear strength of large beams."
 ASCE Struct. Div.,Vol.98,No.ST11,Nov.72,pp.2473-2490.
- 111- R.F.Manuel et al.
 "Deep beam behaviour affected by length and shear span
 variations."
 ACI Jnl.,Vol.68,No.12,Dec.71,pp.954-958.
- 112- H.A.Rawdon,De Parva,C.P.Siess
 "Strength and behavior of deep beams in shear."
 ASCE Struct. Div.,Vol.91,No.ST5,Oct.65,pp.19-41.
- 113- T.Zsutty
 "Shear strength prediction for separate categories of
 simple beam tests."
 ACI Jnl.,Vol.68,Feb.71,pp.138-143.
- 114- G.N.J.Kani
 "How safe are our large concrete beams."
 ACI Jnl.,Vol.64,Mar.67,pp.128-141.

- 127- D.Campbell-Allen,D.F.Rogers
Shrinkage of concrete as affected by size."
Mat. and Struct.,Vol.8,No.45,1975,pp.193-202.
- 128- R.N.Swamy et al.
"The strength and deformation characteristics of high
early strength structural concrete."
Mat. and Struct.,Vol.8,No.48,Nov-Dec.75,pp.413-423.
- 129- A.L.L.Baker
"A criterion of concrete failure."
Instit. of Civ. Eng.,Vol.45,Feb.70,pp.269-278.
- 130- C.M.Sangha,R.K.Dhir
"Strength and complete stress-strain relationships for
concrete, tested in uniaxial compression under different
test conditions."
Mat. and Struct.,Vol.5,No.30,Nov-dec.72,pp.361-370.
- 131- W.H.Price
"Factors influencing concrete strength."
ACI Jnl.,Vol.47,No.6,Feb.51,pp.417-432.
- 132- W.E.Grieb,G.Werner
"Comparison of splitting tensile strength of concrete
with flexural and compressive strengths."
ASTM Jnl.,Vol.62,1962,pp.972-995.
- 133- A.W.Beeby
"The prediction of crack widths in hardened concrete."
The struct. Eng.,Vol.57A,No.1,Jan.79,pp.9-16.
- 134- A.W.Beeby
"An investigation of side cracking in the faces of
beams."
Cement and Conc. Asssoc.,Techn. Rep.,Dec.71.
- 135- K.G.Babu
"Mean steel strain in RC flexural members."
Mat. and Struct.,No.69,May-Jun.79,pp.207-214.
- 136- J.Romuladi,G.B.Pand Batson
"Mechanics of crack arrest in concrete."
ASCE Eng. Mech.,Vol.89,No.EM3,Jun.63,pp.147-168.
- 137- J.Romuladi,G.B.Pand Batson
"Behaviour of RC beams with closely spaced
reinforcement."
ACI Jnl.Vol.60,Jun.63,pp.775-789.
- 138- J.Vaughan
"Application of B & K equipment to strain
measurements."
ISBN 87 87355 08 6, Oct.1975.

